World Journal of Gastroenterology®

Volume 13 Number 43
November 21, 2007

National Journal Award
2005

Baishideng

Editorial Department of *World Journal of Gastroenterology*
77 Shuangta Xijie, Taiyuan 030001, Shanxi Province, China
Telephone: +86-351-4078656
E-mail: wjg@wjgnet.com
http://www.wjgnet.com

ISSN 1007-9327 CN 14-1219/R Local Post Offices Code No. 82-261

World Journal of Gastroenterology www.wjgnet.com Volume 13 Number 43 Nov 21 2007

ISSN 1007-9327
CN 14-1219/R

WJG

World Journal of Gastroenterology®

Indexed and Abstracted in:

Current Contents®/Clinical Medicine, Science Citation Index Expanded (also known as SciSearch®) and Journal Citation Reports/Science Edition, *Index Medicus*, MEDLINE and PubMed, Chemical Abstracts, EMBASE/Excerpta Medica, Abstracts Journals, *Nature Clinical Practice Gastroenterology and Hepatology*, CAB Abstracts and Global Health.
ISI JCR 2003-2000 IF: 3.318, 2.532, 1.445 and 0.993.

Volume 13 Number 43
November 21, 2007
World J Gastroenterol
2007 November 21; 13(43): 5673-5798

Online Submissions
wjg.wjgnet.com
www.wjgnet.com
Printed on Acid-free Paper
世界胃肠病学杂志

National Journal Award
2005

World Journal of Gastroenterology®

Weekly Established in October 1995

Volume 13 Number 43
November 21, 2007

Baishideng

Contents

Contents

World Journal of Gastroenterology
Volume 13 **Number** 43 **November** 21, 2007

World Journal of Gastroenterology
Volume 13 **Number** 43 **November** 21, 2007

Contents

Responsible E-Editor for this issue: Hai-Feng Wang

C-Editor for this issue: Pietro Invernizzi, MD, PhD

Responsible S-Editor for this issue: You-De Chang, PhD

World Journal of Gastroenterology (*World J Gastroenterol , WJG*), a leading international journal in gastroenterology and hepatology, has an established reputation for publishing first class research on esophageal cancer, gastric cancer, liver cancer, viral hepatitis, colorectal cancer, and *H pylori* infection, providing a forum for both clinicians and scientists, and has been indexed and abstracted in Current Contents®/Clinical Medicine, Science Citation Index Expanded (also known as SciSearch®) and Journal Citation Reports/Science Edition, *Index Medicus*, MEDLINE and PubMed, Chemical Abstracts, EMBASE/Excerpta Medica, Abstracts Journals, *Nature Clinical Practice Gastroenterology and Hepatology*, CAB Abstracts and Global Health. ISI JCR 2003-2000 IF: 3.318, 2.532, 1.445 and 0.993. *WJG* is a weekly journal published by *WJG*. The publication date is on 7th, 14th, 21st, and 28th every month. The *WJG* is supported by The National Natural Science Foundation of China, No. 30224801 and No.30424812, which was founded with a name of *China National Journal of New Gastroenterology* on October 1, 1995, and renamed as *WJG* on January 25, 1998.

NAME OF JOURNAL
World Journal of Gastroenterology

RESPONSIBLE INSTITUTION
Department of Science and Technology of Shanxi Province

SPONSOR
Taiyuan Research and Treatment Center for Digestive Diseases, Taiyuan 77, Shuangta Xijie, Taiyuan 030001, Shanxi Province, China

EDITING
Editorial Board of *World Journal of Gastroenterology,* 77 Shuangta Xijie, Taiyuan 030001,
Shanxi Province, China
Telephone: +86-351-4078656
E-mail: wjg@wjgnet.com

PUBLISHING
Editorial Department of *World Journal of Gastroenterology,* 77 Shuangta Xijie, Taiyuan 030001,
Shanxi Province, China
Telephone: +86-351-4078656
E-mail: wjg@wjgnet.com
http://www.wjgnet.com

PRINTING
Beijing Kexin Printing House

OVERSEAS DISTRIBUTOR
Beijing Bureau for Distribution of Newspapers and Journals
(Code No. 82-261)
China International Book Trading Corporation PO Box 399, Beijing, China (Code No. M4481)

PUBLICATION DATE
November 21, 2007

World Journal of Gastroenterology®

Editorial Board

2007-2009

Baishideng

http://www.wjgnet.com E-mail: wjg@wjgnet.com

John L Wallace, *Calgary*
Eric M Yoshida, *Vancouver*

Chile
Silvana Zanlungo, *Santiago*

China
Henry LY Chan, *Hongkong*
Xiao-Ping Chen, *Wuhan*
Zong-Jie Cui, *Beijing*
Da-Jun Deng, *Beijing*
Er-Dan Dong, *Beijing*
Sheung-Tat Fan, *Hong Kong*
Jin Gu, *Beijing*
De-Wu Han, *Taiyuan*
Ming-Liang He, *Hong Kong*
Wayne HC Hu, *Hong Kong*
Chee-Kin Hui, *Hong Kong*
Ching Lung Lai, *Hong Kong*
Kam Chuen Lai, *Hong Kong*
James YW Lau, *Hong Kong*
Yuk Tong Lee, *Hong Kong*
Suet Yi Leung, *Hong Kong*
Wai-Keung Leung, *Hong Kong*
Chung-Mau Lo, *Hong Kong*
Jing-Yun Ma, *Beijing*
Lun-Xiu Qin, *Shanghai*
Yu-Gang Song, *Guangzhou*
Qin Su, *Beijing*
Wai-Man Wong, *Hong Kong*
Hong Xiao, *Beijing*
Dong-Liang Yang, *Wuhan*
Winnie Yeo, *Hong Kong*
Yuan Yuan, *Shenyang*
Man-Fung Yuen, *Hong Kong*
Jian-Zhong Zhang, *Beijing*
Xin-Xin Zhang, *Shanghai*
Shu Zheng, *Hangzhou*

Croatia
Tamara Cacev, *Zagreb*
Marko Duvnjak, *Zagreb*

Cuba
Damian Casadesus Rodriguez, *Havana*

Czech
Milan Jirsa, *Praha*

Denmark
Peter Bytzer, *Copenhagen*
Hans Gregersen, *Aalborg*
Jens H Henriksen, *Hvidovre*
Claus Peter Hovendal, *Odense*
Fin Stolze Larsen, *Copenhagen*
SØren MØller, *Hvidovre*

Egypt
Abdel-Rahman El-Zayadi, *Giza*
Amr Mohamed Helmy, *Cairo*
Sanaa Moharram Kamal, *Cairo*
Ayman Yosry, *Cairo*

Finland
Irma Elisabet Jarvela, *Helsinki*
Katri Maria Kaukinen, *Tampere*
Minna Nyström, *Helsinki*
Pentti Sipponen, *Espoo*

France
Bettaieb Ali, *Dijon*
Corlu Anne, *Rennes*
Denis Ardid, *Clermont-Ferrand*
Charles Paul Balabaud, *Bordeaux*
Soumeya Bekri, *Rouen*
Jacques Belghiti, *Clichy*
Pierre Brissot, *Rennes*
Patrice Philippe Cacoub, *Paris*
Franck Carbonnel, *Besancon*
Laurent Castera, *Pessac*
Bruno Clément, *Rennes*
Jacques Cosnes, *Paris*
Thomas Decaens, *Cedex*
Francoise Lunel Fabiani, *Angers*
Gérard Feldmann, *Paris*
Jean Fioramonti, *Toulouse*
Catherine Guettier, *Villejuif*
Chantal Housset, *Paris*
Juan Lucio Iovanna, *Marseille*
Rene Lambert, *Lyon*
Philippe Mathurin, *Lille*
Tamara Matysiak–Budnik, *Paris*
Francis Mégraud, *Bordeaux*
Richard Moreau, *Clichy*
Thierry Piche, *Nice*
Raoul Poupon, *Paris*
Jean Rosenbaum, *Bordeaux*
Jose Sahel, *Marseille*
Jean-Philippe Salier, *Rouen*
Jean-Yves Scoazec, *Lyon*
Khalid Ahnini Tazi, *Clichy*
Emmanuel Tiret, *Paris*
Baumert F Thomas, *Strasbourg*
MC Vozenin-brotons, *Villejuif*
Jean-Pierre Henri Zarski, *Grenoble*
Jessica Zucman-Rossi, *Paris*

Germany
HD Allescher, *Garmisch-Partenkirchen*
Martin Anlauf, *Kiel*
Rudolf Arnold, *Marburg*
Max G Bachem, *Ulm*
Thomas F Baumert, *Freiburg*
Daniel C Baumgart, *Berlin*
Hubert Blum, *Freiburg*
Thomas Bock, *Tuebingen*
Katja Breitkopf, *Mannheim*
Dunja Bruder, *Braunschweig*
Markus W Büchler, *Heidelberg*
Christa Buechler, *Regensburg*
Reinhard Buettner, *Bonn*
Elke Cario, *Essen*
CF Dietrich, *Bad Mergentheim*
Rainer Josef Duchmann, *Berlin*
Paul Enck, *Tuebingen*
Fred Fändrich, *Kiel*
Ulrich Robert Fölsch, *Kiel*
Helmut Friess, *Heidelberg*
Peter R Galle, *Mainz*
Nikolaus Gassler, *Aachen*
Andreas Geier, *Aachen*
Dieter Glebe, *Giessen*
Burkhard Göke, *Munich*
Florian Graepler, *Tuebingen*
Axel M Gressner, *Aachen*
Veit Gülberg, *Munich*
Rainer Haas, *Munich*
Eckhart Georg Hahn, *Erlangen*
Stephan Hellmig, *Kiel*
Martin Hennenberg, *Bonn*
Johannes Herkel, *Hamburg*
Klaus Herrlinger, *Stuttgart*
Eberhard Hildt, *Berlin*
Joerg C Hoffmann, *Berlin*
Ferdinand Hofstaedter, *Regensburg*
Werner Hohenberger, *Erlangen*
RG Jakobs, *Ludwigshafen*
Jutta Keller, *Hamburg*
Andrej Khandoga, *Munich*
Sibylle Koletzko, *München*
Stefan Kubicka, *Hannover*
Joachim Labenz, *Siegen*
Frank Lammert, *Bonn*
Thomas Langmann, *Regensburg*
Christian Liedtke, *Aachen*
Matthias Löhr, *Mannheim*
Christian Maaser, *Muenster*
Ahmed Madisch, *Dresden*
Michael Peter Manns, *Hannover*
Stephan Miehlke, *Dresden*
Sabine Mihm, *Göttingen*
Silvio Nadalin, *Essen*
Markus F Neurath, *Mainz*
Johann Ockenga, *Berlin*
Florian Obermeier, *Regensburg*
Gustav Paumgartner, *Munich*
Ulrich Ks Peitz, *Magdeburg*
Markus Reiser, *Bochum*
Steffen Rickes, *Magdeburg*
Gerhard Rogler, *Regensburg*
Tilman Sauerbruch, *Bonn*
Dieter Saur, *Munich*
Hans Scherubl, *Berlin*
Joerg Schirra, *Munich*
Roland M Schmid, *München*
Volker Schmitz, *Bonn*
AG Schreyer, *Regensburg*
Tobias Schroeder, *Essen*
Hans Seifert, *Oldenburg*
Manfred V Singer, *Mannheim*
Gisela Sparmann, *Rostock*
Jurgen M Stein, *Frankfurt*
Ulrike Susanne Stein, *Berlin*
Manfred Stolte, *Bayreuth*
Christian P Strassburg, *Hannover*
WR Stremmel, *Heidelberg*
Harald F Teutsch, *Ulm*
Robert Thimme, *Freiburg*
HL Tillmann, *Leipzig*
Tung-Yu Tsui, *Regensburg*
Axel Ulsenheimer, *Munich*
Patrick Veit, *Essen*
Claudia Veltkamp, *Heidelberg*
Siegfried Wagner, *Deggendorf*
Henning Walczak, *Heidelberg*
Fritz von Weizsacker, *Berlin*
Jens Werner, *Heidelberg*
Bertram Wiedenmann, *Berlin*
Reiner Wiest, *Regensburg*
Stefan Wirth, *Wuppertal*
Stefan JP Zeuzem, *Homburg*

Greece
Elias A Kouroumalis, *Heraklion*
Ioannis E Koutroubakis, *Heraklion*
Spiros Sgouros, *Athens*

Hungary
Peter Laszlo Lakatos, *Budapest*
Zsuzsa Szondy, *Debrecen*

Iceland
H Gudjonsson, *Reykjavik*

India
KA Balasubramanian, *Vellore*
Sujit K Bhattacharya, *Kolkata*
Yogesh K Chawla, *Chandigarh*
Radha K Dhiman, *Chandigarh*
Sri Prakash Misra, *Allahabad*
ND Reddy, *Hyderabad*

Iran
Seyed-Moayed Alavian, *Tehran*
Reza Malekzadeh, *Tehran*
Seyed Alireza Taghavi, *Shiraz*

Ireland
Billy Bourke, *Dublin*
Ronan A Cahill, *Cork*
Anthony P Moran, *Galway*

Israel
Simon Bar-Meir, *Hashomer*
Abraham Rami Eliakim, *Haifa*

Yaron Ilan, *Jerusalem*
Avidan U Neumann, *Ramat-Gan*
Yaron Niv, *Pardesia*
Ran Oren, *Tel Aviv*

Italy

Giovanni Addolorato, *Roma*
Luigi E Adinolfi, *Naples*
Domenico Alvaro, *Rome*
V Annese, *San Giovanni Rotond*
Adolfo Francesco Attili, *Roma*
Giovanni Barbara, *Bologna*
Gabrio Bassotti, *Perugia*
Pier Maria Battezzati, *Milan*
Stefano Bellentani, *Carpi*
Antomio Benedetti, *Ancona*
Mauro Bernardi, *Bologna*
Livia Biancone, *Rome*
Luigi Bonavina, *Milano*
Flavia Bortolotti, *Padova*
Giuseppe Brisinda, *Rome*
Giovanni Cammarota, *Roma*
Antonino Cavallari, *Bologna*
Giuseppe Chiarioni, *Valeggio*
Michele Cicala, *Rome*
Amedeo Columbano, *Cagliari*
Massimo Conio, *Sanremo*
Dario Conte, *Milano*
Gino Roberto Corazza, *Pavia*
Francesco Costa, *Pisa*
Antonio Craxi, *Palermo*
Silvio Danese, *Milan*
Roberto De Giorgio, *Bologna*
Giovanni D De Palma, *Naples*
Fabio Farinati, *Padua*
Giammarco Fava, *Ancona*
Francesco Feo, *Sassari*
Stefano Fiorucci, *Perugia*
Andrea Galli, *Firenze*
Valeria Ghisett, *Turin*
Gianluigi Giannelli, *Bari*
Edoardo G Giannini, *Genoa*
Paolo Gionchetti, *Bologna*
Mario Guslandi, *Milano*
Pietro Invernizzi, *Milan*
Giacomo Laffi, *Firenze*
Giovanni Maconi, *Milan*
Lucia Malaguarnera, *Catania*
ED Mangoni, *Napoli*
Giulio Marchesini, *Bologna*
Fabio Marra, *Florence*
Marco Marzioni, *Ancona*
Giuseppe Montalto, *Palermo*
Giovanni Monteleone, *Rome*
Giovanni Musso, *Torino*
Gerardo Nardone, *Napoli*
Valerio Nobili, *Rome*
Luisi Pagliaro, *Palermo*
Francesco Pallone, *Rome*
Fabrizio R Parente, *Milan*
F Perri, *San Giovanni Rotondo*
Raffaele Pezzilli, *Bologna*
A Pilotto, *San Giovanni Rotondo*
Mario Pirisi, *Novara*
Paolo Del Poggio, *Treviglio*
Gabriele Bianchi Porro, *Milano*
Piero Portincasa, *Bari*
Bernardino Rampone, *Siena*
Claudio Romano, *Messina*
Marco Romano, *Napoli*
Gerardo Rosati, *Potenza*
Enrico Roda, *Bologna*
Domenico Sansonno, *Bari*
Vincenzo Savarino, *Genova*
Mario Del Tacca, *Pisa*
Giovanni Tarantino, *Naples*
Roberto Testa, *Genoa*
Pier Alberto Testoni, *Milan*
Dino Vaira, *Bologna*

Japan

Kyoichi Adachi, *Izumo*
Yasushi Adachi, *Sapporo*
Taiji Akamatsu, *Matsumoto*
Sk Md Fazle Akbar, *Ehime*
Takafumi Ando, *Nagoya*
Akira Andoh, *Otsu*
Taku Aoki, *Tokyo*
Masahiro Arai, *Tokyo*
Tetsuo Arakawa, *Osaka*
Yasuji Arase, *Tokyo*
Masahiro Asaka, *Sapporo*
Hitoshi Asakura, *Tokyo*
Takeshi Azuma, *Fukui*
Yoichi Chida, *Fukuoka*
Takahiro Fujimori, *Tochigi*
Jiro Fujimoto, *Hyogo*
Kazuma Fujimoto, *Saga*
Mitsuhiro Fujishiro, *Tokyo*
Yoshihide Fujiyama, *Otsu*
Hirokazu Fukui, *Tochigi*
Hiroyuki Hanai, *Hamamatsu*
Kazuhiro Hanazaki, *Kochi*
Naohiko Harada, *Fukuoka*
Makoto Hashizume, *Fukuoka*
Tetsuo Hayakawa, *Nagoya*
Kazuhide Higuchi, *Osaka*
Keisuke Hino, *Ube*
Keiji Hirata, *Kitakyushu*
Yuji Iimuro, *Nishinomiya*
Kenji Ikeda, *Tokyo*
Fumio Imazeki, *Chiba*
Yutaka Inagaki, *Kanagawa*
Yasuhiro Inokuchi, *Yokohama*
Haruhiro Inoue, *Yokohama*
Masayasu Inoue, *Osaka*
Akio Inui, *Kagoshima*
Hiromi Ishibashi, *Nagasaki*
Shunji Ishihara, *Izumo*
Toru Ishikawa, *Niigata*
Kei Ito, *Sendai*
Masayoshi Ito, *Tokyo*
Hiroaki Itoh, *Akita*
Ryuichi Iwakiri, *Saga*
Yoshiaki Iwasaki, *Okayama*
Terumi Kamisawa, *Tokyo*
Hiroshi Kaneko, *Aichi-Gun*
Shuichi Kaneko, *Kanazawa*
Takashi Kanematsu, *Nagasaki*
Mitsuo Katano, *Fukuoka*
Junji Kato, *Sapporo*
Mototsugu Kato, *Sapporo*
Shinzo Kato, *Tokyo*
Norifumi Kawada, *Osaka*
Sunao Kawano, *Osaka*
Mitsuhiro Kida, *Kanagawa*
Yoshikazu Kinoshita, *Izumo*
Tsuneo Kitamura, *Chiba*
Seigo Kitano, *Oita*
Kazuhiko Koike, *Tokyo*
Norihiro Kokudo, *Tokyo*
Satoshi Kondo, *Sapporo*
Shoji Kubo, *Osaka*
Masato Kusunoki, *Tsu Mie*
Katsunori Iijima, *Sendai*
Shin Maeda, *Tokyo*
Masatoshi Makuuchi, *Tokyo*
Osamu Matsui, *Kanazawa*
Yasuhiro Matsumura, *Chiba*
Yasushi Matsuzaki, *Tsukuba*
Kiyoshi Migita, *Omura*
Tetsuya Mine, *Kanagawa*
Hiroto Miwa, *Hyogo*
Masashi Mizokami, *Nagoya*
Yoshiaki Mizuguchi, *Tokyo*
Motowo Mizuno, *Hiroshima*
Morito Monden, *Suita*
Hisataka S Moriwaki, *Gifu*
Yasuaki Motomura, *Iizuka*
Yoshiharu Motoo, *Kanazawa*
Kazunari Murakami, *Oita*
Kunihiko Murase, *Tusima*
Masahito Nagaki, *Gifu*
Masaki Nagaya, *Kawasaki*
Yuji Naito, *Kyoto*
Hisato Nakajima, *Tokyo*
Hiroki Nakamura, *Yamaguchi*
Shotaro Nakamura, *Fukuoka*
Mikio Nishioka, *Niihama*
Shuji Nomoto, *Nagoya*
Susumu Ohmada, *Maebashi*
Masayuki Ohta, *Oita*
Tetsuo Ohta, *Kanazawa*
Kazuichi Okazaki, *Osaka*
Katsuhisa Omagari, *Nagasaki*
Saburo Onishi, *Nankoku*
Morikazu Onji, *Ehime*
Satoshi Osawa, *Hamamatsu*
Masanobu Oshima, *Kanazawa*
Hiromitsu Saisho, *Chiba*
Hidetsugu Saito, *Tokyo*
Yutaka Saito, *Tokyo*
Isao Sakaida, *Yamaguchi*
Michiie Sakamoto, *Tokyo*
Yasushi Sano, *Chiba*
Hiroki Sasaki, *Tokyo*
Iwao Sasaki, *Sendai*
Motoko Sasaki, *Kanazawa*
Chifumi Sato, *Tokyo*
Shuichi Seki, *Osaka*
Hiroshi Shimada, *Yokohama*
Mitsuo Shimada, *Tokushima*
Tomohiko Shimatan, *Hiroshima*
Hiroaki Shimizu, *Chiba*
Ichiro Shimizu, *Tokushima*
Yukihiro Shimizu, *Kyoto*
Shinji Shimoda, *Fukuoka*
Tooru Shimosegawa, *Sendai*
Tadashi Shimoyama, *Hirosaki*
Ken Shirabe, *Iizuka*
Yoshio Shirai, *Niigata*
Katsuya Shiraki, *Mie*
Yasushi Shiratori, *Okayama*
Masayuki Sho, *Nara*
Yasuhiko Sugawara, *Tokyo*
Hidekazu Suzuki, *Tokyo*
Minoru Tada, *Tokyo*
Tadatoshi Takayama, *Tokyo*
Tadashi Takeda, *Osaka*
Koji Takeuchi, *Kyoto*
Kiichi Tamada, *Tochigi*
Akira Tanaka, *Kyoto*
Eiji Tanaka, *Matsumoto*
Noriaki Tanaka, *Okayama*
Shinji Tanaka, *Hiroshima*
Wei Tang, *Tokyo*
Hideki Taniguchi, *Yokohama*
Kyuichi Tanikawa, *Kurume*
Akira Terano, *Shimotsugagun*
Hitoshi Togash, *Yamagata*
Kazunari Tominaga, *Osaka*
Takuji Torimura, *Fukuoka*
Minoru Toyota, *Sapporo*
Akihito Tsubota, *Chiba*
Shingo Tsuji, *Osaka*
Takato Ueno, *Kurume*
Shinichi Wada, *Tochigi*
Hiroyuki Watanabe, *Kanazawa*
Toshio Watanabe, *Osaka*
Yuji Watanabe, *Ehime*
Chun-Yang Wen, *Nagasaki*
Koji Yamaguchi, *Fukuoka*
Takayuki Yamamoto, *Yokkaichi*
Takashi Yao, *Fukuoka*

Masashi Yoneda, *Tochigi*
Hiroshi Yoshida, *Tokyo*
Masashi Yoshida, *Tokyo*
Norimasa Yoshida, *Kyoto*
Kentaro Yoshika, *Toyoake*
Masahide Yoshikawa, *Kashihara*

Lebanon
Bassam N Abboud, *Beirut*
Ala I Sharara, *Beirut*
Joseph Daoud Boujaoude, *Beirut*

Lithuania
Limas Kupcinskas, *Kaunas*

Macedonia
Vladimir Cirko Serafimoski, *Skopje*

Malaysia
Andrew Seng Boon Chua, *Ipoh*
Khean-Lee Goh, *Kuala Lumpur*
Jayaram Menon, *Sabah*

Mexico
Garcia-Compean Diego, *Monterrey*
E R Marin-Lopez, *Jesús García*
Saúl Villa-Treviño, *México*
JK Yamamoto-Furusho, *México*

Monaco
Patrick Rampal, *Monaco*

Netherlands
Ulrich Beuers, *Amsterdam*
Gerd Bouma, *Amsterdam*
Lee Bouwman, *Leiden*
J Bart A Crusius, *Amsterdam*
Janine K Kruit, *Groningen*
Ernst Johan Kuipers, *Rotterdam*
Ton Lisman, *Utrecht*
Yi Liu, *Amsterdam*
Servaas Morré, *Amsterdam*
Chris JJ Mulder, *Amsterdam*
Michael Müller, *Wageningen*
Amado Salvador Peña, *Amsterdam*
Robert J Porte, *Groningen*
Ingrid B Renes, *Rotterdam*
Andreas Smout, *Utrecht*
RW Stockbrugger, *Maastricht*
Luc JW van der Laan, *Rotterdam*
Karel van Erpecum, *Utrecht*
GP VanBerge-Henegouwen, *Utrecht*

New Zealand
Ian David Wallace, *Auckland*

Nigeria
Samuel Babafemi Olaleye, *Ibadan*

Norway
Trond Berg, *Oslo*
Tom Hemming Karlsen, *Oslo*
Helge Lyder Waldum, *Trondheim*

Pakistan
Muhammad S Khokhar, *Lahore*

Poland
Tomasz Brzozowski, *Cracow*
Robert Flisiak, *Bialystok*
Hanna Gregorek, *Warsaw*
DM Lebensztejn, *Bialystok*
Wojciech G Polak, *Wroclaw*
Marek Hartleb, *Katowice*

Portugal
MP Cecília, *Lisbon*
Miguel Carneiro De Moura, *Lisbon*

Russia
Vladimir T Ivashkin, *Moscow*
Leonid Lazebnik, *Moscow*
Vasiliy I Reshetnyak, *Moscow*

Saudi Arabia
Ibrahim Abdulkarim Al Mofleh, *Riyadh*

Serbia
DM Jovanovic, *Sremska Kamenica*

Singapore
Bow Ho, *Kent Ridge*
Khek-Yu Ho, *Singapore*
Francis Seow-Choen, *Singapore*

Slovakia
Anton Vavrecka, *Bratislava*

Slovenia
Sasa Markovic, *Ljubljana*

South Africa
Michael C Kew, *Parktown*

South Korea
Byung Ihn Choi, *Seoul*
Ho Soon Choi, *Seoul*
M Yeo, *Suwon*
Sun Pyo Hong, *Gyeonggi-do*
Jae J Kim, *Seoul*
Jin-Hong Kim, *Suwon*
Myung-Hwan Kim, *Seoul*
Chang Hong Lee, *Seoul*
Jong Kyun Lee, *Seoul*
Eun-Yi Moon, *Seoul*
Jae-Gahb Park, *Seoul*
Dong Wan Seo, *Seoul*
Dong jin Suh, *Seoul*

Spain
Juan G Abraldes, *Barcelona*
Agustin Albillos, *Madrid*
Raul J Andrade, *Málaga*
Luis Aparisi, *Valencia*
Fernando Azpiroz, *Barcelona*
Ramon Bataller, *Barcelona*
Josep M Bordas, *Barcelona*
Xavier Calvet, *Sabadell*
Andres Cardenas, *Barcelona*
Vicente Carreño, *Madrid*
Jose Castellote, *Barcelona*
Antoni Castells, *Barcelona*
Vicente Felipo, *Valencia*
Juan C Garcia-Pagán, *Barcelona*
Jaime Bosch Genover, *Barcelona*
Jaime Guardia, *Barcelona*
Angel Lanas, *Zaragoza*
María Isabel Torres López, *Jaén*
José M Mato, *Derio*
Juan F Medina, *Pamplona*
MA Muñoz-Navas, *Pamplona*
Julian Panes, *Barcelona*
Miguel Minguez Perez, *Valencia*
Miguel Perez-Mateo, *Alicante*
Josep M Pique, *Barcelona*
Jesús M Prieto, Pamplona
Sabino Riestra, *Pola De Siero*
Luis Rodrigo, *Oviedo*
Manuel Romero-Gómez, *Sevilla*

Sweden
Einar Stefan Björnsson, *Gothenburg*
Curt Einarsson, *Huddinge*
Ulf Hindorf, *Lund*
Hanns-Ulrich Marschall, *Stockholm*
Lars Christer Olbe, *Molndal*
Matti Sallberg, *Stockholm*
Magnus Simrén, *Göteborg*
Xiao-Feng Sun, *Linköping*
Ervin Tóth, *Malmö*
Weimin Ye, *Stockholm*

Switzerland
Chrish Beglinger, *Basel*
Pierre A Clavien, Zurich
Jean-Francois Dufour, *Bern*
Franco Fortunato, *Zürich*
Jean Louis Frossard, *Geneva*
Gerd A Kullak-Ublick, *Zurich*
Pierre Michetti, *Lausanne*
Francesco Negro, *Genève*
Bruno Stieger, *Zurich*
Radu Tutuian, *Zurich*
Stephan Robert Vavricka, *Zurich*
Arthur Zimmermann, *Berne*

Turkey
Yusuf Bayraktar, *Ankara*
Figen Gurakan, *Ankara*
Aydin Karabacakoglu, *Konya*
Serdar Karakose, *Konya*
Hizir Kurtel, *Istanbu*
Osman Cavit Ozdogan, *Istanbul*
Özlem Yilmaz, *Izmir*
Cihan Yurdaydin, *Ankara*

United Arab Emirates
Sherif M Karam, *Al-Ain*

United Kingdom
David Adams, *Birmingham*
NK Ahluwalia, *Stockport*
CG Antoniades, *London*
Anthony TR Axon, *Leeds*
Qasim Aziz, *Manchester*
Nicholas M Barnes, *Birmingham*
Jim D Bell, *London*
Mairi Brittan, *London*
Alastair David Burt, *Newcastle*
Simon Scott Campbell, *Manchester*
Simon R Carding, *Leeds*
Paul Jonathan Ciclitira, *London*
Eithne Costello, *Liverpool*
Tatjana Crnogorac-Jurcevic, *London*
Amar Paul Dhillon, *London*
Emad M El-Omar, *Aberdeen*
Annette Fristscher-Ravens, *London*
Elizabeth Furrie, *Dundee*
Daniel Richard Gaya, *Edinburgh*
Subrata Ghosh, *London*
William Greenhalf, *Liverpool*
Indra Neil Guha, *Southampton*
Peter Clive Hayes, *Edinburgh*
Gwo-Tzer Ho, *Edinburgh*
Anthony R Hobson, *Salford*
Stefan G Hübscher, *Birmingham*
Robin Hughes, *London*
Pali Hungin, *Stockton*
David Paul Hurlstone, *Sheffield*
Rajiv Jalan, *London*
Janusz AZ Jankowski, *Oxford*
Brian T Johnston, *Belfast*
David EJ Jones, *Newcastle*
Michael A Kamm, *Harrow*
Peter Karayiannis, *London*
Laurens Kruidenier, *Harlow*
Patricia F Lalor, *Birmingham*
Hong-Xiang Liu, *Cambridge*
K E L McColl, *Glasgow*
Stuart AC McDonald, *London*

Dermot Patrick Mcgovern, *Oxford*
Giorgina Mieli-Vergani, *London*
Nikolai V Naoumov, *London*
John P Neoptolemos, *Liverpool*
James Neuberger, *Birmingham*
Mark S Pearce, *Newcastle Upon Tyne*
Stephen P Pereira, *London*
D Mark Pritchard, *Liverpool*
Stephen E Roberts, *Swansea*
Marco Senzolo, *Padova*
Soraya Shirazi-Beechey, *Liverpool*
Robert Sutton, *Liverpool*
Simon D Taylor-Robinson, *London*
Paris P Tekkis, *London*
Ulrich Thalheimer, *London*
Nick Paul Thompson, *Newcastle*
David Tosh, *Bath*
Frank Ivor Tovey, *London*
Chris Tselepis, *Birmingham*
Diego Vergani, *London*
Geoffrey Warhurst, *Salford*
Peter James Whorwell, *Manchester*
Roger Williams, *London*
Karen Leslie Wright, *Bath*
Min Zhao, *Foresterhill*

United States

Gary A Abrams, *Birmingham*
Golo Ahlenstiel, *Bethesda*
BS Anand, *Houston*
Frank A Anania, *Atlanta*
M Ananthanarayanan, *New York*
Gavin Edward Arteel, *Louisville*
Jasmohan Singh Bajaj, *Milwaukee*
Jamie S Barkin, *Miami Beach*
Kim Elaine Barrett, *San Diego*
Marc Basson, *Detroit*
Wallace F Berman, *Durham*
Timothy R Billiar, *Pittsburgh*
Edmund J Bini, *New York*
Jennifer D Black, *Buffalo*
Herbert L Bonkovsky, *Farmington*
Andrea D Branch, *New York*
Robert S Bresalier, *Houston*
Alan L Buchman, *Chicago*
Alan Cahill, *Philadelphia*
John M Carethers, *San Diego*
David L Carr-Locke, *Boston*
Ravi S Chari, *Nashville*
Jiande Chen, *Galveston*
Xian-Ming Chen, *Omaha*
Ramsey Chi-man Cheung, *Palo Alto*
William D Chey, *Ann Arbor*
John Y Chiang, *Rootstown*
Parimal Chowdhury, *Arkansas*
Raymond T Chung, *Boston*
James M Church, *Cleveland*
Mark G Clemens, *Charlotte*
Vincent Coghlan, *Beaverton*
David Cronin II, *New Haven*
John Cuppoletti, *Cincinnati*
Mark James Czaja, *New York*
Peter V Danenberg, *Los Angeles*
Kiron Moy Das, *New Brunswick*
Sharon DeMorrow, *Temple*
Deborah L Diamond, *Seattle*
Peter Draganov, *Florida*
Bijan Eghtesad, *Cleveland*
Hala El-Zimaity, *Houston*
Michelle Embree-Ku, *Providence*
Ronnie Fass, *Tucson*
Mark A Feitelson, *Philadelphia*
Ariel E Feldstein, *Cleveland*
Alessandro Fichera, *Chicago*
Chris E Forsmark, *Gainesville*
Chandrashekhar R Gandhi, *Pittsburgh*
Susan L Gearhart, *Baltimore*
Xupeng Ge, *Boston*
John P Geibel, *New Haven*
Xin Geng, *New Brunswick*
Jean-Francois Geschwind, *Baltimore*
Ignacio Gil-Bazo, *New York*
Shannon S Glaser, *Temple*
Ajay Goel, *Dallas*
Julia Butler Greer, *Pittsburgh*
James Henry Grendell, *New York*
David R Gretch, *Seattle*
Stefano Guandalini, *Chicago*
Anna S Gukovskaya, *Los Angeles*
Sanjeev Gupta, *Bronx*
David J Hackam, *Pittsburgh*
Stephen B Hanauer, *Chicago*
Gavin Harewood, *Rochester*
Margaret McLean Heitkemper, *Seattle*
Alan W Hemming, *Gainesville*
Samuel B Ho, *San Diego*
Colin William Howden, *Chicago*
Hongjin Huang, *Alameda*
Jamal A Ibdah, *Columbia*
Atif Iqbal, *Omaha*
Hajime Isomoto, *Rochester*
Hartmut Jaeschke, *Tucson*
Dennis M Jensen, *Los Angeles*
Leonard R Johnson, *Memphis*
Michael P Jones, *Chicago*
Peter James Kahrilas, *Chicago*
AN Kalloo, *Baltimore*
Neil Kaplowitz, *Los Angeles*
Rashmi Kaul, *Tulsa*
Jonathan D Kaunitz, *Los Angeles*
Ali Keshavarzian, *Chicago*
Miran Kim, *Providence*
Joseph B Kirsner, *Chicago*
Leonidas G Koniaris, *Miami*
Burton I Korelitz, *New York*
Robert J Korst, *New York*
Richard A Kozarek, *Seattle*
Michael Kremer, *Chapel Hill*
Shiu-Ming Kuo, *Buffalo*
Daryl Tan Yeung Lau, *Galvesto*
Joel E Lavine, *San Diego*
Dirk J van Leeuwen, *Lebanon*
Glen A Lehman, *Indianapolis*
Alex B Lentsch, *Cincinnati*
Andreas Leodolter, *La Jolla*
Gene LeSage, *Houston*
Ming Li, *New Orleans*
Zhiping Li, *Baltimore*
LM Lichtenberger, *Houston*
GR Lichtenstein, *Philadelphia*
Otto Schiueh-Tzang Lin, *Seattle*
Martin Lipkin, *New York*
Edward V Loftus, *Rocheste*
Robin G Lorenz, *Birmingham*
Michael Ronan Lucey, *Madison*
JD Luketich, *Pittsburgh*
Henry Thomson Lynch, *Omaha*
Patrick M Lynch, *Houston*
Peter J Mannon, *Bethesda*
Charles Milton Mansbach, *Memphis*
John Frank Di Mari, *Texas*
John M Mariadason, *Bronx*
WM Mars, *Pittsburgh*
Laura E Matarese, *Pittsburgh*
Lynne V McFarland, *Washington*
Kevin McGrath, *Pittsburgh*
Harihara Mehendale, *Monroe*
Stephan Menne, *New York*
Howard Mertz, *Nashville*
George W Meyer, *Sacramento*
G Michalopoulos, *Pittsburgh*
James Michael Millis, *Chicago*
Albert D Min, *New York*
Pramod Kumar Mistry, *New Haven*
Smruti Ranjan Mohanty, *Chicago*
Satdarshan Singh Monga, *Pittsburgh*
Timothy H Moran, *Baltimore*
Steven F Moss, *Providence*
Masaki Nagaya, *Boston*
Laura Eleanor Nagy, *Cleveland*
Hiroshi Nakagawa, *Philadelphia*
Douglas B Nelson, *Minneaplis*
Brant K Oelschlager, *Washington*
Curtis T Okamoto, *Los Angeles*
Stephen JD O'Keefe, *Pittsburgh*
Dimitry Oleynikov, *Omaha*
Natalia A Osna, *Omaha*
Stephen J Pandol, *Los Angeles*
Pankaj Jay Pasricha, *Gaveston*
Zhiheng Pei, *New York*
Michael A Pezzone, *Pittsburgh*
CS Pitchumoni, *New Brunswiuc*
Jay Pravda, *Gainesville*
M Raimondo, *Jacksonville*
GS Raju, *Galveston*
Murray B Resnick, *Providence*
Adrian Reuben, *Charleston*
Douglas K Rex, *Indianapolis*
Victor E Reyes, *Galveston*
Richard A Rippe, *Chapel Hill*
Marcos Rojkind, *Washington*
Philip Rosenthal, *San Francisco*
Hemant Kumar Roy, *Evanston*
Shawn David Safford, *Norfolk*
Bruce E Sands, *Boston*
NJ Shaheen, *Chapel Hill*
Harvey L Sharp, *Minneapolis*
Stuart Sherman, *Indianapolis*
Shivendra Shukla, *Columbia*
Alphonse E Sirica, *Virginia*
Shanthi V Sitaraman, *Atlanta*
Shanthi Srinivasan, *Atlanta*
Michael Steer, *Boston*
Gary D Stoner, *Columbus*
Liping Su, *Chicago*
Christina Surawicz, *Seattle*
Gyongyi Szabo, *Worcester*
Yvette Taché, *Los Angeles*
Seng-Lai Tan, *Seattle*
Andrzej Tarnawski, *Long Beach*
Andrzej S Tarnawski, *Orange*
K-M Tchou-Wong, *New York*
Neil D Theise, *New York*
PJ Thuluvath, *Baltimore*
Swan Nio Thung, *New York*
Natalie J Torok, *Sacramento*
RA Travagli, *Baton Rouge*
G Triadafilopoulos, *Stanford*
James F Trotter, *Denver*
Chung-Jyi Tsai, *Lexington*
Andrew Ukleja, *Florida*
Hugo E Vargas, *Scottsdale*
Scott A Waldman, *Philadelphia*
Jian-Ying Wang, *Baltimore*
Steven David Wexner, *Weston*
Keith Tucker Wilson, *Baltimore*
Jacqueline L Wolf, *Boston*
Jackie Wood, *Ohio*
George Y Wu, *Farmington*
Jian Wu, *Sacramento*
Samuel Wyllie, *Houston*
Wen Xie, *Pittsburgh*
Yoshio Yamaoka, *Houston*
Vincent W Yang, *Atlanta*
Francis Y Yao, *San Francisco*
Min You, *Tampa*
Zobair M Younossi, *Virginia*
Liqing Yu, *Winston-Salem*
David Yule, *Rochester*
Ruben Zamora, *Pittsburgh*
Michael E Zenilman, *New York*
Zhi Zhong, *Chapel Hill*

Uruguay

Henry Cohen, *Montevideo*

Online Submissions: wjg.wjgnet.com
www.wjgnet.com
wjg@wjgnet.com

World J Gastroenterol 2007 November 21; 13(43): 5673-5681
World Journal of Gastroenterology ISSN 1007-9327

EDITORIAL

Specifically targeted antiviral therapy for hepatitis C virus

Anna Parfieniuk, Jerzy Jaroszewicz, Robert Flisiak

Anna Parfieniuk, Jerzy Jaroszewicz, Robert Flisiak, Department of Infectious Diseases, Medical University of Bialystok, Zurawia St 14, Bialystok 15540, Poland
Correspondence to: Robert Flisiak, Department of Infectious Diseases, Medical University of Bialystok, Zurawia St 14, Bialystok 15540, Poland. flisiakr@priv.onet.pl
Telephone: +48-85-7416921 Fax: +48-85-7416921
Received: June 19, 2007 Revised: July 29, 2007

Abstract

Hepatitis C virus (HCV) infection affects 180 million people worldwide with the predominant prevalence being infection with genotype 1, followed by genotypes 2 and 3. Standard anti-HCV therapy currently aims to enhance natural immune responses to the virus, whereas new therapeutic concepts directly target HCV RNA and viral enzymes or influence host-virus interactions. Novel treatment options now in development are focused on inhibitors of HCV-specific enzymes, NS3 protease and NS5B polymerase. These agents acting in concert represent the concept of specifically targeted antiviral therapy for HCV (STAT-C). STAT-C is an attractive strategy in which the main goal is to increase the effectiveness of antiviral responses across all genotypes, with shorter treatment duration and better tolerability. However, the emergence of resistant mutations that limit the use of these compounds in monotherapy complicates the regimens. Thus, a predictable scenario for HCV treatment in the future will be combinations of drugs with distinct mechanisms of action. For now, it seems that interferon will remain a fundamental component of any new anti-HCV therapeutic regimens in the near future; therefore, there is pressure to develop forms of interferon that are more effective, less toxic, and more convenient than pegylated interferon.

Key words: Hepatitis C virus; Chronic hepatitis C; Polymerase inhibitors; Protease inhibitors; Cyclophilin B inhibitors

Parfieniuk A, Jaroszewicz J, Flisiak R. Specifically targeted antiviral therapy for hepatitis C virus. *World J Gastroenterol* 2007; 13(43): 5673-5681

http://www.wjgnet.com/1007-9327/13/5673.asp

INTRODUCTION

Hepatitis C virus (HCV) infection affects 180 million people worldwide, about 3% of the world's population. Globally, 3-4 million persons are newly infected each year, with the predominant prevalence being infection with genotype 1, followed by genotypes 2 and 3. The other genotypes, 4, 5, and 6, have specific geographical distributions. The acute phase of infection is asymptomatic in the majority of cases, but leads to chronic infection in about 70%-80% of affected individuals[1,2]. This results in progressive liver disease and eventually liver cirrhosis, with increased risk of hepatocellular carcinoma[3].

HCV is an enveloped virus belonging to the Flaviviridae family. The virion consists of an outer envelope composed of E1 and E2 proteins covering the nucleocapsid, with a single-stranded RNA genome (Figure 1). The HCV genome encodes structural proteins that form the capsid and envelope, as well as non-structural proteins required for virus replication. The latter are potential targets for new drugs aimed at directly affecting HCV. The non-structural components include proteases and helicase (NS2, NS3 and NS4A), a protein responsible for anchoring the replication complex to intracytoplasmic membranes (NS4B), the RNA-binding protein (NS5A), and RNA-dependent RNA polymerase (NS5B). After entering the cell, HCV RNA is released into the cytoplasm. The genome is directly translated by host enzymes. The HCV polyprotein is subsequently processed by the host and viral proteases into structural and non-structural proteins, including NS5B, which is crucial for HCV replication. There are two viral proteases, NS2-3 and NS3. NS2-3 is responsible for cleavage at the NS2/3 site. NS3 catalyses cleavage at four sites: NS3/4A, NS4A/B, NS4B/5A and NS5A/B. The proteolytic activity of NS3 protease is significantly enhanced by heterodimerization with its cofactor NS4B[4].

CURRENT TREATMENT OPTIONS

The therapy currently regarded as the standard consists of pegylated interferon injections administered once weekly, along with daily oral ribavirin. This combination exerts synergistic antiviral effects, although it is efficient in only about 50% of treated individuals. The most important predicting factor appears to be the HCV genotype. Sustained viral response (SVR) expressed as an absence of detectable serum HCV RNA 24 wk after completion of therapy is achieved in only 33%-42% of patients with genotype 1, but in about 90% of those with genotypes 2 and 3[5]. There are patients who do not achieve an SVR due to unresponsiveness or relapse after treatment, as well as those who lack tolerance to adverse events that occur during treatment. Therefore, there is a need for new therapeutic strategies with higher efficacy, shorter

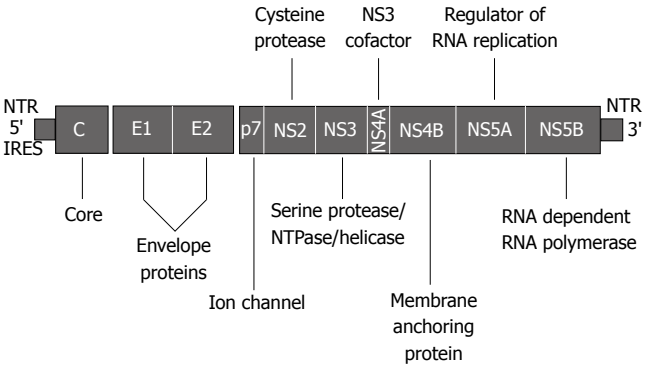

Figure 1 Organization of the HCV genome (adapted from Appel *et al*[4]).

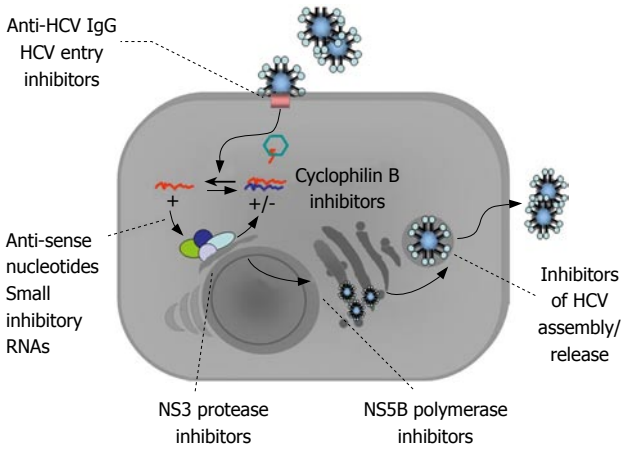

Figure 2 Potential targets for new anti-HCV agents.

treatment duration, convenient routes of administration and favorable side-effect profiles.

The standard anti-HCV therapy currently aims to enhance natural immune responses to the virus; whereas, new therapeutic concepts directly target HCV RNA (anti-sense nucleotides, small inhibitory RNA) and viral enzymes (protease and polymerase inhibitors), or influence host-virus interactions (cyclophilin inhibitors, bavituximab, inhibitors of viral entry) (Figure 2)[6-9]. These findings essentially came from attempts to create an experimental model for studies of the molecular details of the virus and HCV infection of cells. The development of the replicon system and pseudoviruses has greatly contributed to the current knowledge of HCV replication. However, a highlight in recent studies on HCV has been the establishment of a complete cell culture replication system that enables further research into the HCV lifecycle and novel antivirals.

NOVEL ANTIVIRAL AGENTS

Novel treatment options now under intensive development are focused on the inhibitors of HCV-specific enzymes, NS3 protease and NS5B polymerase. The actual protease inhibitors under clinical development are telaprevir and SCH 503034. Among the polymerase inhibitors, several drugs have reached the clinical stage. These include valopicitabine, R1479, HCV-796 and BILB1941. Such agents acting in concert represent the concept of specifically targeted antiviral therapy for HCV (STAT-C). The principle of this new therapeutic strategy is the achievement of higher rates of efficacy, shortened treatment duration, improved tolerability and adherence, oral administration and the possibility for use in special populations (e.g., those with contraindications to interferon). However, the emergence of resistance mutations that limit the use of these compounds in monotherapy complicates the regimens. Thus, a predictable scenario for treatment of HCV in the future will be combinations of drugs with distinct mechanisms of action. Interferon, however, appears pivotal for any new therapeutic regimens.

INTERFERONS IN DEVELOPMENT

Pegylated interferon underpins the current standard of care therapy for HCV. Its immunomodulatory activities with positive pharmacokinetics significantly improve the efficacy of anti-HCV regiments, although the effectiveness of antiviral treatment remains unsatisfactory, especially as regards genotype-1 infections. Another limitation is the frequent occurrence of adverse events, which greatly influence adherence to the treatment regimen. Therefore, there is pressure to develop forms of interferon that are more effective, less toxic, and more convenient than pegylated interferon. Phase 1 clinical trials are in progress with oral forms of interferon (Belerofon; oral interferon alpha). Another goal in the field of interferon development is to obtain forms with a longer half life, which will allow a reduction in the number of injections required and lengthen the period between injections. These agents [IL-29 (PEG-interferon lambda), Belerofon Interferon (long-acting), BLX-883 (Locteron), and Medusa Interferon (Multiferon)] are mostly in the first or second phase of their clinical development. Omega interferon, which is in phase Ⅱ development, is used in an implantable infusion pump that releases a steady amount of interferon for about 1 mo[10]. Albinterferon (IFN-α2b genetically fused to human albumin) and interferon β-1a (REBIF) have reached phase Ⅲ development. Albinterferon is a protein that combines the antiviral properties of IFN-α2b with the prolonged half-life of human serum albumin. Clinical trials have shown that albinterferon administered every 2 wk exerts an antiviral efficacy comparable to that of Peg-IFN-α2a, with a similar frequency of occurrence of adverse events and laboratory abnormalities[11]. Consensus interferon (Infergen) administered daily is currently in phase Ⅳ clinical trials, and research evaluating its usefulness in treatment of prior non-responders is ongoing, with promising interim results[12,13].

PROTEASE INHIBITORS

Telaprevir (VX-950), an investigational oral selective inhibitor of HCV NS3/4A protease[14], appears to be the one of most advanced therapeutic agents that specifically target the HCV lifecycle. Clinical phase Ⅱb studies utilizing VX-950 are ongoing. These include the PROVE

1 and PROVE 2 trials that have enrolled 260 and 320 treatment-naïve HCV genotype 1 patients, respectively, and the PROVE 3 study in patients with HCV genotype 1, previously treated by standard of care therapy (at least one prior course of peginterferon with ribavirin).

The phase Ⅰb studies showed that VX-950 had potent anti-HCV activity in monotherapy, which led to a rapid decline in HCV RNA of about 3 log within 3 d in all dosage groups (450 mg q8h, 750 mg q8h and 1250 mg q12h), both in genotype 1 treatment-naïve patients and non-responders to prior treatment. In the optimal dose group, 750mg q8h, the highest plasma concentration was achieved with a 4.4 log reduction in HCV RNA load at d 14. When sub-optimal doses were applied, maximal HCV RNA reduction was seen after 3-7 d treatment, with any following increase in viral load being related to the selection of HCV variants less sensitive to VX-950[15,16]. Moreover, other studies have reported that the abovementioned HCV RNA fluctuations, as well as alanine aminotransferase (ALT) levels during treatment correlated with the concentration of neopterin - a monocyte/macrophage-derived factor that can be considered an indicator of inflammatory activity during the course of chronic C hepatitis[17,18]. Furthermore, the ultrasound evaluation of perihepatic lymph nodes (PLNs) in HCV-infected individuals undergoing treatment with telaprevir alone showed a significant reduction in PLN volume after 14 d therapy. This suggests that VX-950 may have the ability to reduce inflammatory activity in liver tissue; however, this research is limited by a lack of objective parameters for inflammatory activity, such as histopathological evaluation[19].

The HCV NS3 protease diversity determined before administration of VX-950 appears to have no predictive impact for the effectiveness of antiviral responses[20]. Whereas, identification of HCV NS3 protease variants after 14 d treatment demonstrates the emergence of mutations that implicate varying decreases in sensitivity to VX-950, low-level resistance characterized by V36A/M, T54A, R155K/T, and A156S mutations, and high-level resistance determined by the emergence of A156V/T, V36A/M-R155K/T, and V36A/M-A156V/T variants. Each dosage group has a distinct mutation pattern that results from the different levels of drug pressure on the variants selected. It has been suggested that these drug-resistant variants pre-exist at a minimal frequency before the introduction of treatment, because of the low fidelity of HCV polymerase and the high rate of HCV replication. Resistant variants appear to be less fit and have lower replication rates compared to wild type; therefore, they may not be detected prior to treatment[21,22].

Further studies of VX-950 administered with peginterferon, with or without ribavirin, have confirmed the advantageous effect of combination therapy on virus selection. Data presented at the American Association for the Study of Liver Diseases (AASLD) Meeting in 2006 demonstrated a 5.5 log HCV RNA drop when VX-950 was combined with peginterferon α2a *vs* a 1 log drop in those receiving peginterferon alone, and a 4 log decrease in monotherapy with VX-950 at d 14 of the study[23]. With regard to selection of the resistant variant, this study provides evidence of the suppressing effect of peginterferon when it is included in a combination therapy regimen, or is applied as a follow-on after discontinuation of VX-950, thus indicating that VX-950-resistant variants remain sensitive to the standard care therapy. This observation is consistent with *in vitro* research confirming the decreased replication capacity of resistant variants while the sensitivity to interferon is fully retained[22]. Interestingly, in a few patients receiving VX-950 alone, the higher level resistant variant A156V/T emerged, but was subsequently suppressed by therapy with VX-950 followed by peginterferon and ribavirin. In this study, all patients receiving peginterferon and ribavirin subsequent to 14 d treatment with VX-950 had undetectable HCV RNA at the end of wk 24. However, the discontinuation of therapy at that point in individuals with undetectable HCV RNA at wk 12, resulted in relapses in two of the four patients from the VX-950 monotherapy group, and one of six from the VX-950 with peginterferon group, which showed the advantages of combination therapy over monotherapy[23,24]. The interim results after 12 wk of the PROVE 1 study, the first major phase Ⅱ clinical trial to evaluate VX-950, are now available. Analysis shows a definitely higher incidence of undetectable HCV RNA [limit of detection (LOD) 10 IU/mL] at wk 12 in patients receiving VX-950 in combination with peginterferon and ribavirin, in contrast to those receiving standard therapy (88% *vs* 52%). The frequency of adverse events was comparable in the telaprevir-treated and control groups. However, discontinuation due to adverse events was higher in the telaprevir than in the control groups, 9% *vs* 3%. The adverse events most frequently reported in the telaprevir group included rashes (3%), gastrointestinal disorders and anemia. The incidence of serious adverse events in the telaprevir groups was about 3% compared to 1% in the control[25]. Further research on telaprevir that aimed to assess its activity against the NS3/4A proteases of HCV genotypes 2, 3 and 4 was presented at the European Association for the Study of the Liver (EASL) Meeting in 2007. *In vitro* studies have demonstrated that the VX-950 activity against genotypes 2a, 2b, 3a and 4a is similar to that for genotypes 1a or 1b. Moreover, NS3/4A protease heterogeneity seems to have an unremarkable impact on VX-950 suppressive activity. Hence, it has been suggested that the majority of genotype-specific polymorphic sequences are located peripherally to the active sites of HCV protease, and do not affect binding of the agent molecule[26]. This investigation confirms the necessity for further research in this subject area. By contrast to the above are observations of telaprevir activity in a liver biopsy model of HCV infection. Cell cultures from liver biopsies of patients with genotype 1 and non-genotype 1 HCV were exposed to VX-950, which resulted in a significant decrease in HCV genotype 1 RNA, but only a minimal effect in non-genotype 1 HCV[27]. Thus further studies are required.

Another HCV protease inhibitor, SCH 503034, orally bioavailable with satisfactory pharmacokinetics and a good safety profile, is being tested in a phase Ⅱ clinical trial[28]. *In vitro* studies have determined its anti-viral activity on its

own, and an additive effect in combination with interferon α-2b[29,30]. Monotherapy with SCH 503034, at a dose of 400 mg q8h, in HCV-genotype-1-infected non-responders to prior standard therapy resulted in a 2.06 log reduction of the mean maximum viral load during the 14 d period of observation. Moreover, the HCV RNA decline correlated with ALT activity, and both of these parameters appeared to be dose-dependent. It is important to mention that the frequency of adverse events was comparable to the control group receiving a placebo[31]. Similar to telaprevir, further research into combination therapy with SCH 503034 and peginterferon has shown advantages over monotherapy with SCH 503034 or peginterferon. The mean maximum HCV RNA decline was dose-dependent, 2.4 log and 2.9 log for 200 mg q8h and 400 mg q8h, respectively, of SCH 503034 with peginterferon[32]. Another study designed to evaluate the antiviral effects of a combination of an NS3 protease inhibitor with a polymerase inhibitor strongly supports the concept of STAT-C. In this research, genotype 1b HCV replicon cells, wild-type, as well as replicons with reduced susceptibility to protease inhibitors or polymerase inhibitors, were exposed to a combination of SCH 503034 with the polymerase inhibitor HCV-796. The results were encouraging; the antiviral effect of these two agents was additive, with a favorable cross-resistance profile. Furthermore, the emergence of resistant viral variants was less frequent compared to that for monotherapy[33].

ITMN-191, a novel agent with a high genetic barrier to emergence of resistance mutations, is in preclinical development and has been shown to retain significant potency against variants with decreased sensitivity to other protease inhibitors[34]. Other *in vitro* studies have shown that ITMN-191 displays synergistic antiviral activity in combination with interferon[35,36], as well as HCV polymerase inhibitor R1479[37].

Recently, the clinical trials for BILB2061, another specific and potent inhibitor of HCV NS3 protease, were halted due to drug-induced cardiotoxicity[38].

ACH-806 is a novel anti-HCV agent, currently in phase Ⅰ/Ⅱ clinical studies, which has a distinct mechanism of action. Preclinical data have demonstrated that ACH-806 inhibits HCV genotype 1 replication *via* binding to NS4A and consequently blocks the formation of HCV replication complexes[39]. Resistance induction studies in replicon cells have shown a lack of cross resistance between ACH-806 and protease or polymerase inhibitors; thus confirming its different mode of action. Interestingly, viral quasispecies resistant to protease or polymerase inhibitors remain sensitive to ACH-806 and vice versa[40]. *In vitro* studies of a combination of ACH-806 with telaprevir or valopicitabine or interferon have demonstrated potent antiviral effects, which are synergistic when cells are exposed to ACH-806 with telaprevir or ACH-806 with valopicitabine. Hence the authors have concluded that ACH-806 could in the future become a potent component of STAT-C. Clinical studies preformed on genotype 1 HCV-infected subjects have shown an ~ 1 log reduction in HCV RNA at d 5. Further research on ACH-806 has been limited because of reversible nephrotoxicity reported in a clinical trial[41].

POLYMERASE INHIBITORS

The inhibitors of HCV NS5B polymerase influence different steps in RNA synthesis, from initiation to elongation through binding to the enzyme's active sites. Valopicitabine (NM283) appears the most advanced orally bioavailable pro-drug of a ribonucleoside analogue that displays an ability to sufficiently inhibit HCV NS5B polymerase. It is currently in phase Ⅱ clinical development. It has been shown that NM283 given as monotherapy exhibits significant, dose-related antiviral activity in both treatment-naïve and non-responders to prior interferon therapy. This effect was marked and synergistic, with a mean HCV RNA reduction of 2.7 log at d 28 when NM283 was administered in combination with peginterferon[42]. Studies in genotype 1 HCV-infected treatment-naïve patients showed an intense HCV RNA decline of about 4 log at wk 24 when NM283 was included in the regimen[43]. However evaluation of the side effects, mainly gastrointestinal and hematological disorders at higher doses, resulted in revision of the dosages. Interestingly, at higher doses, NM283 developed superior rapid response rates, although after 12, 24 and 36 wk of treatment the results were similar in all the different dose groups. Hence, low-dose NM283 in combination with peginterferon seems to display marked antiviral effects with fewer adverse events[43,44]. Moreover, there are promising results of *in vitro* research into the efficacy of NM283 against HCV variants resistant to protease inhibitors. All mutations tested conferring resistance to protease inhibitors were sensitive to NM283, thus supporting the advantages of combination therapy. As well, only a single mutation (S282T), described in the highly conserved B domain of NS5B, has so far been identified as determining moderate resistance to NM283[45]. In a separate study, a combination of two agents with distinct mechanisms of action, NM283 and SCH 503034, revealed enhanced anti-replicon activity, without observed cross-resistance[46]. These data support the initiative to develop combination regimens for treatment of HCV infections.

Other polymerase inhibitors currently in clinical development are nucleoside analogue R1479 (prodrug R1626) and non-nucleoside analogues HCV-796 and BILB1941. In phase I trials, R1626 has been shown to induce the greatest viral load reduction in genotype 1 HCV-infected patients, so far reported among this class of antiviral agents. It was a 3.7 log mean HCV RNA decline for 4500 mg q12h at d 14, and a 2.6 log decline for the lower dose of 3000 mg q12h, but with better tolerability[47]. *In vitro* analysis of the antiviral effects exerted by combinations of R1479 with interferon or ribavirin have demonstrated synergistic effects, whereas with other direct antivirals the effects were additive[48]. Another compound, HCV-796, when utilized in monotherapy exhibited dose-related anti-HCV activity across multiple genotypes, and with a good tolerability profile. Although, a selection of variants with reduced susceptibility was observed, they retained sensitivity to

interferon[49]. Associated studies of combined HCV-796 and peginterferon have confirmed the increased antiviral response to therapy, which was more intense in non-genotype 1 HCV[50]. In a clinical evaluation, polymerase inhibitor BILB 1941 showed anti-HCV activity; however, a high discontinuation rate due to adverse events within the group with appropriate pharmacokinetics was observed[51].

Several novel compounds are now being tested in preclinical trials; these include PSI-6130, GSK 625433, A-848837, A-837093 and AG-021541[52-56]. Additional studies should determine whether these polymerase inhibitors reach a clinical development stage in the future.

CYCLOPHILIN INHIBITORS

The favorable complementary elements of various prospective therapies seem to be the cyclophilin inhibitors, which exhibit peculiar mechanisms of action based on targeting of virus-host interactions. Cyclophilin B (Cyp B) has been shown to serve as a cellular cofactor of the NS5B RNA-dependent RNA polymerase that promotes HCV replication[57,58]. Thus the blocking of Cyp B appears to be an attractive target for the development of new anti-HCV agents[59-61]. The first compound shown to exhibit inhibitory properties with reference to cyclophilins was cyclosporin A (CsA)[60-62]. It was shown that its antiviral activity against HCV was distinct from its immunosuppressive function, which was dependent on anti-calcineurin activity[60-63]. Clinical studies on a regimen based on a combination of CsA with interferon-α demonstrated a high antiviral potency compared to that with interferon alone[63]. However, the immunosuppressive function of CsA limits its usefulness in anti-HCV therapy. Moreover, there are various opinions regarding the benefits of administering CsA *vs* tacrolimus in post-liver transplantation management of individuals with HCV infection[64,65]. The available data are limited, and the results are equivocal[66,67]. Thus, further studies are required in this area.

The first synthesized CsA derivate found to be devoid of immunosuppressive activity was NIM811. It has been investigated in regard to its anti-HIV inhibitory features[68,69]. Recent studies have confirmed its anti-HCV activity *in vitro*. The reduction of HCV RNA in replicon cells was more potent, even at low concentrations, compared to CsA. Moreover, NIM811 shows activity against HCV in replicons with high resistance to protease or polymerase inhibitors. Also, combinations of NIM811 with other groups of HCV inhibitors display at least additive effects[71]. Analogous results, with potentially synergistic effects, have been obtained when HCV replicon cells were exposed to a combination of NIM811 with interferon-α[72]. The anti-HCV activity of NIM-811 exerted at low drug concentrations infers reduced potential side effects from the therapy. Hence, *in vivo* evaluations of the safety profile, pharmacokinetics and anti-HCV activity need to be undertaken.

The first oral non-immunosuppressive cyclophilin B inhibitor, Debio 025, to enter into clinical trials displayed potent antiviral effects in chimeric mice, and the effect was enhanced in combination with pegylated interferon[72]. *In vitro* studies have demonstrated that Debio 025 has a unique potency for clearing HCV replicon cells of virus when used alone or in combination with other antivirals. The combination of Debio 025 with interferon α-2a results in additive to slightly synergistic antiviral effects. Resistant replicon cells, selected by passage in increasing concentrations of Debio 025, are sensitive to protease or polymerase inhibitors and interferon[73]. Moreover, Debio 025 exerts antiviral activity against wild-type HCV, as well as HCV replicons resistant to protease or polymerase inhibitors. The emergence of resistant variants to protease inhibitors (VX-950, BILB 2061) is restrained by the presence of Debio 025[74]. Clinical research shows that Debio 025 exerts both anti-HIV and anti-HCV activity in HIV/HCV co-infected subjects. The anti-HIV effect at d 15 was a 1 log decrease in viral load when the dose was 1200 mg q12h. HCV viremia decline was more profound, reaching 3.6 log at d 15. However, at this dose, transitional hyperbilirubinemia led to the discontinuation of treatment in some patients[6]. Debio 025 has been shown to exert anti-HCV activity in both genotype 1 and non-genotype 1 infections. Interestingly, no signals of emerging mutation appeared during the period of observation, which suggests a possible ability for this agent to suppress selection of resistant variants[75].

Recently the novel non-immunosuppressive CsA derivate, SCY-635, has been evaluated in preclinical studies that have demonstrated its favorable properties as an anti-HCV agent. Compared to CsA, this compound has good affinity with cyclophilin, and exerts potent antiviral activity with suitable pharmacokinetics and lower cytotoxicity. The combination of SCY-635 with interferon-α has antiviral effects on HCV replicon cells that range form additive to synergistic; thus supporting the need for more evaluations of this drug in anti-HCV treatment options[7].

CONCLUSION

Specifically targeted antiviral therapy, through interference in the replication cycle, leads to the selection of resistant variants[76-78]. This observation has been confirmed in several studies focusing on STAT-C agents as used in monotherapy. Combination therapy displays higher antiviral efficacy and has a fundamental impact on the selection of HCV strains with concomitantly reduced sensitivity and decreased viral fitness. It has also been shown that protease and polymerase inhibitors demonstrate advantageous cross-resistance profiles with improved anti-HCV activity, which supports the STAT-C development initiatives. Interestingly, the introduction of interferon to regimens based on novel compounds not only augments antiviral effects, but has a strong suppressive activity against the emergence of resistant mutations. Considering this, it is seems unlikely that interferon will be eliminated from antiviral regimens in the near future.

STAT-C presents an attractive strategy, one in which the main goal is to increase the effectiveness of antiviral responses across all genotypes, with shorter

Table 1 Anti-HCV agents currently under clinical development

Compound		Clinical advancement nt	Viral efficacy	Resistance (HCV resistant variants)	Remarks
Protease inhibitors	Telaprevir	Ⅱ	(dose-750 mg q8h; genotype-1)	Low level: V36A/M, T54A, R155K/T, A156S	Rash, GI and hematological adverse events (AE)
	(VX-950)	PROVE-1, 2, 3	VLR = 3 log d 3 VLR = 4.4 log: d 14 VLR = 5.5 log: d 14 when combined with PEG-IFNa2a	High level: A156V/T, V36A/M-R155K/T, V36A/M-A156V/T; After 14 d of treatment	
	SCH 503034	Ⅱ	(dose 400 mg q8h; genotype-1) VLR = 2.06 log d 14 VLR = 2.9 log: when combined with PEG-IFN	Low to moderate levels: V170A T54A A156S High level: A156T	Frequency of AE comparable to control group receiving placebo
Inhibitor of protease cofactor NS4A	ACH-806	Ⅰ / Ⅱ	VLR = 1 log: d 5	Single mutation at N-terminus of NS3; lack of cross resistance to any of the polymerase inhibitors or protease inhibitors now under development	Reversible nephrotoxicity
Polymerase inhibitors	Valopicitabine (NM283)	Ⅱ	VLR = 0.8 log: d 28 VLR = 2.7 log: d 28, when combined with PEG-IFN VLR = 4.24 log: wk 24, when combined with PEG-IFN	S282T	GI and hematological AE
	R1479 (R1626)	Ⅱ	VLR = 3.7 log for 4500 mg q12h at d 14, VLR = 2.6 log for 3000 mg q12h	no data	Mild to moderate hematological AE with increasing doses
	HCV-796	Ⅱ	VLR = 1.4-1.5 log: d 4 VLR = 3.3-3.5 log: d 14, when combined with PEG-IFN	C316Y	Mild to moderate headache-the most frequent AE; no treatment-emergent serious AE
	BILB 1941	Ⅰ	Data incomplete due to high discontinuation rate	No data	GI AE
Cyclophilin inhibitors	DEBIO 025	Ⅰ	VLR = 3.6 log: d 14 of monotherapy	No breakthrough during the treatment	Transitional hyperbilirubinemia

treatment duration and better tolerability. Recent studies have shown that these aims are within reach. Novel therapeutic agents are already in advanced clinical development; listed here in Table 1. Although there are many limitations pertaining to the STAT-C strategy; including variable bioavailability, and different effects exerted against various HCV genotypes and even quasispecies. A disadvantage of direct interference in the virus replication cycle is the increased rate of resistant mutations, but this could be ameliorated by the use of multiply agents with different mechanisms of actions. In combination with interferon, these drugs could augment antiviral effects and reduce some of the toxic side effects of this cytokine. On the other hand, the toxicity of new agents needs to be carefully evaluated, along with their pharmacokinetics, safety and effective doses. New regimens will also need to be worked out. Currently, it appears that interferon will remain as an element of anti-HCV therapy in the near future; indeed its effectiveness could be elevated by the introduction of new drugs.

REFERENCES

1 **Hepatitis C--global prevalence (update)**. *Wkly Epidemiol Rec* 2000; **75**: 18-19

2 **Barrera JM**, Bruguera M, Ercilla MG, Gil C, Celis R, Gil MP, del Valle Onorato M, Rodés J, Ordinas A. Persistent hepatitis C viremia after acute self-limiting posttransfusion hepatitis C. *Hepatology* 1995; **21**: 639-644

3 **Alter HJ**. HCV natural history: the retrospective and prospective in perspective. *J Hepatol* 2005; **43**: 550-552

4 **Appel N**, Schaller T, Penin F, Bartenschlager R. From structure to function: new insights into hepatitis C virus RNA replication. *J Biol Chem* 2006; **281**: 9833-9836

5 **Fried MW**, Shiffman ML, Reddy KR, Smith C, Marinos G, Gonçales FL, Häussinger D, Diago M, Carosi G, Dhumeaux D, Craxi A, Lin A, Hoffman J, Yu J. Peginterferon alfa-2a plus ribavirin for chronic hepatitis C virus infection. *N Engl J Med* 2002; **347**: 975-982

6 **Flisiak R**, Horban A, Kierkus J, Stanczak J, Cielniak I, Stanczak GP, Wiercinska-Drapalo A, Siwak E, Higersberger J, Aeschlimann C, Grosgurin P, Nicolas V, Durmont JM, Porchet H, Crabbe R, Scalfaro P. The cyclophilin inhibitor DEBIO-025 has a potent dual anti-HCV activity in treatment-naive HIV/HCV co-infected subjects. *Hepatology* 2006; **44** Suppl 1: S609

7 **Houck DR**. Preclinical evaluation of SCY-635, a cyclophilin inhibitor with potent anti-HCV activity. *Hepatology* 2006; **44**

Suppl 1: S534
8 **Godofsky EW**, Shan JS. Phase I single-dose study of bavituximab, a chimeric anti-phosphatidyl serine monoclonal antibody, in subjects with chronic hepatitis C. *Hepatology* 2006; **44** Suppl 1: S236
9 **Matsumura T**, Kato T, Hu Z, Juteau JM, Vaillant A, Liang JT. A novel class of amphipathic DNA polymers inhibits hepatitis C virus infection by blocking viral entry. *Hepatology* 2006; **44** Suppl 1: S693
10 **Novozhenov V**, Zakharova N, Vinogradova E, Nikiton I, Gorbakov V, Yakovlev A, Pak S, Rafalski V, Bogomolov P, Alessi T, Blanchett D, Lang W, Lengecker P, McNally J, McHutchison J. Phase 2 study of omega interferon alone or in combination with ribavirin in subjects with chronic hepatitis C genotype-1 infection. *J Hepatol* 2007; **46** Suppl 1: S8
11 **Zeuzem S**, Benhamou Y, Bain V, Shouval D, Pianko S, Flisiak R, Grigorescu M, Rehak V, Yoshida E, Kaita K, Cronin P, Pulkstenis E, Subramanian M. Antiviral response at week 12 following completion of treatment with albinterferon α-2b plus ribavirin in genotype-1, IFN-naive, chronic hepatitis C patients. *J Hepatol* 2007; **46** Suppl 1: S293
12 **Chen K**, Seraphin P, Murphy L, Shah N. Consensus interferon and ribavirin in patients with chronic hepatitis C who were nonresponders to prior therapy with either interferon alpha and ribavirin or pegylated interferon and ribavirin. *J Hepatol* 2005; **42** Suppl 1: S670
13 **Ghalib R**, Levine C, Mouti M, Weinstein J, Schwartz A, Cheng S. Early viral response to consensus interferon plus ribavirin therapy in patients who are nonresponders or relapsers to prior PEG IFN plus ribavirin therapy. *Hepatology* 2005; **42** Suppl 1: S686
14 **Perni RB**, Almquist SJ, Byrn RA, Chandorkar G, Chaturvedi PR, Courtney LF, Decker CJ, Dinehart K, Gates CA, Harbeson SL, Heiser A, Kalkeri G, Kolaczkowski E, Lin K, Luong YP, Rao BG, Taylor WP, Thomson JA, Tung RD, Wei Y, Kwong AD, Lin C. Preclinical profile of VX-950, a potent, selective, and orally bioavailable inhibitor of hepatitis C virus NS3-4A serine protease. *Antimicrob Agents Chemother* 2006; **50**: 899-909
15 **Reesink HW**, Zeuzem S, Weegink CJ, Forestier N, Vliet A, Wetering de Rooij J, McNair L, Purdy S, H.M. C, Jansen PL. Final result of a phase 1b, multiple-dose study of VX-950, a hepatitis C virus protease inhibitor. *Hepatology* 2005; **42** Suppl 1: S234
16 **Reesink HW**, Zeuzem S, Weegink CJ, Forestier N, van Vliet A, van de Wetering de Rooij J, McNair L, Purdy S, Kauffman R, Alam J, Jansen PL. Rapid decline of viral RNA in hepatitis C patients treated with VX-950: a phase Ib, placebo-controlled, randomized study. *Gastroenterology* 2006; **131**: 997-1002
17 **Gelderblom HC**, Zeuzem S, Weegink CJ, Forestier N, McNair L, Purdy S, Jansen PL, Reesink H. Decline in serum neopterin concentration correlated with HCV RNA decline during administration of VX-950, a hepatitis C virus protease inhibitor. *Hepatology* 2005; **42** Suppl 1: S533
18 **Gelderblom HC**, Zeuzem S, Weegink CJ, Forestier N, McNair L, Purdy S, Jansen PL, Reesink H. Neopterin and ALT as markers of inflammation in chronic hepatitis C patients during administration of the HCV NS3-4A protease inhibitor telaprevir (VX-950) in combination with peginterferon alpha 2a. *J Hepatol* 2007; **46** Suppl 1: S225
19 **Friedrich-Rust M**, Forestier N, Sarrazin C, Reesink H, Herrmann E, Zeuzem S. Ultrasound evaluation of perihepatic lymph nodes during antiviral therapy with the protease inhibitor telaprevir (VX-950) in patients with chronic hepatitis C infection. *J Hepatol* 2007; **46** Suppl 1: S205
20 **Kieffer T**, Sarrazin C, Bartels D, Muh U, Welker M, Lin C, Grossman T, Weegink CJ, Purdy S, Reesink H, Kwong AD, Zeuzem S. Genetic heterogeneity in the HCV NS3 protease of untreated genotype 1 patients has little effect on the sensitivity to VX-950. *Hepatology* 2005; **42** Suppl 1: S537
21 **Sarrazin C**, Kieffer T, Bartels D, Hanzelka B, Muh U, Welker M, Wincheringer D, Lin C, Grossman T, Purdy S, Weegink CJ, Reesink H, Zeuzem S, Kwong AD. Characterization of viral variants in the HCV NS3 protease domain of genotype 1 in patients that are selected during 14 days of dosing with VX-950. *Hepatology* 2005; **42** Suppl 1: S751
22 **Chu HM**, Zhou Y, Bartels D, Khunvichai A, Rao BG, Kwong AD, Lin C. Telaprevir (VX-950)-resistant variants exhibit reduced replication capacity compared to wild-type HCV in vivo and in vitro. *J Hepatol* 2007; **46** Suppl 1: S230
23 **Kieffer T**, Sarrazin C, Miller J, Traver S, Zhou Y, Bartels D, Hanzelka B, Muh U, Lin C, Reesink H, Kwong AD, Zeuzem S. Combination of telaprevir (VX-950) and Peg-INF alpha suppresses both wild type virus and resistance variants in HCV genotype 1-infected patients in a 14-day phase 1b study. *Hepatology* 2006; **44** Suppl 1: S222
24 **Forestier N**, Weegink CJ, Purdy S, McNair L, Jansen PL, Zeuzem S, Reesink H. Current status of subjects receiving peginterferon-alfa-2a (Peg-IFN) and ribavirin (RBV) after a 14-day study of the hepatitis C protease inhibitor telaprevir (VX-950), with Peg-IFN. *Hepatology* 2006; **44** Suppl 1: S614
25 **McHutchison JG**, Everson GT, Gordon S, Jacobson I, Kauffman R, McNair L, Muir A. Results of an interim analysis of a phase 2 study of telaprevir (VX-950) with peginterferon alfa-2a and ribavirin in previously untreated subjects with hepatitis C. *J Hepatol* 2007; **46** Suppl 1: S296
26 **Lin C**, Hanzelka B, Muh U, Kovari L, Bartels D, Tigges AM, Miller J, Rao BG, Kwong AD. Telaprevir (VX-950) is a potent inhibitor of HCV NS3 proteases derived from genotype non-1 HCV-infected patients. *J Hepatol* 2007; **46** Suppl 1: S8
27 **Hibbert L**, Foster GR. Effects of telaprevir (VX950) in a liver biopsy model of HCV infection: genotype-1 virions are inhibited in vitro but other genotypes are less responsive. *J Hepatol* 2007; **46** Suppl 1: S227
28 **Preston RA**, Alonso AB, Feely W, Gupta S, Deckman D, Marchisin D, Kantesaria B, Hughes E. SCH 503034, an oral HCV protease inhibitor, is well-tolerated in patients with varying degrees of hepatic impairment. *J Hepatol* 2007; **46** Suppl 1: S207
29 **Malcolm BA**, Arasappan A, Bennett F, Bogen SL, Chase R, Chen K, Chen T, Ingravallo P, Jao E, Kong J, Lahser F, Liu R, Liu YT, Lovey R, McCormick J, Njoroge FG, Saksana A, Skelton A, Tong X, Venkatraman S, Wright-Minogue J, Xia E, Girijavallabhan V. SCH 503034, a mechanism-based inhibitor of hepatitis C virus (HCV) NS3 protease suppresses polyprotein maturation and enhances the antiviral activity of alpha interferon-a-2b (INF). *Hepatology* 2005; **42** Suppl 1: S535
30 **Malcolm BA**, Liu R, Lahser F, Agrawal S, Belanger B, Butkiewicz N, Chase R, Gheyas F, Hart A, Hesk D, Ingravallo P, Jiang C, Kong R, Lu J, Pichardo J, Prongay A, Skelton A, Tong X, Venkatraman S, Xia E, Girijavallabhan V, Njoroge FG. SCH 503034, a mechanism-based inhibitor of hepatitis C virus NS3 protease, suppresses polyprotein maturation and enhances the antiviral activity of alpha interferon in replicon cells. *Antimicrob Agents Chemother* 2006; **50**: 1013-1020
31 **Zeuzem S**, Sarrazin C, Rouzier R, Tarral A, Brion N, Forestier N, Gupta S, Deckman D, Fellows K, Hussain M, Cutler D, Zhang J. Anti-viral activity of SCH 503034, a HCV protease inhibitor, administered as monotherapy in hepatitis C genotype-1 (HCV-1) patients refractory to pegylated interferon (Peg-IFN-alpha). *Hepatology* 2005; **42** Suppl 1: 233A
32 **Zeuzem S**, Sarrazin C, Wagner F, Rouzier R, Forestier N, Gupta S, Hussain M, Shah A, Cutler D, Zhang J. Combination therapy with the HCV protease inhibitor, SCH 503034, plus Peg-Intron in hepatitis C genotype-1 Peg-Intron non-responders: phase 1b results. *Hepatology* 2005; **42** Suppl 1: 276A
33 **Howe AY**, Ralston R, Chase R, Tong X, Skelton A, Flint M, Mullen S, Broom C, Emini EA. Favourable cross-resistance profile of two novel hepatitis C virus inhibitors, SCH-503034 and HCV-796, and enhanced anti-replicon activity mediated by the combined use of both compounds. *J Hepatol* 2007; **46** Suppl 1: S165
34 **Seiwert SD**, Hong J, Lim SR, Wang T, Tan H, Blatt LM. Sequence variation of NS3/4A in HCV replicons exposed to ITMN-191 concentrations encompassing those likely to be achieved following clinical dosing. *J Hepatol* 2007; **46** Suppl 1: S244

35 **Tan H**, Seiwert SD, Blatt LM. In vitro synergistic antiviral activity of ITMN-191, an orally active inhibitor of the hepatitis C virus (HCV) NS3/4A protease, in combination with Peg-Interferon alfa-2a. *Hepatology* 2006; **44** Suppl 1: 534A

36 **Blatt LM**, Tan H, Seiwert SD. ITMN-191 concentrations achieved in the liver of animals promote HCV replicon clearance in vitro and this effect is enhanced by Peg-IFN alpha-2a. *J Hepatol* 2007; **46** Suppl 1: S219

37 **Seiwert SD**, Tan H, Blatt LM. Additive to synergistic antiviral effects of an NS3/4A protease inhibitor (ITMN-191) and an NS5B RNA-dependent RNA polymerase inhibitor (R1479) in an HCV replicon system. *J Hepatol* 2007; **46** Suppl 1: S167

38 **Hinrichsen H**, Benhamou Y, Wedemeyer H, Reiser M, Sentjens RE, Calleja JL, Forns X, Erhardt A, Cronlein J, Chaves RL, Yong CL, Nehmiz G, Steinmann GG. Short-term antiviral efficacy of BILN 2061, a hepatitis C virus serine protease inhibitor, in hepatitis C genotype 1 patients. *Gastroenterology* 2004; **127**: 1347-1355

39 **Huang M**, Sun Y, Yang W, Hou H, Fabrycki J, Nie X, Sanchez A, Zhao Y, Phadke A. ACH-806: a potent inhibitor of HCV replication with a novel mechanism of action. *J Hepatol* 2007; **46** Suppl 1: S221

40 **Yang W**, Zhao Y, Fabrycki J, Hou X, Nie X, Sun Y, Phadke A, Agarwal A, Deshpande M, Huang M. Induction of resistance by a novel class of compounds active against hepatitis C virus with no cross-resistance to NS3 protease and NS5B polymerase inhibitors. *Hepatology* 2006; **44** Suppl 1: S536

41 **Pottage JCJ**, Lawitz E, Mazur D, Wyles D, Vargas H, Ghalib R, Gugliotti R, Donohue M, Robison H. Short-term antiviral activity and safety of ACH-806 (GS-9132), an NS4A antagonist, in HCV genotype 1 infected individuals. *J Hepatol* 2007; **46** Suppl 1: S294

42 **O'Brien C**, Godofsky EW, Rodriguez-Torres M, Afdhal N, Pockros P, Lawitz E, Bzowej N, Rustgi V, Sulkowski M, Sherman K, Jacobson I, Chao G, Knox S, Pietropaolo K, Brown NA. Randomized trial of valopicitabine (NM283) alone or with peg-interferon, vs. retreatment with peg-interferon plus ribavirin (PEGIFN/RBV) in hepatitis C patients with previous non-response to PEGIFN/RBV: first interim results. *Hepatology* 2005; **42** Suppl 1: S234

43 **Lawitz E**, Nguyen TT, Younes Z, Santoro J, Gitlin N, McEniry D, Chasen R, Goff J, Dieterich D, Knox S, Kleber K, Belanger B, Brown NA. Clearance of HCV RNA with valopicitabine (NM283) plus peg-interferon in treatment-naive patients with HCV-1 infection: results at 24 and 48 weeks. *J Hepatol* 2007; **46** Suppl 1: S9

44 **Lawitz E**, Nguyen TT, Younes Z, Santoro J, Gitlin N, McEniry D, Chasen R, Goff J, Knox S, Kleber K, Belanger B, Brown NA, Dieterich D. Valopicitabine (NM283) plus peg-interferon in treatment-naive hepatitis C treatment-naive hepatitis C patients with HCV genotype-1 infection: HCV RNA clearance during 24 weeks of treatment. *Hepatology* 2006; **44** Suppl 1: S223

45 **Bichko V**, Lallos L, Soubasakos M, LaColla M, Tausek MM, Gillum J, Standring DN. Valopicitabine (NM283) is fully active against known HCV protease resistance mutations in vitro. *J Hepatol* 2007; **46** Suppl 1: S163

46 **Ralston R**, Bichko V, Chase R, LaColla M, Lallos L, Skelton A, Soubasakos M, Tausek M, Tong X, Standring D. Combination of two hepatitis C virus inhibitors, SCH 503034 and NM107, provides enhanced anti-replicon activity and suppresses emergence of resistant replicons. *J Hepatol* 2007; **46** Suppl 1: S298

47 **Roberts S**, Cooksley G, Dore G, Robson R, Shaw D, Berns H, Brandl M, Fettner S, Hill G, Ipe D, Klumpp K, Mannino M, O' Mara E, Tu Y, Washington C. Results of a phase 1b, multiple dose study of R1626, a novel nucleoside analog targeting HCV polymerase in chronic HCV genotype 1 patients. *Hepatology* 2006; **44** Suppl 1: S692

48 **Jiang WR**, Chiu S, Ali S, Chapman M, Daniel C, Kretz T, Cammack N, Symons J, Klumpp K. In vitro antiviral interactions of a novel HCV inhibitor R1479 with interferon alpha-2-a, ribavirin and other HCV inhibitors. *Hepatology* 2006; **44** Suppl 1: S533

49 **Villano S**, Howe A, Raible D, Harper D, Speth J, Bichier G. Analysis of HCV NS5B genetic variants following monotherapy with HCV-796, a non-nucleoside polymerase inhibitor, in treatment-naive HCV-infected patients. *Hepatology* 2006; **44** Suppl 1: S607

50 **Villano S**, Raible D, Harper D, Speth J, Chandra P, Shaw P, Bichier G. Antiviral activity of the non-nucleoside polymerase inhibitor, HCV-796, in combination with pegylated interferon alfa-2b in treatment-naive patients with chronic HCV. *J Hepatol* 2007; **46** Suppl 1: S24

51 **Erhardt A**, Wedemeyer H, Benhamou Y, Moellekens C, Forns X, Pol S, Calleja JL, Ross S, Spangenberg HC, Garcia-Samaniego J, Fuchs M, Enriquez J, Wiegand J, Stern J, Wu K, Nehmiz G, Steffgen J. Safety, pharmacokinetics and antiviral effect of BILB1941, a novel HCV RNA polymerase inhibitor, after 5 days oral treatment in patients with chronic hepatitis C. *J Hepatol* 2007; **46** Suppl 1: S222

52 **Wagner R**, Larson D, Bosse T, Kati W, Mo HM, Koev G, Masse S, Jiang W, Liu Y, Montgomery D, Middleton T, Beno D, Lanford R, Kohlbrenner W, Kempf D, Molla A. Discovery, characterization and anti-HCV activity of a novel NS5B inhibitor. *Hepatology* 2006; **44** Suppl 1: S236

53 **Furman PA**, Murakami E, Bao H, Symons J, Otto MJ. Inhibition of HCV replication by PSI-6130: mechanism of biochemical activation and inhibition. *J Hepatol* 2007; **46** Suppl 1: S224

54 **Gray F**, Amphlett E, Bright H, Chambers L, Cheasty A, Fenwick R, Haigh D, Hartley D, Howes P, Jarvest R, Mirzai F, Nerozzi F, Parry N, Slater M, Smith S, Thommes P, Wilkinson C, Williams E. GSK625433; a novel and highly potent inhibitor of the HCV NS5B polymerase. *J Hepatol* 2007; **46** Suppl 1: S225

55 **Molla A**, Wagner R, Lu L, He D, Chen CM, Koev G, Masse S, Cai Y, Klein C, Beno D, Hernandez L, Krishnan P, Pithawalla R, Pilot-Matias T, Middleton T, Lanford R, Kati W, Kempf D. Characterization of pharmacokinetic/pharmacodynamic parameters for the novel HCV polymerase inhibitor A-848837. *J Hepatol* 2007; **46** Suppl 1: S234

56 **Shi ST**, Herlihy KJ, Gonzalez J, Patick AK, Duggal R. In vitro resistance studies of AG-021541, a novel nonnucleoside inhibitor of the hepatitis C virus RNA- dependent RNA polymerase. *Hepatology* 2006; **44** Suppl 1: S534

57 **Watashi K**, Ishii N, Hijikata M, Inoue D, Murata T, Miyanari Y, Shimotohno K. Cyclophilin B is a functional regulator of hepatitis C virus RNA polymerase. *Mol Cell* 2005; **19**: 111-122

58 **Heitman J**, Cullen BR. Cyclophilin B escorts the hepatitis C virus RNA polymerase: a viral achilles heel? *Mol Cell* 2005; **19**: 145-146

59 **Gallay P**, Flisiak R, Horban A, Aeschlimann C, Dumont JM, Porchet H, Scalfaro P, Crabbe R. The reduction of both cyclophilin B and HCV-RNA by the cyclophilin inhibitor Debio-025 confirms the importance of cyclophilin B for HCV replication in man. *J Hepatol* 2007; **46** Suppl 1: S296

60 **Goto K**, Watashi K, Murata T, Hishiki T, Hijikata M, Shimotohno K. Evaluation of the anti-hepatitis C virus effects of cyclophilin inhibitors, cyclosporin A, and NIM811. *Biochem Biophys Res Commun* 2006; **343**: 879-884

61 **Watashi K**, Shimotohno K. Chemical genetics approach to hepatitis C virus replication: cyclophilin as a target for anti-hepatitis C virus strategy. *Rev Med Virol* 2007; **17**: 245-252

62 **Nakagawa M**, Sakamoto N, Enomoto N, Tanabe Y, Kanazawa N, Koyama T, Kurosaki M, Maekawa S, Yamashiro T, Chen CH, Itsui Y, Kakinuma S, Watanabe M. Specific inhibition of hepatitis C virus replication by cyclosporin A. *Biochem Biophys Res Commun* 2004; **313**: 42-47

63 **Inoue K**, Sekiyama K, Yamada M, Watanabe T, Yasuda H, Yoshiba M. Combined interferon alpha2b and cyclosporin A in the treatment of chronic hepatitis C: controlled trial. *J Gastroenterol* 2003; **38**: 567-572

64 **Mueller AR**, Platz KP, Blumhardt G, Bechstein WO, Steinmüller T, Christe W, Hopf U, Lobeck H, Neuhaus P. The optimal immunosuppressant after liver transplantation according to diagnosis: cyclosporine A or FK506? *Clin*

Transplant 1995; **9**: 176-184
65 **Villamil F**, Levy G, Grazi GL, Mies S, Samuel D, Sanjuan F, Rossi M, Lake J, Munn S, Mühlbacher F, Leonardi L, Cillo U. Long-term outcomes in liver transplant patients with hepatic C infection receiving tacrolimus or cyclosporine. *Transplant Proc* 2006; **38**: 2964-2967
66 **Hilgard P**, Kahraman A, Lehmann N, Seltmann C, Beckebaum S, Ross RS, Baba HA, Malago M, Broelsch CE, Gerken G. Cyclosporine versus tacrolimus in patients with HCV infection after liver transplantation: effects on virus replication and recurrent hepatitis. *World J Gastroenterol* 2006; **12**: 697-702
67 **Berenguer M**, Aguilera V, Prieto M, San Juan F, Rayón JM, Benlloch S, Berenguer J. Effect of calcineurin inhibitors on survival and histologic disease severity in HCV-infected liver transplant recipients. *Liver Transpl* 2006; **12**: 762-767
68 **Billich A**, Hammerschmid F, Peichl P, Wenger R, Zenke G, Quesniaux V, Rosenwirth B. Mode of action of SDZ NIM 811, a nonimmunosuppressive cyclosporin A analog with activity against human immunodeficiency virus (HIV) type 1: interference with HIV protein-cyclophilin A interactions. *J Virol* 1995; **69**: 2451-2461
69 **Rosenwirth B**, Billich A, Datema R, Donatsch P, Hammerschmid F, Harrison R, Hiestand P, Jaksche H, Mayer P, Peichl P. Inhibition of human immunodeficiency virus type 1 replication by SDZ NIM 811, a nonimmunosuppressive cyclosporine analog. *Antimicrob Agents Chemother* 1994; **38**: 1763-1772
70 **Lin K**, Ma S, Boerner JE, Huang MM, Ryder NS, Weidmann B, Cooreman MP. NIM811 exhibits potent anti-HCV activity in vitro and represents a novel approach for viral hepatitis C therapy. *Hepatology* 2005; **42** Suppl 1: S536
71 **Ma S**, Boerner JE, TiongYip C, Weidmann B, Ryder NS, Cooreman MP, Lin K. NIM811, a cyclophilin inhibitor, exhibits potent in vitro activity against hepatitis C virus alone or in combination with alpha interferon. *Antimicrob Agents Chemother* 2006; **50**: 2976-2982
72 **Inoue K**, Umehara T, Watanabe T, Durmont JM, Scalfaro P, Yoshiba M, Kohara M. Non immunosupressive cyclosporin Debio-025 with interferon shows synergistic anti-HCV effect in chimeric mouse. *Hepatology* 2006; **44** Suppl 1: S238
73 **Paeshuyse J**, Coelmont L, Kaul A, Vliegen I, de Clercq E, Rosenwirth B, Dumont JM, Scalfaro P, Bartenschlager R, Neyts J. The Cyclophilin inhibitor Debio-025 is a potent inhibitor of hepatitis C virus replication in vitro. *Hepatology* 2006; **44** Suppl 1: S346
74 **Coelmont L**, Paeshuyse J, Kaptein S, Vliegen I, Kaul A, De Clercq E, Rosenwirth B, Scalfaro P, Crabbe R, Bartenschlager R, Dumont JM, Neyts J. The Cyclophilin Inhibitor Debio-025 is a Potent Inhibitor of Hepatitis C Virus Replication in vitro With a Unique Resistance Profile. *Antivir Res* 2007; **74**: S139
75 **Herrmann E**, Flisiak R, Horban A, Crabbe R, Porchet H, Nicolas V, Scalfaro P, Zeuzem S. Viral kinetics during 14-day treatment with Debio-025 demostrate efficient blocking of viral replication in different HCV genotypes without signs of emerging viral resistance. *J Hepatol* 2007; **46** Suppl 1: S40
76 **Lin C**, Gates CA, Rao BG, Brennan DL, Fulghum JR, Luong YP, Frantz JD, Lin K, Ma S, Wei YY, Perni RB, Kwong AD. In vitro studies of cross-resistance mutations against two hepatitis C virus serine protease inhibitors, VX-950 and BILN 2061. *J Biol Chem* 2005; **280**: 36784-36791
77 **Lin C**, Lin K, Luong YP, Rao BG, Wei YY, Brennan DL, Fulghum JR, Hsiao HM, Ma S, Maxwell JP, Cottrell KM, Perni RB, Gates CA, Kwong AD. In vitro resistance studies of hepatitis C virus serine protease inhibitors, VX-950 and BILN 2061: structural analysis indicates different resistance mechanisms. *J Biol Chem* 2004; **279**: 17508-17514
78 **Tong X**, Chase R, Skelton A, Chen T, Wright-Minogue J, Malcolm BA. Identification and analysis of fitness of resistance mutations against the HCV protease inhibitor SCH 503034. *Antiviral Res* 2006; **70**: 28-38

S- Editor Ma N **L- Editor** Kerr C **E- Editor** Liu Y

Online Submissions: wjg.wjgnet.com
www.wjgnet.com
wjg@wjgnet.com

World J Gastroenterol 2007 November 21; 13(43): 5682-5686
World Journal of Gastroenterology ISSN 1007-9327

EDITORIAL

Persistent occult hepatitis B virus infection: Experimental findings and clinical implications

Patricia M Mulrooney-Cousins, Tomasz I Michalak

Patricia M Mulrooney-Cousins, Tomasz I Michalak, Molecular Virology and Hepatology Research, Division of BioMedical Science, Faculty of Medicine, Health Sciences Centre, Memorial University, St. John's, NL A1B 3V6, Canada
Supported by operating research grants from the Canadian Institutes of Health Research, Canada and the Canada Research Chair Program, and the Canada Foundation for Innovation
Correspondence to: Tomasz I Michalak, MD, PhD, Molecular Virology and Hepatology Research, Faculty of Medicine, Health Science Centre, Memorial University, 300 Prince Philip Drive, St. John's, NL A1B 3V6, Canada. timich@mun.ca
Telephone: +1-709-7777301 Fax: +1-709-7778279
Received: July 24, 2007 Revised: September 5, 2007

Abstract

Hepatitis B virus (HBV) is a highly pathogenic virus that causes chronic liver diseases in millions of people globally. In addition to a symptomatic, serologically evident infection, occult persistent HBV carriage has been identified since nucleic acid amplification assays of enhanced sensitivity became introduced for detection of hepadnaviral genomes and their replicative intermediates. Current evidence indicates that occult HBV infection is a common and long-term consequence of resolution of acute hepatitis B. This form of residual infection is termed as secondary occult infection (SOI). The data from the woodchuck model of HBV infection indicate that exposure to small amounts of hepadnavirus can also cause primary occult infection (POI) where virus genome, but no serological makers of exposure to virus, are detectable, and the liver may not be involved. However, virus replicates at low levels in the lymphatic system in both these forms. We briefly summarize the current understanding of the nature and characteristics of occult hepadnaviral persistence as well as of its documented and expected pathological consequences.

Key words: Hepatitis B virus; Hepadnaviruses; Woodchuck hepatitis virus; Hepadnaviral hepatitis; Occult viral persistence; Hepadnavirus lymphotropism; Primary occult infection; Secondary occult infection; Virus reactivation

Mulrooney-Cousins PM, Michalak TI. Persistent occult hepatitis B virus infection: Experimental findings and clinical implications. *World J Gastroenterol* 2007; 13(43): 5682-5686

http://www.wjgnet.com/1007-9327/13/5682.asp

INTRODUCTION

Despite the availability of effective prophylactic vaccines, hepatitis caused by hepatitis B virus (HBV) remains one of the most troublesome infectious diseases responsible for significant morbidity and mortality in the world. HBV-induced chronic hepatitis B (CHB), defined as a prolonged liver inflammation accompanied by HBV surface antigen (HBsAg) in serum for longer than 6 mo, develops in up to 10% of individuals infected as adults and in about 85% of individuals exposed in the neonatal period and early childhood[1,2]. Consequently, up to 400 million people worldwide are afflicted with serum HBsAg-positive chronic infection, which in high endemic areas is mainly acquired by vertical virus transmission[3]. Furthermore, it is estimated that as much as one third of the world population have been exposed to HBV[4]. Many of these individuals may unknowingly carry the virus. It is assumed that, due to low virus loads in many of the cases, HBV may not be identifiable by commonly used serological assays based on detection of HBsAg and that the infection is often asymptomatic or has non-specific symptoms. This serologically and clinically unapparent infection makes the true global incidence of HBV hard to estimate. Consequently, the pathogenic significance of HBV might be much greater than that currently assumed.

OCCULT HBV INFECTION

The clinical data and the findings from animal models accumulated in the past ten years strongly argue that persistent, serologically silent, i.e., serum HBsAg-negative, HBV infection is a natural consequence of resolved acute hepatitis B, but it may also occur following an asymptomatic exposure to HBV, and may have serious pathological and epidemiological repercussions. Another important aspect of infections with HBV and other related viruses, that has been known for a long time but remained controversial and/or not fully realized, is the fact that the immune system, in addition to the liver, is the site of active hepadnaviral replication and long-term persistence.

Occult HBV infection is defined as the existence of HBV DNA in the serum, cells of the lymphatic (immune) system, and/or hepatic tissue in the absence of serum HBsAg. Most frequently, occult HBV infection follows

resolution of acute hepatitis and continues indefinitely after clearance of HBsAg and biochemical improvement in liver function[5-9]. For this reason, this form of infection is termed as residual or secondary occult infection or SOI, in opposite to primary occult infection or POI, which will be discussed later. Serological testing in SOI normally reveals the presence of antibodies to HBV core antigen (anti-HBc), which are now recognized not only as a valuable marker of prior exposure to HBV but also as an indicator suggesting actually progressing occult HBV infection. Nonetheless, recent estimates suggest that up to 20% of individuals with occult HBV carriage evidenced by HBV DNA detection could be nonreactive for anti-HBc or any other serological indicator of exposure to HBV[7]. It also is of note that the detection of naturally acquired antibodies to HBsAg (anti-HBs) does not exclude the existence of occult infection[5-7,9].

DETECTION OF OCCULT HEPADNAVIRAL PERSISTENCE

One of the main current challenges in diagnosis of occult HBV infection is the relatively low sensitivity of HBV DNA detection assays. The present assays are based on different approaches to amplification of HBV DNA by polymerase chain reaction (PCR) and their lowest detection limits range between 200 and 1000 virus genome copies, which are also referred to as virus genome equivalents (vge) per mL of plasma or serum. Although these assays are adequate to detect prodromal and symptomatic HBV infections and to monitor the progress of antiviral therapy, they are yet not sufficiently sensitive to identify occult infection in the majority of the individuals affected, where serum loads are usually below 100 vge per mL, as well as to determine whether virus was indeed completely eradicated following antiviral treatment[9]. In contrast to the clinical assays, the current research tests, which in our laboratory apply nested PCR and detection of resulting amplicons by nucleic acid hybridization (NAH), i.e., PCR/NAH, identify hepadnaviral DNA at loads below 10 vge/mL[10,11]. Furthermore, by testing of serial samples of serum and peripheral blood mononuclear cells (PBMC) and, when feasible, liver biopsies, and by amplifying different non-overlapping regions of the virus genome, detection of occult infection is greatly enhanced[9]. Application of these ultrasensitive assays to investigation of clinical materials and animal models, particularly the woodchuck model of hepatitis B, led to identification in the last decade of occult hepadnavirus infection as a new, distinctive entity and to delineation of its unique characteristics. However, due to yet limited population-based studies and relatively low sensitivity of the assays approved for clinical testing, the full impact of this infection remains to be determined. Nonetheless, with the recent introduction of clinical HBV nucleic acid testing (HBV NAT) in many parts of the world, significant progress in this area is expected.

EXPERIMENTAL OCCULT HBV INFECTION IN THE WOODCHUCK MODEL

Many of the characteristics of occult HBV infection have been originally identified in the woodchuck model of hepatitis B[5]. Woodchuck hepatitis virus (WHV) infecting the Eastern North American woodchuck (*Marmota monax*) is accepted as the most adequate, natural model of human HBV infection, hepatitis B and HBV-induced hepatocellular carcinoma (HCC). WHV closely resembles HBV in the structure, biology, and in the patterns and outcomes of the liver diseases induced. Much of the basic understanding of the natural course, requirements for transmission, molecular and immunological properties of occult hepadnaviral carriage, and its long-term pathological ramifications is owed to the woodchuck-WHV experimental system[10-15].

Occult WHV infection was first identified as a residual, life-long persistent infection in woodchucks who apparently completely resolved experimental acute hepatitis and developed anti-WHs (antibodies to WHV surface antigen, WHsAg)[10]. Analysis of sequential sera, PBMC and liver biopsies collected during the lifespan of these animals, as well as autopsy lymphatic and hepatic tissues, using sensitive PCR/NAH assays, identified WHV DNA in all three compartments, i.e., serum, lymphoid cells and the liver. In addition, the WHV replicating intermediates, covalently closed circular DNA (cccDNA), and virus mRNA were consistently found in the cells of the lymphatic system and the liver. Anti-WHc (equivalent of anti-HBc) persisted in all animals for life. This form of WHV infection become later termed as SOI[5,14]. In addition and unexpectedly, a low grade, intermittent liver inflammation was diagnosed throughout the remaining life in the majority of the woodchucks who apparently completely resolved acute hepatitis[10]. Not less importantly, one fifth of the animals developed HCC in 3-5 years after recovery and despite anti-WHs presence[10]. The same rate of HCC development was reported in woodchucks recovered from acute hepatitis which were examined by other investigators[16]. Most recently, it has also been shown that residual WHV in animals with SOI can be reactivated by treatment with an immunosuppressive agent, Cyclosporin A, leading to transiently serum WHsAg-positive infection[17]. Taken together, the data accumulated indicate that despite resolution of acute hepatitis, the replication of WHV continues for life, albeit at very low levels, both in the liver and the lymphatic system, that limited inflammatory process continues in hepatic tissue, and that the silently persisting virus may retain its oncogenic potency. This implies that although the immune system is able to resolve acute hepatitis and can keep persistently propagating hepadnavirus under relative control, it is unable to eradicate the virus completely[10,14]. The same conclusion was recently reached when bicistronic WHV core-gamma interferon (IFN) DNA vaccine was found to be able to prevent WHV hepatitis, but could not mount sterile immunity and prevent establishment of occult infection[18]. Furthermore, it became apparent that the detection of anti-WHc in the absence of other serological indicators of infection is a reliable indicator of occult WHV persistence[15]. This state, similarly as strong HBV-specific cytotoxic T cell (CTL) and T helper lymphocyte responses detectable years after resolution of acute hepatitis B[19,20], is likely a consequence of sustained restimulation of the immune system with a

viral protein produced during low-level virion assembly[15]. The high degree of compatibility between WHV and HBV infections and the data from studies on otherwise healthy anti-HBc-positive individuals[21,22] suggest that the occurrence of isolated anti-HBc could also be of value in identifying occult HBV persistence.

The virus recovered from woodchucks with SOI remains infectious. It was observed that WHV harvested from PBMC isolated during SOI and *ex vivo* stimulated with lipopolysaccharide (LPS) induced classical acute WHV hepatitis in virus-naive animals[10]. Furthermore, woodchuck dams with SOI were found to transmit virus to offspring, however, the infection induced frequently displays characteristics different than those of SOI[11]. Thus, WHV DNA and WHV cccDNA was harboured only in the lymphatic system, but not in the liver, and in the absence of serological markers of infection, including anti-WHc antibodies. This form of hepadnaviral infection was later named as primary occult infection or POI[14]. Interestingly, POI, in contrast to SOI, is not associated with protection from reinfection and hepatitis after challenge with liver pathogenic doses of WHV[11]. In subsequent studies, the same profile of occult infection was experimentally induced in adult animals by intravenous injections with WHV doses lower than 1000 virions[14]. At the same time, it was also established that WHV quantities higher than 1000 virions, in addition to infecting the lymphatic system, consistently cause classical acute hepatitis. This revealed that doses greater than 1000 virions are liver pathogenic in woodchucks[14]. From these data it was inferred that the threshold level of WHV required to infect lymphoid cells is 100 to 1000-fold lower than that to infect hepatocytes. WHV sequence variation was not responsible for the induction of these two contrasting forms of infection[14].

At the present time, POI is the entity which has not yet been convincingly identified in humans. However, the detection of occult HBV DNA-positive, anti-HBc-negative infection may suggest its existence. The persistence of trace amounts of replicating virus, especially at the extrahepatic locations, could have an impact in terms of unforeseen virus transmission and induction of disorders which are not yet considered to be related to hepadnaviral infection. Small quantities of the virus carried across the placenta may induce POI, similarly to CHB developing in neonates born to mothers with serum HBsAg-positive infection.

OCCULT HEPADNAVIRAL INFECTION AND THE HOST'S IMMUNE SYSTEM

Since the cells of the immune system are clearly the site of WHV propagation, independent of whether infection is symptomatic or occult, it became of interest to enumerate the cells carrying the virus in different forms of experimentally induced infection. By applying *in situ* PCR combined with flow cytometric quantification of cells containing amplified WHV core gene sequences, the proportion of WHV DNA-positive circulating lymphoid cells was found to range from 3.4% to 20.4% (mean 9.6%) in serum WHsAg-positive hepatitis, as compared to 1.1% to 14.6% (mean 4.8%) in occult WHV infection[13]. There was no difference between SOI and POI in the numbers of infected cells.

In terms of WHV-specific T cell responses, recent studies have shown that animals with POI display weak but evident, persistent and multispecific virus-specific T cell proliferative reactivity and that this cellular response does not provide protection against challenge with liver pathogenic doses of WHV[23] (Gujar *et al*, manuscript in preparation). The existence of active peripheral WHV-specific T cell response and innate immune cell activation in the livers of animals with SOI have also been established[12] (Gujar *et al*, manuscript in preparation). Overall, the findings in experimental SOI in woodchucks are closely compatible with those reported for humans convalescent from acute hepatitis B[19,20].

PRIMARY VERSUS SECONDARY OCCULT WHV INFECTION

In summary, experimental occult hepadnaviral infection occurs in two distinctive forms, as primary and secondary infection. POI is induced upon exposure to WHV doses at or below 1000 vge and engages the lymphatic system, although the infection with time may also spread to the liver[11,14]. Animals with POI carry virus in serum and lymphoid cells at levels which are comparable with those occurring in SOI and mount virus-specific T cell proliferative response, but they do not have serological (immunovirological) markers of infection and they are not protected from challenge with liver pathogenic doses of the virus. On the other hand, in SOI, a low-level replication of the virus progresses in both the liver and the lymphatic system, anti-WHc and frequently anti-WHs are detectable, and the animals are protected from hepatitis when re-exposed to liver pathogenic doses of WHV. Moreover, while SOI can be accompanied by low grade, protracted liver inflammation and HCC may finally develop, the liver is entirely normal in POI and a possible development of hepatoma has not yet been assessed.

IMPLICATIONS OF OCCULT HEPADNAVIRAL PERSISTENCE

Given the high degree of similarity between WHV and HBV and infections induced by these viruses, it is important to recognize the impact of silent HBV persistence in terms of its overall incidence, infectivity and pathogenic consequences. The previous clinical and research focus on the liver as essentially the only reservoir of HBV has somehow restricted characterization of extrahepatic sites of hepadnaviral replication and its potential pathological consequences. Recent studies are bringing occult HBV infection and the virus' lymphotropic nature to the forefront. Some of the cardinal works on occult HBV infection were accomplished by examining lymphoid cells of patients with resolved acute hepatitis B where HBV DNA sequences were found[19,24,25]. Furthermore, immunological studies showed that vigorous CTL and T cell proliferative

responses specific against HBV antigens persisted for years after recovery[19,20]. Many case reports also indicate that immunosuppression caused by chemotherapy[26,27], immunomodulatory agents[28], or immune deficiencies, such as HIV infection[29] or hematological malignancies[30], can reactivate occult infection. As in woodchucks with SOI, mild necroinflammation has been documented in liver samples obtained many years after recovery from acute hepatitis B[31,32]. Liver fibrosis and cirrhosis of unknown origin has now been explained by occult HBV infection in many retrospective studies[33,34]. There also is strong evidence for the risk of HCC development in patients with occult HBV[35-38] and this risk is further elevated in alcoholics[39] and in patients with other liver ailments, like hepatitis C[40]. Interestingly, convincing evidence points to the conservation of the HBV genome sequence in occult infection, negating the possibility that faulty HBsAg production accounts for all incidences of occult infection[32,41]. On the other hand, studies demonstrating the passage of HBV in non-liver cells, such as stem cells[42,43] and bone marrow[44], and by blood donations collected from individuals with occult HBV[45] are increasingly frequent in the literature. Recent estimates suggest that transient HBV DNA levels of up to 10^4 vge/mL can be found in sera from apparently healthy individuals with occult infection, which evade detection by current clinical assays, especially when testing is done on single serum or plasma samples[9,46].

CONCLUSION

The seriousness of the consequences of occult HBV infection is yet not fully recognized. Accumulated evidence indicate that occult HBV can be both a source of virus contamination in blood and organ donations, as well as the reservoir from which full blown hepatitis can arise. The oncogenic potency of occult HBV persistence becomes progressively evident. This silent infection can also affect the progression and outcomes of other viral diseases, particularly hepatitis C. It can be expected that while the burden of CHB will decrease with time due to introduction of more effective antiviral therapies, occult HBV infection could become a main concern. Understanding in its entirety of the nature and consequences of this form of HBV persistence should be of a high priority and this quest has already been initiated.

REFERENCES

1 **Ganem D**, Prince AM. Hepatitis B virus infection--natural history and clinical consequences. *N Engl J Med* 2004; **350**: 1118-1129
2 **Michalak TI**. Immunology of hepatitis B virus. In: Colacino JM, Heinz BA. Hepatitis Prevention and Treatment. Basel, Switzerland: Birkhäuser Verlang, 2004: 87-105
3 **Lok AS**, McMahon BJ. Chronic hepatitis B. *Hepatology* 2001; **34**: 1225-1241
4 **Lavanchy D**. Hepatitis B virus epidemiology, disease burden, treatment, and current and emerging prevention and control measures. *J Viral Hepat* 2004; **11**: 97-107
5 **Michalak TI**. Occult persistence and lymphotropism of hepadnaviral infection: insights from the woodchuck viral hepatitis model. *Immunol Rev* 2000; **174**: 98-111
6 **Bréchot C**, Thiers V, Kremsdorf D, Nalpas B, Pol S, Paterlini-Bréchot P. Persistent hepatitis B virus infection in subjects without hepatitis B surface antigen: clinically significant or purely "occult"? *Hepatology* 2001; **34**: 194-203
7 **Torbenson M**, Thomas DL. Occult hepatitis B. *Lancet Infect Dis* 2002; **2**: 479-486
8 **Raimondo G**, Pollicino T, Cacciola I, Squadrito G. Occult hepatitis B virus infection. *J Hepatol* 2007; **46**: 160-170
9 **Michalak TI**, Pham TNQ, Mulrooney-Cousins PM. Molecular diagnosis of occult hepatitis C and hepatitis B virus infections. *Future Virol* 2007; **2**: 451-465
10 **Michalak TI**, Pardoe IU, Coffin CS, Churchill ND, Freake DS, Smith P, Trelegan CL. Occult lifelong persistence of infectious hepadnavirus and residual liver inflammation in woodchucks convalescent from acute viral hepatitis. *Hepatology* 1999; **29**: 928-938
11 **Coffin CS**, Michalak TI. Persistence of infectious hepadnavirus in the offspring of woodchuck mothers recovered from viral hepatitis. *J Clin Invest* 1999; **104**: 203-212
12 **Hodgson PD**, Michalak TI. Augmented hepatic interferon gamma expression and T-cell influx characterize acute hepatitis progressing to recovery and residual lifelong virus persistence in experimental adult woodchuck hepatitis virus infection. *Hepatology* 2001; **34**: 1049-1059
13 **Mulrooney PM**, Michalak TI. Quantitative detection of hepadnavirus-infected lymphoid cells by in situ PCR combined with flow cytometry: implications for the study of occult virus persistence. *J Virol* 2003; **77**: 970-979
14 **Michalak TI**, Mulrooney PM, Coffin CS. Low doses of hepadnavirus induce infection of the lymphatic system that does not engage the liver. *J Virol* 2004; **78**: 1730-1738
15 **Coffin CS**, Pham TN, Mulrooney PM, Churchill ND, Michalak TI. Persistence of isolated antibodies to woodchuck hepatitis virus core antigen is indicative of occult infection. *Hepatology* 2004; **40**: 1053-1061
16 **Korba BE**, Wells FV, Baldwin B, Cote PJ, Tennant BC, Popper H, Gerin JL. Hepatocellular carcinoma in woodchuck hepatitis virus-infected woodchucks: presence of viral DNA in tumor tissue from chronic carriers and animals serologically recovered from acute infections. *Hepatology* 1989; **9**: 461-470
17 **Menne S**, Cote PJ, Butler SD, Toshkov IA, Gerin JL, Tennant BC. Immunosuppression reactivates viral replication long after resolution of woodchuck hepatitis virus infection. *Hepatology* 2007; **45**: 614-622
18 **Wang J**, Gujar SA, Cova L, Michalak TI. Bicistronic woodchuck hepatitis virus core and gamma interferon DNA vaccine can protect from hepatitis but does not elicit sterilizing antiviral immunity. *J Virol* 2007; **81**: 903-916
19 **Rehermann B**, Ferrari C, Pasquinelli C, Chisari FV. The hepatitis B virus persists for decades after patients' recovery from acute viral hepatitis despite active maintenance of a cytotoxic T-lymphocyte response. *Nat Med* 1996; **2**: 1104-1108
20 **Penna A**, Artini M, Cavalli A, Levrero M, Bertoletti A, Pilli M, Chisari FV, Rehermann B, Del Prete G, Fiaccadori F, Ferrari C. Long-lasting memory T cell responses following self-limited acute hepatitis B. *J Clin Invest* 1996; **98**: 1185-1194
21 **Hoofnagle JH**, Seeff LB, Bales ZB, Zimmerman HJ. Type B hepatitis after transfusion with blood containing antibody to hepatitis B core antigen. *N Engl J Med* 1978; **298**: 1379-1383
22 **Marusawa H**, Uemoto S, Hijikata M, Ueda Y, Tanaka K, Shimotohno K, Chiba T. Latent hepatitis B virus infection in healthy individuals with antibodies to hepatitis B core antigen. *Hepatology* 2000; **31**: 488-495
23 **Gujar SA**, Michalak TI. Primary occult hepadnavirus infection induces both virus-specific and generalized T cell responses in the absence of virus-specific humoral immunity. *Hepatology* 2006; **44**: 536A
24 **Michalak TI**, Pasquinelli C, Guilhot S, Chisari FV. Hepatitis B virus persistence after recovery from acute viral hepatitis. *J Clin Invest* 1994; **93**: 230-239
25 **Murakami Y**, Minami M, Daimon Y, Okanoue T. Hepatitis B virus DNA in liver, serum, and peripheral blood mononuclear cells after the clearance of serum hepatitis B virus surface

antigen. *J Med Virol* 2004; **72**: 203-214
26 **Lok AS**, Liang RH, Chiu EK, Wong KL, Chan TK, Todd D. Reactivation of hepatitis B virus replication in patients receiving cytotoxic therapy. Report of a prospective study. *Gastroenterology* 1991; **100**: 182-188
27 **Hui CK**, Cheung WW, Zhang HY, Au WY, Yueng YH, Leung AY, Leung N, Luk JM, Lie AK, Kwong YL, Liang R, Lau GK. Kinetics and risk of de novo hepatitis B infection in HBsAg-negative patients undergoing cytotoxic chemotherapy. *Gastroenterology* 2006; **131**: 59-68
28 **Madonia S**, Orlando A, Scimeca D, Olivo M, Rossi F, Cottone M. Occult hepatitis B and infliximab-induced HBV reactivation. *Inflamm Bowel Dis* 2007; **13**: 508-509
29 **Chamorro AJ**, Casado JL, Bellido D, Moreno S. Reactivation of hepatitis B in an HIV-infected patient with antibodies against hepatitis B core antigen as the only serological marker. *Eur J Clin Microbiol Infect Dis* 2005; **24**: 492-494
30 **Lalazar G**, Rund D, Shouval D. Screening, prevention and treatment of viral hepatitis B reactivation in patients with haematological malignancies. *Br J Haematol* 2007; **136**: 699-712
31 **Yuki N**, Nagaoka T, Yamashiro M, Mochizuki K, Kaneko A, Yamamoto K, Omura M, Hikiji K, Kato M. Long-term histologic and virologic outcomes of acute self-limited hepatitis B. *Hepatology* 2003; **37**: 1172-1179
32 **Bläckberg J,** Kidd-Ljunggren K. Occult hepatitis B virus after acute self-limited infection persisting for 30 years without sequence variation. *J Hepatol* 2000; **33**: 992-997
33 **Bréchot C**. Pathogenesis of hepatitis B virus-related hepatocellular carcinoma: old and new paradigms. *Gastroenterology* 2004; **127**: S56-S61
34 **Ikeda K**, Marusawa H, Osaki Y, Nakamura T, Kitajima N, Yamashita Y, Kudo M, Sato T, Chiba T. Antibody to hepatitis B core antigen and risk for hepatitis C-related hepatocellular carcinoma: a prospective study. *Ann Intern Med* 2007; **146**: 649-656
35 **Paterlini P**, Gerken G, Nakajima E, Terre S, D'Errico A, Grigioni W, Nalpas B, Franco D, Wands J, Kew M. Polymerase chain reaction to detect hepatitis B virus DNA and RNA sequences in primary liver cancers from patients negative for hepatitis B surface antigen. *N Engl J Med* 1990; **323**: 80-85
36 **Pollicino T**, Squadrito G, Cerenzia G, Cacciola I, Raffa G, Craxi A, Farinati F, Missale G, Smedile A, Tiribelli C, Villa E, Raimondo G. Hepatitis B virus maintains its pro-oncogenic properties in the case of occult HBV infection. *Gastroenterology* 2004; **126**: 102-110
37 **Donato F**, Gelatti U, Limina RM, Fattovich G. Southern Europe as an example of interaction between various environmental factors: a systematic review of the epidemiologic evidence. *Oncogene* 2006; **25**: 3756-3770
38 **Huo TI**, Wu JC, Lee PC, Chau GY, Lui WY, Tsay SH, Ting LT, Chang FY, Lee SD. Sero-clearance of hepatitis B surface antigen in chronic carriers does not necessarily imply a good prognosis. *Hepatology* 1998; **28**: 231-236
39 **Yotsuyanagi H**, Hashidume K, Suzuki M, Maeyama S, Takayama T, Uchikoshi T. Role of hepatitis B virus in hepatocarcinogenesis in alcoholics. *Alcohol Clin Exp Res* 2004; **28**: 181S-185S
40 **Chemin I**, Trépo C. Clinical impact of occult HBV infections. *J Clin Virol* 2005; **34** Suppl 1: S15-S21
41 **Pollicino T**, Raffa G, Costantino L, Lisa A, Campello C, Squadrito G, Levrero M, Raimondo G. Molecular and functional analysis of occult hepatitis B virus isolates from patients with hepatocellular carcinoma. *Hepatology* 2007; **45**: 277-285
42 **Knöll A**, Boehm S, Hahn J, Holler E, Jilg W. Long-term surveillance of haematopoietic stem cell recipients with resolved hepatitis B: high risk of viral reactivation even in a recipient with a vaccinated donor. *J Viral Hepat* 2007; **14**: 478-483
43 **Seth P**, Alrajhi AA, Kagevi I, Chaudhary MA, Colcol E, Sahovic E, Aljurf M, Gyger M. Hepatitis B virus reactivation with clinical flare in allogeneic stem cell transplants with chronic graft-versus-host disease. *Bone Marrow Transplant* 2002; **30**: 189-194
44 **Iwai K**, Tashima M, Itoh M, Okazaki T, Yamamoto K, Ohno H, Marusawa H, Ueda Y, Nakamura T, Chiba T, Uchiyama T. Fulminant hepatitis B following bone marrow transplantation in an HBsAg-negative, HBsAb-positive recipient; reactivation of dormant virus during the immunosuppressive period. *Bone Marrow Transplant* 2000; **25**: 105-108
45 **Liu CJ**, Lo SC, Kao JH, Tseng PT, Lai MY, Ni YH, Yeh SH, Chen PJ, Chen DS. Transmission of occult hepatitis B virus by transfusion to adult and pediatric recipients in Taiwan. *J Hepatol* 2006; **44**: 39-46
46 **Allain JP**. Occult hepatitis B virus infection. *Transfus Clin Biol* 2004; **11**: 18-25

S- Editor Liu Y **L- Editor** Rippe RA **E- Editor** Lu W

Online Submissions: wjg.wjgnet.com
www.wjgnet.com
wjg@wjgnet.com

World J Gastroenterol 2007 November 21; 13(43): 5687-5691
World Journal of Gastroenterology ISSN 1007-9327

REVIEW

Carbohydrate malabsorption in patients with non-specific abdominal complaints

Peter Born

Peter Born, Department of Internal Medicine, Tirschenreuth District Hospital, Tirschenreuth 95643, Germany
Correspondence to: Professor Peter Born, MD, Department of Internal Medicine, Tirschenreuth District Hospital, St. Peter-Strasse 31, Tirschenreuth 95643, Germany. peter.born@krankenhaus-tirschenreuth.de
Telephone: +49-9631-875204
Received: July 12, 2007 Revised: August 31, 2007

Abstract

Non-specific abdominal complaints are a considerable problem worldwide. Many patients are affected and many differential diagnoses have to be considered. Among these, carbohydrate malabsorption seems to play an important role. However, so far, only incomplete absorption of lactose is broadly accepted, while the malabsorption of fructose and sorbitol is still underestimated, although in many parts of the world it is much more frequent. Despite the success of dietary interventions in many patients, there are still a lot of unanswered questions that make further investigations necessary.

Key words: Non-specific abdominal disorders; Carbohydrate malabsorption; Fructose; Sorbitol; Lactose; Dietary intervention

Born P. Carbohydrate malabsorption in patients with non-specific abdominal complaints. *World J Gastroenterol* 2007; 13(43): 5687-5691

http://www.wjgnet.com/1007-9327/13/5687.asp

INTRODUCTION

The incomplete absorption of carbohydrates may cause serious problems for the affected patients, and is a frequent cause of so-called non-specific abdominal complaints. Non-specific abdominal complaints are characterized by a lack of morphological or biochemical abnormalities in the affected patients[1,2]. These complaints are a major problem throughout the world, with up to 30% of the population in Western countries being affected. Although only a minority seek medical attention, some 20%-50% of patients are referred to gastroenterologists so because of these non-specific complaints[2]. A study in Germany[3] has reported similar data, with 30% of the population being affected. A quarter of the patients required medical treatment, and no other diagnosis could be established in two-thirds of the cases. Similar findings have been described in Africa[4]; the rates appear to be lower in Asia, although they are still substantial, with a prevalence of up to 10% being reported[5].

There is a wide range of symptoms; the predominant ones are pain, flatulence, constipation and diarrhea. These symptoms should always be distinguished from those such as anemia, weight loss, bleeding and fever, which may indicate more dangerous conditions[6].

CARBOHYDRATE MALABSORPTION

Pathogenesis

Carbohydrates are a major source of calories in the diet. They may be ingested as monosaccharides, disaccharides, oligosaccharides or polysaccharides. During their passage from the mouth to the small intestine, they are broken down enzymatically until, in the small intestine, brush-border enzymes hydrolyze them into monosaccharides, which can be absorbed by various carrier systems[7].

The most important carbohydrates that routinely cause clinical abdominal complaints are lactose, fructose, and the sugar alcohol sorbitol. Lactose has long been recognized as one of the most important nutrients, and fructose and sorbitol have become increasingly important following recommendations to increase fruit and vegetable consumption, and also as a result of their use as sweeteners in dietary preparations and so-called sugar-free sweets. Further disorders such as sucrase-isomaltase deficiency or lack of trehalase are rare or only of regional importance, and are not discussed in this paper, although in affected patients, diets free from these sugars are very successful.

Malabsorption may result from congenital or acquired defects of single transport systems (primary malabsorption), or from impairment of the epithelial surface of the small intestine, due to general intestinal diseases such as celiac disease or Crohn's disease, which impede the absorption of all carbohydrates (secondary malabsorption). In secondary malabsorption, treatment is directed at the underlying disease, and successful therapy can lead to the normalization of carbohydrate absorption. In primary malabsorption, selective interventions are necessary.

Lactose is split by the enzyme lactase (β-d-

galactosidase), derived from the brush border of the enterocytes, into galactose and glucose, which can be absorbed by a special carrier system. The most frequently associated deficiency is primary lactase deficiency in adults. In these patients, lactase activity gradually declines during early life, and symptoms may occur as early as late childhood. Congenital lactase deficiency is rare and already affects neonates[8].

Several carriers, such as the GLUT family, are known to be involved in the transport of monosaccharides. GLUT-5 is the most important carrier currently known for the absorption of fructose. A deficiency in GLUT-5 leads to incomplete absorption or malabsorption of fructose[9,10]. Sorbitol is only sparsely absorbed, and is therefore used therapeutically as an osmotic laxative. Absorption is thought to take place through passive diffusion[11-13].

Congenital and acquired deficiencies are recognized. An important aspect is that the presence of glucose stimulates GLUT-5 activity, while sorbitol blocks it[9]. These data from animal intestinal perfusion tests (in most cases rat jejunum) confirm previous clinical and experimental data, which show that addition of glucose to fructose in patients known to have fructose malabsorption can prevent malabsorption, and suppress the occurrence of the accompanying symptoms. In contrast, the presence of sorbitol may aggravate malabsorption and the symptoms[13-17]. However, the mechanisms of carbohydrate absorption are still not completely understood.

There are also data that indicate an additional role for other factors in fructose metabolism, such as GLUT-2, which is capable of stimulating absorption[10].

Prevalence

Lactase deficiency is the most common enzymatic defect worldwide, although there are considerable regional differences in its prevalence. The majority of people in Asia and Africa, as well as the aboriginal populations of America and Australia, are affected, while in Europe, there are very low rates (under 10%) in the north, with a strong increase (up to 70%-100%) in regions further south, such as in Italy and Turkey.

There have been many studies reporting high malabsorption rates for fructose and sorbitol. Depending on the dosage and concentration, the reported data are closely comparable. After the ingestion of 50 g fructose dissolved in 250 mL water (corresponding to the traditional lactose test), there are malabsorption rates of about 60%-70%[15,18,19], while the rates are about 40% after a dosage of 25 g in 250 mL, the concentration now most commonly used[14,20]. Similar values have also been documented in children[21,22]. With regard to sorbitol, the test dosages used are less standardized, but even after an intake of 10 g, malabsorption rates can reach 100%[12,19,23].

For all of these sugars, it should be noted that the malabsorption rates are quite similar in patients and healthy controls. While some 50% of those with malabsorption of fructose and sorbitol have no concomitant symptoms, the symptomatic rates for lactose malabsorption are much more varied, with only a few people being symptomatic in some populations, despite high malabsorption rates.

Symptoms

The clinical symptoms of carbohydrate malabsorption include flatulence, abdominal cramps and pain, diarrhea, and sometimes even headache, usually after the ingestion of a product containing the incompletely absorbed sugar. There are no symptoms specific for a single sugar. However, there are data showing that, in patients (mainly females) with fructose and sorbitol malabsorption, diet can improve not only gastrointestinal disturbances, but also mood[24]. An association with reduced plasma levels of tryptophan has been discussed as a possible mechanism for this[25].

The gastrointestinal symptoms are thought to be provoked by the increased osmotic load of the sugar, with an augmented intraluminal volume (water) and a consequent acceleration of intestinal passage. Gas production and diarrhea occur in connection with the bacterial flora in the colon, the unabsorbed sugar presenting as a substrate for increased bacterial fermentation. Moreover, the capacity of the colon to absorb the surplus water plays a role in the pathogenesis of diarrhea.

In view of these etiologic factors, it is of particular interest that many patients report that initial symptoms develop after an infection (mostly gastrointestinal) or after antibiotic therapy, although it must be assumed that malabsorption has been present since childhood. Irritable bowel syndrome (which probably often includes patients with carbohydrate malabsorption) has also been reported to develop in connection with infections, both inside and outside the gastrointestinal tract[26,27]. In two small series, our own group has shown that the degradation of the malabsorbed sugar in stool cultures correlates with the occurrence of symptoms and a different pattern of short-chain free fatty acids[28,29].

It may therefore be speculated that the symptoms of carbohydrate malabsorption depend on the pattern of the colonic flora. A further argument in favor of this view is the observation that, in volunteers in whom more than one type of malabsorption is detected, the symptoms occur either after each malabsorption or after none[30].

Diagnosis

Carbohydrate malabsorption can be detected using direct or indirect methods. Using a cecal tube to measure the amount of unabsorbed sugar after oral ingestion is not practicable for routine purposes. Measurement of enzymatic activity in intestinal biopsies is a valuable tool for quantifying disaccharidase activity. It is therefore suitable for diagnosing lactase insufficiency, but is rarely used. Indirect methods are more widely used. Measurement of blood sugar after lactose ingestion was formerly a widespread method, but it declined in importance with the introduction of hydrogen exhalation tests. Direct measurement of ingested sugar in blood or urine is applicable for xylose.

By far the most frequently used method nowadays is the hydrogen exhalation test. After ingestion of the test sugar, the amount of hydrogen in the exhaled gas is measured. If there is incomplete absorption, part of

the ingested sugar passes into the colon, in which it is metabolized by bacteria into hydrogen, methane, carbon dioxide and free fatty acids. A small amount of hydrogen is absorbed and exhaled during the first passage through the lungs. An increase in hydrogen of more than 20 parts per million is considered to indicate malabsorption[31-33]. The extent of the hydrogen increase does not correlate either with the patients' symptoms or with the degree of malabsorption[34]. Hydrogen tests are only able to detect or exclude malabsorption. It should be pointed out that to avoid false-negative results, the presence of hydrogen-producing bacteria should be confirmed by carrying out a lactulose test (as lactulose is a disaccharide that cannot be absorbed by humans and therefore causes an increase in hydrogen). False-positive results due to bacterial overgrowth or accelerated orocecal transit can also be reduced with this test[35].

Concomitant measurement of blood glucose may improve the accuracy of lactose tests and should be mandatory in all fructose tests, in order to detect rare cases of fructose intolerance, which may mimic the symptoms of fructose malabsorption, but can cause severe hypoglycemia and even death after the ingestion of fructose. There is also some evidence that parallel methane assessment may improve the accuracy of the hydrogen test, but the data are sparse and require further evaluation[36]. The use of ^{13}C exhalation tests also requires further evaluation[37].

Therapy

Avoidance of the malabsorbed sugar is still the treatment of choice. In patients with lactose malabsorption, the addition of lactase (most conveniently in liquids) is an alternative, as well as the consumption of lactose-free milk products. Patients with fructose malabsorption can choose fruits and vegetables that have an equal ratio of fructose and glucose. In liquids, the addition of glucose can prevent malabsorption and its symptoms, but does not appear appropriate from the point of view of healthy nutrition. For sorbitol malabsorption, restricting sorbitol intake is the best method of preventing symptoms. In the same way that glucose can reduce malabsorption when administered along with fructose, adding sorbitol to fructose may aggravate the symptoms, and this should be taken into account when establishing the dietary regimen. For all sugars, small amounts are tolerated by most patients. Ingesting them along with or after other nutrients further improves tolerance.

The diet and its effects are often an important method of establishing a diagnosis of clinically relevant carbohydrate malabsorption. As mentioned above, many people are affected by malabsorption, but by no means are all symptomatic. Improvement after dietary adjustment and recurrence of symptoms when dietary errors occur is still the best way of confirming the diagnosis. There have been few studies that have documented the beneficial effects of dietary changes in patients with fructose and sorbitol malabsorption. In addition, there are methodological problems in all of these studies, including those by our own group. The diet itself is sometimes not clearly described; patient compliance with the diet is difficult to assess; there are no control groups, so that the role of a placebo effect is difficult to assess; and there are inadequacies in the way in which the patients' dietary behavior is recorded.

Nevertheless, the available data are fairly consistent. In our own study, which had both prospective and retrospective parts (in order to assess the placebo effect), symptomatic improvement of 60%-100%, depending on the degree of patient compliance, was observed to a similar degree in both arms of the study[38]. Fernandez-Banares et al[39] have reported similar results and were able to show that the treatment effect was long-lasting, with the positive effects of the diet being maintained at 12 mo. Shepherd and Gibson have confirmed these data in a group of 62 patients[40]. The largest study (so far available only as an abstract, so far as we are aware), including 1320 patients, documented an improvement after dietary changes in 87.5% of the patients[41]. In a more recent study including 90 selected patients with non-specific abdominal complaints, we observed a high rate of carbohydrate malabsorption (lactose 34%, fructose 61%, and sorbitol 91%)[42]. After dietary information had been provided, the patients reported significant improvement in 75% of cases, depending on the extent of compliance. The study by Ledochowski *et al*[24], which has shown that dietary changes in patients with fructose malabsorption have a beneficial effect on gastrointestinal complaints and also on mood, as documented by improvements in depression score, has already been mentioned above. However, there are also contradictory data that show that only avoiding one sugar (with proven malabsorption) may not be sufficient for patients with irritable bowel syndrome[43,44].

The phenomenon that patients with non-specific abdominal complaints frequently report improvement in their symptoms for several weeks after colonoscopy (thought to be due to bowel preparation with cleansing of the colon) underlines the possible role of bacteria in the colon. Treatments involving antibiotics[45,46], attempts to reduce colonic bacterial fermentation[47], and administration of probiotics[48] therefore require further investigation.

Open questions

Although carbohydrate malabsorption appears to play an important role in patients suffering from non-specific abdominal complaints, there are several problems with this diagnosis that should not be overlooked. In the first place, diagnosis using hydrogen tests is still problematic, particularly if the increase is borderline. The threshold value of 20 p.p.m. requires further evaluation, as there may be significant variations in methane production in the colon, among other factors. Moreover, hydrogen tests are not capable of quantifying the amount of malabsorption. Symptoms do not always occur during the test, even in patients who are considered to be symptomatic. Assessing the clinical relevance of the diagnosis may therefore sometimes be difficult.

The etiology of the symptoms is not fully understood. If the data published by our own group, which show that symptoms occur after each malabsorbed sugar or after none (see above), are reproducible, it would theoretically mean that no patient should become symptom-free, since

physiological malabsorption of carbohydrates is essential for the colonocytes. Moreover, if the data showing that there is a beneficial effect of carbohydrate malabsorption on the short-chain free fatty acid ratio, and especially on the increase in butyrate, are confirmed[29], this might also raise doubts about whether treatment is advantageous at all in the longer term.

CONCLUSION

Carbohydrate malabsorption is a common phenomenon not only in patients, but also in healthy individuals. In patients suffering from non-specific abdominal complaints, it is therefore very difficult sometimes to clarify whether the malabsorption that has been detected is definitely the cause of the symptoms. On the other hand, many patients with these symptoms and confirmed malabsorption appear to benefit considerably from dietary interventions, thus underlining the importance of diagnosing carbohydrate malabsorption. Another advantage of diagnostic work-up, including hydrogen exhalation tests, is that the results may provide evidence of other diseases that feature in the differential diagnosis of non-specific abdominal complaints, such as intestinal bacterial overgrowth or alterations in the orocecal transit times.

As pointed out above, however, there are still a considerable number of open questions in this field, so that further controlled studies are urgently necessary. The first step for the scientific community is to accept that, in addition to the widely accepted condition of lactose malabsorption, malabsorption of other sugars such as fructose and sorbitol also occurs and may be at least as important, or perhaps even more, than lactose malabsorption.

REFERENCES

1 **Manning AP**, Thompson WG, Heaton KW, Morris AF. Towards positive diagnosis of the irritable bowel. *Br Med J* 1978; **2**: 653-654
2 **Thompson WG**, Dotevall G, Drossman DA, Heaton KW, Kruis W. Irritable bowel syndrome: guidelines for the diagnosis. *Gastroenterol Int* 1989; **2**: 92-95
3 **Hotz J,** Kark W. Non-ulcer dyspepsia syndrome. Classification, diagnostic verification, etiology and possibilities for treatment. *Med Klin* (Munich) 1992; **87**: 21-27
4 **Olubuyide IO**, Olawuyi F, Fasanmade AA. A study of irritable bowel syndrome diagnosed by Manning criteria in an African population. *Dig Dis Sci* 1995; **40**: 983-985
5 **Chang FY**, Lu CL. Irritable bowel syndrome in the 21st century: perspectives from Asia or South-east Asia. *J Gastroenterol Hepatol* 2007; **22**: 4-12
6 **Costa F**, Mumolo MG, Marchi S, Bellini M. Differential diagnosis between functional and organic intestinal disorders: is there a role for non-invasive tests? *World J Gastroenterol* 2007; **13**: 219-223
7 **Drozdowski LA**, Thomson AB. Intestinal sugar transport. *World J Gastroenterol* 2006; **12**: 1657-1670
8 **Terjung B**, Lammert F. Lactose intolerance: new aspects of an old problem. *Dtsch Med Wochenschr* 2007; **132**: 271-275
9 **Ledochowski M**, Widner B, Fuchs D. Fruktosemalabsorption. *J Ernährungsmed* 2000; **2**: 10-14
10 **Helliwell PA**, Richardson M, Affleck J, Kellett GL. Regulation of GLUT5, GLUT2 and intestinal brush-border fructose absorption by the extracellular signal-regulated kinase, p38 mitogen-activated kinase and phosphatidylinositol 3-kinase intracellular signalling pathways: implications for adaptation to diabetes. *Biochem J* 2000; **350** Pt 1: 163-169
11 **Islam MS**, Sakaguchi E. Sorbitol-based osmotic diarrhea: possible causes and mechanism of prevention investigated in rats. *World J Gastroenterol* 2006; **12**: 7635-7641
12 **Corazza GR**, Strocchi A, Rossi R, Sirola D, Gasbarrini G. Sorbitol malabsorption in normal volunteers and in patients with coeliac disease. *Gut* 1988; **29**: 44-48
13 **Rumessen JJ**. Fructose and related food carbohydrates. Sources, intake, absorption, and clinical implications. *Scand J Gastroenterol* 1992; **27**: 819-828
14 **Rumessen JJ**, Gudmand-Høyer E. Absorption capacity of fructose in healthy adults. Comparison with sucrose and its constituent monosaccharides. *Gut* 1986; **27**: 1161-1168
15 **Truswell AS**, Seach JM, Thorburn AW. Incomplete absorption of pure fructose in healthy subjects and the facilitating effect of glucose. *Am J Clin Nutr* 1988; **48**: 1424-1430
16 **Götze H**. Kohlenhydratmalabsoprtion. *TW Pädiatr* 1990; **3**: 60-66
17 **Born P**, Kamenisch W, Müller S, Paul F. Fruktosemalabsorption-Normalisierung durch Glukosezugabe. *Verdauungskrankheiten* 1991; **9**: 239-241
18 **Ravich WJ**, Bayless TM, Thomas M. Fructose: incomplete intestinal absorption in humans. *Gastroenterology* 1983; **84**: 26-29
19 **Born P**, Kamenisch W, Barina W, Paul F. Hohe Raten von Fruktose-und Sorbitmalabsorption. *Ärztl Lab* 1989; **35**: 309-310
20 **Born P**, Zech J, Stark M, Classen M, Lorenz R. Carbohydrate substitutes: comparative study of intestinal absorption of fructose, sorbitol and xylitol. *Med Klin* (Munich) 1994; **89**: 575-578
21 **Götze H**, Mahdi A. Fructose malabsorption and dysfunctional gastrointestinal manifestations. *Monatsschr Kinderheilkd* 1992; **140**: 814-817
22 **Hoekstra JH**, van Kempen AA, Bijl SB, Kneepkens CM. Fructose breath hydrogen tests. *Arch Dis Child* 1993; **68**: 136-138
23 **Jain NK**, Rosenberg DB, Ulahannan MJ, Glasser MJ, Pitchumoni CS. Sorbitol intolerance in adults. *Am J Gastroenterol* 1985; **80**: 678-681
24 **Ledochowski M**, Widner B, Bair H, Probst T, Fuchs D. Fructose- and sorbitol-reduced diet improves mood and gastrointestinal disturbances in fructose malabsorbers. *Scand J Gastroenterol* 2000; **35**: 1048-1052
25 **Ledochowski M**, Widner B, Murr C, Sperner-Unterweger B, Fuchs D. Fructose malabsorption is associated with decreased plasma tryptophan. *Scand J Gastroenterol* 2001; **36**: 367-371
26 **Marshall JK**, Thabane M, Garg AX, Clark WF, Salvadori M, Collins SM. Incidence and epidemiology of irritable bowel syndrome after a large waterborne outbreak of bacterial dysentery. *Gastroenterology* 2006; **131**: 445-450; quiz 660
27 **McKeown ES**, Parry SD, Stansfield R, Barton JR, Welfare MR. Postinfectious irritable bowel syndrome may occur after non-gastrointestinal and intestinal infection. *Neurogastroenterol Motil* 2006; **18**: 839-843
28 **Born P**, Zech J, Lehn H, Classen M, Lorenz R. Colonic bacterial activity determines the symptoms in people with fructose-malabsorption. *Hepatogastroenterology* 1995; **42**: 778-785
29 **Born P**, Bauch C, Ulm K, Kamereck K, Classen M, Scheppach W. Fecal bacterial activity in symptomatic carbohydrate malabsorption: effect on the fecal short-chain fatty acid ratio. *Z Gastroenterol* 2000; **38**: 623-626
30 **Born P**, Bauch C, Zech J, Lorenz R, Classen M. Kohlenhydratmalabsorption-die Rolle der Kolonbakterien bei der Entstehung der Symptome. *Verdauungskrankheiten* 1997; **15**: 205-208
31 **Calloway DH**, Murphy EL. The use of expired air to measure intestinal gas formation. *Ann N Y Acad Sci* 1968; **150**: 82-95
32 **Levitt MD**. Production and excretion of hydrogen gas in man. *N Engl J Med* 1969; **281**: 122-127
33 **Levitt MD**, Donaldson RM. Use of respiratory hydrogen (H2) excretion to detect carbohydrate malabsorption. *J Lab Clin Med* 1970; **75**: 937-945

34 **Symons P**, Jones MP, Kellow JE. Symptom provocation in irritable bowel syndrome. Effects of differing doses of fructose-sorbitol. *Scand J Gastroenterol* 1992; **27**: 940-944
35 **Born P**, Hannig C, Braig C, Lorenz R, Classen M. Der H2-Test Lactulose: Notwendigkeit und Probleme. *Verdauungskrankheiten* 1992; **10**: 202-205
36 **Rumessen JJ**, Nordgaard-Andersen I, Gudmand-Høyer E. Carbohydrate malabsorption: quantification by methane and hydrogen breath tests. *Scand J Gastroenterol* 1994; **29**: 826-832
37 **Hoekstra JH**, van den Aker JH, Kneepkens CM, Stellaard F, Geypens B, Ghoos YF. Evaluation of 13CO2 breath tests for the detection of fructose malabsorption. *J Lab Clin Med* 1996; **127**: 303-309
38 **Born P**, Vierling T, Paul F. Effect of diet in symptomatic fructose malabsorption. *Eur J Gastroenterol Hepatol* 1994; **6**: 701-704
39 **Fernández-Bañares F**, Rosinach M, Esteve M, Forné M, Espinós JC, Maria Viver J. Sugar malabsorption in functional abdominal bloating: a pilot study on the long-term effect of dietary treatment. *Clin Nutr* 2006; **25**: 824-831
40 **Shepherd SJ**, Gibson PR. Fructose malabsorption and symptoms of irritable bowel syndrome: guidelines for effective dietary management. *J Am Diet Assoc* 2006; **106**: 1631-1639
41 **Janetschek P**, Gantert F, Böckmann U. Malabsorption and impact of diet: underestimated relevance in the diagnosis of dyspeptic symptoms (abstract). *Gut* 2001; **49** (Suppl III): 2122
42 **Born P**, Sekatcheva M, Rösch T, Classen M. Carbohydrate malabsorption in clinical routine: a prospective observational study. *Hepatogastroenterology* 2006; **53**: 673-677
43 **Parker TJ**, Woolner JT, Prevost AT, Tuffnell Q, Shorthouse M, Hunter JO. Irritable bowel syndrome: is the search for lactose intolerance justified? *Eur J Gastroenterol Hepatol* 2001; **13**: 219-225
44 **Fritz E**, Hammer J, Vogelsang H. Fructose-free diet does not improve GI symptoms in fructose-intolerant patients if irritable bowel syndrome is reported. *Z Gastroenterol* 2002; **40**: G20
45 **Pimentel M**, Park S, Mirocha J, Kane SV, Kong Y. The effect of a nonabsorbed oral antibiotic (rifaximin) on the symptoms of the irritable bowel syndrome: a randomized trial. *Ann Intern Med* 2006; **145**: 557-563
46 **Lembcke B**, Fölsch UR, Caspary WF, Ebert R, Creutzfeldt W. Influence of metronidazole on the breath hydrogen response and symptoms in acarbose-induced malabsorption of sucrose. *Digestion* 1982; **25**: 186-193
47 **Dear KL**, Elia M, Hunter JO. Do interventions which reduce colonic bacterial fermentation improve symptoms of irritable bowel syndrome? *Dig Dis Sci* 2005; **50**: 758-766
48 **Schutz E**. The treatment of intestinal diseases with Mutaflor. A multicenter retrospective study. *Fortschr Med* 1989; **107**: 599-602

S- Editor Liu Y **L- Editor** Kerr C **E- Editor** Yin DH

Online Submissions: wjg.wjgnet.com
www.wjgnet.com
wjg@wjgnet.com

World J Gastroenterol 2007 November 21; 13(43): 5692-5698
World Journal of Gastroenterology ISSN 1007-9327

GASTRIC CANCER

Metastatic suppressor genes inactivated by aberrant methylation in gastric cancer

Jian-Feng Wang, Dong-Qiu Dai

Jian-Feng Wang, Department of Surgical Oncology, the First Affiliated Hospital, China Medical University, Dalian University Affiliated Xinhua Hospital, Shenyang 110001, Liaoning Province, China
Dong-Qiu Dai, Department of Surgical Oncology, the First Affiliated Hospital, China Medical University, Shenyang 110001, Liaoning Province, China
Supported by the National Natural Science Foundation of China, No.30271477 and No.30572162; and the Special Scientific Research Foundation for Doctors, State Education Ministry, No.20050159001
Correspondence to: Dong-Qiu Dai, Department of Surgical Oncology, the First Affiliated Hospital, China Medical University, Shenyang 110001, Liaoning Province, China. daidq63@163.com
Telephone: +86-24-83283555
Received: June 28, 2007 Revised: August 8, 2007

Abstract

AIM: To screen out the differentially methylated DNA sequences between gastric primary tumor and metastatic lymph nodes, test the methylation difference of gene *PTPRG* between primary gastric tumor and metastatic lymph nodes, and test the regulatory function of 5-aza-2-deoxycytidine which is an agent with suppression on methylation and the level of methylation in gastric cancer cell line.

METHODS: Methylated DNA sequences in genome were enriched with methylated CpG islands amplification (MCA) to undergo representational difference analysis (RDA), with MCA production of metastatic lymph nodes as tester and that of primary tumor as driver. The obtained differentially methylated fragments were cloned and sequenced to acquire the base sequence, which was analyzed with bioinformatics. With methylation-specific PCR (MSP) and RT-PCR, methylation difference of gene *PTPRG* was detected between primary tumor and metastatic lymph nodes in 36 cases of gastric cancer. Methylation of gene *PTPRG* and its regulated expression were observed in gastric cancer cell line before and after being treated with methylation-suppressive agent.

RESULTS: Nineteen differentially methylated sequences were obtained and located at 5′ end, exons, introns and 3′ end, in which KL59 was observed to be located at 9p21 as the first exon of gene *p16* and KL22 to be located at promoter region of *PRPRG*. KL22, as the probes, was hybridized with driver, tester and 3-round RDA products respectively with all positive signals except with the driver. Significant difference was observed in both methylation rate of gene *PTPRG* and PTPRG mRNA expression rate between primary tumor and metastatic lymph nodes. Demethylation of gene *PTPRG*, with recovered expression of PTPRG mRNA, was observed after gastric cancer cell line being treated with methylation-suppressive agent.

CONCLUSION: Difference exists in DNA methylation between primary tumor and metastatic lymph nodes of gastric cancer, with MCA-RDA as one of the good analytical methods. Significant difference exists in methylation of gene *PTPRG* between primary tumor and metastatic lymph nodes of gastric cancer. Methylation level in gastric cancer cell line can be decreased by 5-aza-2′-deoxycytidine, which is the methylation-suppressive agent, with PTPRG expression being recovered.

Key words: Gastric cancer; Methylated CpG islands amplification; Representational difference analysis; DNA methylation; gene *PTPRG*

Wang JF, Dai DQ. Metastatic suppressor genes inactivated by aberrant methylation in gastric cancer. *World J Gastroenterol* 2007; 13(43): 5692-5698

http://www.wjgnet.com/1007-9327/13/5692.asp

INTRODUCTION

Metastasis of gastric cancer, at the genetic level, is caused by mutations or loss of corresponding cancer suppressor genes, while at epigenetic level it is caused by low expression of metastasis-suppression genes due to multiple reasons, in which gene hypermethylation is an important mechanism[1-3]. A genome with methylation at CpG is usually accompanied by inactivation of genes in that region. If not, on the contrary, it is usually accompanied by active expression of genes in the region. The aberrant hypermethylation of CpG islands in transcription regulatory region of metastasis-inhibition genes relating to gastric cancer causes these genes to be in silence and this fact will induce the metastasis of gastric cancer[4-6]. Most of previous analytic methods on methylation can only analyze the methylation condition of a known gene,

but cannot analyze that of a whole genome. Methylated CpG islands amplification (MCA) methods, combined with representative difference analysis (RDA), can analyze effectively the condition of methylation in a whole genome, especially good at detecting unknown methylated fragments.

In this research, gene methylation difference was detected between primary tumor and metastatic lymph nodes of gastric cancer using MCA-RDA method, to screen out genes relating to metastasis of gastric cancer, which further underwent analysis on methylation difference with methods, including methylation-specific PCR, in order to define further the mechanism of metastasis of gastric cancer.

MATERIALS AND METHODS

Subjects

Pathological specimens, including tumor tissues and metastatic lymph nodes, taken from 36 gastric cancer patients hospitalized in Surgical Oncology Ward of the First Affiliated Hospital of China Medical University, were included in this study. The tumor tissues and suspected metastatic lymph nodes, after resecting from the patients, were promptly placed into a liquid nitrogen tank. Each tumor tissue and lymph node was cut into two pieces, one piece was kept in liquid nitrogen and the other underwent HE pathological staining to examine whether a true metastasis had occurred. In addition, gastric cancer line SGC7901 was also included in this study.

Extraction of DNA and total RNA

Hydroxybenzene-chloroform extraction method was adopted to extract DNA of the genome, and total RNA was extracted with TRIZOL reagent according to the manufacturer's instruction.

MCA

MCA was adopted to obtain CpG islands enriched with methylation. The CpG island region of DNA mixture extracted from tumor tissues and metastatic lymph nodes of 5 cases of gastric cancer were enriched with MCA, respectively. Firstly, 5 μg of DNA of genome was digested with 100U *Sma*I endonuclease (provided by NEB, not functional on methylated sites) for 6 h to cut the unmethylated -CCCGGG- sites to form the blunt ends, and also digested with 20U *Xma*I enzyme (provided by NEB) for 16 h to cut the methylated -CCCGGG- sites to form the sticky -CCCGGG- ends. Then T4DNA (Promega) was used to connect corresponding adaptor RXMA 24/12, with RXMA24 fragment as the primer to amplify the DNA fragments with adaptor, which were incubated for 5 min at 72℃, followed by pre-denaturalization for 3 min at 95℃, 30 amplification cycles for 1 min at 95℃ and 3 min at 72℃, and a final extension for 10 min at 72℃, to enrich methylated fragments of DNA from both tumor tissues and metastatic lymph nodes. The products were electrophoresed on 15 g/L agarose gel containing ethidium bromide[7].

Table 1 Adaptor used in MCA-RDA and their sequence

Adaptor	Sequence
RXMA24	5'-AGCACTCTCCAGCCTCTCACCGAC-3'
RXMA12	5'-CCGGGTCGGTGA-3'
JXMA24	5'-ACCGACGTCGACTATCCATGAACC-3'
JXMA12	5'-CCGGGGTTCATG -3'
NMCA24	5'-GTTAGCGGACACAGGGCGGGTCAC-3'
NMCA12	5'-CCGGGTGACCCG-3'

RDA

The methylated DNA fragments obtained from tumor and metastatic lymph nodes were underwent representative difference analysis. The adaptor of methylated CpG fragments taken from tumor and metastatic lymph nodes was cut-off with *Sma*I being used for tumor tissue to form blunt ends as the driver, and with *Xma*I being used for metastatic lymph nodes to form sticky ends to be connected with new ends as the tester. Tester and driver were underwent 3 cycles of hybridization RDA analysis in a ratio of 1:80, 1:400 and 1:800, respectively. After each analysis, the adaptor was cut off with *Xma*I, with new adaptor being added. The adaptors used in the 3 cycles of analysis were NMCA24/12, JXMA24/12 and NMCA24/12, with different extension temperature for different connectors. The sequence of each connector is listed in Table 1. The products were analyzed on 15 g/L agarose gel containing ethidium bromide[8].

Cloning, sequencing and analysis of similarity

Products of the 3rd cycle of RDA analysis as well as pCAT®3-Control carrier (Promega) were treated with *Xma*I to cut their ends into sticky ones, which were connected with T4 ligase and transformed into competent bacteria JM109 for incubation with matrix containing Ampicillin. Positive clones were selected and cultivated in matrix containing antibiotics at 37℃. Then plasmid DNA was extracted, and was underwent to cleavage with *Xma*I, and to electrophoresis; then the more than 100 bp and the clones of more than 100 bp cleavage products were selected and delivered to bio-company (Combined Gene Company) for sequencing. The obtained sequence were underwent repeated sequence analysis with Repeatmasker. BLAST system was used to carry out similarity analysis, with relationship between cloned sequence and corresponding genes being analyzed *via* GenBank.

Dot blot

The differentially methylated fragments of KL22 obtained from MCA-RDA analysis were labeled with digoxin, using random primer method to form the probe. With this latter hybridization analysis was carried out on the 1st, 2nd, 3rd round RDA. MCA products of tumor or metastatic lymph nodes, respectively, in a volume of 5 μL for each sample, were dotted onto nylon membrane with positive electricity.

Cell cultivation and methylation intervention

Gastric cancer cell line was subcultured according to

Table 2 MSP primers of gene *PTPRG*

Methylated primers	5'-GTTCGTTCGTTTTTTCGTTC-3' 5'-CATACTCCTAAAAATTATAACTCCGAC-3'
Unmethylated primers	5'-TTTTGTTTGTTTGTTTTTTTGTTTG-3' 5'-AATCCATACTCCTAAAAATTATAACTCCA-3'

Table 3 RT-PCR primers of *PTPRG* gene

PTPRG primer	5'-CTAATAAGGGATGTTCACATGAAGC-3' 5'-CTGTATTTTAATGGAGTGGATAGCA-3'
β-actin primer	5'-AAATCGTGCGTGACATTAA-3' 5'-CTCGTCATACTCCTGCTTG-3'

standard methods and then randomized into two groups, one of them was treated with 5 μmol/L 5-Aza-2'-deoxycytidine and cultured for 5 d.

Methylation-specific PCR (MSP)

Sodium hydrogen sulfite was used for DNA modification, and then sodium hydrogen sulfite was eliminated from DNA with Wizard DNA Clean-up kit (Promega). The samples were amplified through 30 cycles, each amplification cycle consisting of denaturation at 95℃ for 40 s, primers annealing at 65℃ (unmethylation) or at 60℃ (methylation) for 40 s and extension at 72℃ for 60 s. Cycles were preceded by incubation at 95℃ for 3 min to ensure full denaturation of the target gene, and finally by an extra incubation at 72℃ for 10 min to ensure full extension of the products. PCR was carried out with methylated primer and unmethylated primer, respectively. The primers adopted are listed in Table 2. The PCR products were analyzed on 20 g/L agarose gel[9].

RT-PCR

RNA was reverse transcribed into cDNA as the template, which was amplified through 30 cycles, each amplification cycle consisting of denaturation at 94℃ for 40 s, primers annealing at 57℃ for 30 s and extension at 72℃ for 60 s. Cycles were preceded by incubation at 94℃ for 2 min to ensure full denaturation of the target gene, and finally by an extra incubation at 72℃ for 10 min to ensure full extension of the products.

Meanwhile, β-actin was adopted as internal control. The sequences of primers are listed in Table 3. The products were electrophoresed on 15 g/L agarose gel.

Statistical analysis

Chi-square test was adopted to verify the difference of PTPRG methylation rate and PTPRG mRNA expression between gastric tumor and metastatic lymph nodes, as well as the difference on absent expression of PTPRG mRNA between negative and positive group of methylated nodular PTPRG. Rectilinear regression was used to test the correlation between PTPRG methylation rate and metastatic lymph nodes number. SPSS11.0 software was used to process the data.

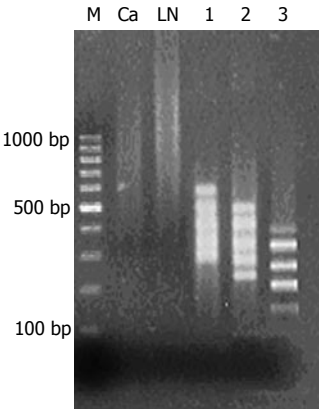

Figure 1 Methylated CpG islands amplification (MCA) and representational difference analysis (RDA). M: Marker; Ca: MCA products of gastric cancer tissues; LN: MCA products of metastatic lymph nodes; lanes 1-3: The 1st to the 3rd round RDA products. After methylated CpG islands amplification (MCA) of genome DNA of primary tumor and metastatic lymph nodes, bright smears were observed between 300 bp and 2000 bp, which were the concentrated methylated CpG islands. From the 1st to the 3rd cycle of analysis, fragments with methylation difference decreased gradually and the straps gradually became clear. In the 3rd RDA analysis, 5 straps of different methylation were observed.

RESULTS

MCA

After methylated CpG islands amplification (MCA) of genome DNA of primary tumor and metastatic lymph nodes, bright smear was observed between 300 and 2000 bp, which were the concentrated methylated CpG islands (Figure 1).

RDA

MCA products of metastatic lymph nodes were adopted as the tester and MCA products of primary tumor as the driver to carry out 3 cycles of RDA analysis, which resulted in 100-500-bp fragments with methylation difference. From the 1st to the 3rd cycle of analysis, fragments with methylation difference decreased gradually and the straps gradually became clear. In the 3rd RDA analysis, 5 straps of different methylation were observed (Figure 1).

Cloning, sequencing and analysis on homology

Ninety-six positive clones were selected to undergo sequencing analysis, 19 of them demonstrated the sequence longer than 100 bp. KL8 appeared for 21 times, while KL22 11 times, KL59 4 times, and both KL40 and KL71 for twice. No repeated sequence, such as ALU, was found after repeated sequencing analysis. Table 4 shows the 19 sequence characteristics. All sequences were of length between 100 bp and 400 bp, with GC content beyond 50%. Analysis showed these fragments to be distributed into various regions in the genome, including 5' ends, exons, introns and 3' ends, in which KL59 was situated at 9p21 as the first extron of gene *p16*, with 100% similarity rate, and KL22 was situated at 3p21, in the promoter region of gene *PTPRG*.

Dot blot

KL122 sequence was labeled with digoxin to form the

Table 4 Features of fragments with different methylation

Fragment	Length (bp)	GC %	CpG/GpC	Chromosome Positioning	Similarity rate %	S	E
KL2	198	55.0	0.5625	1q23.1	100	404	e-110
KL5	106	71.2	0.7142	15	100	222	e-56
KL6	159	59.4	1.0714	1p36.31-36.23	98	141	2e-31
KL8	194	61.1	0.8461	2q33.3	99	396	e-108
KL14	347	72.3	0.9811	4p15	100	585	e-165
KL19	258	58.3	0.7692	5p15.1	97	480	e-133
KL22	332	64.1	0.7027	3p21	99	527	e-147
KL23	287	70.7	1.0606	1q42.1-43	98	458	e-126
KL33	136	53.2	0.9629	2p24.3-24.1	100	129	6e-28
KL40	255	66.2	1.1428	4p16.1	99	404	e-110
KL55	268	65.6	0.7894	18	92	231	e-152
KL59	282	64.5	0.6471	9p21	100	571	e-160
KL68	251	62.5	0.6000	4	87	173	4e-39
KL71	213	69.9	0.8260	10p12.1	100	434	e-119
KL74	341	69.5	0.7317	9p21	99	668	0
KL79	225	61.3	0.4782	13q13	98	458	e-127
KL82	403	67.4	0.8043	8q21.2	99	383	e-104
KL87	275	51.9	1.0000	11	97	515	e-144
KL95	360	70.8	0.7608	Xp22.3	100	726	0

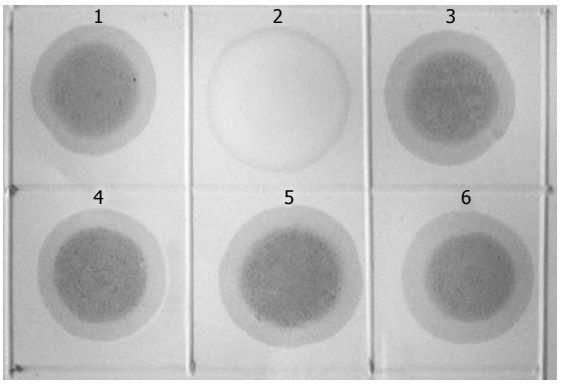

Figure 2 Dot blot analysis. 1: Positive control; 2: MCA products of gastric cancer tissues; 3: MCA products of metastatic lymph nodes; and 4-6: the first to the third round RDA products. KL122 sequence was labeled with digoxin to form the probe; with this latter the three rounds MCA-RDA products were undergone hybridization analysis with testers and drivers. Positive results were observed in all products of the three-round RDA as well as in testers, while negative one in drivers.

probe, with which the three rounds MCA-RDA products underwent hybridization analysis with testers and drivers. Positive results were observed in all products of the 3-round RDA as well as in testers, while negative one in drivers (Figure 2).

Gene PTPRG methylation rate of primary tumor and metastatic lymph nodes of gastric cancer

A positive band was observed at 158 bp of non-methylation PCR of primary tumor, with a positive rate of 77.78% (28/36), while that of metastatic lymph nodes was 63.89% (23/36) ($P > 0.05$). A positive strap was observed at 150 bp of methylation PCR of metastatic lymph nodes, with a positive rate of 52.78% (19/36), while that of primary tumor was 25.0% (9/36) ($P < 0.05$) (Figure 3 and Table 5). Linear correlation was observed between MSP positive rate of metastatic lymph nodes and the number of metastatic nodes ($r = 0.882$, $P < 0.001$, Figure 4).

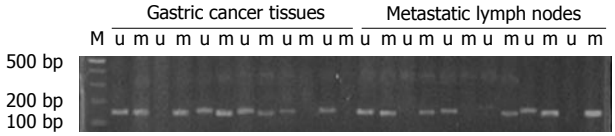

Figure 3 Methylation-specific PCR (MSP) of gene *PTPRG*. M: Marker; u: Unmethylated (158 bp); m: Methylated (150 bp). A positive band was observed at 158 bp of non-methylation PCR of primary tumor, with a positive rate of 77.78% (28/36), while that of metastatic lymph nodes was 63.89% (23/36). A positive strap was observed at 150 bp of methylation PCR of metastatic lymph nodes, with a positive rate of 52.78% (19/36), while that of primary tumor was 25.0% (9/36) ($P < 0.05$).

Table 5 Methylation and mRNA expression of gene *PTPRG n* (%)

Tissue	*PTPRG* gene methylation		PTPRG mRNA expression
	U	M	
Primary tumor	28 (77.78)	9 (25.0)	18 (50.0)
Metastatic lymph nodes	23 (63.89)	19 (52.78)[a]	9 (25.0)[a]
Before cell line treatment	+	+	-
After cell line treatment	+	-	+

[a]$P < 0.05$. U: Unmethylation; M: Methylation.

A positive strap was observed at 177 bp in RT-PCR of gene *PTPRG* of primary tumor, with a positive rate of 50.0% (18/36) and a 177-bp positive band was observed in metastatic lymph nodes, with a positive rate of 25.0% (9/36) ($P < 0.05$), (Figure 5, Table 5).

Relationship between methylation of PTPRG in metastatic lymph nodes and absent expression of mRNA

Among 19 cases of positive PTPRG methylation in metastatic lymph nodes, there was only one case of positive expression of PTPRG mRNA, with the positive rate of 5.26%, while 9 cases of positive expression existed among 17 cases of negative PTPRG methylation, with the positive rate of 52.9% ($P < 0.01$), (Table 6).

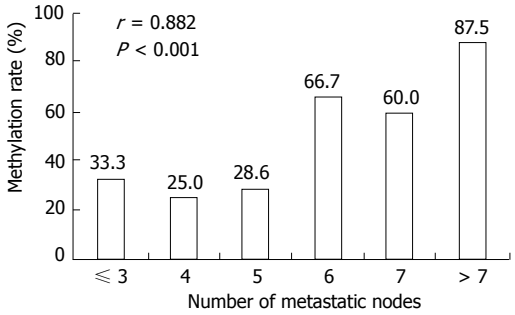

Figure 4 Relationship between number of metastatic lymph nodes and positive rate of PTPRG methylation.

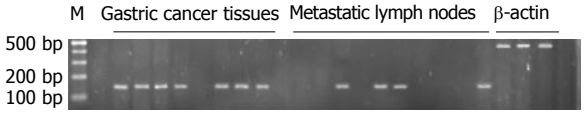

Figure 5 PTPRG mRNA expression of gastric cancer tissues and metastatic lymph nodes. M: Marker. Gastric cancer tissues: Products of *PTPRG* gene (177 bp) of gastric cancer tissues; Metastatic lymph nodes: Products of *PTPRG* gene (177 bp) of metastatic lymph nodes; β-actin: 483 bp. RT-PCR showed a positive strap at 177 bp in gene *PTPRG* of primary tumor, with a positive rate of 50.0% (18/36), while a 177-bp positive band was observed in metastatic lymph nodes, with a positive rate of 25.0% (9/36) ($P < 0.05$).

PTPRG methylation level and its mRNA expression in gastric cell line SGC7901 before and after the treatment with 5-aza-2'-deoxycytidine

Before the treatment, a positive band was observed at 158 bp in unmethylated PCR, while a positive band was seen at 150 bp in methylated PCR of gastric cancer cell line. After the treatment, a positive band was also observed at 158 bp in unmethylated PCR, but no positive band was seen in methylated PCR (Figure 6, Table 5). PTPRG mRNA expression of cell line was negative before treatment, while a weak positive band was seen at 177 bp after treatment (Figure 7, Table 5).

DISCUSSION

Based on previous researches, a group containing methyl exists in every 100 nucleotide acids in human DNA, which is usually combined onto 5'-C position. Almost all methylated cytosine residues appear on the 5'-GC-3' nucleotide acid in the symmetrical sequence. This kind of sequence is not randomly distributed, but concentrated to GC-enriched islands (CpG islands), which usually situates at the position in or near transcription regulatory region. Sensitivity of methylation on all CpG is not the same, and the methylation level at the site of CpG can be changed[10-12]. Prevalent hypomethylation and local hypermethylation exist in genome of cancer tissue, for example, hypermethylation on promoters of p16, E-cadherin, and genes encoding hormone receptors and genes of DNA repair, and genes inhibiting the genesis of blood vessels may induce the absent or low expression of these gene and improve the oncogenesis and metastasis. Therefore, research on methylation of genome provides a new route to study the oncogenesis and metastasis of cancer[13-17].

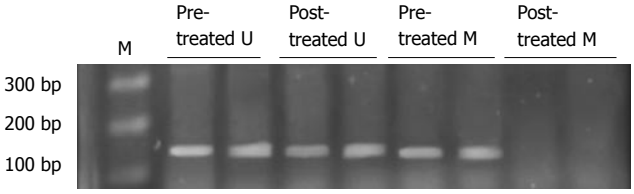

Figure 6 Methylation-specific PCR (MSP) of gene *PTPRG* in gastric cell line before and after the treatment with 5-aza-2'-deoxycytidine. M: Marker; U: Unmethylated; M: Methylated. Before the treatment, a positive band was observed at 158 bp in unmethylated PCR, while a positive band was seen at 150 bp in methylated PCR of gastric cancer cell line. After the treatment, a positive band was also observed at 158 bp in unmethylated PCR, but no positive band was seen in methylated PCR.

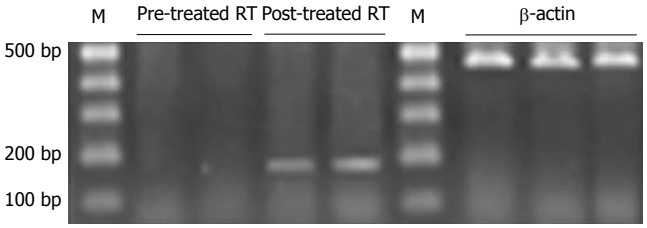

Figure 7 PTPRG mRNA expression of cell line before and after the treatment with 5-aza-2'-deoxycytidine. M: Marker; Pre-treated RT: PTPRG mRNA expression before the treatment with 5-aza-2'-deoxycytidine; Post-treated RT: PTPRG mRNA expression after the treatment with 5-aza-2'-deoxycytidine.

Table 6 The relationship between PTPRG methylation in metastatic lymph nodes and absent expression of mRNA.

PTPRG methylation	PTPRG mRNA expression (%)	
	+	-
+	1 (5.26)	18 (94.73)
-	9 (52.94)	8 (47.05)

$\chi^2 = 10.17$, $P < 0.01$.

MCA technique is a new approach which has recently been adopted for research on gene methylation, which can be applied promptly and efficiently to the research on the whole genome methylation, with specific advantage especially for research on methylation condition of various unknown genes. Through the optimization of PCR condition, it is almost fit for every gene containing two adjacent *Sma*I restriction sites. The content of CpG is different in CpG islands, so different PCR primers and reaction conditions are needed, such as RXMA and RMCA. Thus RXMA seems to be more fit for this research. Through the optimization on the reaction condition, RXMA may yield MCA product steadily. It needs to point out that high quality sample of DNA is needed for MCA experiment, so generally wax-embedded sample is not considered in the case, in which only some sites can be detected, but not in total, among all sites in the CpG islands, which is only sensitive to partially digested products by *Sma*I, with distance shorter than 1000

bp between every two *Sma*I constriction sites. Generally speaking, GC content of MCA's products is high; in this case if only an optimized PCR reaction system is adopted with high GC content, a satisfactory result can be made. RDA is a relatively mature technique adopted to screen out accurately the different fragments between two groups of DNA. In this research, we combined MCA and RDA to screen out the differentially methylated fragments between primary tumor and metastatic lymph nodes of gastric cancer, to explore the gene with alteration in methylation involved within process of metastatic lymph nodes. It provides a relatively accurate method with high efficiency, and it is fit for the primary screening out large quantities of metastasis-suppressive genes. It may be considered a high flux analytical method.

Phosphorylation of tyrosine residue is the important characteristic of many cellular signals transmission, influencing a number of vital biological processes including growth and differentiation of cells, adjustment of cell cycle, cell apoptosis and transference. Phosphorylation and dephosphorylation of tyrosine are adjusted by tyrosine kinase (TK) and tyrosine phosphatase (TP), respectively. Despite several tyrosine kinases have been recognized to correlate to oncogenesis directly through activating the mutant of cells *in vivo*, only a small amount of tyrosine phosphatase is known to correlate oncogenesis[18,19]. Gene *PTPRG* is a member belonging to the classic tyrosine phosphatase gene family, which includes receptor genes and non-receptor genes. *PTPRG* is a member of receptor gene, and is situated at 3p14 chromosome[20-22]. Previous researches observed methylation extinguishments of other genes that belong to the same family of *PTPRG*, such as *PTPRN2*, *PTPRO*, *etc*, in hepatic cancer[23]. *PTPRG* mutation is often found in colon cancer, lung cancer and kidney cancer, with conclusive identification on the role of *PTPRG* as one of tumor-inhibition genes[18,24]. However, there is a little information in literature regarding the extinguishments of *PTPRG* on epigenetic level. Based on recent studies, its deactivation on epigenetic level occurs in skin T-cell lymphoma. A study has demonstrated that a significant difference exists on *PTPRG* methylation in metastatic lymph nodes compared to primary tumor[9]. The silencing of genomic induced by methylation mainly consists of the methylation in promoter and in the first exon[9].

Methylation-specific PCR (MSP) revealed a significant difference in the positive methylation rate of PRPGR in primary tumor of gastric cancer (25.0%) compared to in metastatic lymph nodes (52.78%) ($P < 0.05$)[25,26]; this fact which further proved that the differentially methylated fragments we screened out were accurate. The significant linear correlation existing between positive rates of methylated *PTPRG* and numbers of metastatic nodes suggests that there is certain relationship between *PTPRG* methylation and metastatic lymph nodes of gastric cancer. In addition, a significant difference in *PTPRG* mRNA expression was observed between primary gastric tumor and metastatic lymph nodes, suggesting that product of *PTPRG* gene exerts suppressive effect against metastatic lymph nodes of gastric cancer. It is because of the down-regulated PTPRG, that the metastatic lymph nodes of gastric cancer was promoted.

PTPRG methylation exists in gastric cancer cell line. RT-PCR analysis demonstrated that PTPRG is not expressed in the cell line. However, MSP result of the cell line was negative and RT-PCR result was weakly positive after treatment with 5-aza-2'-deoxycytidine as the methylation suppressor; this fact, suggested that methylation of this gene was suppressed after the treatment with 5-aza-2'-deoxycytidine, so the MSP result was negative and the expression of PTPRG was partially recovered[27,28].

Among all 19 cases of positive methylation of PTPRG in metastatic lymph nodes, there was only one case of positive expression of PTPRG mRNA (positive rate of 5.26%), while among 17 cases of negative methylation of PTPRG, there were 9 cases of positive expression of PTPRG mRNA (positive rate of 52.9%) ($P < 0.05$); this result further implies that methylation in promoter region of PTPRG might be the mechanism of its being distinguished. However, the concrete mechanism of this gene involved in metastatic lymph nodes of gastric cancer is not clear yet, and it is waiting for the further research.

COMMENTS

Background

Metastasis of gastric cancer, at the genetic level, is caused by mutation or loss of corresponding cancer suppressor genes, while at epigenetic level it is caused by low expression of metastasis-suppression genes due to multiple reasons, among which gene hypermethylation is an important mechanism.

Research frontiers

Methylated CpG islands amplification (MCA) methods, combined with representative difference analysis (RDA), can analyze wholly and effectively the condition of methylation in a whole genome, especially good at detecting unknown methylated fragments.

Innovations and breakthroughs

In this research, gene methylation difference was detected between primary tumor and metastatic lymph nodes of gastric cancer using MCA-RDA method, to screen out genes relating to metastasis of gastric cancer, which further underwent analysis on methylation difference by methylation specific PCR, in order to define further the mechanism of metastasis of gastric cancer.

Applications

This observation might be of potential value in gene therapy of gastric cancer.

Peer review

The manuscript looked at the potential role of the *PTPRG* gene as metastatic suppressor gene, by comparing methylation status and LOI between the primary tumor and lymph nodes metastasis in 36 cases. Additionally, gastric cancer cell line was treated with 5-aza-2'-deoxycytidine (inhibitor of methylation) and gene expression was investigated. This study proved the hypothesis by demonstrating a significant difference in the level of methylation between the primary tumor and metastasis.

REFERENCES

1 **Toyota M**, Itoh F, Imai K. DNA methylation and gastrointestinal malignancies: functional consequences and clinical implications. *J Gastroenterol* 2000; **35**: 727-734

2 **Rashid A**, Shen L, Morris JS, Issa JP, Hamilton SR. CpG island methylation in colorectal adenomas. *Am J Pathol* 2001; **159**: 1129-1135

3 **Cowled P**, Kanter I, Leonardos L, Jackson P. Uroplakin Ib gene transcription in urothelial tumor cells is regulated by CpG methylation. *Neoplasia* 2005; **7**: 1091-1103

4 **Teodoridis JM**, Hall J, Marsh S, Kannall HD, Smyth C, Curto J, Siddiqui N, Gabra H, McLeod HL, Strathdee G, Brown R. CpG island methylation of DNA damage response genes in advanced ovarian cancer. *Cancer Res* 2005; **65**: 8961-8967

5 **Costello JF**, Frühwald MC, Smiraglia DJ, Rush LJ, Robertson GP, Gao X, Wright FA, Feramisco JD, Peltomäki P, Lang JC, Schuller DE, Yu L, Bloomfield CD, Caligiuri MA, Yates A, Nishikawa R, Su Huang H, Petrelli NJ, Zhang X, O'Dorisio MS, Held WA, Cavenee WK, Plass C. Aberrant CpG-island methylation has non-random and tumour-type-specific patterns. *Nat Genet* 2000; **24**: 132-138

6 **Toyota M**, Ahuja N, Suzuki H, Itoh F, Ohe-Toyota M, Imai K, Baylin SB, Issa JP. Aberrant methylation in gastric cancer associated with the CpG island methylator phenotype. *Cancer Res* 1999; **59**: 5438-5442

7 **Toyota M**, Ho C, Ahuja N, Jair KW, Li Q, Ohe-Toyota M, Baylin SB, Issa JP. Identification of differentially methylated sequences in colorectal cancer by methylated CpG island amplification. *Cancer Res* 1999; **59**: 2307-2312

8 **Lisitsyn N**, Lisitsyn N, Wigler M. Cloning the differences between two complex genomes. *Science* 1993; **259**: 946-951

9 **Esteller M**, Hamilton SR, Burger PC, Baylin SB, Herman JG. Inactivation of the DNA repair gene O6-methylguanine-DNA methyltransferase by promoter hypermethylation is a common event in primary human neoplasia. *Cancer Res* 1999; **59**: 793-797

10 **Siegfried Z**, Cedar H. DNA methylation: a molecular lock. *Curr Biol* 1997; **7**: R305-R307

11 **Tycko B**. Epigenetic gene silencing in cancer. *J Clin Invest* 2000; **105**: 401-407

12 **Catteau A**, Harris WH, Xu CF, Solomon E. Methylation of the BRCA1 promoter region in sporadic breast and ovarian cancer: correlation with disease characteristics. *Oncogene* 1999; **18**: 1957-1965

13 **Jaenisch R**, Bird A. Epigenetic regulation of gene expression: how the genome integrates intrinsic and environmental signals. *Nat Genet* 2003; **33** Suppl: 245-254

14 **Dong C**, Yoon W, Goldschmidt-Clermont PJ. DNA methylation and atherosclerosis. *J Nutr* 2002; **132**: 2406S-2409S

15 **Robertson KD**, Jones PA. DNA methylation: past, present and future directions. *Carcinogenesis* 2000; **21**: 461-467

16 **Choi IS**, Wu TT. Epigenetic alterations in gastric carcinogenesis. *Cell Res* 2005; **15**: 247-254

17 **Issa JP**. Epigenetic variation and human disease. *J Nutr* 2002; **132**: 2388S-2392S

18 **Wang Z**, Shen D, Parsons DW, Bardelli A, Sager J, Szabo S, Ptak J, Silliman N, Peters BA, van der Heijden MS, Parmigiani G, Yan H, Wang TL, Riggins G, Powell SM, Willson JK, Markowitz S, Kinzler KW, Vogelstein B, Velculescu VE. Mutational analysis of the tyrosine phosphatome in colorectal cancers. *Science* 2004; **304**: 1164-1166

19 **van Doorn R**, Zoutman WH, Dijkman R, de Menezes RX, Commandeur S, Mulder AA, van der Velden PA, Vermeer MH, Willemze R, Yan PS, Huang TH, Tensen CP. Epigenetic profiling of cutaneous T-cell lymphoma: promoter hypermethylation of multiple tumor suppressor genes including BCL7a, PTPRG, and p73. *J Clin Oncol* 2005; **23**: 3886-3896

20 **Van Poucke M**, Yerle M, Chardon P, Jacobs K, Genêt C, Mattheeuws M, Van Zeveren A, Peelman LJ. A refined comparative map between porcine chromosome 13 and human chromosome 3. *Cytogenet Genome Res* 2003; **102**: 133-138

21 **Kholodnyuk ID**, Szeles A, Yang Y, Klein G, Imreh S. Inactivation of the human fragile histidine triad gene at 3p14.2 in monochromosomal human/mouse microcell hybrid-derived severe combined immunodeficient mouse tumors. *Cancer Res* 2000; **60**: 7119-7125

22 **Matsuyama A**, Shiraishi T, Trapasso F, Kuroki T, Alder H, Mori M, Huebner K, Croce CM. Fragile site orthologs FHIT/FRA3B and Fhit/Fra14A2: evolutionarily conserved but highly recombinogenic. *Proc Natl Acad Sci USA* 2003; **100**: 14988-14993

23 **Motiwala T**, Ghoshal K, Das A, Majumder S, Weichenhan D, Wu YZ, Holman K, James SJ, Jacob ST, Plass C. Suppression of the protein tyrosine phosphatase receptor type O gene (PTPRO) by methylation in hepatocellular carcinomas. *Oncogene* 2003; **22**: 6319-6331

24 **LaForgia S**, Morse B, Levy J, Barnea G, Cannizzaro LA, Li F, Nowell PC, Boghosian-Sell L, Glick J, Weston A. Receptor protein-tyrosine phosphatase gamma is a candidate tumor suppressor gene at human chromosome region 3p21. *Proc Natl Acad Sci USA* 1991; **88**: 5036-5040

25 **Herman JG**, Graff JR, Myöhänen S, Nelkin BD, Baylin SB. Methylation-specific PCR: a novel PCR assay for methylation status of CpG islands. *Proc Natl Acad Sci USA* 1996; **93**: 9821-9826

26 **Deng G**, Chen A, Hong J, Chae HS, Kim YS. Methylation of CpG in a small region of the hMLH1 promoter invariably correlates with the absence of gene expression. *Cancer Res* 1999; **59**: 2029-2033

27 **Fang JY**, Lu J, Chen YX, Yang L. Effects of DNA methylation on expression of tumor suppressor genes and proto-oncogene in human colon cancer cell lines. *World J Gastroenterol* 2003; **9**: 1976-1980

28 **Liu LH**, Xiao WH, Liu WW. Effect of 5-Aza-2'-deoxycytidine on the P16 tumor suppressor gene in hepatocellular carcinoma cell line HepG2. *World J Gastroenterol* 2001; **7**: 131-135

S- Editor Liu Y **L- Editor** Kumar M **E- Editor** Li HY

Online Submissions: wjg.wjgnet.com
www.wjgnet.com
wjg@wjgnet.com

World J Gastroenterol 2007 November 21; 13(43): 5699-5706
World Journal of Gastroenterology ISSN 1007-9327

Characteristics and pathological mechanism on magnetic resonance diffusion-weighted imaging after chemoembolization in rabbit liver VX-2 tumor model

You-Hong Yuan, En-Hua Xiao, Jian-Bin Liu, Zhong He, Ke Jin, Cong Ma, Jun Xiang, Jian-Hua Xiao, Wei-Jian Chen

You-Hong Yuan, Jian-Bin Liu, Department of Radiology, Hunan Province People's Hospital, Changsha 410005, Hunan Province, China
En-Hua Xiao, Zhong He, Cong Ma, Jun Xiang, Department of Radiology, the Second Xiang-Ya Hospital, Central South University, Changsha 410005, Hunan Province, China
Ke Jin, Wei-Jian Chen, Department of Pathology, Hunan Province Children's Hospital, Changsha 410005, Hunan Province, China
Jian-Hua Xiao, Department of Epidemiology, Center for Disease Control of Hunan Province, Changsha 410005, Hunan Province, China
Supported by the National Natural Science Foundation of China, No. 30070235, 30470508
Correspondence to: Dr. You-Hong Yuan, Department of Radiology, Hunan Province People's Hospital, Changsha 410005, Hunan Province, China. heyuanyouhong@yahoo.com.cn
Telephone: +86-731-2278047 Fax: +86-731-2278011
Received: June 5, 2007 Revised: August 17, 2007

Abstract

AIM: To investigate dynamic characteristics and pathological mechanism of signal in rabbit VX-2 tumor model on diffusion-weighted imaging (DWI) after chemoembolization.

METHODS: Forty New Zealand rabbits were included in the study and forty-seven rabbit VX-2 tumor models were raised by implanting directly and intrahepatically after abdominal cavity opened. Forty VX-2 tumor models from them were divided into four groups. DWI was performed periodically and respectively for each group after chemoembolization. All VX-2 tumor samples of each group were studied by pathology. The distinction of VX-2 tumors on DWI was assessed by their apparent diffusion coefficient (ADC) values. The statistical significance between different time groups, different area groups or different b-value groups was calculated by using SPSS12.0 software.

RESULTS: Under b-value of 100 s/mm^2, ADC values were lowest at 16 h after chemoembolization in area of VX-2 tumor periphery, central, and normal liver parenchyma around tumor, but turned to increase with further elongation of chemoembolization treatment. The distinction of ADC between different time groups was significant respectively (F = 7.325, P < 0.001; F = 2.496, P < 0.048; F = 6.856, P < 0.001). Cellular edema in the area of VX-2 tumor periphery or normal liver parenchyma around tumor, increased quickly in sixteen h after chemoembolization but, from the 16th h to the 48th h, cellular edema in the area of normal liver parenchyma around tumor decreased gradually and that in the area of VX-2 tumor periphery decreased lightly at, and then increased continually. After chemoembolization, Cellular necrosis in the area of VX-2 tumor periphery was more significantly high than that before chemoembolization. The areas of dead cells in VX-2 tumors manifested low signal and high ADC value, while the areas of viable cells manifested high signal and low ADC value.

CONCLUSION: DWI is able to detect and differentiate tumor necrotic areas from viable cellular areas before and after chemoembolization. ADC of normal liver parenchyma and VX-2 tumor are influenced by intracellular edema, tissue cellular death and microcirculation disturbance after chemoembolization.

Key words: Liver; VX-2 tumor; Diffusion-weighted imaging; Apparent diffusion coefficient; Chemoembolization

Yuan YH, Xiao EH, Liu JB, He Z, Jin K, Ma C, Xiang J, Xiao JH, Chen WJ. Characteristics and pathological mechanisms on magnetic resonance diffusion-weighted imaging after chemoembolization in rabbit liver VX-2 tumor model. *World J Gastroenterol* 2007; 13(43): 5699-5706

http://www.wjgnet.com/1007-9327/13/5699

INTRODUCTION

Transcatheter arterial chemoembolization (TACE) is a kind of classic interventional therapy and it is commonly performed to treat the unresectable hepatocellular carcinoma and secondary liver cancers. The major goal of chemoembolization is to destroy the tumor. It is very important to evaluate obviously progression of hepatic tumors and differentiate accurately the areas and degrees of necrotic tumor from that of viable tumor before and after chemoembolization.

As reported, ultrasound (US), digital subtraction

angiography (DSA), computed tomography (CT) and magnetic resonance imaging (MRI) are usually used to diagnose and evaluate the progression of hepatic tumor but they have their respective defects. US is able to comprehend the size, blood provision and liquefied or cystic areas of tumor but it can not differentiate necrotic tumor from viable tumor[1,2]. DSA can infer necrotic tumor and viable tumor from the degree of tumor stain. CT can manifest the areas of iodized oil and necrotic or viable tumor but, because density of iodized oil is very high on CT, some areas of necrotic or viable tumor are easily covered before and after chemoembolization[3-5]. MRI is not affected by high density of iodized oil and it is more valuable than US and CT in evaluating the progression of the tumor and in differentiating necrotic from viable tumor. The signals of coagulative necrotic areas of tumor are low on T1- and T2-weighted imaging after chemoembolization and there are no enhanced in MR enhancement scanning[6-11].

Diffusion-weighted imaging is a kind of new functional imaging technology having been developed in recent years and it is the only one method which is able to reflect non-woundingly water molecular diffusion *in vivo*. It has been generally accepted that it is valuable in diagnosing qualitatively and quantitatively cerebral ischemia in hyper-inchoate period[12-14] and, at the same time, many studies of hepatic pathological changes on DWI have been reported[15-17]. ADC values of benign lesions, such as hepatic cysts and hemangiomas, were higher than those of malignant lesions, such as hepatocellular carcinomas and metastases on DWI, as reported by Ichikawa *et al*[15,16], Yamashita *et al*[17], Taouli *et al*[18], Sun *et al*[19]. Colagrande *et al*[20], indicating that the signals of tumor coagulative necrotic areas were lower in comparison with those of tumor viable areas. Kamel *et al*[21] confirmed, in their clinical investigation of 8 case of hepatocellular carcinomas, by image-pathology, that ADC would become high directly with the degree of tumor cellular necrosis increasing and that the signals of 6 tumors were higher than those of normal parenchyma on DWI. Geschwind *et al*[22] demonstrated that the signals of VX-2 tumor necrotic areas were low and that ADC in the area of tumor necrosis were significantly greater than those in the area of viable tumor after chemoembolization.

As indicated by findings of above preliminary experiments, DWI, especially ADC, has potential values in reflecting characteristics of liver pathological changes and of differentiation to benign tumor from malignant one.

There has been no dynamically and image-pathologically investigated report on the characteristics of hepatocellular carcinomas on DWI after chemoembolization. The purpose of our experiment is to investigate dynamic characteristics and pathological mechanism of signal with DWI in rabbit VX-2 tumor model after chemoembolization, which is the most valuable animal model of hepatocellular carcinoma for imaging investigations. Moreover the aim is to evaluate the contribution of DWI in differentiating of tumor viable cells to necrotic ones.

MATERIALS AND METHODS

Animals and establishment of VX-2 tumor model

Animal studies were carried out under the supervision of a veterinarian according to the guidelines on the Use of Laboratory Animals of the Ministry of Public Health of China. All animals were provided by the Laboratory Animal Center of the Second Xiangya Hospital and all protocols were approved by the Animal Use and Care Committee of the Second Xiangya Hospital.

Forty New Zealand rabbits were included in the study. Twenty-two were male rabbits and eighteen were female, weighed 1.7 to 2.5 kg, aged 5 to 6 mo. All of them were healthy. Forty-seven rabbit VX-2 tumor models were raised by implanting the tumor directly and intrahepatically after the abdominal cavity was opened. The VX-2 tumor strain of rabbit was provided by the Fourth Military Medical University.

Forty VX-2 tumor models were layered and randomly chosen from forty-seven VX-2 tumor models and were divided into four groups, including control group (non-interventional group, namely group A) and investigation group (at the 16th h after chemoembolization, at the 32nd h after chemoembolization, at the 48th h after chemoembolization, namely group B, C, and D, respectively). Otherwise, ten cases were randomly chosen from all data were carried out by DWI for all rabbits of group B, C and D at 6th h after chemoembolization and the data was put into group of the 6th h after chemoembolization, as one of investigation groups, namely E group.

Chemoembolization protocol

After DWI at the 21st d after implantation, trans-hepaticartery catheterization chemoembolization was directly and respectively carried out for all rabbits of B, C and D group in the Animal Operating Room of the Second Xiangya Hospital.

First, once rabbits were anesthetized by injecting 3% soluble pentobarbitone and the skin of abdomen was disinfected, then we exposed organs of the hepatic hilar region by incising the skin and vagina musculi recti abdominis. Arteria coeliaca, arteria hepatica communis, arteria hepatica propria, arteria gastroduodenalis, portal vein *etc* were recognized. Second, we drew off arteria gastroduodenalis, we occluded its distalpart and dropped a little attenuated aethocaine on it. Third, we punctured the arteria gastroduodenalis and put plastic transfixion pins or scalp acupunctures into it; the top of transfixion pins were put in arteria hepatica propria. Fourth, we fixed the microtubular or transfixion pins and then infused iodized oil (0.3 mL/kg) and pharmorubicin (2 mg/kg) into arteria hepatica. At last, abdominal membrane, musculature and cutaneous were sutured layer by layer after the liver and other organs in abdominal cavity stopped bleeding.

Magnetic resonance imaging protocol

After animals were anesthetized by injecting 3% soluble pentobarbitone into auriborder vein at a dose of 1 mL/kg or at different doses based on different animal status to make sure that the breathing of animals was slow and stable, DWI(axial) was carried respectively and periodically out a 1.5-Tesla Signa Twinspeed MR scanner (General Electron Medical Systems, USA) using a small diameter cylindrical brain radiofrequency coil before chemoembolization and at the 6th h, the 16th h, the 32nd

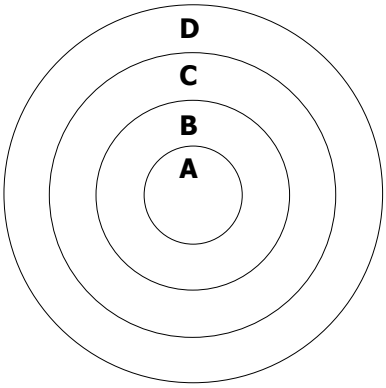

Figure 1 **A**: The area of VX-2 tumor center; **B**: The area of VX-2 tumor periphery; **C**: The area of VX-2 tumor outer layer; **D**: The normal liver parenchyma area around tumor when the values of ADC and signals were measured on DWI and samples were investigated pathologically.

h and the 48th h after chemoembolization. The scanning parameters of DWI included spin echo echoplanar imaging (SE-EPI) series, b-value 100 and 300 s/mm^2, repetition time (TR) 6000 ms, echo time (TE) 45 ms, 20 cm × 15 cm field of view (FOV), 8 number of excitations (NEX), 2 mm thickness layer, 0.5 mm Space, 128 × 128 matrix, *etc*.

ADC values and signal values in the area of VX-2 tumor periphery, in the VX-2 tumor center and in the normal liver parenchyma around tumor (Figure 1) were obtained by using Function Software in GE workstation. Three different regions of interest (ROIs) (50 mm^2 each area) were chosen in the area of normal liver parenchyma (area D in Figure 1) and we measured their ADC values and signal values. The average value of above was considered as the ADC value or the signal value of normal liver parenchyma around tumor. The thickness of area A and B in Figure 1 was respectively two fifth diameter of VX-2 tumor. By the same methods, the average value of three different ROIs ADC values or signal values in area B was considered as the ADC value or the signal value of VX-2 tumor periphery area; ADC value or signal value of area A was its ADC value or signal value of VX-2 tumor center area. All measurements were finished cooperatively by two senior attending physicians or associate professors.

Pathology protocol

All of the rabbits in each group were euthanized by injecting an overdose of 3% soluble pentobarbitone into auriborder vein when DWI was respectively carried out before chemoembolization, and after the 16 h, the 32 h and 48 from chemoembolization. We got layer by layer VX-2 samples under the condition of asepsis (Figure 1) and made them fixed in the formaldehyde solution for 24 h before being embedded in mineral wax. Each VX-2 tumor was divided into the outer layer area, the periphery area and the center area (Figure 1) so that samples included four parts: VX-2 tumor center area, VX-2 tumor periphery area, VX-2 tumor outer layer area and normal liver parenchyma around tumor.

All samples were investigated respectively under 100 × and 400 × microscope and the emphases were on investigating cellular edema in the VX-2 tumor and normal liver parenchyma around tumor.

Edema index was used to estimate the degree of cellular edema, which was the contrast of edema cell number to total cells under microscope. Manifestations of edema cells under microscope included cell body increasing, unclear cellular membrane and intracytoplasm vacuolar or ballooning degeneration; the latter was the most important manifestation of edema cell. Two campus visualises under 400 × microscope were obtained randomly in the zone of non-necrosis. The number of edema cells and total cell number were counted by two external doctors not from our study team with double blind method. Otherwise, we investigated specially the degree of tumor cellular necrosis and the abnormity of cell membrane. Statistical analysis based on apparent diffusion coefficient (ADC) value of ROIs and edema index, the distinction between different area groups, different time groups and different b-value groups was respectively estimated. The statistical significance was calculated by analysis of variance (ANOVA) or analysis of non-parameter by using SPSS software (version 12.0; SPSS, Tokyo, Japan)

RESULTS

Image manifestations of hepatic VX-2 tumor before and after chemoembolization

ADC values and signal values of VX-2 tumors were shown in Table 1 and Figures 2-5.

The distinction between ADC in the area of VX-2 tumor periphery, tumor center or normal parenchyma around tumor was respectively significant ($F = 14.366$, $P < 0.001$; $F = 4.674$, $P = 0.033$; $F = 23.054$, $P < 0.001$) with b-value 100 s/mm^2 and with b-value is 300 s/mm^2 was respectively significant ($F = 14.366$, $P < 0.001$; $F = 4.674$, $P = 0.033$; $F = 23.054$, $P < 0.001$). Signals in the area of VX-2 tumor periphery, tumor center and normal parenchyma around tumor b-value was 100 s/mm^2 were higher than with b-value was 300 s/mm^2 ($F = 112.874$, $P < 0.001$; $F = 83.455$, $P < 0.001$; $F = 135.455$, $P < 0.001$).

When b-value was 100 s/mm^2, the distinction of ADC in the area of VX-2 tumor periphery, tumor center and normal parenchyma around tumor among group A, B, C, D and E was respectively significant($F = 7.325$, $P < 0.001$; $F = 2.496$, $P = 0.048$; $F = 6.856$, $P < 0.001$). The distinction of signal in the area of VX-2 tumor periphery among group A, B, C, D and E was significant ($F = 3.005$, $P < 0.05$) but that in the area of VX-2 tumor center and normal parenchyma around tumor was not significant ($F = 1.399$, $P > 0.05$; $F = 2.146$, $P > 0.05$).

Manifestations of VX-2 tumor pathology

Observed by the naked eye, most surfaces of normal hepatic parenchyma around VX-2 tumor were paler in investigation group than those in control group and there was embolization of unequal areas but well-circumscribed. The tumors were hard and there was clear demarcation. The cavities of unequal size were found in the area of VX-2 tumors because kermesinus liquid had run off after the tumors werfae cut open.

Under microscope, some edema cells containing ballooning degeneration were observed in the area of normal parenchyma around VX-2 tumor. Inequality

Table 1 ADC values of tumor and normal parenchyma after Chemoembolization

Group	VX-2 tumor periphery areas		VX-2 tumor center areas		Hepatic normal parenchyma	
	b = 100	b = 300	b = 100	b = 300	b = 100	b = 300
Control	1.71 ± 0.27	1.48 ± 0.23	1.77 ± 0.36	1.55 ± 0.30	2.71 ± 0.42	2.30 ± 0.40
6 h	1.56 ± 0.40	1.36 ± 0.18	1.97 ± 0.49	1.79 ± 0.37	2.44 ± 0.53	1.87 ± 0.31
16 h	1.24 ± 0.22	1.12 ± 0.20	1.56 ± 0.40	1.69 ± 0.35	2.10 ± 0.54	1.65 ± 0.37
32 h	1.48 ± 0.37	1.23 ± 0.16	1.99 ± 0.32	1.66 ± 0.31	2.10 ± 0.49	1.97 ± 0.29
48 h	1.57 ± 0.23	1.40 ± 0.18	2.04 ± 0.54	1.82 ± 0.27	2.43 ± 0.33	2.06 ± 0.23
Total	1.51 ± 0.33	1.32 ± 0.23	1.87 ± 0.45	1.70 ± 0.32	2.36 ± 0.51	1.97 ± 0.38

Data are expressed as mean ± SD × 10^{-3} mm^2/s; ADC: Apparent diffusion coefficient.

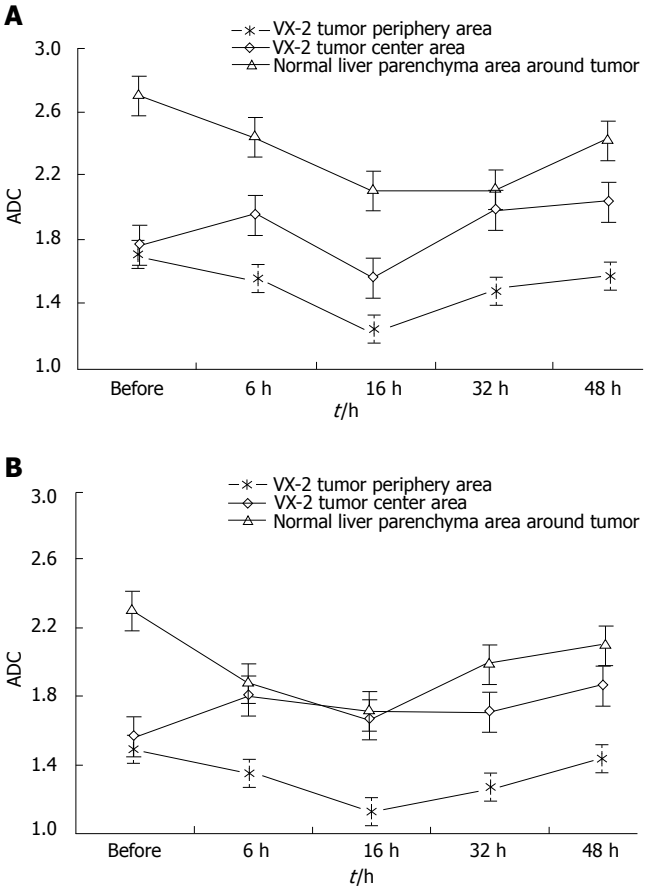

Figure 2 ADC values of different areas on DWI after chemoembolization. **A**: B-value was 100 s/mm^2; **B**: B-value was 300 s/mm^2.

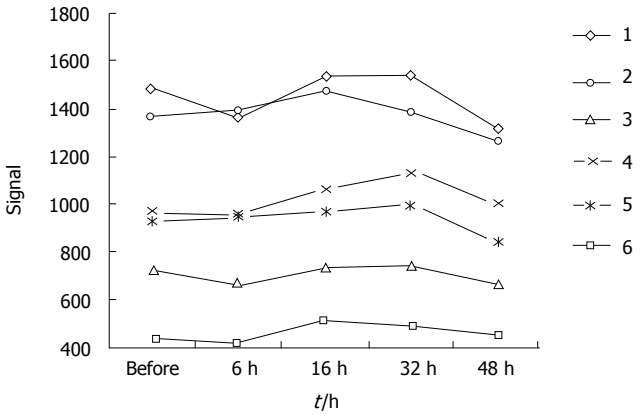

Figure 3 Signal values on DWI when area and b-value was different after chemoembolization. Areas: 1-signal of VX-2 tumor periphery area when b-value was 100 s/mm^2; 2-signal of VX-2 tumor center area when b-value was 100 s/mm^2; 3-signal of the normal liver parenchyma area around tumor when b-value was 100 s/mm^2; 4-signal of VX-2 tumor periphery area when b-value was 300 s/mm^2; 5-signal of VX-2 tumor center area when b-value was 300 s/mm^2; 6-signal of the normal liver parenchyma area around tumor when b-value was 300 s/mm^2.

of size, round or ellipse or strip tumor nests could be observed in different areas of VX-2 tumor. The degree of cell edema and necrosis were more obvious in group B,C and D (after chemoembolization) than group A (before chemoembolization), the necrotic areas were more in the area of VX-2 tumor center than those in the area of tumor periphery or tumor outer layer, and most areas of tumor center were necrotic in some VX-2 tumors.

Edema cells showed their volume increased obviously, kytoplasm dyeing thinly and obvious ballooning degeneration (Figure 6 and 7). Dynamical information of cellular edema and necrosis were counted in Tables 2 and 3.

DISCUSSION

The signal and ADC characteristics of many hepatic pathological changes on DWI have been reported in recent years[23-26]. DWI has significant and potential clinical application values in detecting, diagnosing and differentiating tumors earlier. From what has been determined when DWI was investigated by Yuan *et al* in rabbit liver VX-2 tumor model, VX-2 tumor is a solid tumor and its body mainly consists of tumor nests and other cells so that its water molecule diffusion motion is obviously restricted, the signal of them is significantly high and ADC is significantly low.

The signals in VX-2 tumors were higher than those in the area of normal parenchyma around tumor while ADC values were lower than those in the area of normal parenchyma after chemoembolization, and the tendency of the signal and ADC in VX-2 tumors and in the area of normal parenchyma was basically the same. The signals in VX-2 tumors were uneven, the signals in the area of tumor center were lower than that in the area of tumor periphery, while those in the 48 h after chemoembolization were lower than that before chemoembolization. The areas of low signal and high signal were observed in VX-2 tumor and ADC of them was higher than that in the equal signal area of VX-2 tumor or in the area of normal parenchyma. Accordingly with pathology, the areas of low signal in VX-2 tumor were coagulation necrosis, those of high signal were liquid or cystic tissue,

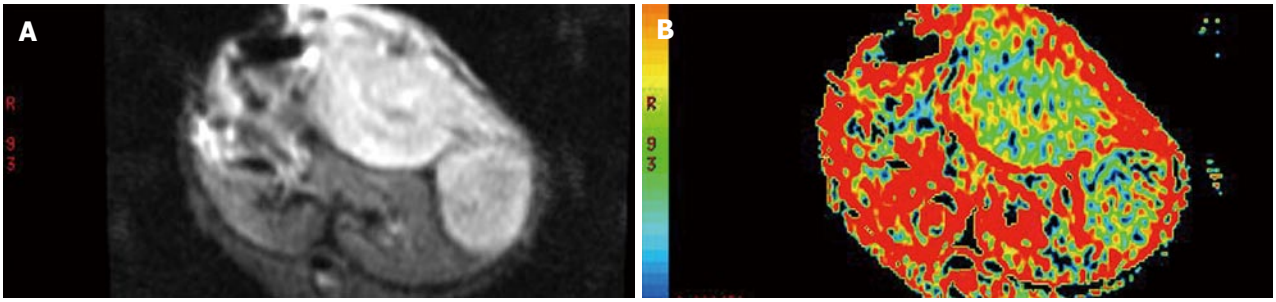

Figure 4 Image manifestations of hepatic VX-2 tumor on DWI and ADC map when b-value was 100 s/mm^2 at 6 h after chemoembolization **A**: High signal and distinct margin of VX-2 tumor on DWI; **B**: Low signal of it on the ADC map.

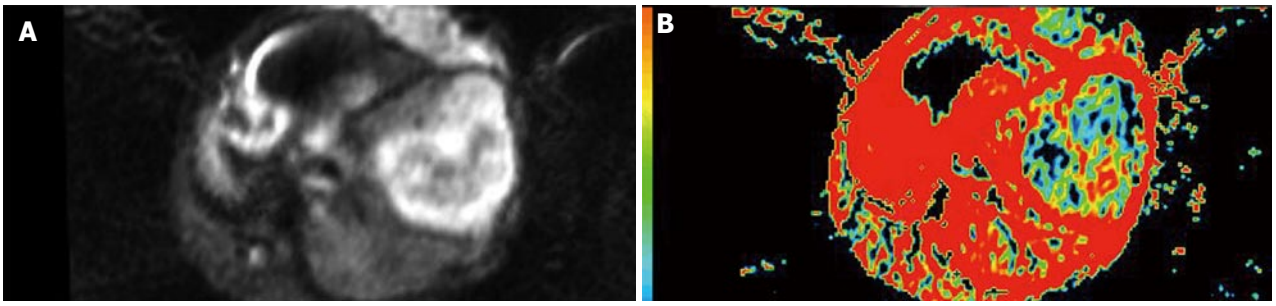

Figure 5 Image manifestations of hepatic VX-2 tumor on DWI and ADC map when b-value was 100 s/mm^2 at 48 h after chemoembolization **A**: High and uneven signal and distinct margin of VX-2 tumor on DWI; **B**: Low and uneven signal of it on the ADC map.

and other areas except low signal and high signal areas in the lump were viable tumor cells. Moreover, necrotic areas in VX-2 tumors after chemoembolization were more than those before chemoembolization. When coagulation necrosises/necroses takes place in the tumor because of insufficient blood provision, cellular membrane will break and the limitation of water molecular motion in the tumor decreases greatly so that the signals is reduced while ADC values are upgraded. After coagulation necroses have been liquefied or become cystic, cell lysis and leakier cell membranes can no longer compartmentalize water molecules and allow free diffusion to take place so that ADC values increase greatly. Nyway the signals of above mentioned liquefied or cystic areas are higher than those of coagulative necrosis areas, even viable tumor areas or normalparenchyma. It can be explained by the presence of greater amounts of extracellular water molecules within the necrotic region which is a kind of long T2-value contribution constitution and the b-value is 100 or 300 s/mm^2, a small b-value, in diffusion-weighted imaging scanning so that the signals of above are affected significantly by "shine-through".

At 6 h after chemoembolization, the signals in the area of tumor centers decreased slightly while ADC increased slightly, the signals in the area of tumor periphery and normal parenchyma increased significantly while ADC decreased at different degrees. However, pathology demonstrated that the degree of cellular necrosis in the area of normal parenchyma before chemoembolization was the same of that after chemoembolization while in the area of tumor periphery areas before chemoembolization was much more than after chemoembolization.

Accordingly with what discussed above, the signal increasing and ADC decreasing cannot completely be explained by tumor cellular necrosis after chemoembolization. The dynamic mechanisms of water molecular diffusion decreasing and the signal increasing while ADC values decreasing after cerebral infarction have been investigated by many investigators in recent years, and it is not completely comprehended yet, but most of them demonstrated it was connected with cytotoxic edema, microcirculation disturbance, temperature or abnormality of cellular membrane permeability, *etc*[27-31]. A series of clinical and animal experimental investigations by Xie *et al*[28], Han *et al*[29] and Marks *et al*[30] have demonstrated that the cytotoxic edema after embolization had significant influences on the change of water molecules diffusion. Because of dysfunctional Na-K pump due to early hypoxia after embolization, the density of intra-cellular electrolyte increases and then also water molecules of intra-cells increase significantly, while extra-cell water molecules decrease significantly, so that ADC starts decreasing while the signal starts increasing. When intracellular edema reaches to the biggest degree, ADC of constitution will decrease to the lowest and it will maintain at a low degree if intracellular edema maintains or if there are constitution edema originating from the blood vessel. ADC of constitution will start increasing after cellular membrane has been broken and cells have dissolved; it will reach the biggest when constitution has been liquefied and become cystic.

After chemoembolization, ADC in the area of VX-2 tumor periphery and normal parenchyma decreased quickly wuth ther bottom at biggest in the 16th h and

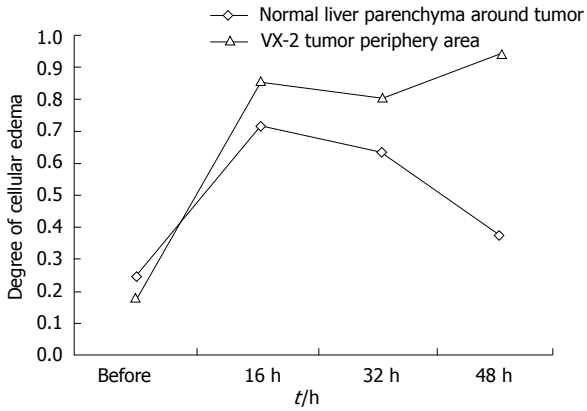

Figure 6 Cellular edema of different areas after chemoembolization.

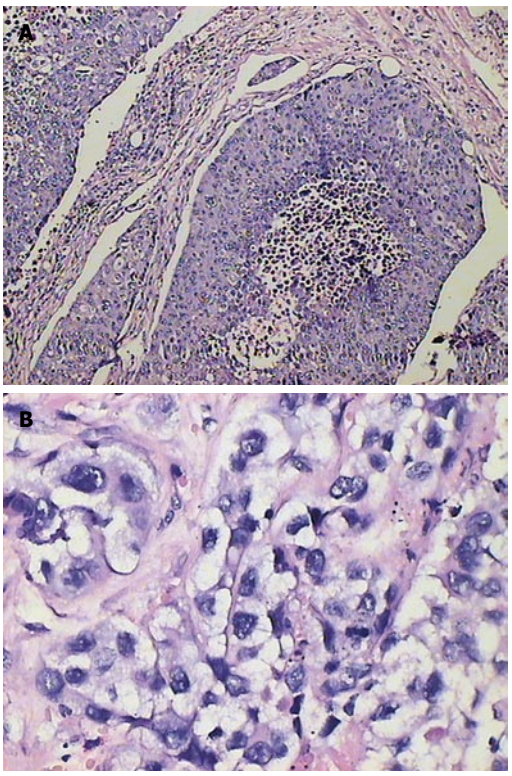

Figure 7 **A**: Cell nest of VX-2 tumor and wide zone of necrosis in the tumor(x 100) and **B**: cellular edema in the VX-2 tumor (x 400).

then increased gradually but they were significantly lower in the 48th h after chemoembolization than those before chemoembolization. Pathology demonstrated the degree of cellular edema in the area of VX-2 tumor and normal parenchyma were significant higher after chemoembolization than before chemoembolization and it reaching a peak at 16th h after chemoembolization and then decreased gradually. The signal and ADC changes in the area of VX-2 tumor and normal parenchyma were significantly relative to cellular edema. The function of Na-K pump decreases or misses because of ischemia and hypoxia from chemoembolization and toxic action from chemotherapeutic drug; the degree of intra-cell edema also increases significantly after chemoembolization so that ADC starts decreasing. With intracellular edema lessening

Table 2 Dynamic information of cellular edema after chemoembolization (%) (mean ± SD)

	Control	16 h	32 h	48 h
Normal parenchyma	24.90 ± 11.69	72.12 ± 34.48	63.89 ± 29.87	38.00 ± 24.57
Tumor periphery areas	18.16 ± 10.35	86.06 ± 16.01	81.18 ± 20.03	96.66 ± 4.76

Table 3 Manifestations of VX-2 tumor pathology after chemoembolization

	Cellular membrane		Cellular necrosis			
	0	1	0	1	2	3
Normal parenchyma (Control)	8	2	7	3		
Tumor periphery areas (Control)	10				9	1
Normal parenchyma (16 h)	7	3	7	1	2	
Tumor periphery areas (16 h)	10			2	4	4
Normal parenchyma (32 h)	7	3	7	1	2	
Tumor periphery areas (32 h)	10				3	7
Normal parenchyma (48 h)	6	4	8	2		
Tumor periphery areas (48 h)	10				4	6

Cellular membrane: 0-clear and complete; 1-unclear and non-complete. Cellular necrosis: 0-cellular structure existing and cellular membrane complete; 1-many cells dissolving and cellular membrane disappearing; 2-minute cellular coagulation necrosis; 3-extensive cellular coagulation necrosis.

or cell breaking, ADC values will increase gradually. The dynamic changes of ADC can reflect the degree of tumor cellular edema and cellular necrosis.

However, after chemoembolization, ADC in the area of VX-2 tumor periphery and normal parenchyma increased gradually but the signals decreased gradually from the 16th h to the 48th h after chemoembolization; the signals were lower in the 48th h than those before chemoembolization. Pathology demonstrated that the degree of cellular edema in the area of normal parenchyma reached a peak in the 16th h and then decreased gradually but that in the area of tumor periphery reached a peak in the 16th h and then increased continually after chemoembolization. The degree of cellular edema in the area of tumor periphery was significantly lower than that in the area of normal parenchyma. Double blood-provision from hepatic artery and portal system plus our protocols of transcatheter hepaticarterial chemoembolization can explain it. Selective catheterization was not carried out in our experiments so that ischemia and hypoxia took place in the VX-2 tumor and normal parenchyma at the same time and ADC decreased because of intracellular edema. The degree of cellular edema in VX-2 tumor was higher than that in the area of normal parenchyma after chemoembolization because 95%-99% blood provision of hepatocellular carcinoma comes from hepatic artery while 70%-75% blood provision of normal parenchyma comes from portal system and others comes from hepatic artery. Blood provision from portal system would recover step by step after chemoembolization so that the degree of cellular edema in the area of normal parenchyma decreased significantly but that in VX-2

tumor increased continually from the 16 h to the 48 h after chemoembolization. Otherwise, as reported by Yang *et al*[31], blood provision decreasing could lead to ADC decreasing and ADC reflected blood provision to a certain degree when b-value was small in diffusion-weighted imaging scanning. Since b-value was small in our scanning, ADC could be affected by blood provision after chemoembolization.

Necrotic tumor manifests low signal and high ADC value, while viable tumor manifests high signal and low ADC value after chemoembolization. DWI has potential ability in detecting and differentiating viable tumor from necrotic tumor and, besides water molecular diffusion, intracellular edema, microcirculation disturbance and tumor necrosis from chemoembolization are significantly relative to ADC changing dynamically.

ACKNOWLEDGMENTS

We thank the staff of the Radiology Department and the Laboratory Animal Center of the Second Xiangya Hospital for their help, especially Ying-Si He.

COMMENTS

Background

Transcatheter arterial chemoembolization (TACE) is a kind of classic interventional therapy and it is commonly performed to treat the unresectable hepatocellular carcinoma and most secondary liver cancers. The major goal of chemoembolization is to destroy the tumor. Ultrasound (US), digital subtraction angiography (DSA), computed tomography (CT) and magnetic resonance imaging (MRI) are usually used to diagnose and to evaluate the progression of hepatic tumor but they have their respective defects. Diffusion-weighted imaging is a kind of new functional imaging technology having been developed in recent years and it is the only one method which is able to reflect non-woundingly water molecular diffusion *in vivo*. Geschwind *et al* demonstrated that the signals of VX-2 tumor necrotic areas were low and ADC of them were significantly greater in the area of tumor necrosis than those in the area of viable tumor after chemoembolization. Therefore, we believe that DWI, especially ADC, has potential values in reflecting characteristics of liver pathological changes and differentiating benign tumor from malignant one.

Research frontiers

Many studies of hepatic pathological changes on DWI have been reported. ADC values of benign lesions, such as hepatic cysts and hemangiomas, were higher than those of malignant lesions, such as hepatocellular carcinomas and metastases on DWI and many studies also indicated that the signals of tumor coagulative necrotic areas were lower in comparison with that of tumor viable areas. There has been no dynamically and image-pathologically investigated report on the characteristics of hepatocellular carcinomas on DWI after chemoem-bolization.

Innovations and breakthroughs

Our study clearly showed that necrotic tumor manifested low signal and high ADC value while viable tumor manifested high signal and low ADC value after chemoembolization. DWI would have potential ability in detecting and differentiating viable tumor from necrotic tumor and, besides water molecular diffusion, intracellular edema, microcirculation disturbance and tumor necrosis from chemoembolization were significantly relative to ADC changing dynamically.

Applications

Physicians can apply this knowledge to evaluate obviously progression of hepatic tumors and differentiate accurately the areas and degrees of necrotic tumor from that of viable tumor before and after chemoembolization.

Peer review

This is an interesting, well designed, and written study on a problem of real clinical significance.

REFERENCES

1 **Morimoto M**, Shirato K, Sugimori K, Kokawa A, Tomita N, Saito T, Imada T, Tanaka N, Nozawa A, Numata K, Tanaka K. Contrast-enhanced harmonic gray-scale sonographic-histologic correlation of the therapeutic effects of transcatheter arterial chemoembolization in patients with hepatocellular carcinoma. *AJR Am J Roentgenol* 2003; **181**: 65-69

2 **Kubota K**, Hisa N, Nishikawa T, Fujiwara Y, Murata Y, Itoh S, Yoshida D, Yoshida S. Evaluation of hepatocellular carcinoma after treatment with transcatheter arterial chemoembolization: comparison of Lipiodol-CT, power Doppler sonography, and dynamic MRI. *Abdom Imaging* 2001; **26**: 184-190

3 **Ebied OM**, Federle MP, Carr BI, Pealer KM, Li W, Amesur N, Zajko A. Evaluation of responses to chemoembolization in patients with unresectable hepatocellular carcinoma. *Cancer* 2003; **97**: 1042-1050

4 **Kim HC**, Kim AY, Han JK, Chung JW, Lee JY, Park JH, Choi BI. Hepatic arterial and portal venous phase helical CT in patients treated with transcatheter arterial chemoembolization for hepatocellular carcinoma: added value of unenhanced images. *Radiology* 2002; **225**: 773-780

5 **Shankar S**, vanSonnenberg E, Morrison PR, Tuncali K, Silverman SG. Combined radiofrequency and alcohol injection for percutaneous hepatic tumor ablation. *AJR Am J Roentgenol* 2004; **183**: 1425-1429

6 **Minami Y**, Kudo M, Kawasaki T, Kitano M, Chung H, Maekawa K, Shiozaki H. Transcatheter arterial chemoembolization of hepatocellular carcinoma: usefulness of coded phase-inversion harmonic sonography. *AJR Am J Roentgenol* 2003; **180**: 703-708

7 **Zhang Z**, Wu M, Chen H, Chen D, He J. Percutaneous radiofrequency ablation combined with transcatheter arterial chemoembolization for hepatocellular carcinoma. *Zhonghua Waike Zazhi* 2002; **40**: 826-829

8 **Seki T**, Tamai T, Ikeda K, Imamura M, Nishimura A, Yamashiki N, Nakagawa T, Inoue K. Rapid progression of hepatocellular carcinoma after transcatheter arterial chemoembolization and percutaneous radiofrequency ablation in the primary tumour region. *Eur J Gastroenterol Hepatol* 2001; **13**: 291-294

9 **Chan JH**, Tsui EY, Luk SH, Yuen MK, Cheung YK, Wong KP. Detection of hepatic tumor perfusion following transcatheter arterial chemoembolization with dynamic susceptibility contrast-enhanced echoplanar imaging. *Clin Imaging* 1999; **23**: 190-194

10 **Tsui EY**, Chan JH, Cheung YK, Cheung CC, Tsui WC, Szeto ML, Lau KW, Yuen MK, Luk SH. Evaluation of therapeutic effectiveness of transarterial chemoembolization for hepatocellular carcinoma: correlation of dynamic susceptibility contrast-enhanced echoplanar imaging and hepatic angiography. *Clin Imaging* 2000; **24**: 210-216

11 **Lövblad KO**, Wetzel SG, Somon T, Wilhelm K, Mehdizade A, Kelekis A, El-Koussy M, El-Tatawy S, Bishof M, Schroth G, Perrig S, Lazeyras F, Sztajzel R, Terrier F, Rüfenacht D, Delavelle J. Diffusion-weighted MRI in cortical ischaemia. *Neuroradiology* 2004; **46**: 175-182

12 **Na DG**, Thijs VN, Albers GW, Moseley ME, Marks MP. Diffusion-weighted MR imaging in acute ischemia: value of apparent diffusion coefficient and signal intensity thresholds in predicting tissue at risk and final infarct size. *AJNR Am J Neuroradiol* 2004; **25**: 1331-1336

13 **O'Donnell ME**, Tran L, Lam TI, Liu XB, Anderson SE. Bumetanide inhibition of the blood-brain barrier Na-K-Cl cotransporter reduces edema formation in the rat middle cerebral artery occlusion model of stroke. *J Cereb Blood Flow Metab* 2004; **24**: 1046-1056

14 **Ichikawa T**, Haradome H, Hachiya J, Nitatori T, Araki T. Diffusion-weighted MR imaging with a single-shot echoplanar sequence: detection and characterization of focal hepatic lesions. *AJR Am J Roentgenol* 1998; **170**: 397-402

15 **Ichikawa T**, Haradome H, Hachiya J, Nitatori T, Araki T. Diffusion-weighted MR imaging with single-shot echo-planar imaging in the upper abdomen: preliminary clinical experience in 61 patients. *Abdom Imaging* 1999; **24**: 456-461

16 **Yamashita Y**, Tang Y, Takahashi M. Ultrafast MR imaging of the abdomen: echo planar imaging and diffusion-weighted imaging. *J Magn Reson Imaging* 1998; **8**: 367-374
17 **Taouli B**, Martin AJ, Qayyum A, Merriman RB, Vigneron D, Yeh BM, Coakley FV. Parallel imaging and diffusion tensor imaging for diffusion-weighted MRI of the liver: preliminary experience in healthy volunteers. *AJR Am J Roentgenol* 2004; **183**: 677-680
18 **Sun XJ**, Quan XY, Liang W, Wen ZB, Zeng S, Huang FH, Tang M. Quantitative study of diffusion weighted imaging on magnetic resonance imaging in focal hepatic lesions less than 3 cm. *Zhonghua Zhongliu Zazhi* 2004; **26**: 165-167
19 **Colagrande S**, Politi LS, Messerini L, Mascalchi M, Villari N. Solitary necrotic nodule of the liver: imaging and correlation with pathologic features. *Abdom Imaging* 2003; **28**: 41-44
20 **Kamel IR**, Bluemke DA, Ramsey D, Abusedera M, Torbenson M, Eng J, Szarf G, Geschwind JF. Role of diffusion-weighted imaging in estimating tumor necrosis after chemoembolization of hepatocellular carcinoma. *AJR Am J Roentgenol* 2003; **181**: 708-710
21 **Geschwind JF**, Artemov D, Abraham S, Omdal D, Huncharek MS, McGee C, Arepally A, Lambert D, Venbrux AC, Lund GB. Chemoembolization of liver tumor in a rabbit model: assessment of tumor cell death with diffusion-weighted MR imaging and histologic analysis. *J Vasc Interv Radiol* 2000; **11**: 1245-1255
22 **Somford DM**, Marks MP, Thijs VN, Tong DC. Association of early CT abnormalities, infarct size, and apparent diffusion coefficient reduction in acute ischemic stroke. *AJNR Am J Neuroradiol* 2004; **25**: 933-938
23 **Brugières P**, Thomas P, Maraval A, Hosseini H, Combes C, Chafiq A, Ruel L, Breil S, Peschanski M, Gaston A. Water diffusion compartmentation at high b values in ischemic human brain. *AJNR Am J Neuroradiol* 2004; **25**: 692-698
24 **Mitsias PD,** Ewing JR, Lu M, Khalighi MM, Pasnoor M, Ebadian HB, Zhao Q, Santhakumar S, Jacobs MA, Papamitsakis N, Soltanian-Zadeh H, Hearshen D, Patel SC, Chopp M. Multiparametric iterative self-organizing MR imaging data analysis technique for assessment of tissue viability in acute cerebral ischemia. *AJNR Am J Neuroradiol* 2004; **25**: 1499-1508
25 **Moteki T**, Horikoshi H, Oya N, Aoki J, Endo K. Evaluation of hepatic lesions and hepatic parenchyma using diffusion-weighted reordered turboFLASH magnetic resonance images. *J Magn Reson Imaging* 2002; **15**: 564-572
26 **Wang JL**, Xie JX. Assessment of hemodynamics and pathophysiology of acute cerebral ischemia with MR perfusion-weighted imaging and dynamic diffusion-weighted imaging. *Zhonghua Fangshexue Zazhi* 1998; **32**: 370-374
27 **Xiao XH**, Kong XQ, Jiang Li, Jiang L, Wang YM, Xu HB, Li LY, Tang YF. An experimental study on acute cerebral ischemia and reperfusion with magnetic resonance diffusion weighted imaging. *Zhonghua Fangshexue Zazhi* 1999; **33**: 662-666
28 **Xie JX**, Fu Y, Zhang Y. The change of water cellular diffusion motion and its clinical application. *Beijing Daxue Xuebao* (Yixueban) 2001; **33**:109-112
29 **Han HB**, Xie JX. Application of EPI diffusion- weighted and Gd DTPA2 perfusion imaging in the diagnosis of brain ischemia. *Zhonghua Fangshexue Zazhi* 1998; **32**: 364-369
30 **Marks MP**, de Crespigny A, Lentz D, Enzmann DR, Albers GW, Moseley ME. Acute and chronic stroke: navigated spin-echo diffusion-weighted MR imaging. *Radiology* 1996; **199**: 403-408
31 **Yang ZH**, Xie JX, Zhang YW, HU BF. Study on diffusion-weighted imaging in cirrhotic liver. *Zhongguo Yixue Yingxiang Jishu* 2002; **9**: 907-909

S- Editor Zhu LH **L- Editor** Li M **E- Editor** Yin DH

Online Submissions: wjg.wjgnet.com
www.wjgnet.com
wjg@wjgnet.com

World J Gastroenterol 2007 November 21; 13(43): 5707-5717
World Journal of Gastroenterology ISSN 1007-9327

BASIC RESEARCH

Concurrent repletion of iron and zinc reduces intestinal oxidative damage in iron- and zinc-deficient rats

Sreedhar Bodiga, Madhavan Nair Krishnapillai

Sreedhar Bodiga, Madhavan Nair Krishnapillai, Department of Biophysics, National Institute of Nutrition, Hyderabad 500007, Andhra Pradesh, India
Supported by the Indian Council of Medical Research
Correspondence to: Dr. Madhavan Nair Krishnapillai, Department of Biophysics, National Institute of Nutrition, Indian Council of Medical Research, Jamai-Osmania PO, Hyderabad 500007, Andhra Pradesh, India. nairthayil@hotmail.com
Telephone: +91-40-27008921 Fax: +91-40-27019074
Received: June 15, 2007 Revised: August 16, 2007

Abstract

AIM: To understand the interactions between iron and zinc during absorption in iron- and zinc-deficient rats, and their consequences on intestinal oxidant-antioxidant balance.

METHODS: Twenty-four weanling Wistar-Kyoto rats fed an iron- and zinc-deficient diet (< 6.5 mg Fe and 4.0 mg Zn/kg diet) for 4 wk were randomly divided into three groups (n = 8, each) and orally gavaged with 4 mg iron, 3.3 mg zinc, or 4 mg iron + 3.3 mg zinc for 2 wk. On the last day of repletion, 3 h before the animals were sacrificed, they received either 37 mBq of ^{55}Fe or ^{65}Zn, to study their localization in the intestine, using microautoradiography. Hemoglobin, iron and zinc content in plasma and liver were measured as indicators of iron and zinc status. Duodenal sections were used for immunochemical staining of ferritin and metallothionein. Duodenal homogenates (mitochondrial and cytosolic fractions), were used to assess aconitase activity, oxidative stress, functional integrity and the response of antioxidant enzymes.

RESULTS: Concurrent repletion of iron- and zinc-deficient rats showed reduced localization of these minerals compared to rats that were teated with iron or zinc alone; these data provide evidence for antagonistic interactions. This resulted in reduced formation of lipid and protein oxidation products and better functional integrity of the intestinal mucosa. Further, combined repletion lowered iron-associated aconitase activity and ferritin expression, but significantly elevated metallothionein and glutathione levels in the intestinal mucosa. The mechanism of interactions during combined supplementation and its subsequent effects appeared to be due to modulation of cytosolic aconitase, which in turn influenced the labile iron pool and metallothionein levels, and hence reduced intestinal oxidative damage.

CONCLUSION: Concurrent administration of iron and zinc corrects iron and zinc deficiency, and also reduces the intestinal oxidative damage associated with iron supplementation.

Key words: Iron; Zinc; Absorption; Intestine; Aconitase; Ferritin; Metallothionein; Oxidative damage

Bodiga S, Krishnapillai MN. Concurrent repletion of iron and zinc reduces intestinal oxidative damage in iron- and zinc-deficient rats. *World J Gastroenterol* 2007; 13(43): 5707-5717

http://www.wjgnet.com/1007-9327/13/5707.asp

INTRODUCTION

Iron-deficiency anemia is frequently the result of low intake of dietary iron, and high intake of phytate and tannins, which inhibit iron absorption. An iron-deficient population can generally have zinc deficiency, due to similar influences of various dietary factors on iron and zinc absorption[1]. There is strong evidence in humans that a blockage of zinc absorption is a consequence of daily intake of high amounts of iron[2]. Studies in pregnant women also provide evidence that the absorption of supplemental iron is lower from multimineral antenatal supplements, particularly in the presence of high calcium and magnesium than when it is administered alone[3,4]. It has therefore become evident during the past decade that deficiencies of iron and zinc co-exist, and those vulnerable groups may benefit from iron as well as zinc supplementation, rather than individual supplementation with these minerals. However, iron and zinc are known to interact, either at the site of absorption or post-absorptively, because of competition for similar transport pathways[5-8]. Moreover, these two minerals have opposing effects on oxidant-antioxidant balance in either iron- or zinc-deficient intestines[8,9]. As mineral supplementation programs are designed for populations at risk of both iron and zinc deficiencies, understanding of quantitative and qualitative aspects of the potential of the two metals is critical. Iron and zinc have been found to interact antagonistically at the site of absorption, and this interaction helps in reducing the iron-mediated generation of hydroxyl radicals and

subsequent intestinal oxidative damage during repletion in a single mineral deficiency[8,9]. Other cascading effects of such interactions are the reduction of iron and zinc uptake, aconitase activity, and ferritin expression in the intestinal mucosa. Besides, zinc induction of metallothionein in the intestinal mucosa helps to restore its functional integrity[8]. However, absorption of these two minerals is regulated at the intestinal level[10,11], and hence the nature and extent of interactions may differ when the deficiencies co-exist, because of molecular adaptations that modulate the absorption of these minerals. Therefore, in the present study, we depleted iron and zinc in weanling rats and studied the nature of the interactions between two metals, and their consequences on intestinal oxidant-antioxidant balance; finally we postulated a probable mechanism.

MATERIALS AND METHODS

Animals and diets

This study employed a typical depletion-repletion design for understanding the potential interactions of iron and zinc during supplementation in iron- and zinc-deficient rats. The Institutional Animal Ethical and Bio-safety Committee of the National Institute of Nutrition approved the study.

Twenty-four weanling female Wistar-Kyoto rats, (National Center for Laboratory Animal Science at the National Institute of Nutrition, Hyderabad, India) weighing 35-45 g, were fed an egg-albumin-based, semi-synthetic, purified iron- and zinc-deficient diet (< 6.5 mg Fe and 4.0 mg Zn/kg diet) for 4 wk (Table 1). Rats were housed individually in polypropylene cages with stainless steel wire floors (45 cm × 16 cm, 7.5 mm mesh, 1 mm wire diameter) to prevent coprophagy, in a room maintained at 23℃ and 60% humidity, with a 12-h light: dark cycle. Deionized distilled water, in plastic bottles with stainless steel sippers, was freely available to all rats. Body weight was recorded weekly and blood was collected by orbital sinus puncture for determination of iron and zinc status at the end of depletion and repletion.

Oral repletion of iron and/or zinc

At the end of depletion phase, rats were randomly divided into three groups and assigned to either Fe, Zn and Fe + Zn groups for repletion (n = 8, each). In order to achieve complete repletion of both the minerals, while minimizing the intestinal oxidative damage, we used a dose of 4 mg iron and 3.3 mg zinc for repletion. Force feeding was performed daily during the repletion period, either with a dose of 4.0 mg iron (Fe group), 3.3 mg zinc (Zn group) or a combination of 4.0 mg iron and 3.3 mg zinc (Fe + Zn group) in 1.0 mL 0.01 mol/L HCl, via an orogastric plastic tube, for 2 wk[12]. During this period, the rats were fed an iron- and zinc-deficient diet *ad libitum*. The doses were prepared by dissolving $FeSO_4$ and $ZnSO_4$ salts, either individually or in combination, in dilute HCl[8]. Administration of 0.01 mol/L HCl alone to the rats had no significant effect on the parameters studied[12]. Therefore, vehicle controls were not included in the present study. All the rats were fasted for 16 h before administering the last dose for uptake studies and for studying various other parameters.

Table 1 Composition of the iron and zinc-deficient diet

Ingredient	Concentration g/kg diet
Egg albumin powder	220
Cornstarch	293
Sucrose	300
Cellulose	40
Peanut oil	70
Mineral mixture[1]	35
Vitamin mixture[1]	10
DL-methionine	4

[1]Mineral and vitamin mixture were formulated according to AIN (1993), but mineral mixture was devoid of iron and zinc salts (4.0 mg Zn and 6.5 mg Fe/kg diet) during depletion and repletion.

Uptake of iron and zinc; immunolocalization of ferritin and metallothionein in the duodenum

Three rats, each from the Fe and Zn repleted groups, along with six rats from the Fe + Zn repleted group (three each for ^{55}Fe and ^{65}Zn) were randomly selected. Fe group rats received 4.0 mg Fe with 37 mBq of ^{55}Fe (specific activity, 46.9 mCi/g), Zn group rats received 3.3 mg Zn with 37 mBq of ^{65}Zn (specific activity, 1.14 Ci/g), and the Fe + Zn group rats received 4.0 mg Fe and 3.3 mg Zn with either 37 mBq of ^{55}Fe (n = 3) or 37 mBq of ^{65}Zn (n = 3) (BRIT, Mumbai, India). The rats were killed after collecting blood. Proximal 10-cm portion of the duodenum was excised for mucosa collection. Samples of liver were collected from the rats for iron and zinc determination by atomic absorption spectrophotometry.

The tissues were placed immediately on ice, trimmed of excess fat and mesentery, and weighed. The intestinal segments were flushed with ice-cold saline. Of the 10-cm portion, the first 2.0 cm was used for studying iron and zinc uptake, and localization of their responsive proteins, while the remaining portion was saved and processed for obtaining mucosal homogenates. The 2.0-cm portion was placed in 10% neutral-buffered formalin for 12 h, washed in PBS for 24 h, using a "Swiss roll" technique[13] to evaluate the entire longitudinal section on one slide and embedded in paraffin at 58℃. Multiple serial sections of 4-μm thickness were obtained from these blocks. These sections were dewaxed, defatted, mounted on chrome alum-gelatin coated slides, and dip-coated with Amersham LM1 photographic emulsion (Amersham, UK). These were then exposed for 30 d in a light-proof desiccator at 4℃, before developing and fixing in Kodak D-19 developer and Kodak Rapid fix (Kodak, Rochester NY), respectively. Sections were stained with Mayer's hematoxylin and eosin, and then examined using a Nikon Microfot-FX microscope (Nikon, Japan) at 100 × magnification, and photographed. In separate serial sections, localization of ferritin and metallothionein was probed using immunohistochemistry. Briefly, dewaxed and defatted sections were incubated overnight with a 1:500 dilution of rabbit anti-rat liver ferritin[12], or 1:50 dilution

of metallothionein antibody (Clone E9; Dako Corp, Carpinteria, CA), or with IgG from non-immune rabbit serum. The specific binding was detected by biotinylated goat anti-rabbit IgG and avidin-biotin peroxidase complex (Sigma, St. Louis, MO) using hydrogen peroxide and diaminobenzidine. The endogenous peroxidase was quenched with 0.3% hydrogen peroxide in 100% methanol for 15 min. The sections were counterstained with hematoxylin and eosin and observed by light microscopy at 250 × magnification, and photographed.

Preparation of intestinal mucosa

We used the remaining 7-cm intestinal segment from the radioisotope-treated animals and the whole segment from non radioisotope-treated animals, for preparation of intestinal homogenates. All the animals were sufficiently repleted for 2 wk. However, radioisotope-treated animals received an additional dose of iron and/or zinc at the end of repletion. This single additional dose is unlikely to contribute much to the nutrient status compared to animals that have not received radioisotope.

The duodenal segments collected from each rat in ice-cold 1.15% KCl were scraped and a 10% homogenate of the mucosal suspension was prepared in 1.15% KCl containing 0.5 mmol/L butylated hydroxy tolune (to prevent *ex vivo* peroxidation) as described previously[12]. The homogenate was subjected to differential centrifugation (Sorvall RC-5B, Du Pont Instruments, CT) at 800 *g* for 30 min, 12 000 *g* for 30 min, and 100 000 *g* for 1 h at 4℃, and the respective supernatants were collected and stored at -20℃ until further analysis. The protein content in these supernatants was determined using a modified Lowry method, with BSA as the standard.

Iron and zinc content in diet, plasma and liver

Iron and zinc concentrations in the diet, liver, mineral solutions and plasma were determined by atomic absorption spectrophotometry using a SpectrAA-400 atomic absorption spectrometer (Varian, Sunnyvale, Melbourne, Australia). The mineral deficient diet fed to the rats was digested with concentrated nitric acid and 70% perchloric acid by method (Ⅱ) A of the Analytical Methods Committee (1960)[14]. One g of liver tissue was ashed in a muffle furnace at 600℃ for 6 h and was used to prepare the mineral solution.

Markers of functional integrity

Activity of alkaline phosphatase and lys-ala-dipeptidyl aminopeptidase was measured in the 12 000 *g* supernatant to assess the functional integrity of the intestinal mucosa, because of the differential localization of these two enzymes within the mucosal cells: the maximum activity of the former towards the upper half of the villus, and that of the latter towards the lower half[8,12]. Alkaline phosphatase activity was determined using β-glycerophosphate and lys-ala-dipeptidyl aminopeptidase activity was measured using lys-ala-7-amido-4-methyl coumarin.

Markers of oxidative stress

The amount of thiobarbituric acid-reactive substance (TBARS) in the 12 000 *g* supernatant was measured using malondialdehyde as a standard, and was quantified, using a reverse-phase silica-based C18 column, according to Templar *et al*[15]. Elution was done for 10 min at a flow rate of 1.2 mL/min with 65% 50 mmol/L KH_2PO_4-KOH, pH 7.0, and 35% methanol buffer, while monitoring at 532 nm. Protein carbonyls were estimated by incubation of 1 mL of the 100 000 *g* supernatant with 10 mmol/L dinitrophenyl hydrazine (DNPH) for 1 h in the dark, followed by protein precipitation with trichloroacetic acid according to the method of Reznick & Packer[16]. The final DNPH and lipid-free precipitate was dissolved in 6 mol/L guanidine hydrochloride and the absorbance was read at 375 nm. The amount of protein in the final pellet was quantified at 280 nm using BSA in guanidine hydrochloride as a standard.

Antioxidant status

Activity of total superoxide dismutase (SOD), glutathione peroxidase (100 000 *g* supernatant), Mn-SOD and catalase (12 000 *g* supernatant) was determined as previously described[17-19]. Glutathione (reduced GSH and oxidized GSSH) levels were determined using HPLC equipped with a fluorimetric detector (excitation at 350 nm and emission at 420 nm), according to Pastore *et al*[20]. Briefly, thiols were extracted using sulfosalicylic acid and injected onto a 150 mm × 4.6 mm Hypersil ODS column, equilibrated with 30 mmol/L ammonium nitrate and 40 mmol/L ammonium formate buffer, pH 3.6. For GSH determinations, $NaBH_4$ was substituted with 2 mmol/L EDTA-DTT. The thiols were eluted from the column with a 6-min gradient of acetonitrile (0-4 min, 0%-30% acetonitrile; 4-5 min, 30%-100% acetonitrile; 5-6 min, 100% acetonitrile) at a flow rate of 1.5 mL/min.

Activity of duodenal mucosal aconitase

The activity of aconitase in cytosolic (100 000 *g* supernatant) and mitochondrial (12 000 *g* pellet) was measured by a coupled isocitrate dehydrogenase reaction, monitored at 37℃ (Cary 100 Bio UV-Vis spectrophotometer, Varian Inc., CA) at 340 nm for 1 h [21,22].

Statistical analysis

Statistical analysis was performed using SPSS/PC+, version 5.0 (SPSS, Chicago, IL, USA). Comparison among the three groups was tested by one-way ANOVA with post-hoc multiple comparison tests. For measurements of body weight and iron and zinc status, comparisons were made with littermates maintained in the animal colony. The values were considered significantly different at $P < 0.05$.

RESULTS

Body weight changes

Rats fed an iron- and zinc-deficient diet for 4 wk weighed 57% less than their littermates in the animal colony (62.0 ± 8.0 g and 108.2 ± 7.5 g, respectively). However, the final bodyweight of Fe-, Zn- and Fe + Zn-repleted rats was similar, but weighed 50% of their littermates (95.6 ± 10.2 g and 190.0 ± 14.8 g).

Iron and zinc status

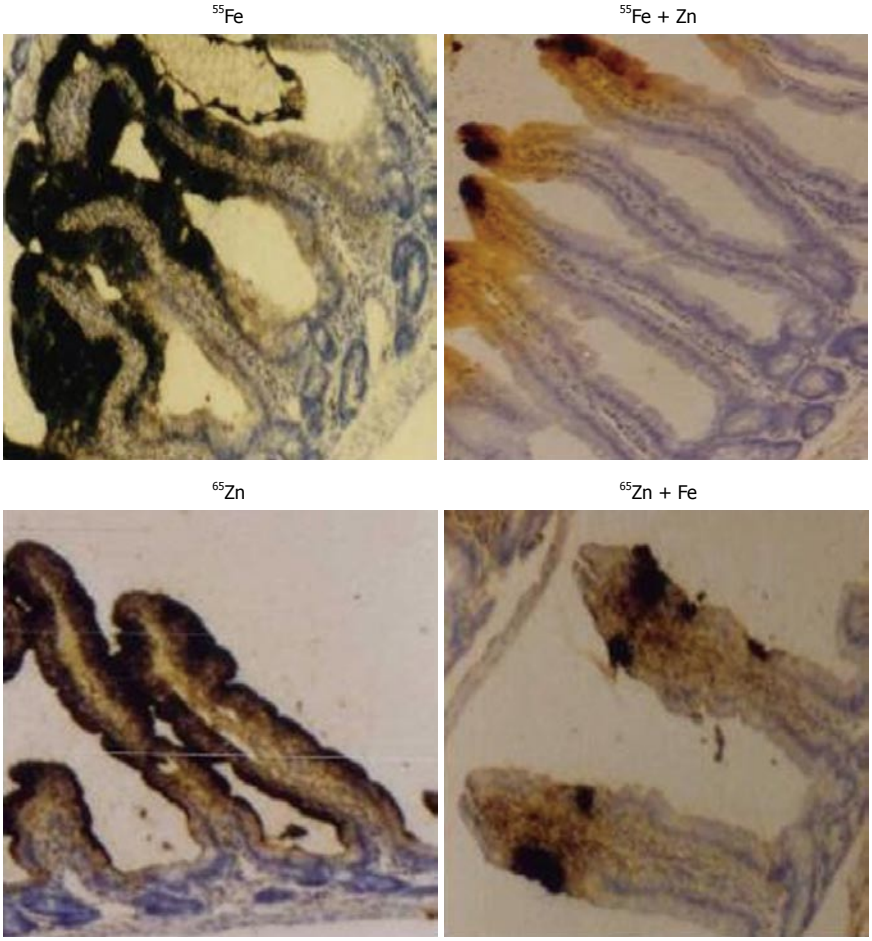

Figure 1 Zn reduces uptake of ^{55}Fe and Fe reduces uptake of ^{65}Zn during combined administration: A representative microautoradiogram of the duodenal mucosa of ^{55}Fe in Fe (top left), Fe + Zn (top right), ^{65}Zn in Zn (bottom left). and Fe + Zn (bottom right) groups. Iron and zinc deficient rats were orally administered 37mBq of ^{55}Fe and 4.0 mg Fe and/or 37mBq of ^{65}Zn and 3.3 mg Zn. Presence of black spots in the intestinal mucosa indicates the presence of the radioactivity (× 100).

Table 2 Iron and zinc status after concurrent depletion and repletion

Group	Hemoglobin (g/L)	Iron		Zinc	
		Plasma (μmol/L)	Liver (μg/g)	Plasma (μmol/L)	Liver (μg/g)
-Fe - Zn	82.0^{a} ± 3.2	65.0^{a} ± 4.6	-	12.3^{a} ± 2.0	-
Fe	126.9^{b} ± 3.0	94.8^{b} ± 7.2	192.8^{a} ± 12.5	13.0^{a} ± 1.8	22.8^{a} ± 4.5
Zn	80.0^{a} ± 2.8	64.0^{a} ± 5.5	43.7^{b} ± 6.6	29.6^{b} ± 3.0	48.6^{b} ± 4.6
Fe + Zn	106.8^{c} ± 3.0	82.4^{c} ± 3.8	157.5^{c} ± 7.7	20.5^{c} ± 3.2	37.1^{c} ± 4.2

Iron and zinc deficient (-Fe-Zn) rats were administered 4.0 mg Fe and/or 3.3 mg Zn/day for 2 wk; Fe: Iron administered group; Zn: Zinc administered group; Fe + Zn: Iron and zinc administered group; Number of animals was 8 in each group. Values are mean ± SD; means with different superscripts are significantly different with $P < 0.05$.

Iron and zinc depletion were confirmed by lowered hemoglobin and plasma zinc concentrations compared to their littermates in the animal colony, which were fed an iron- and zinc-adequate diet (35.0 mg Fe and 30.0 mg Zn/kg diet). Concurrent depletion of iron and zinc resulted in reduction of hemoglobin to 58%, plasma iron to 86% and plasma zinc to 38% compared to littermates. A significant lowering in all the above measured variables indicated the co-existence of iron and zinc deficiency in the experimental rats (Table 2). On repletion, hemoglobin and plasma and liver iron concentrations were significantly higher in the Fe and Fe + Zn groups compared to the Zn group (Table 2). Among the iron-repleted groups, iron status was significantly higher in the Fe than in the Fe + Zn group. Similarly, plasma and liver zinc concentrations were significantly higher in the Zn and Fe + Zn groups than in the Fe group. However, the Fe + Zn group showed significantly lower zinc status compared to the Zn group (Table 2).

Uptake of ^{55}Fe and ^{65}Zn; immunolocalization of ferritin and metallothionein in intestinal mucosa

To understand the effect of interactions following concurrent repletion of iron and zinc to depleted rats, we looked for their presence in the site of absorption. Uptake of ^{55}Fe and ^{65}Zn at the end of repletion in the intestinal mucosa was reduced in Fe + Zn-supplemented rats compared with Fe- or Zn-supplemented rats, respectively (Figure 1). Intestinal ferritin concentration was higher in the Fe than in the Fe + Zn group (Figure 2, upper panel). Identically, metallothionein concentration in the intestinal mucosa was high and appeared similar in the Zn and Fe + Zn groups, but relatively weak in the Fe group (Figure 2, Lower panel).

Intestinal oxidative stress and its functional integrity

Interactions between iron and zinc and their functional relevance to intestinal oxidative stress were assessed by as TBARS and protein carbonyls. TBARS and protein carbonyl concentrations were 1.5-fold higher in the Fe than in the Fe + Zn group. These indices did not differ in the Zn and Fe + Zn groups (Figure 3A and B). Activity

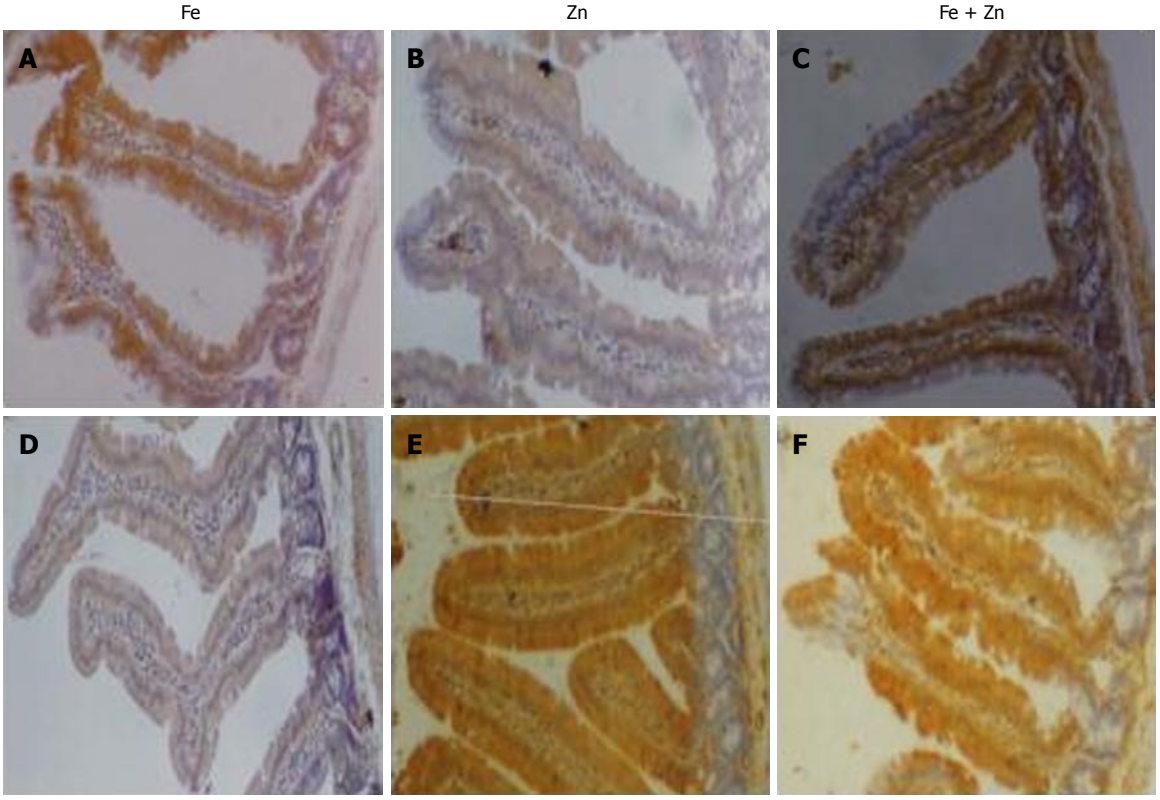

Figure 2 Zn reduces ferritin but enhances metallothionein abundance in the intestinal mucosa: A representative photomicrograph of the immunohistochemical localization of ferritin (top panel) and metallothionein (bottom panel) in the intestinal mucosa of Fe, Zn and Fe + Zn repleted groups. The staining intensity indicates the abundance of ferritin and metallothionein (× 250).

of the marker enzymes alkaline phosphatase and lys-ala-dipeptidyl aminopeptidase in the intestinal mucosa was about 20% lower in the Fe than in the Fe + Zn group. The activity did not differ between the Zn and Fe + Zn groups (Figure 3C and D).

Antioxidant status

Activity of intestinal SOD and glutathione peroxidase, except Mn-SOD, was significantly higher in the Fe than in the Zn and Fe + Zn groups. Catalase activity was significantly higher in the Fe and Fe + Zn groups compared to the Zn group. These enzyme activities did not differ between the Zn and Fe + Zn groups (Figure 4A-D), except for catalase activity. Glutathione concentration was significantly lower in the Fe than in the Zn and Fe + Zn groups. On the other hand, oxidized glutathione (GSSG) concentration was significantly higher in the Fe than in the Zn and Fe + Zn groups (Figure 5A and B).

Intestinal aconitase activity

Activity of cytosolic and mitochondrial aconitase was measured as an indicator of the cellular labile iron pool. Activity was higher in the Fe group, but lowered significantly in the Zn and Fe + Zn groups. Activity in the Fe + Zn group was higher than that in the Zn group (Figure 6A and B).

DISCUSSION

In the light of high prevalence of anemia, emerging incidence of zinc deficiency, and interactions during supplementation, we studied the interactive effects of iron and zinc repletion on oxidant/antioxidant status in combined deficient rats. Metabolic studies and supplementation trials suggest an antagonistic relationship between iron and zinc, in which zinc reduces the positive effects of iron supplementation and vice versa. For example, inorganic iron was found to compete for absorption with zinc when given to adults in solution in ratios > 2:1[2]. Zinc absorption in fasting pregnant Peruvian women treated with Fe or Fe + Zn was significantly reduced compared with non-metals supplemented women[23]; which indicates a post-absorptive effect of iron on zinc absorption. In women treated only with Fe, plasma zinc concentrations was also lower, compared with controls. Conversely, there were smaller improvements in hemoglobin and serum ferritin concentrations in Indonesian children treated both with Fe and Zn than in children treated with Fe alone[24]. Two recent studies on iron and zinc supplementation of Indonesian infants show that iron and zinc interactions occur when they are given as supplements[25,26]. In the study by Dijkhuizen *et al*, infants were treated with iron alone (10 mg/d), zinc alone (10 mg/d), both elements together (10 + 10 mg/d) and placebo from 4 to 10 mo of age. Supplementation significantly reduces the prevalence of iron deficiency anemia and zinc deficiency. Iron supplementation does not negatively affect plasma zinc concentration, and zinc supplementation does not increase the prevalence of anemia. However, combined iron and zinc supplementation is less efficacious than iron supplementation alone in reducing the prevalence

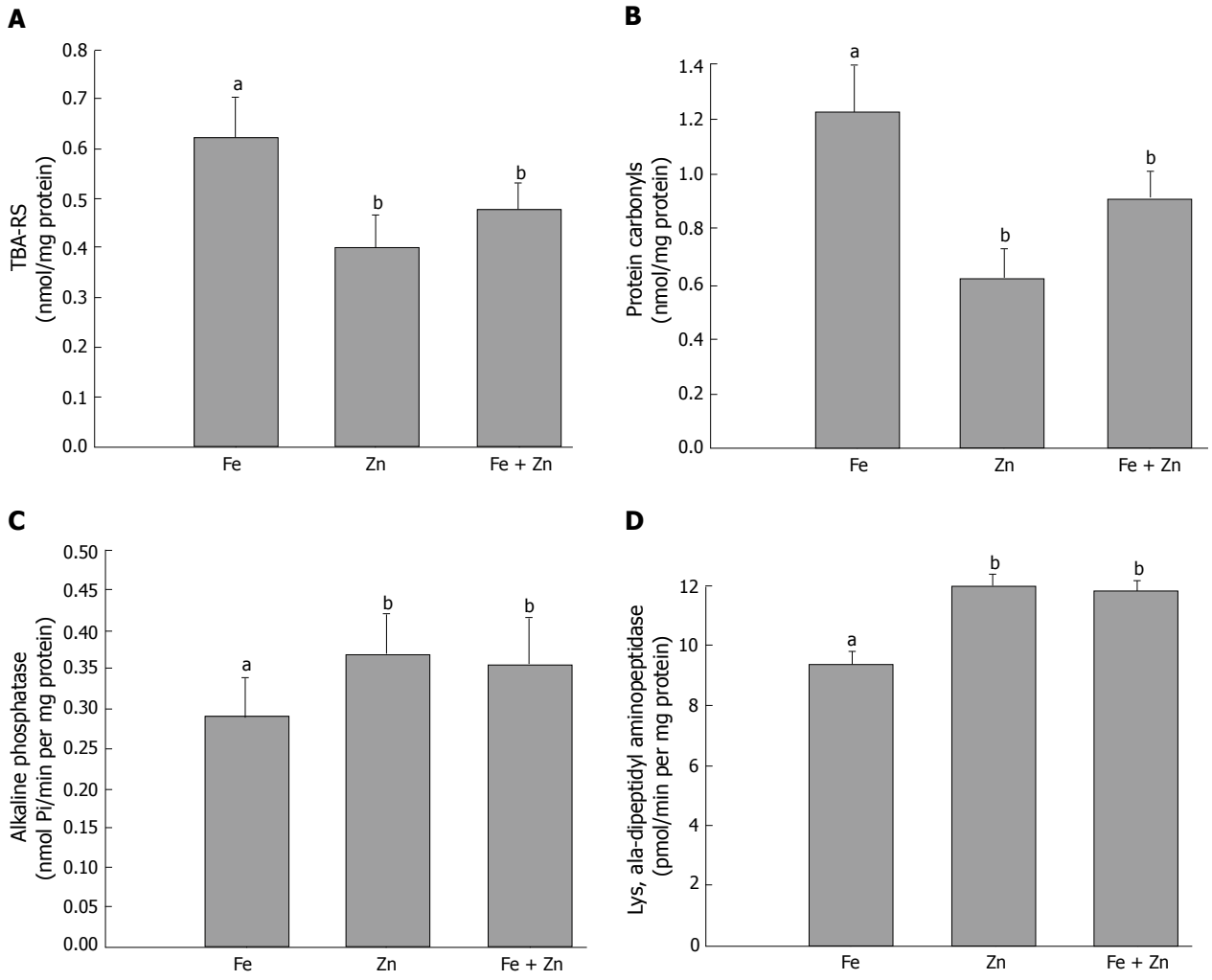

Figure 3 Iron increases intestinal oxidative stress and lowers functional integrity: Concentrations of thiobarbituric acid-reactive substances (TBA-RS) and protein carbonyls (**A** and **B**) as indicators of oxidative stress, and activities of alkaline phosphatase and lys-ala-dipeptidyl aminopeptidase (**C** and **D**), as markers of mucosal functional integrity, in the intestinal mucosa of iron and zinc deficient rats treated with iron and/or zinc. Fe: Iron administered group; Zn: Zinc administered group; Fe + Zn: Iron and zinc administered group; Number of animals: 7 in each group. Vertical columns and error bars represent mean and SD respectively; Bars with different superscripts are significantly different with $P < 0.05$ among groups.

of anemia (20% *vs* 38% reduction) and in increasing hemoglobin and plasma ferritin concentrations. In the study by Lind *et al*, infants received the same treatments, but from 6 to 12 mo of age. After supplementation, the Fe group had higher hemoglobin and serum ferritin than the Fe + Zn group; this fact indicates an effect of zinc on iron absorption. The Zn group had higher serum zinc than the placebo group, whereas this was not the case for the Fe and Fe + Zn groups, this fact suggests an effect of iron on zinc absorption. Thus, supplementation with Fe + Zn is less efficacious than single supplements alone in improving iron and zinc status, with evidence of negative interactions between iron and zinc when a combined supplement is given. However, the crucial question is whether such interactions between iron and zinc have any functional consequences for intestinal oxidative stress and functional integrity.

Both these nutrients are essential for growth, and in populations in which deficiencies of these minerals co-exist, stunting of growth has been reported[27]. Depletion of both iron and zinc in the diet has a significant impact on the growth of rats, and causes a marked reduction in iron and zinc status. Thus, the model developed in the present study had characteristic clinical and sub-clinical manifestations of iron and zinc deficiency, respectively. Although several studies have examined the effect of iron supplementation on zinc absorption, few have considered the effect of zinc supplementation on iron absorption. The molar ratio of iron and zinc seems to be critical in determining the interactive effects. One study has shown that zinc inhibited iron absorption when the zinc-iron ratio was 1.14:1 (1:1 molar ratio), but not when it was 0.36:1 (0.4:1 molar ratio)[28]. Another study has shown that a zinc-iron ratio of 5:1 significantly reduced iron absorption from an aqueous solution, but did not affect heme iron absorption from a hamburger meal in humans[29]. In the present study, we used a 1:1 molar ratio for repletion of iron- and zinc-deficient rats.

Several possible sites of interaction during transfer from the apical membrane into the intestinal cytosolic compartment, and from the basolateral membrane into plasma have been suggested by Fairweather-Tait[30].

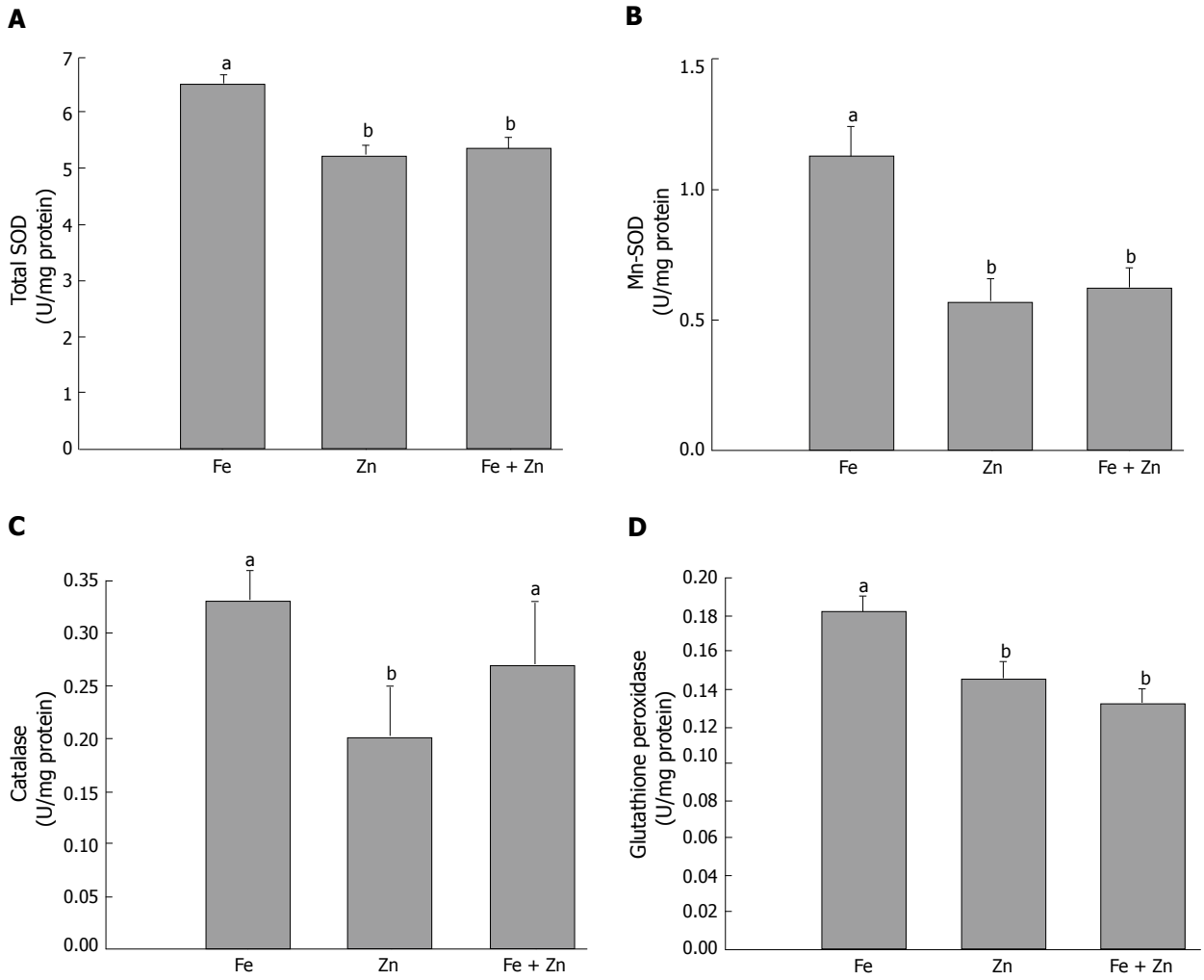

Figure 4 Changes in antioxidant enzyme activities due to iron and zinc repletion: Activity levels of superoxide dismutase (SOD, **A** and **B**), catalase (**C**) and glutathione peroxidase (Gpx, **D**) in the small intestinal mucosa of rats during repletion with iron and/or zinc. Total SOD activity indicates the activity of Cu, Zn-SOD and Mn-SOD. Fe: Iron administered group; Zn: Zinc administered group; Fe + Zn: Iron and zinc administered group; Number of animals: 8 in each group. Vertical columns and error bars represent mean and SD respectively; bars with different superscripts are significantly different with $P < 0.05$.

The possibility of iron and zinc inhibiting each other's intestinal uptake through competition for a common pathway, has been studied by measuring ferritin and metallothionein concentrations, and aconitase activity in the site of absorption. Intestinal uptake of iron and zinc was significantly reduced in the presence of the other metal during repletion in rats with combined deficiencies of iron and zinc. This may have been due to increased competition between iron and zinc for the ligands/transporters at the site of absorption. Reduced uptake of ^{55}Fe or ^{65}Zn in the Fe + Zn group compared to the Fe or Zn groups provides clear evidence for their antagonistic interaction during repletion. Reduced plasma and liver iron and zinc concentrations in the Fe + Zn group compared to individual supplementation groups suggests that iron and zinc interactions affect not only the uptake, but also retention of these minerals. Thus, this study clearly demonstrates that a combined supplement is less efficacious than a single supplement in improving iron or zinc status.

Another intriguing possible site of interaction between iron and zinc is the duodenal transport protein divalent cation transporter 1 (DCT-1). DCT-1 appears to be a key transporter that is involved in iron absorption, but can also transport many other metals, including zinc[31]. It is possible that iron and zinc can inhibit each other's absorption by competing for DCT-1, and their effects are expected to be most noticeable when one metal is in relative excess compared with the other, or when both deficiencies co-exist. Although we have not studied DCT-1 expression, the influence of iron and zinc on their responsive proteins clearly suggests that both interact at the site of absorption during concurrent repletion.

The intestine is vulnerable to oxidative damage during iron and/or zinc depletion and repletion. Incessant pulses of iron during repletion leave excess unabsorbed iron in the intestinal mucosa, which is a potential pro-oxidant. Moreover, electron paramagnetic resonance spectroscopy in rats has shown that oral iron therapy with ferrous sulfate results in iron-mediated oxidative stress, through hydroxyl radicals in the small intestine. This stress-stimuli results in a decrease in cell turnover, shortening of microvillus height, and partial or complete erosion of the microvilli in the duodenum[32-34]. On the

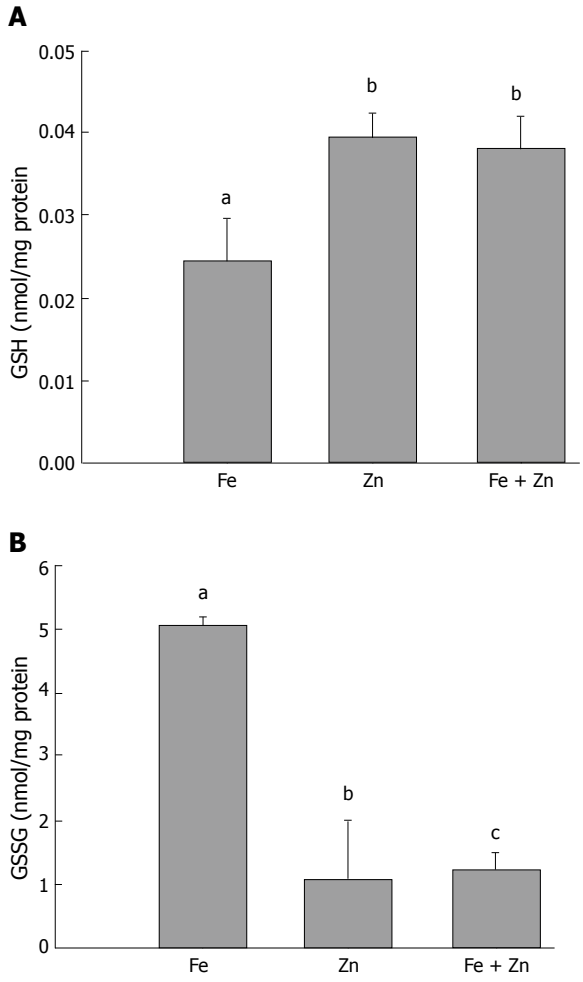

Figure 5 Altered intestinal mucosal redox status: Changes in the levels of GSH (Panel **A**) and GSSG (Panel **B**) in the intestinal mucosa at the end of repletion for 2 wk with iron and/or zinc. Vertical columns and error bars represent mean and SD respectively; bars with different superscripts are significantly different with $P < 0.05$.

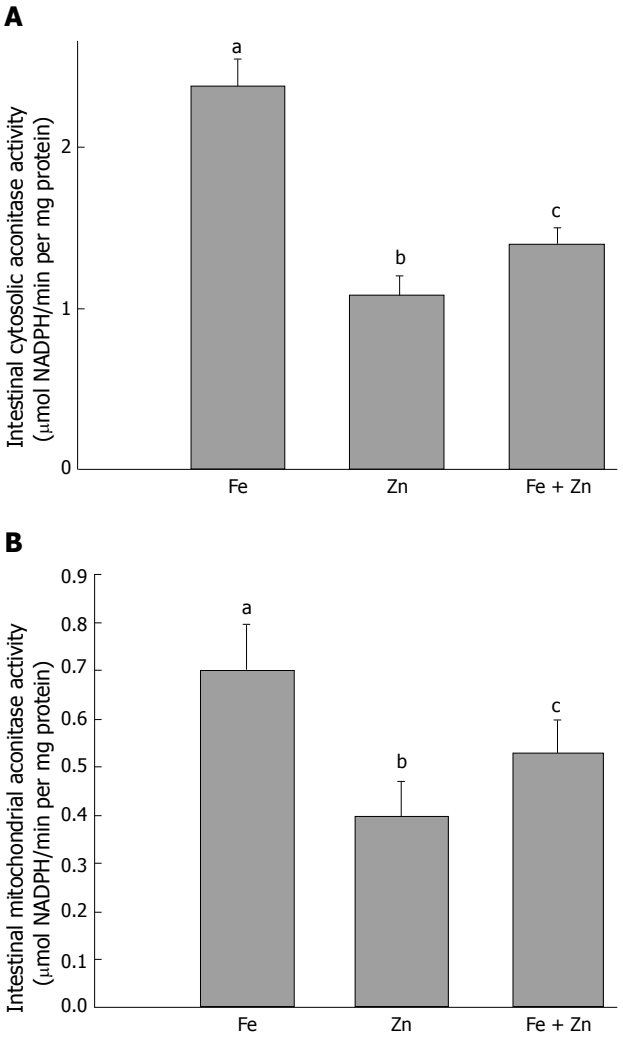

Figure 6 Intestinal aconitase activity in response to iron and/or zinc repletion: Response of intestinal cytosolic (Panel **A**) and mitochondrial (Panel **B**) aconitase to intestinal iron content and as a functional indicator of oxidative stress after 2 wk of oral iron and/or zinc administration. Fe: Iron administered group; Zn: Zinc administered group; Fe + Zn: Iron and zinc administered group. Number of animals :is 8 in each group. Vertical columns and error bars represent mean and SD respectively; bars with different superscripts are significantly different with $P < 0.05$.

other hand, zinc deficiency impairs intestinal antioxidant capacity by lowering the expression of metallothionein, an effective scavenger of hydroxyl radicals that can play a major role in the development of oxidative damage. In an earlier study, we have shown increased hydroxyl radical production, associated decrease in turnover of intestinal epithelial cells, and compromised functional integrity of the mucosa, when iron-deficient rats were repleted with 8.0 mg Fe[12]. This dose may be relatively high and could have produced structural and functional impairment at the site of absorption. To reduce these effects, we used 4.0 mg Fe for repletion and maintained a 1:1 molar ratio of iron and zinc in the present study. Iron repletion resulted in significantly higher levels of peroxidation products, i.e., TBARS and protein carbonyls in the intestinal mucosa, even with lower doses of iron. This also decreased the alkaline phosphatase and dipeptidase activity, which indicates compromised functional integrity. Although zinc negatively affected iron uptake, concurrent repletion of iron and zinc significantly reduced the oxidative damage and improved the functional integrity. The reason for the beneficial effects with co-administration of iron and zinc may be due to the changes in antioxidant balance. We have observed increased localization of metallothionein in the intestinal mucosa during zinc repletion. These findings support the view that zinc *per se* can act at various levels and exert its antioxidant effect. Incorporation of zinc along with iron in supplements seems to be efficacious in improving the antioxidant capacity.

To determine the role of antioxidant defense enzymes in reducing iron-induced oxidative damage, activity of SOD, catalase and glutathione peroxidase were determined. Cu, Zn-SOD was more active in the Fe group compared to that in the Zn and Fe + Zn groups. On the other hand, Mn-SOD activity was similar in all three groups. This indicates that the formation of superoxide anion and its conversion to hydrogen peroxide is greater in the cytosolic compartment than in the mitochondria. The other antioxidant enzyme that showed a difference in the Fe and Zn + Fe groups was glutathione peroxidase (Gpx), which implies that reduction of peroxides to water was more prevalent in the Fe than in the Fe + Zn group.

No increase was observed in the catalase activity of iron-treated animals, which suggests that hydrogen peroxide conversion to water was similar among all groups, but was compensated by an increase in Gpx in the Fe group. This increase in Gpx is indicative of excess formation of organic peroxides in the Fe group, which may have enhanced oxidative stress. In a recent study, we have shown that zinc *per se* can reduce iron-mediated production of hydroxyl radicals and thereby protect against oxidative stress[8]. Hence, concurrent administration of iron and zinc or zinc alone substantially enhances the intestinal non-enzymatic antioxidant capacity. In addition, we have observed in zinc-supplemented groups, increased intestinal metallothionein concentrations, which has been reported to be more effective than GSH on a molar basis for preventing oxidative damage of various cellular components[35]. Quenching of hydroxyl radicals by sulfhydryl groups in metallothionein, releasing zinc and its subsequent uptake by the membranes can protect both cellular components and membranes against oxidative damage[36,37]. Thus, zinc-induced metallothionein not only reduces the oxidative stress, but also improves the functional integrity of the mucosa.

Control of iron uptake and storage through regulation of transferrin receptor and ferritin proteins represents an important avenue through which cellular iron homeostasis is modulated and maintained[38,39]. The expression of ferritin and transferrin receptor is linked to iron status through the action of two iron-regulated RNA-binding proteins, iron regulatory proteins, IRP1 and IRP2. Iron regulates the RNA-binding function of IRP1 and IRP2 through fundamentally different mechanisms[40,41]. For IRP1, which is a bifunctional protein, iron inhibits RNA-binding activity by promoting assembly of an iron-sulfur cluster in the binding protein, thereby converting it to cytosolic aconitase[42]. Walter *et al*[43] has suggested that iron deficiency can induce the IRP-mediated cellular iron signaling pathway, which leads to enhanced intracellular iron levels. Therefore, we assessed the activity of cytosolic and mitochondrial aconitase. Cytosolic aconitase activity was found to be suppressed in the presence of zinc in the Fe + Zn group compared to that in the Fe group. A decrease in cytosolic aconitase activity implies a decrease in cellular iron availability in the presence of zinc, or inhibition of aconitase *per se* by zinc. It has been shown that zinc competitively inhibits duodenal cytosolic aconitase activity[22]. Reduced ferritin protein in the intestinal mucosa of the Fe + Zn group when compared to that of the Fe group supports the decrease in cytosolic aconitase activity in the Fe + Zn group. We also observed a decrease in mitochondrial aconitase activity in the Fe + Zn compared to the Fe group. This may have been due to a decrease in citrate availability or post-transcriptional regulation by IRP1, as reported by Chen *et al*[44]. Nevertheless, zinc seems to act as a buffer against free-radical damage invoked by the presence of free iron. The presence of zinc during supplementation had a significant effect on the levels of various antioxidants, including GSH and metallothionein.

Thus, this study clearly demonstrates that the interactions between iron and zinc during absorption in iron- and zinc-deficient rats are mutually antagonistic. Competition of iron and zinc for common transporters (DMT1) at the site of absorption results in reduced uptake of these minerals during concurrent administration. The presence of zinc during iron administration also influences aconitase activity, ferritin expression and thereby the labile iron pool. Furthermore, zinc induction of metallothionein and scavenging of hydroxyl radicals helps to control iron-mediated oxidative stress.

COMMENTS

Iron deficiency is the single most common nutritional disorder worldwide and the main cause of anemia in infancy, childhood and pregnancy. It is prevalent in most of the developing world, where it coexists with other micronutrient deficiencies such as zinc, vitamin A and folate. The exact prevalence of zinc deficiency is not known, but it is estimated that the magnitude might not be too different from that for iron deficiency. This is probably because the diet of populations in the developing world is based mainly on foodstuffs that have low iron and zinc concentrations, and with a poor bioavailability of these minerals. Combined supplementation with iron and zinc in target populations may be effective in preventing deficiencies of these micronutrients, but knowledge of their potential interactions when given together is inadequate.

Research frontiers

Combined supplementation with both micronutrients is one strategy that can be used to improve the iron and zinc status of a population. However, there is concern about the negative interactions between these two minerals. Studies performed in humans have shown an inhibitory effect of zinc on iron absorption, but it is not well established whether this interaction depends on the absolute amount of iron and zinc in the supplement and/or on the molar ratio between these two minerals, or on nutritional status. This information could help design rational guidelines for iron and zinc supplementation programs. A review of the randomized trials that have assessed the effects of iron and zinc supplementation on iron and zinc status shows that zinc supplementation alone does not appear to have a clinically important negative effect on iron status. However, when zinc is given with iron, iron indicators do not improve as greatly as when iron is given alone. In most of the studies, iron supplementation did not affect the biochemical status of zinc, but the data are not clear regarding morbidity outcomes. Although some trials have shown that joint iron and zinc supplementation has less effect on biochemical or functional outcomes than supplementation with either mineral alone, there is no strong evidence to discourage joint supplementation. Supplementation programs that provide iron and zinc together are an efficient way to provide both micronutrients, provided the benefits of individual supplementation are not lost. Further research is needed before health policies on joint supplementation programs can be established.

Innovations and breakthroughs

Oral iron supplementation is a widely used practice to correct iron-deficiency anemia. Exposure of iron-deficient intestine to large doses of iron is known to induce oxidative damage, which leads to loss of functional integrity and reduced mucosal cell turnover. Intestinal conditioning with anti-oxidants during iron administration has been shown to suppress iron-induced oxidative damage. Zinc is known to protect cells from peroxidative damage by inducing metallothionein and maintaining sulfhydryl group stability. Nevertheless, co-administration of iron and zinc may antagonize each other with respect to absorption. In the present study, we showed that although combined supplementation of iron and zinc marginally inhibits iron uptake, it significantly attenuates oxidative stress by induction of metallothionein and elevation of GSH level. Furthermore, the presence of zinc *in situ* reduced the iron-induced hydroxyl radical production in the intestinal mucosa, as assessed by electron paramagnetic resonance spectroscopy. These results strongly suggest a protective role for zinc on iron-induced oxidative stress, which might have implications in anemia control programs.

Applications

Supplementation with multiple micronutrients is an appealing strategy for the prevention and treatment of anemia and common morbidities that affect women and young children. However, drawing definitive conclusions regarding the

potential benefit or harm of joint supplementation, based on a variety of study designs, target populations and outcome measures, has proven challenging.

Terminology

Nutrient-nutrient interactions: Although the term interaction denotes a bidirectional effect, many interactions are unidirectional, i.e., one nutrient affects the biological disposition of another, which remains more or less passive. Bidirectional interactions are most common among nutrients with similar physicochemical properties and that share a common mechanism of absorption or metabolism. Some uni- or bidirectional interactions are affected by the presence of a third dietary constituent. Nutrient interactions are not usually additive. From the physiological standpoint, nutrient interactions can occur at several different levels: (1) In the diet. The mode of preparation of diets may be as important as their composition in determining nutrient interactions. For example, cooking in an alkaline medium may decrease the interaction between ascorbic acid and iron by destroying the vitamin; (2) In the intestinal lumen. Interactions at this level have received the most attention, because they determine the true availability of a nutrient for translocation through the enterocytes. Most luminal interactions consist of direct nutrient-nutrient interactions, but certain nutrients can indirectly affect the absorption of others by modifying gastrointestinal physiological activities. For example, certain dietary fibers can stimulate gastrointestinal hormone secretion or inhibit micellar formation, thus indirectly affecting nutrient absorption (Table 2); (3) In the post-absorptive phase. Many interactions take place after the process of absorption has been completed. These interactions may be in the form of physiological synergism, such as the effect of vitamin A and zinc on the visual process, or between vitamin A and iron mobilization. Conversely, negative interactions may affect circulating or storage levels of nutrients.

Peer review

In this study, the authors investigated the nature of interactions between iron and zinc, and their consequences on intestinal oxidant-antioxidant balance. They demonstrated that the interactions between iron and zinc during absorption in iron- and zinc-deficient rats were antagonistic. They demonstrated that the antioxidant status was significantly lower in the Fe than in the Zn and Fe + Zn groups, whereas the aconitase activity was higher in the Fe than in the Zn and Fe + Zn groups. In conclusion, they reported that the competition of iron and zinc for common transporters such as DCT-1, at the site of absorption, resulted in reduced uptake of Fe and Zn during concurrent administration. Moreover, they suggested that zinc induction of metallothionein and scavenging of hydroxyl radicals assisted in controlling iron-mediated oxidative stress.

REFERENCES

1 **Lonnerdal B**. Dietary factors influencing zinc absorption. *J Nutr* 2000; **130**: 1378S-1383S
2 **Solomons NW**. Competitive interaction of iron and zinc in the diet: consequences for human nutrition. *J Nutr* 1986; **116**: 927-935
3 **Seligman PA**, Caskey JH, Frazier JL, Zucker RM, Podell ER, Allen RH. Measurements of iron absorption from prenatal multivitamin--mineral supplements. *Obstet Gynecol* 1983; **61**: 356-362
4 **Babior BM**, Peters WA, Briden PM, Cetrulo CL. Pregnant women's absorption of iron from prenatal supplements. *J Reprod Med* 1985; **30**: 355-357
5 **Solomons NW**, Ruz M. Zinc and iron interaction: Concepts and perspectives in the developing world. *Nutr Res* 1997; **17**: 177-189
6 **Isfaoun A**, Bureau F, Mouly-Boudey M, Drosdowsky M, Arhan P, Bougle D. Relationships between iron and zinc metabolism: predictive value of digestive absorption on tissue storage. *J Trace Elem Med Biol* 1997; 11: 23-27
7 **Bougle D**, Isfaoun A, Bureau F, Neuville D, Jauzac P, Arhan P. Long-term effects of iron:zinc interactions on growth in rats. *Biol Trace Elem Res* 1999; **67**: 37-48
8 **Sreedhar B**, Subramaniyan R, Nair KM. A protective role for zinc on intestinal peroxidative damage during oral iron repletion. *Biochem Biophys Res Commun* 2004; **318**: 992-997
9 **Sreedhar B**, Nair KM. Modulation of aconitase, metallothionein, and oxidative stress in zinc-deficient rat intestine during zinc and iron repletion. *Free Radic Biol Med* 2005; **39**: 999-1008
10 **Lonnerdal B**. Trace element nutrition in infants. *Annu Rev Nutr* 1989; **9**: 109-125
11 **Lombard M**, Chua E, O'Toole P. Regulation of intestinal non-haem iron absorption. *Gut* 1997; **40**: 435-439
12 **Srigiridhar K**, Nair KM. Iron-deficient intestine is more susceptible to peroxidative damage during iron supplementation in rats. *Free Radic Biol Med* 1998; **25**: 660-665
13 **Moolenbeek C**, Ruitenberg EJ. The "Swiss roll": a simple technique for histological studies of the rodent intestine. *Lab Anim* 1981; **15**: 57-59
14 **Analytical Methods Committee Methods of destruction of organic matter.** *Analyst* 1960; **85**: 643-656
15 **Templar J**, Kon SP, Milligan TP, Newman DJ, Raftery MJ. Increased plasma malondialdehyde levels in glomerular disease as determined by a fully validated HPLC method. *Nephrol Dial Transplant* 1999; **14**: 946-951
16 **Reznick AZ**, Packer L. Oxidative damage to proteins: spectrophotometric method for carbonyl assay. *Methods Enzymol* 1994; **233**: 357-363
17 **Marklund S**, Marklund G. Involvement of the superoxide anion radical in the autoxidation of pyrogallol and a convenient assay for superoxide dismutase. *Eur J Biochem* 1974; **47**: 469-474
18 **Aebi HE**. Catalase. In: Bergmeyer HU. editor. Methods in Enzymatic analysis [Vol.Ⅲ]. Weinheim, Germany: Verlag Chemiel, 1983: 273-282 [Book chapter]
19 **Paglia DE**, Valentine WN. Studies on the quantitative and qualitative characterization of erythrocyte glutathione peroxidase. *J Lab Clin Med* 1967; **70**: 158-169
20 **Pastore A**, Massoud R, Motti C, Lo Russo A, Fucci G, Cortese C, Federici G. Fully automated assay for total homocysteine, cysteine, cysteinylglycine, glutathione, cysteamine, and 2-me rcaptopropionylglycine in plasma and urine. *Clin Chem* 1998; **44**: 825-832
21 **Rose IA**, O'Connell EL. Mechanism of aconitase action. I. The hydrogen transfer reaction. *J Biol Chem* 1967; **242**: 1870-1879
22 **Sreedhar B**, Nair KM. Iron dependence and zinc inhibition of duodenal cytosolic aconitase of rat. *Indian J Biochem Biophys* 2004; **41**: 250-253
23 **O'Brien KO**, Zavaleta N, Caulfield LE, Wen J, Abrams SA. Prenatal iron supplements impair zinc absorption in pregnant Peruvian women. *J Nutr* 2000; **130**: 2251-2255
24 **Schultink W**, Merzenich M, Gross R, Shrimpton R, Dillon D. Effects of iron zinc supplementation on the iron, zinc, and vitamin A status of anaemic preschool children in Indonesia. *Food Nutr Bull* 1997; **18**: 311-317
25 **Dijkhuizen MA**, Wieringa FT, West CE, Martuti S, Muhilal. Effects of iron and zinc supplementation in Indonesian infants on micronutrient status and growth. *J Nutr* 2001; **131**: 2860-2865
26 **Lind T**, Lonnerdal B, Stenlund H, Gamayanti IL, Ismail D, Seswandhana R, Persson LA. A community-based randomized controlled trial of iron and zinc supplementation in Indonesian infants: effects on growth and development. *Am J Clin Nutr* 2004; **80**: 729-736
27 **Rosado JL**. Separate and joint effects of micronutrient deficiencies on linear growth. *J Nutr* 1999; **129**: 531S-533S
28 **Crofton RW**, Gvozdanovic D, Gvozdanovic S, Khin CC, Brunt PW, Mowat NA, Aggett PJ. Inorganic zinc and the intestinal absorption of ferrous iron. *Am J Clin Nutr* 1989; **50**: 141-144
29 **Rossander-Hulten L**, Brune M, Sandstrom B, Lonnerdal B, Hallberg L. Competitive inhibition of iron absorption by manganese and zinc in humans. *Am J Clin Nutr* 1991; **54**: 152-156
30 **Fairweather-Tait SJ**. Iron-zinc and calcium-Fe interactions in relation to Zn and Fe absorption. *Proc Nutr Soc* 1995; **54**: 465-473
31 **McMahon RJ**, Cousins RJ. Regulation of the zinc transporter ZnT-1 by dietary zinc. *Proc Natl Acad Sci USA* 1998; **95**: 4841-4846
32 **Srigiridhar K**, Nair KM. Protective effects of antioxidant enzymes and GSH in vivo on iron mediated lipid peroxidation

in gastrointestinal tract of rat. *Indian J Biochem Biophys* 1997; **34**: 402-405
33 **Srigiridhar K**, Nair KM. Supplementation with alpha-tocopherol or a combination of alpha-tocopherol and ascorbic acid protects the gastrointestinal tract of iron-deficient rats against iron-induced oxidative damage during iron repletion. *Br J Nutr* 2000; **84**: 165-173
34 **Srigiridhar K**, Nair KM, Subramanian R, Singotamu L. Oral repletion of iron induces free radical mediated alterations in the gastrointestinal tract of rat. *Mol Cell Biochem* 2001; **219**: 91-98
35 **Abel J**, de Ruiter N. Inhibition of hydroxyl-radical-generated DNA degradation by metallothionein. *Toxicol Lett* 1989; **47**: 191-196
36 **Thornalley PJ**, Vasak M. Possible role for metallothionein in protection against radiation-induced oxidative stress. Kinetics and mechanism of its reaction with superoxide and hydroxyl radicals. *Biochim Biophys Acta* 1985; **827**: 36-44
37 **Thomas JP**, Bachowski GJ, Girotti AW. Inhibition of cell membrane lipid peroxidation by cadmium- and zinc-metallothioneins. *Biochim Biophys Acta* 1986; **884**: 448-461
38 **Theil EC**. Iron regulatory elements (IREs): a family of mRNA non-coding sequences. *Biochem J* 1994; **304** (Pt 1): 1-11
39 **Eisenstein RS**, Kennedy MC, Beinert H. In: Silver S, Walden W, editors. Metal Ions in Gene Regulation. New York: Chapman and Hall, Inc., 1997: 157-216
40 **Guo B**, Phillips JD, Yu Y, Leibold EA. Iron regulates the intracellular degradation of iron regulatory protein 2 by the proteasome. *J Biol Chem* 1995; **270**: 21645-21651
41 **Henderson BR**, Kuhn LC. Differential modulation of the RNA-binding proteins IRP-1 and IRP-2 in response to iron. IRP-2 inactivation requires translation of another protein. *J Biol Chem* 1995; **270**: 20509-20515
42 **Kennedy MC**, Mende-Mueller L, Blondin GA, Beinert H. Purification and characterization of cytosolic aconitase from beef liver and its relationship to the iron-responsive element binding protein. *Proc Natl Acad Sci USA* 1992; **89**: 11730-11734
43 **Walter PB**, Knutson MD, Paler-Martinez A, Lee S, Xu Y, Viteri FE, Ames BN. Iron deficiency and iron excess damage mitochondria and mitochondrial DNA in rats. *Proc Natl Acad Sci USA* 2002; **99**: 2264-2269
44 **Chen OS**, Schalinske KL, Eisenstein RS. Dietary iron intake modulates the activity of iron regulatory proteins and the abundance of ferritin and mitochondrial aconitase in rat liver. *J Nutr* 1997; **127**: 238-248

S- Editor Liu Y **L- Editor** Kerr C **E- Editor** Li HY

Online Submissions: wjg.wjgnet.com
www.wjgnet.com
wjg@wjgnet.com

World J Gastroenterol 2007 November 21; 13(43): 5718-5724
World Journal of Gastroenterology ISSN 1007-9327

BASIC RESEARCH

Silencing SMYD3 in hepatoma demethylates RIZI promoter induces apoptosis and inhibits cell proliferation and migration

Li-Bo Chen, Jun-Yao Xu, Zhen Yang, Guo-Bin Wang

Li-Bo Chen, Guo-Bin Wang, Hepatobiliary center, Union Hospital of Huazhong University of Science & Technology, Wuhan 430022, Hubei province, China
Jun-Yao Xu, Department of General Surgery, The Second Affiliated Hospital of Sun Yat-seu University, Guangzhou 510120, Guangdong province, China
Zhen Yang, Department of integrated surgery, Tongji Hospital of Huazhong University of Science & Technology, Wuhan 430030, Hubei province, China
Supported by National Natural Science Foundation of China, No 30200273 & 30672067
Correspondence to: Li-Bo Chen, Hepatobiliary center, Union Hospital of Huazhong University of Science and Technology, Wuhan 430022, Hubei province, China. libo_chen@hotmail.com
Telephone: +86-27-85351623 Fax: +86-27-85776343
Received: April 04, 2007 Revised: July 31, 2007

Abstract

AIM: To investigate the role of SMYD3 in hepatocellular carcinoma (HCC) development and progression and to verify whether its regulation activity was through RIZ1 inactivation.

METHODS: Expression of SMYD3 in HCC cell lines and tissues were measured; silencing of SMYD3 by RNA interference (RNAi) was effectuated, hepatoma cell proliferation, migration and apoptosis were tested, with RIZ1 CpG promoter methylation, and corresponding mRNA expression were investigated.

RESULTS: SMYD3 over-expression in HCC was associated with RIZ1 hypermethylation and mRNA down-expression. Suppression of SMYD3 expression de-methylated RIZ1 CpG promoter ($P < 0.01$) and increased RIZ1 mRNA expression ($P < 0.01$). Consequently, SMYD3 down-expression with RIZ1 de-methylation strongly inhibited hepatoma cell growth (MTT inhibitory rates: Pgenesil-1-s1 60.95% ± 7.97%, Pgenesil-1-s2 72.14% ± 9.68% *vs* Pgenesil-1-hk 6.89% ± 4.12%, $P < 0.01$) and migration (Pgenesil-1-s1 4.24% ± 1.58%, Pgenesil-1-s1 4.87% ± 0.73% *vs* Pgenesil-1 19.03% ± 4.63%, Pgenesil-1-hk 19.95% ± 5.21%, $P < 0.01$) and induced apoptosis (FCM subG1 phase Pgenesil-1-s1 19.07% ± 1.78%, Pgenesil-1-s2 17.68% ± 2.36% *vs* Pgenesil-1 0.47% ± 0.12%, Pgenesil-1-hk 1.46% ± 0.28%, $P < 0.01$. TUNEL-positive cells: Pgenesil-1-s1 40.24% ± 5.18%, Pgenesil-1-s2 38.48% ± 4.65% *vs* Pgenesil-1 2.18% ± 1.34%, Pgenesil-1-hk 2.84% ± 1.22%, $P < 0.01$) in HepG2 cells.

CONCLUSION: These results demonstrate that SMYD3 plays a critical role in the carcinogenesis and progression of HCC. The proliferation, migration induction and apoptosis inhibition activities of SMYD3 may be mediated through RIZ1 CpG promoter hypermethylation.

Key words: SMYD3; Hepatocellular carcinoma; Retinoblastoma protein-interacting zinc finger gene; Histone methyltransferase; DNA methylation

Chen LB, Xu JY, Yang Z, Wang GB. Silencing SMYD3 in hepatoma demethylates RIZI promoter induces apoptosis and inhibits cell proliferation and migration. *World J Gastroenterol* 2007; 13(43): 5718-5724

http://www.wjgnet.com/1007-9327/13/5718.asp

INTRODUCTION

Hepatocellular carcinoma (HCC) is one of the most common malignancies worldwide, generally long-term survival is disappointing. Epigenetics, defined as heritable changes in gene expression that are not coded in the DNA sequence itself, is increasingly linked with tumorigenesis[1,2]. It is well established that DNA methylation, nucleosomal histone post-translational modifications such as methylation, acetylation/deacetylation, phosphorylation ADP-ribosylation, and ubiquitination, and other epigenetic patterns are central to proper gene expression. Increasing evidence shows that disrupting epigenetic patterns can induce carcinogenesis or affect the outcome of cancer[3,4]. Among these, histone methylation is considered to be critical for transcriptional regulation and seems to play an important role in tumor epigenetic modification. Recently, SMYD3 was identified and characterized to specifically methylate histone H3 at lysine 4 (K4), and this activity is indeed dependent on an intact SET domain, an evolutionarily conserved protein module shown to facilitate histone methyltransferase activity[5]. Expression of SMYD3 was frequently enhanced in colorectal carcinoma (CRC), breast cancer tissue, as well as HCC, and elevated *SMYD3* expression was involved in the growth of CRC, breast cancer and HCC cells[5-7]. Although transcriptional activation of downstream genes including *Nkx2.8* and *WNT10B* gene has been reported[5,6], the effect of SMYD3 on HCC development and the underlining mechanism remains unclear.

Inactivation of tumor suppressive genes (TSGs) plays an important role in carcinogenesis. RIZ1, a typical

TSG with H3-K9 methyltransferase activity, was shown to lose its expression and tumor-suppressing activity in many types of human tumors including HCC[8], CRC[9], breast cancer[10], prostate cancer[11] and gastric cancer[12]. Adenovirus-mediated RIZ1 expression causes G2-M cell cycle arrest and/or apoptosis in breast cancer, liver cancer, and microsatellite instability-positive colon cancer cells. Adenovirus RIZ1 can also inhibit growth of colon cancer xenografts[13]. Previous data suggest that the RIZ locus is a target of frequent deletion in HCC, but a more common way of RIZ inactivation in HCC may not involve mutations that alter peptide sequences, but by CpG promoter hypermethylation[14].

Therefore, we sought to explore whether targeting of SMYD3 expression can inhibit the development of HCC, and determine whether the biological function of SMYD3 in HCC development and progression is mediated through RIZ1 inactivation. We found SMYD3 was significantly overexpressed in HCC cell lines, but not in normal hepatocellular cells and peri-cancerous tissues. Silencing of SMYD3 by RNAi remarkably inhibited HCC cell proliferation and migration, and induced apoptosis *in vitro*. Furthermore, RIZ1 was under-expressed in HCC cells with its promoter hypermethylated, while inhibition of SMYD3 demethylated RIZ1 and recovered its expression in HCC cells. Our results indicated that SMYD3 plays pro-oncological function in HCC development and progression; thus the activity of SMYD3 in HCC may be partly through its activity on RIZ1 promoter hypermethylation and RIZ1 inactivity.

MATERIALS AND METHODS

Cell lines

HCC cell lines HepG2 and Hep3B were purchased from the American Type Culture Collection (Rockville, MD). HCC cell line SMMC-7721 and liver cell line L-02 were generous gifts from Dr. Danhui Weng (HUST, China). The cells were cultured in Dulbecco's modified Eagle's medium (Gibco-BRL, Carlsbad, CA) supplemented with 10% fetal bovine serum (Gibco-BRL).

RT-PCR

Total RNA was extracted using Trizol reagent (Takara, Tokyo, Japan). RT-PCR was performed with the Advantage RT-PCR kit (Takara), according to the manufacturer's protocol. PCR setting: Initial denaturation at 94℃ for 3 min before 18 cycles (for *GAPDH*) or 30 cycles (for *SMYD3* and *RIZ1*) at 94℃ for 30 s, 50℃ for 45 s and 72℃ for 60 s. The sets of primers are listed in Supplementary Information Table S1.

shRNA construction and transfection

The Pgenesil-1 vector containing the U6 promoter region was purchased from Genesil Biotechnology Corporation (Wuhan, China). Plasmids expressing siRNAs were prepared by cloning double-stranded oligonucleotides into the Pgenesil-1 vector. The sets of primers are listed in Supplementary Information Table S1. Positive clones were identified by restriction digestion and confirmed by sequencing. The resulting plasmids were designated as Pgenesil-1-s1, Pgenesil-1-s2 and negative control Pgenesil-1-hk. Transfection was performed by Lipofectamine 2000 reagent (Invitrogen, Carlsbad, CA) in accordance with the manufacturer's protocol.

Western blot analysis

Proteins were prepared by homogenization of cells in lysis buffer (10 mmol/L Tris-HCl, pH 8.0; 140 mmol/L NaCl; 5 mmol/L EDTA; 0.25 g/L NaN_3; 10 g/L Triton X-100; 10 g/L deoxycholate; 1 g/L SDS; 0.5 mmol/L PMSF; 1 g/L leupeptin; 1 g/L aprotinin). Protein concentration was determined by the Lowry method (Bio-Rad, Hercules, CA). Proteins were resolved (30 μg per lane) in 120 g/L sodium dodecyl sulfate-polyacrylamide gel electrophoresis and was transblotted onto a PVDF membrane (Amersham, Arlington Heights, IL). Membranes were blocked in 50 mL/L non-fat milk overnight and subsequently incubated with 1:2000 rabbit polyclonal anti-SMYD3 antibody (a generous gift from Dr. Ryuji Hamamoto of the University of Tokyo, Tokyo, Japan), or anti-β-actin (1:5000 dilution, Sigma, St. Louis, MO) for 1 h and then with secondary anti-rabbit IgG-horseradish-peroxidase antibody for 1 h at room temperature. Immunoreactive proteins were visualized by means of enhanced chemiluminescence reagent (Pierce Biotechnology, Rockford, IL) and exposure to autoradiographic film.

Proliferation assay of HepG2 cell

MTT experiments were carried out using the cell proliferation kit (Roche Diagnostics, Indianapolis, IN), according to the manufacturer's manual. Briefly, stable transfected and parental HepG2 cells were seeded at a density of 5×10^3 cells/well in 96-well plates and allowed to grow for 48 h and then 20 μL 5 g/L MTT was added. After incubation for 4 h, DMSO 200 g/L was added to each well to dissolve crystals. After 5 min incubation at 37℃, absorbance was measured at 570 nm. Assays were performed in triplicate.

Migration assay of HepG2 cell

This assay for the invasiveness of cells was based on the principle of Boyden chamber (BD Biosciences, San Diego, CA) and performed according to the manufacturer's protocol. Briefly, the top compartment was prepared by coating the filter with diluted Matrigel and incubated for 30 min. A suspension of 1×10^4 cells in serum-free medium was inoculated in the upper chamber, and conditioned media obtained from NIH3T3 cells was placed in the lower compartment of the chamber, as a chemoattractant. After 24 h incubation, noninvasive cells were removed with a cotton swab. The cells which migrated through the filter and adhered to the lower surface of the filter were fixed with methanol, stained with hematoxylin, and counted manually in 5 randomly selected microscopic fields. Assays were performed in triplicate. The data were reported as the percentage of cells successfully passing through the Matrigel and filter relative to those migrating through the control filter.

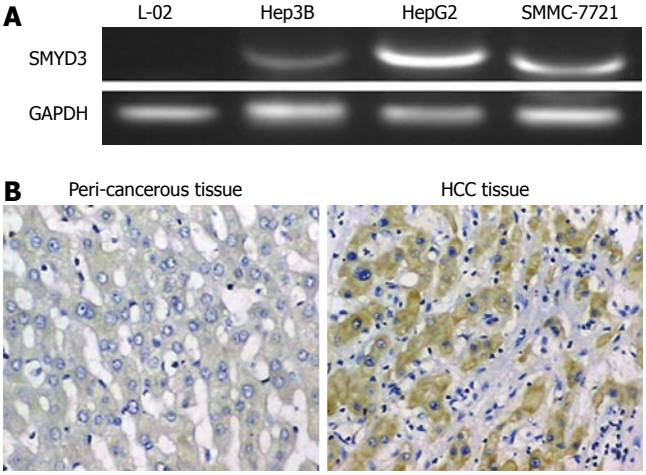

Figure 1 Enhanced expression of SMYD3 in HCC. **A**: The expression of SMYD3 genes was determined by RT-PCR and GAPDH served as an internal control; **B**: Representative images of immunohistochemical staining of accumulated SMYD3 protein in HCC tissue, but not in peri-cancerous tissue.

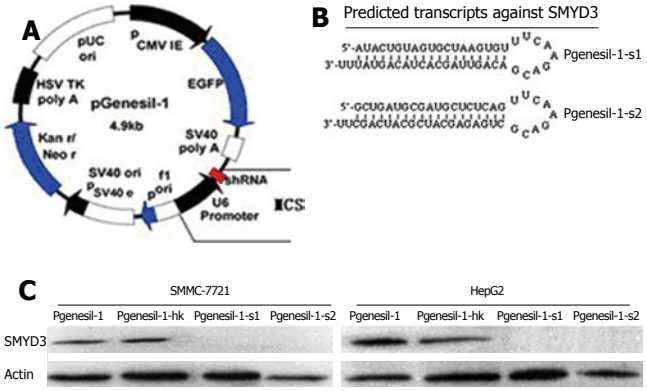

Figure 2 RNAi specifically inhibits SMYD3 expression in HCC cell lines. **A**: Schematic drawing of the Pgenesil-1 vector; **B**: The predicted secondary structures of the Pgenesil-1-s1 and Pgenesil-1-s2 transcripts target SMYD3 are shown; **C**: 48h after transfection, Western blot analysis showed the inhibitory effect of plasmids expressing SMYD3 shRNAs in HepG2 and SMMC-7721 cells.

FCM analysis

HepG2 cells, 1×10^6, were seeded in 60-mm dishes and transfected with SMYD3-RNAi-plasmids at 60%-80% confluence. Then, 48 h after transfection, cells were deprived of serum for 36 h. Afterwards, cells were harvested, fixed in 700 mL/L ethanol and washed with 1 × PBS and suspended in 50 mg/L propidium iodide. DNA content was determined by flow cytometry using a Becton-Dickinson FACSCalibur (Becton Dickinson, Bedford, MA). Results were analyzed by ModFit LT2.0 and Cellquest software. Assays were performed in triplicate.

TUNEL assay

Apoptotic cells were identified with the *In Situ* Cell Death Detection kit (Roche Applied Science, Shanghai, China) using the protocol recommended by the manufacturer. In brief, HepG2 cells were grown on coverslips. The next day, cells were transfected with SMYD3-RNAi-plasmids. At 48 h after transfection, cells were deprived of serum for 36 h. Coverslips with adherent cells were fixed in 40 g/L paraformaldehyde for 1 h at room temperature and permeabilized with 1 g/L Triton X-100 for 2 min on ice. DNA fragments were labeled with the TdT-mediated dUTP nick end labeling (TUNEL) reaction mixture for 60 min at 37℃ in a humidified atmosphere in the dark. Diaminobenzidine was used to mark the apoptotic cells (brown staining). Cells were counted manually in six randomly selected microscopic fields for each sample. The apoptosis index was defined by the percentage of apoptotic cells among the total cells of each sample.

RIZ1 promoter methylation specific PCR assay

Methylation Specific PCR (MSP) assay was performed according to the procedure described by Fang *et al*[15]. In brief, 1 μg of the genomic DNA was modified by sodium bisulfide using the CpGenome DNA Modification Kit (Intergen, Purchase, NY) in accordance with the manufacturer's instructions. Modified DNA was amplified by two different primer pairs specific to the unmethylated (U) and methylated (M) *RIZ1* sequences, respectively. The sets of primers are listed in Supplementary Information Table S1. The PCR amplification was performed for a total of 45 cycles with an annealing temperature of 68℃ and 60℃ for M-sequences and U-sequences, respectively. The PCR products were then analyzed using a 35 g/L agarose gel.

Statistical analysis

SPSS 13.0 was used to analyze the data. Statistical significance was assessed by comparing mean ± SD with Student's *t* test for independent groups. $P < 0.05$ was considered statistically significant.

RESULTS

Enhanced SMYD3 expression in HCC cell lines

To determine whether SMYD3 gene is overexpressed in HCC cell lines, we compared the level of SMYD3 gene expression in normal human hepatocellular cell line L-02 to that of three HCC cell lines. RT-PCR analysis revealed that SMYD3 was overexpressed in all HCC cells, but absent in L-02 cells (Figure 1). These data indicate that enhanced SMYD3 expression is involved in a majority of HCC.

RNAi specifically inhibits SMYD3 expression in HCC cell lines

To inhibit SMYD3 expression in HCC cells, we used a DNA-based siRNA method (Figure 2A). Two siRNAs targeting different 21 sequences of human SMYD3 were cloned into Pgensil-1 vector to express RNA, which is expected to fold back to form a hairpin loop structure after being transcribed. The hairpin dsRNA can then be further cleaved by Dicer to generate a 21-nucleotide siRNA, the active form for the RNAi effect (Figure 2B). We used HepG2 and SMMC-7721 cells, which overexpress SMYD3 abundantly. Forty eight hours after transfection, Pgenesil-1-s1 and Pgenesil-1-s2 markedly knocked down SMYD3 expression in these cells, as determined by Western blot analysis. The specificity of RNAi targeting SMYD3 was shown by transfection with Pgenesil-1-hk which had no effect on SMYD3 expression (Figure 2C).

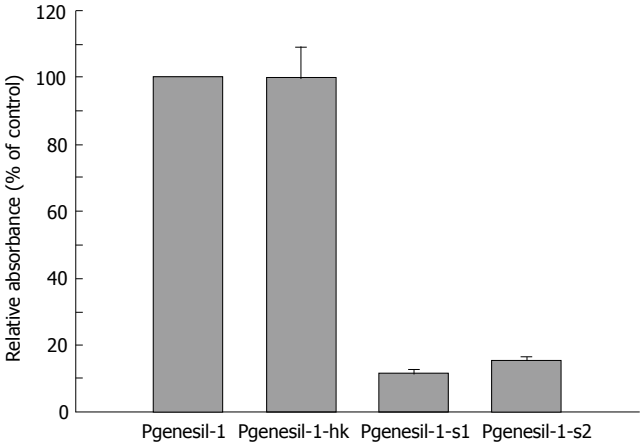

Figure 3 Inhibition of SMYD3 reduces hepatoma cell proliferation (MTT assays).

Inhibition of SMYD3 reduces hepatoma cell proliferation

MTT assay was used to examine the inhibitory effect of RNAi against SMYD3 on cell growth in HepG2 cells. Suppression of SMYD3 expression significantly inhibited cell growth compared to the cells transfected with control plasmid Pgenesil-1. Pgenesil-1-hk, which did not suppress expression of SMYD3, was shown to have little inhibitory effect on growth of HepG2 cells, compared to Pgenesil-1 (Figure 3). The growth inhibitory effect of the plasmids was consistent with their gene silencing effect. Therefore, SMYD3 RNAi significantly suppressed the growth of HeG2 cells *in vitro*, indicating that SMYD3 may be involved in the regulation of cell proliferation.

Inhibition of SMYD3 reduces hepatoma cell migration

The HepG2 cell line has been characterized as a highly invasive hepatocellular cancer cell line. To determine whether SMYD3 gene knockdown by RNAi could reduce its invasive potential, an *in vitro* invasion assay was performed. As shown in Figure 4, HepG2 cells were greatly deprived of invasiveness by depletion of SMYD3 gene expression. The percentage of invasive cells was decreased by 3-4 fold in Pgenesil-1-s1 and Pgenesil-1-s2 treated groups, compared to Pgenesil-1 treated groups. No significant decrease of invasive cells was observed in Pgenesil-1-hk treated cells. These results demonstrate that SMYD3 not only plays a pivotal role in the process of development, but it also is involved in tumor cell migration.

Inhibition of SMYD3 promotes apoptosis in hepatoma cells

Flow cytometry analysis showed that after 48 h of transfection and 36 h serum deprivation, the number of cells in the sub G1 phase was 19.07 ± 1.78% and 17.68 ± 2.36% in HepG2 cells transfected with Pgenesil-1-s1 and Pgenesil-1-s2, respectively, while only 0.47% ± 0.12% and 1.46% ± 0.28% cells were observed in HepG2 cells transfected with Pgenesil-1 and Pgenesil-1-hk, respectively (Figure 5A). These results possibly suggest the induction of apoptosis. To confirm whether silencing of SMYD3 can induce apoptosis in HCC cells following serum deprivation, TUNEL assay was performed. The number

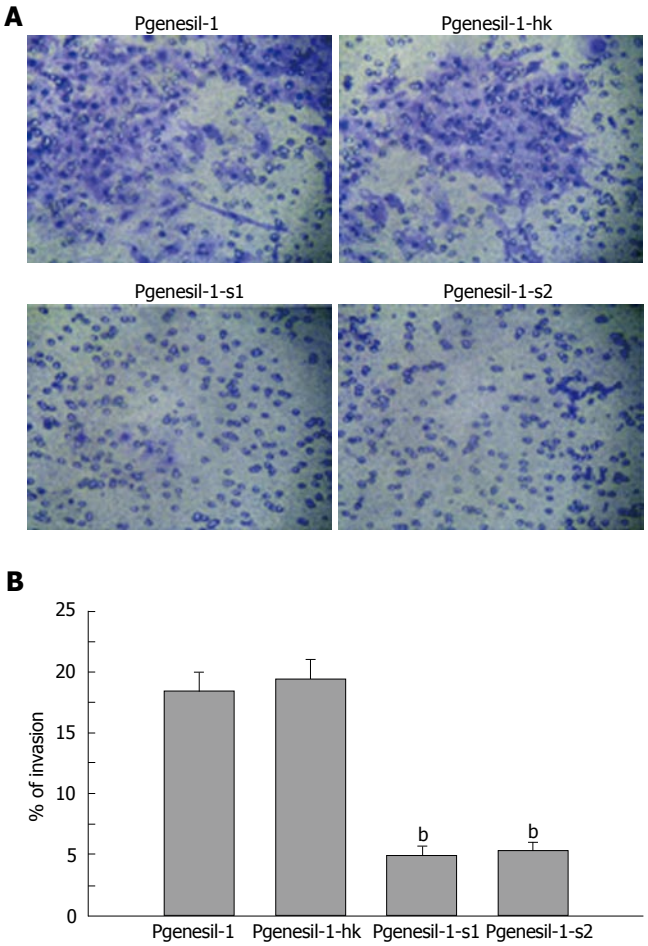

Figure 4 Inhibition of SMYD3 reduces hepatoma cell migration. **A**: Representative cells (blue) invade through Matrigel and membrane; **B**: The percentage of cells successfully passing through the matrigel and membrane ($P < 0.01$).

of TUNEL-positive cells was 40.24% ± 5.18% and 38.48% ± 4.65% in HepG2 cells transfected with Pgenesil-1-s1 and Pgenesil-1-s2, respectively. Only 2.18% ± 1.34% and 2.84% ± 1.22% were TUNEL positive in control cells transfected with Pgenesil-1 and Pgenesil-1-hk, $P < 0.01$, respectively (Figure 5B). These results indicate that inhibition of SMYD3 by RNAi significantly promoted apoptosis in HepG2 cells following serum deprivation.

Inhibition of SMYD3 de-methylates RIZ1 promoter CpG islands and re-expresses RIZ1 in hepatoma cells

Through MSP and RT-PCR, we observed that the RIZ1 promoter was totally methylated with the lack expression of RIZ1 mRNA in HepG2 cells. After inhibition of SMYD3 by Pgenesil-1-s1, the RIZ1 promoter was found partial methylated in HepG2 cells, consistent with the change of RIZ1 mRNA (Figure 6). These results suggest that the activity of SMYD3 may be regulated through RIZ1 CpG promoter hypermethylation and RIZ1 inactivation.

DISCUSSION

Among epigenetic regulatory ways, histone methylation, perhaps more than any other form of modification, has demonstrated the power of modifications over DNA-

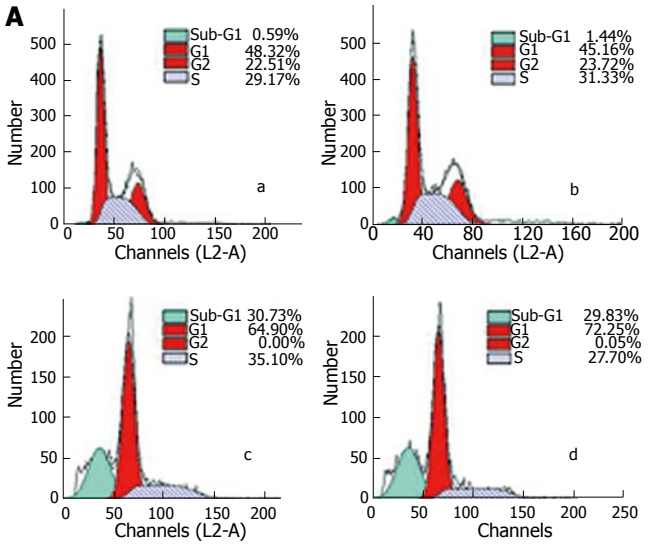

Figure 5 Inhibition of SMYD3 promotes apoptosis in hepatoma cells upon serum deprivation. **A**: FCM analysis of HepG2 cells 48 h after transfection ($P < 0.01$). **B**: TUNEL assay of cell apoptosis with siRNA suppression of SMYD3 expression in HepG2 (brown staining cells) ($P < 0.01$).

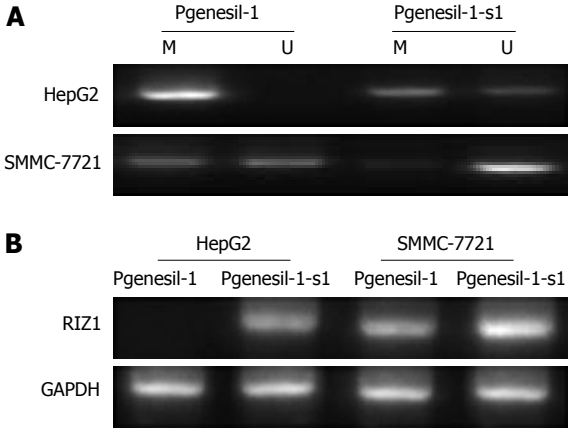

Figure 6 Inhibition of SMYD3 de-methylates RIZ1 promoter CpG islands and reexpresses RIZ1 in hepatoma Cells. **A**: Methylation specific PCR (MSP) assay of RIZ1 promoter. M: Methylated; U: Unmethylated; **B**: RIZ1 mRNA expression, GAPDH served as internal control (RT-PCR).

based functions, regulating fundamental processes such as gene transcription and DNA repair[16]. SMYD3, a gene located in 1q44 chromosome, encodes a protein with HMTase activity specifically on histone H3 at K4, and is involved in carcinogenesis and tumor progression[5]. In the present study, we confirmed that SMYD3 is overexpressed in HCC cell lines. To further investigate the function of SMYD3 in HCC carcinogenesis and tumor progression, RNAi technology was applied to specifically knock down SMYD3 expression in HCC cell lines. We demonstrated that depletion of SMYD3 reduced hepatoma cell growth, migration and induced cell apoptosis upon serum deprivation. Our findings suggest that SMYD3 plays pro-oncologic role in HCC development and progression. Interestingly, our results show that the expression level of SMYD3 in Hep3B cells differs significantly from that in HepG2 and SMMC-7721 cells. We hypothesized that the difference is possibly due to the HBV infectious state of the cells that we used; HBV positive in Hep3B, but negative in HepG2 and SMMC-7721 cells. However, this hypothesis needs to be further clarified.

SMYD3 is considered to function through its H3-K4 histone metylation, regulating expression of Nkx2.8[17,18], Wnt10B[19,20] and other genes involved in hepatoma cell-cycle regulation, cell proliferation and apoptosis. SMYD3 also upregulates genes linked to cell adhesion and invasion, such as ITGA5[21], COLQ[22], SELL[23], NEURL[24], and PECAM1[25], which may be responsible for cell migration regulatory role of SMYD3 in our experiment. To investigate whether SMYD3 might act on HCC oncological activity through TSG inactivation, we examined if RIZ1 activity could be regulated by SMYD3 in different hepatoma cells. RIZ1 was found to be downregulated in HepG2 cells with its promoter CpG hypermethylated, which was in line with enhanced SMYD3 expression, while knockdown of SMYD3 demethylated RIZ1 promoter and upregulated RIZ1 expression in these cells. In addition, different SMYD3 expression levels in hepatoma cells was also consistent with RIZ1 promoter methylation and mRNA expression in hepatoma cells in our results (data not shown) and in other results. HepG2 cells have been shown to lack RIZ1 expression due to promoter hypermethylation; in contrast, Hep3B cells do not show *RIZ1* promoter hypermethylation and express RIZ1 mRNA[26,27]. These results strongly suggest that SMYD3 plays a role in HCC development and progression, partly through RIZ1 promoter hypermethylation and RIZ1 inactivation.

As a histone/protein methyltransferase, SMYD3 mainly acts on histones or proteins; therefore, the mechanism by which SMYD3 regulate RIZ1 promoter CpG islands needs to be further clarified. SMYD3 includes a putative 428-amino acid protein containing a SET domain (codons 148-239) which is HMT, and a zf-MYND domain (codons 49-87), a typical zinc finger domain. The presence of a MYND-type zinc-finger domain in SMYD3 suggests that SMYD3 can recognize and bind particular sequences present in the promoter region of downstream genes through its MYND zinc finger. The specific SMYD3

binding elements (SBE) in target DNA are 5'-CCCTCC-3' or 5'-GGAGGG-3', which are present in the promoter regions of SMYD3 downstream genes, such as Nkx2.8[5]. It is interesting to note that one SBE, 5'-GGAGGG-3', is present in the promoter region of RIZ1[27]. A typical zinc finger domain in SMYD3 and SBE sequence in RIZ1 promoter strongly suggests that SMYD3 may act on RIZ1 promoter through its zf-MYND domain recognizing and binding to the SBE within the RIZ1 promoter. However, SMYD3 may also recognize SBE in other genes, such as DNA methyltransferases (DNMT), which are crucial for DNA methylation[28], and sequentially regulates RIZ1 promoter hypermethylation. There is other evidence suggesting that histone modification may interact with DNA methylation or may regulate DNA methylation[29]. In mammals, H3K9 methylation and CpG methylation shows a complex interplay in which each mark can influence the activity of the other.

Our results imply that, besides their gene-transacting role, SMYD3 and other H3-K4 methyltransferases might influence carcinogenesis and tumor progression by silencing TSGs through DNA methylation. In mammals, DNA methylation must be catalyzed by DNA methyltransferases, whether SMYD3 directly regulates DNMT expression, or SMYD3 changes the local conformation of RIZ1 promoter to facilitate DNMT congregation needs to be further investigated. Moreover, SMYD3 can di- and tri-methylate H3-K4, if its DNA methylation activity is dependent on H3-K4 transactivation, the H3-K4 hypermethylation patterns also needs to be established.

COMMENTS

Background

SMYD3, a H3K4 methyltransferase, was shown to be enhanced expressed in HCC, and involved in the growth of hepatocellular carcinoma (HCC) cells. Although transcriptional activation of downstream genes including Nkx2.8 and WNT10B gene was reported, the effect of SMYD3 on HCC development and the underlining mechanism remain unclear. RIZ1, one typical TSG with H3-K9 methyltransferase activity, was shown to lose its expression and tumor-suppressing activity in HCC, RIZ inactivation in HCC was mainly through its CpG promoter hypermethylation. In this article, whether SMYD3 regulates HCC proliferation, apoptosis and migration through RIZ1 promoter hypermethylation was initially investigated.

Research frontiers

In previous studies, histone metylation were thought to be irreversible. However, in recent studies, histone demethylase was found, which means that histone can be hypermethylated or demethylated in regulating gene expression. Since histone modification play important epigenetic regulating roles in gene transcription, this may provide new target for carcinoma therapy through hypermethylating or demethylating histone.

Innovations and breakthroughs

This article suggests H3-T4 histone methyltransferase regulates HCC biology, not only through oncogene transcription, but through interacting with H3-K9 HMT which mainly plays inhibitory role in oncogene expression, and through inhibiting TSG expression by promoter hypermethylation. These findings deepen our understanding of the interaction of different histone modification ways in gene transcription modification.

Applications

Clarifying the regulating models of H3-K4 methyltransferase, such as SMYD3, represents a potentiality for understanding oncogene expression and tumor suppressive gene under-expression in carcinogenesis and progress. By deepened understanding the key role of SMYD3 in HCC development may also provide new target for carcinoma treatment.

Terminology

SMYD3 SET and MYND domain-containing protein 3; RIZ1 retinoblastoma protein-interacting zinc finger gene1; TSG tumor suppressive gene; HMT Histone methyltransferase; DNMT DNA methyltransferases.

Peer review

The manuscript describes studies showing that several HCC cell lines and one HCC tissue sample express SMYD3 and is well described.

REFERENCES

1 **Egger G**, Liang G, Aparicio A, Jones PA. Epigenetics in human disease and prospects for epigenetic therapy. *Nature* 2004; **429**: 457-463

2 **Lund AH**, van Lohuizen M. Epigenetics and cancer. *Genes Dev* 2004; **18**: 2315-2335

3 **Yu J**, Zhang H, Gu J, Lin S, Li J, Lu W, Wang Y, Zhu J. Methylation profiles of thirty four promoter-CpG islands and concordant methylation behaviours of sixteen genes that may contribute to carcinogenesis of astrocytoma. *BMC Cancer* 2004; **4**: 65

4 **Alaminos M**, Dávalos V, Ropero S, Setién F, Paz MF, Herranz M, Fraga MF, Mora J, Cheung NK, Gerald WL, Esteller M. EMP3, a myelin-related gene located in the critical 19q13.3 region, is epigenetically silenced and exhibits features of a candidate tumor suppressor in glioma and neuroblastoma. *Cancer Res* 2005; **65**: 2565-2571

5 **Hamamoto R**, Furukawa Y, Morita M, Iimura Y, Silva FP, Li M, Yagyu R, Nakamura Y. SMYD3 encodes a histone methyltransferase involved in the proliferation of cancer cells. *Nat Cell Biol* 2004; **6**: 731-740

6 **Hamamoto R**, Silva FP, Tsuge M, Nishidate T, Katagiri T, Nakamura Y, Furukawa Y. Enhanced SMYD3 expression is essential for the growth of breast cancer cells. *Cancer Sci* 2006; **97**: 113-118

7 **Frank B**, Hemminki K, Wappenschmidt B, Klaes R, Meindl A, Schmutzler RK, Bugert P, Untch M, Bartram CR, Burwinkel B. Variable number of tandem repeats polymorphism in the SMYD3 promoter region and the risk of familial breast cancer. *Int J Cancer* 2006; **118**: 2917-2918

8 **Jiang GL**, Liu L, Buyse IM, Simon D, Huang S. Decreased RIZ1 expression but not RIZ2 in hepatoma and suppression of hepatoma tumorigenicity by RIZ1. *Int J Cancer* 1999; **83**: 541-546

9 **Chadwick RB**, Jiang GL, Bennington GA, Yuan B, Johnson CK, Stevens MW, Niemann TH, Peltomaki P, Huang S, de la Chapelle A. Candidate tumor suppressor RIZ is frequently involved in colorectal carcinogenesis. *Proc Natl Acad Sci USA* 2000; **97**: 2662-2667

10 **He L**, Yu JX, Liu L, Buyse IM, Wang MS, Yang QC, Nakagawara A, Brodeur GM, Shi YE, Huang S. RIZ1, but not the alternative RIZ2 product of the same gene, is underexpressed in breast cancer, and forced RIZ1 expression causes G2-M cell cycle arrest and/or apoptosis. *Cancer Res* 1998; **58**: 4238-4244

11 **Suzuki M**, Shigematsu H, Shivapurkar N, Reddy J, Miyajima K, Takahashi T, Gazdar AF, Frenkel EP. Methylation of apoptosis related genes in the pathogenesis and prognosis of prostate cancer. *Cancer Lett* 2006; **242**: 222-230

12 **Piao Z**, Fang W, Malkhosyan S, Kim H, Horii A, Perucho M, Huang S. Frequent frameshift mutations of RIZ in sporadic gastrointestinal and endometrial carcinomas with microsatellite instability. *Cancer Res* 2000; **60**: 4701-4704

13 **Jiang GL**, Huang S. Adenovirus expressing RIZ1 in tumor suppressor gene therapy of microsatellite-unstable colorectal cancers. *Cancer Res* 2001; **61**: 1796-1798

14 **Nishimura T**, Nishida N, Itoh T, Komeda T, Fukuda Y, Ikai I, Yamaoka Y, Nakao K. Discrete breakpoint mapping and shortest region of overlap of chromosome arm 1q gain and 1p loss in human hepatocellular carcinoma detected by

semiquantitative microsatellite analysis. *Genes Chromosomes Cancer* 2005; **42**: 34-43

15 **Fang W**, Piao Z, Buyse IM, Simon D, Sheu JC, Perucho M, Huang S. Preferential loss of a polymorphic RIZ allele in human hepatocellular carcinoma. *Br J Cancer* 2001; **84**: 743-747

16 **Yoo CB**, Jones PA. Epigenetic therapy of cancer: past, present and future. *Nat Rev Drug Discov* 2006; **5**: 37-50

17 **Apergis GA**, Crawford N, Ghosh D, Steppan CM, Vorachek WR, Wen P, Locker J. A novel nk-2-related transcription factor associated with human fetal liver and hepatocellular carcinoma. *J Biol Chem* 1998; **273**: 2917-2925

18 **Kajiyama Y**, Tian J, Locker J. Regulation of alpha-fetoprotein expression by Nkx2.8. *Mol Cell Biol* 2002; **22**: 6122-6130

19 **Benhaj K**, Akcali KC, Ozturk M. Redundant expression of canonical Wnt ligands in human breast cancer cell lines. *Oncol Rep* 2006; **15**: 701-707

20 **Kirikoshi H**, Katoh M. Expression of WNT7A in human normal tissues and cancer, and regulation of WNT7A and WNT7B in human cancer. *Int J Oncol* 2002; **21**: 895-900

21 **Koike T**, Kimura N, Miyazaki K, Yabuta T, Kumamoto K, Takenoshita S, Chen J, Kobayashi M, Hosokawa M, Taniguchi A, Kojima T, Ishida N, Kawakita M, Yamamoto H, Takematsu H, Suzuki A, Kozutsumi Y, Kannagi R. Hypoxia induces adhesion molecules on cancer cells: A missing link between Warburg effect and induction of selectin-ligand carbohydrates. *Proc Natl Acad Sci USA* 2004; **101**: 8132-8137

22 **Deprez P**, Inestrosa NC, Krejci E. Two different heparin-binding domains in the triple-helical domain of ColQ, the collagen tail subunit of synaptic acetylcholinesterase. *J Biol Chem* 2003; **278**: 23233-23242

23 **Johansson FK**, Göransson H, Westermark B. Expression analysis of genes involved in brain tumor progression driven by retroviral insertional mutagenesis in mice. *Oncogene* 2005; **24**: 3896-3905

24 **Kondoh N**, Wakatsuki T, Ryo A, Hada A, Aihara T, Horiuchi S, Goseki N, Matsubara O, Takenaka K, Shichita M, Tanaka K, Shuda M, Yamamoto M. Identification and characterization of genes associated with human hepatocellular carcinogenesis. *Cancer Res* 1999; **59**: 4990-4996

25 **Frachon S**, Gouysse G, Dumortier J, Couvelard A, Nejjari M, Mion F, Berger F, Paliard P, Boillot O, Scoazec JY. Endothelial cell marker expression in dysplastic lesions of the liver: an immunohistochemical study. *J Hepatol* 2001; **34**: 850-857

26 **Ricketts SL**, Carter JC, Coleman WB. Identification of three 11p11.2 candidate liver tumor suppressors through analysis of known human genes. *Mol Carcinog* 2003; **36**: 90-99

27 **Robert MF**, Morin S, Beaulieu N, Gauthier F, Chute IC, Barsalou A, MacLeod AR. DNMT1 is required to maintain CpG methylation and aberrant gene silencing in human cancer cells. *Nat Genet* 2003; **33**: 61-65

28 **Jackson JP**, Lindroth AM, Cao X, Jacobsen SE. Control of CpNpG DNA methylation by the KRYPTONITE histone H3 methyltransferase. *Nature* 2002; **416**: 556-560

29 **Johnson L**, Cao X, Jacobsen S. Interplay between two epigenetic marks. DNA methylation and histone H3 lysine 9 methylation. *Curr Biol* 2002; **12**: 1360-1367

S- Editor Ma N **L- Editor** Rippe RA **E- Editor** Yin DH

Online Submissions: wjg.wjgnet.com
www.wjgnet.com
wjg@wjgnet.com

World J Gastroenterol 2007 November 21; 13(43): 5725-5730
World Journal of Gastroenterology ISSN 1007-9327

RAPID COMMUNICATION

CYP2E1 Rsa I polymorphism impacts on risk of colorectal cancer association with smoking and alcohol drinking

Chang-Ming Gao, Toshiro Takezaki, Jian-Zhong Wu, Min-Bin Chen, Yan-Ting Liu, Jian-Hua Ding, Haruhiko Sugimura, Jia Cao, Nobuyuki Hamajima, Kazuo Tajima

Chang-Ming Gao, Jian-Zhong Wu, Min-Bin Chen, Yan-Ting Liu, Jian-Hua Ding, Division of Epidemiology, Jiangsu Province Institute of Cancer Research, Nanjing 210009, Jiangsu Province, China
Toshiro Takezaki, Department of International Island and Community Medicine, Kagoshima University Graduate School of Medical and Dental Sciences, 8-35-1 Sakuragaoka, Kagoshima 890-8544, Japan
Haruhiko Sugimura, First Department of Pathology, Hamamatsu University School of Medicine, Hamamatsu 431-3192, Japan
Jia Cao, Molecular Toxicology Laboratory, Third Military Medical Universit School of Public Healthy, Chongqing 400038, China
Nobuyuki Hamajima, Department of Preventive Medicine Biostatistics and Medical Decision Making, Nagoya University School of Medicine, Nagoya 466-8550, Japan
Kazuo Tajima, Division of Epidemiology and Prevention, Aichi Cancer Center Research Institute, Nagoya 464-8681, Japan
Supported by a Grant-in Aid for International Scientific Research, Special Cancer Research, No.11137311, from the Ministry of Education, Science, Sports, Culture and Technology of Japan, and by a Major International (Regional) Joint Research Projects, No. 30320140461 from the National Natural Science Foundation of China
Correspondence to: Kazuo Tajima, Division of Epidemiology and Prevention, Aichi Cancer Center Research Institute, Nagoya 464-8681, Japan. ktajima@aichicc.jp
Telephone: +81-52-7642970 Fax: +81-52-7635233
Received: March 7, 2007 Revised: July 31, 2007

Abstract

AIM: To investigate associations between the *Rsa* I polymorphism of *CYP2E1* and risk of colorectal cancer.

METHODS: A case-control study was conducted with 315 colorectal cancer cases (105 colon, 210 rectal) and 439 population-based controls in Jiangsu Province of China. Genomic DNA samples were assayed for restriction fragment length polymorphisms in *CYP2E1* by PCR amplification followed by digestion with *Rsa* I. Information on smoking and alcohol drinking was collected using a questionnaire. Odds ratios (ORs) were estimated with an unconditional logistic model.

RESULTS: The proportional distribution of the *CYP2E1 Rsa* I c1/c1, c1/c2 and c2/c2 genotypes were 61.4%, 35.6% and 3.0% in controls, 60.6%, 33.7% and 5.8% in colon cancer cases, and 58.4%, 34.0% and 7.7% in rectal cancer cases, respectively. A significant difference was noted between controls and rectal cancer cases (P = 0.029), the c2/c2 genotype being associated with elevated OR (adjusted age, sex and status of the smoking and alcohol drinking) for rectal cancer (1.64, 95% CI, 1.12-2.41, *vs* c1 allele carriers), but not for colon cancer. In interaction analysis between the *CYP2E1 Rsa* I genotype and smoking and drinking habits, we found a significant cooperative action between the c2/c2 genotype and alcohol drinking in the sex-, age-adjusted ORs for both colon (4.74, 95% CI, 1.10-20.40) and rectal (5.75, 95% CI, 1.65-20.05) cancers. Among non-smokers, the *CYP2E1 Rsa* I c2/c2 genotype was also associated with elevated ORs in the two sites (1.95, 95% CI, 0.99-3.86 and 2.30, 95% CI, 1.32-3.99).

CONCLUSION: The results of the present study suggest that the *CYP2E1* c2/c2 genotype increases susceptibility to rectal cancer and the gene-environmental interactions between the *CYP2E1* polymorphism and smoking or alcohol drinking exist for colorectal neoplasia in general.

Key words: *CYP 2E1*; Gene polymorphism; Smoking; Alcohol drinking; Colorectal cancer

Gao CM, Takezaki T, Wu JZ, Chen MB, Liu YT, Ding JH, Sugimura H, Cao J, Hamajima N, Tajima K. *CYP2E1 Rsa* I polymorphism impacts on risk of colorectal cancer associated with smoking and alcohol drinking *World J Gastroenterol* 2007; 13(43): 5725-5730

http://www.wjgnet.com/1007-9327/13/5725.asp

INTRODUCTION

CYP2E1, a member of the cytochrome P450 superfamily, is involved in the metabolic activation of many low-molecular-weight compounds such as N-nitrosamines, aniline, vinyl chloride, urethane and alcohol[1]. N-nitrosamines present in tobacco and diet are well-recognized carcinogens involved in tumor development at various sites. Functional *CYP2E1* gene polymorphisms might therefore impact on susceptibility to cancer development.

A substitution polymorphism (G1259C) detected using the restriction enzymes *Pst* I or *Rsa* I has been associated

with decreased *CYP2E1* activity/inducibility[2-5]. The *Dra* I polymorphism is also associated with altered activity of *CYP2E1*, although *Dra* I is located in intron 6 and is not thought to affect gene transcription[6]. Activity of *CYP2E1* is also modulated by various physiological determinants, such as obesity[7], fasting[7] and liver dysfunction[8] and can be induced by ethanol[9]. In contrast, dietary isothiocyanates[10] and garlic[11,12], as well as some drugs, such as disulfiram[13] and chlormethiazole[14], inhibit its activity. A number of environmental factors may thus modify the cancer risk through altered *CYP2E1* enzyme activity.

Previous studies have shown inconsistent findings on *CYP2E1* polymorphism associations with cancer risk. Some studies demonstrated the common genotype or alleles to confer greater risk of oral[15], pharyngeal[15], esophageal[16,17] liver[18] and lung[19,20] cancers. On the other hand, increased risk of oral[21], nasopharyngeal[22], liver[23] and colorectal[24,25] cancers was observed with the rare genotype or allele carriers in other studies. Furthermore, some case-control studies failed to find a significant association between *CYP2E1* polymorphisms and risk of neoplasia of the oral cavity and pharynx[26], esophagus[27], stomach[28,29], lung[30-33], bladder[34] and colorectum[35]. The reasons for these inconsistent results are not clear, but one problem is a lack of sufficient investigation of gene-environmental interactions, including links with dietary and smoking habits. We hypothesized that environmental factors may alter the enzyme activity of *CYP2E1* and therefore modify cancer susceptibility due to *CYP2E1* polymorphisms. One earlier study in our laboratory showed that gene-environment interactions between the *CYP2E1* polymorphism and smoking have the potential to alter susceptibility to gastric cancer[36].

To investigate possible relations between *CYP2E1 Rsa* I polymorphisms and environmental factors (smoking and alcohol drinking) on the risk of colorectal cancers, we conducted a population-based case-control study in Jiangsu province, China.

MATERIALS AND METHODS

Subjects

We recruited colorectal cancer cases using data of Cancer Registries in Huian and Jintan Cities of Jiangsu Province of China, and also recruited cases who visited Jiangsu Province Cancer Hospital from these cities from August 2000 to September 2002. All were histopathologically diagnosed as having a primary colorectal cancer. Physicians at the hospital asked eligible cases to participate in our study, and doctors or nurses interviewed the subjects and collected blood samples from a peripheral vein after obtaining informed consent. Population-based controls were selected from healthy residents in eight villages or towns of Huian and Jintan Cities. Doctors of the public health center randomly selected one or two controls for each case, after matching for ethnicity, sex and age within 2 years using the records of residents at the local governmental office, and then asked eligible residents for their participation. Interviews and blood collection were performed as for the cancer cases. A few patients and residents refused to participate in our study, but the response rates were 97% for cases and 93% for controls. The ethics committee of Jiangsu Province Institute of Cancer Research approved this study.

Environmental factors

The items of our questionnaire covered smoking and drinking habits. Smokers were divided into never- and ever-smokers (current and former). Drinkers also were divided into two groups ($\geq$ 2 times/mo and < 2 times/mo) according to drinking frequency.

DNA extraction and genotyping of the CYP2E1

Whole blood was collected into EDTA-coated tubes and centrifuged for 15 min, and the buffy coat layer was isolated. Genomic DNA was extracted from 200 μL of buffy coat using a Qiagen QIAamp DNA Blood Mini Kit (QIAGEN Inc., Valencia, CA). The method for genotyping of the *CYP2E1* has been previously described[30]. In brief, PCR was used to amplify the transcription regulation region of *CYP2E1* that includes the *Rsa* I enzyme recognition site[3]. The primers were 5'-CCAGTCGAGTCTACATTGTCA and 5'-TTCATTCT GTCTTCTAACTGG. The PCR product was subjected to *Rsa* I restriction enzyme digestion and samples were then analyzed by electrophoresis in 5% polyacrylamide gels. There were three genotypes of *CYP2E1* resulting from digestion with the restriction enzyme *Rsa* I : the common homozygote c1/c1; the heterozygote c1/c2; and the rare homozygote c2/c2. Among 754 examined samples, PCR products could not be visualized for 2 cases and 6 controls.

Statistical analysis

Associations between the *Rsa* I polymorphism and colorectal cancer risk were estimated by OR, using the unconditional logistic regression model. We calculated adjusted ORs for age (continuous), sex, smoking and drinking habits. To investigate gene-environmental interactions, we also calculated (stratified analysis) ORs according to combinations of the *CYP2E1* genotypes and habits of the smoking and drinking, with *Rsa* I c1 allele carriers as the reference. The procedure LOGISTIC from the statistical package SAS was employed for the calculations. The probability of Hardy-Weinberg equilibrium was assessed by the χ^2 test.

RESULTS

Numbers of subjects were 190 male and 125 female with colorectal cancer, and 223 male and 216 female controls (Table 1). The proportion of females in controls was significant higher than in colorectal cases but the mean age did not differ between cases and controls. The proportional distributions of smokers and alcohol drinkers were significant higher in colorectal cancer cases than in controls.

The distributions of *CYP2E1 Rsa* I c1/c1, c1/c2 and c2/c2 genotypes were 61.4%, 35.6% and 3.0%, respectively, in controls, 59.1%, 33.9% and 7.0% in colorectal cases, 60.6%, 33.7% and 5.8% in colon cancer cases, and 58.4%, 34.0% and 7.7% in rectal cancer cases (Table 1). The proportional distribution significantly differed

Table 1 Background characteristics of colorectal cancer cases and their controls

	Controls *n* (%)	Colorectal cancer *n* (%)	Colon cancer *n* (%)	Rectal cancer *n* (%)
All of the subjects	439 (100.0)	315 (100.0)	105 (100.0)	210 (100.0)
Gender				
Males	223 (50.8)	190 (60.3)	65 (61.9)	125 (59.5)
Females	216 (49.2)	125 (39.7)	40 (38.1)	85 (40.5)
χ^2_{MH} (*P*)		6.70 (0.010)	4.19 (0.041)	4.34 (0.037)
Age (yr)				
< 40	42 (9.6)	44 (14.0)	14 (13.3)	30 (14.3)
40-49	75 (17.1)	54 (17.1)	15 (14.3)	39 (18.6)
50-59	150 (34.2)	88 (27.9)	30 (28.6)	58 (27.6)
60-69	131 (29.8)	85 (29.0)	26 (24.8)	59 (28.1)
> 70	41 (9.3)	44 (14.0)	20 (19.1)	24 (11.4)
χ^2_{MH} (*P*)		9.37 (0.053)	10.23 (0.037)	5.69 (0.224)
Mean age ± SD	55.7 ± 11.0	55.3 ± 12.7	56.4 ± 13.4	54.7 ± 12.3
P (*t* test)		0.6172	0.6325	0.3159
Smoking status				
Nonsmoker	284 (64.7)	176 (55.9)	61 (58.1)	115 (54.8)
Courrent and former	155 (35.3)	139 (44.1)	44 (41.9)	95 (45.2)
χ^2_{MH} (*P*)		5.99 (0.014)	1.59 (0.208)	5.91 (0.015)
Alcohol status				
Nondrinker	327 (74.5)	176 (55.9)	65 (61.9)	120 (57.1)
Current and former	112 (25.5)	139 (44.1)	50 (38.1)	90 (42.9)
χ^2_{MH} (*P*)		28.58 (0.000)	14.19 (0.000)	19.90 (0.000)
CYP 2E1 genotypes[1]				
c1/c1	266 (61.4)	185 (59.1)	63 (60.6)	122 (58.4)
c1/c2	154 (35.6)	106 (33.9)	35 (33.7)	71 (34.0)
c2/c2	13 (3.0)	22 (7.0)	6 (5.8)	16 (7.7)
χ^2_{MH} (*P*)		6.58 (0.037)	1.91 (0.385)	7.07 (0.029)

[1]Six controls and two cases were excluded because of unknown CYP2E1 genotype.

Table 2 CYP2E1 genotypes and risk of colorectal cancer

	Genotype	Cases (*n*)	Controls (*n*)	OR[1] (95% CI)	OR[2] (95% CI)
Colorectal cancer					
	c1/c1	185	266	1.00	1.00
	c1/c2	106	154	0.99 (0.72-1.35)	0.99 (0.72-1.35)
	c2/c2	22	13	1.54 (1.07-2.19)	1.55 (1.08-2.22)
Colon Cancer					
	c1/c1	63	266	1.00	1.00
	c1/c2	35	154	0.96 (0.61-1.52)	0.95 (0.60-1.51)
	c2/c2	6	13	1.36 (0.82-2.25)	1.40 (0.84-2.33)
Rectal cancer					
	c1/c1	122	266	1.00	1.00
	c1/c2	71	154	1.01 (0.71-1.44)	1.01 (0.71-1.44)
	c2/c2	16	13	1.61 (1.09-2.36)	1.64 (1.12-2.41)

[1]ORs were adjusted for age and sex in a logistic regression model. [2]ORs were adjusted for age, sex and status of smoking and alcohol drinking.

between control and colorectal (χ^2_{MH} = 6.58, P = 0.037) or rectal (χ^2_{MH} = 7.07, P = 0.029) cancer cases. The allelic distribution of the *Rsa* I polymorphism for controls was in Hardy-Weinberg equilibrium (χ^2 = 2.77, P > 0.05). It shows that the controls from general population are representative. The *CYP2E1 Rsa* I c2/c2 genotype was associated with significantly increased ORs for colorectal cancer (sex-, age- and habits of smoking and alcohol drinking adjusted OR = 1.55, 95% CI, 1.08-2.22) and rectal cancer (adjusted OR = 1.64, 95% CI, 1.12-2.41) (Table 2).

Table 3 shows the results of the multivariable analysis of smoking, alcohol drinking and *CYP2E1 Rsa* I c2/c2 genotypes and risk of colorectal cancer. The smoking habit was not associated with any increased OR for colon or rectal cancer, but alcohol drinking was linked with elevated ORs for colon (1.68, 95% CI, 0.97-2.89) and rectal (2.08,

Table 3 Logistic regression analysis on smoking, alcohol drinking and CYP2E1 c2/c2 genotypes and risk of colorectal cancer

	Colorectal cancer OR[1] (95% CI)	Colon cancer OR[1] (95% CI)	Rectal cancer OR[1] (95% CI)
Smoking	1.01 (0.69-1.47)	0.84 (0.49-1.44)	1.08 (0.70-1.67)
Alcohol drinking	1.91 (1.31-2.80)	1.68 (0.97-2.89)	2.08 (1.36-3.19)
CYP2E1 c2/c2	1.50 (1.05-2.15)	1.34 (0.81-2.23)	1.58 (1.08-2.32)

[1]Logistic regression model included age (continuous), sex, smoking (nonsmoker, current + former smoker), alcohol drinking (nondrinker, current + former drinker) and *CYP2E1* genotype (c1/c1 + c1/c2, c2/c2).

Table 4 Interaction between the *CYP2E1* genotype and the status of smoking and alcohol drinking, and the odds ratios (ORs) for colorectal cancer

	CYP2E1 genotype	Controls	Colorectal cancer		Colon cancer		Rectal cancer	
		n	*n*	OR[1] (95% CI)	*n*	OR[1] (95% CI)	*n*	OR[1] (95% CI)
Smoker								
No	c1/c1 + c1/c2	275	162	1.00	57	1.00	105	1.00
No	c2/c2	5	14	2.20 (1.31-3.70)	4	1.95 (0.99-3.86)	10	2.30 (1.32-3.99)
Yes	c1/c1 + c1/c2	145	129	1.34 (0.93-1.92)	41	1.11 (0.66-1.88)	88	1.48 (0.98-2.25)
Yes	c2/c2	8	8	1.41 (0.50-3.96)	2	0.91 (0.18-4.57)	6	1.75 (0.57-5.42)
Drinker								
No	c1/c1 + c1/c2	313	174	1.00	62	1.00	112	1.00
No	c2/c2	9	10	1.41 (0.89-2.24)	2	1.09 (0.50-2.38)	8	1.55 (0.95-2.53)
Yes	c1/c1 + c1/c2	107	117	1.86 (1.28-2.68)	36	1.50 (0.89-2.55)	81	2.07 (1.37-3.14)
Yes	c2/c2	4	12	5.42 (1.65-17.40)	4	4.74 (1.10-20.40)	8	5.75 (1.65-20.05)

[1]ORs were adjusted for age and sex.

95% CI, 1.36-3.19) cancers. The *CYP2E1 Rsa* I c2/c2 genotype significantly increased the OR for rectal cancer (1.58, 95% CI, 1.08-2.32).

Table 4 shows the results of interaction analysis of the *CYP2E1 Rsa* I polymorphism with smoking and alcohol drinking habits. Among nonsmokers, *Rsa* I c2/c2 was associated with elevated ORs for colon (1.95, 95% CI, 0.99-3.86) and rectal (2.30, 95% CI, 1.32-3.99) cancers. Among smokers with the *Rsa* I c2/c2 genotype, no increase in the OR for colon cancer was observed, and the slightly increased OR for rectal cancer also was not statistically significant.

Among carriers of the *Rsa* I c1 allele, alcohol drinking was significantly associated with an elevated OR for rectal cancer (2.07, 95% CI, 1.37-3.14). As compared with non-drinkers with the *Rsa* I c1 allele, drinkers with RsaI c2/c2 genotype had significant increased ORs for colon cancer (4.74, 95% CI, 1.10-20.40) and rectal cancer (5.75, 95% CI, 1.65-20.05).

DISCUSSION

The present study revealed a significant association between the *CYP2E1 Rsa* I c2/c2 genotype and risk of rectal cancer, as well as a notable interaction with smoking or alcohol drinking as environmental factors.

Previous investigations showed inconsistent findings. As regards colorectal cancer, Kiss *et al*[24] found the *CYP2E1* c2 allele to be significantly associated with colorectal cancer (OR: 1.91, 95% CI, 1.05-3.52) in a Hungarian population. Yu *et al*[25] found the *CYP2E1 Pst* I c2 allele to be a susceptibility factor for colorectal cancer, especially for colon cancer, and there is an apparent gene-environment interaction with salted food in a Chinese population. In a study from the Netherlands, although calculation of crude ORs revealed an increased risk for colorectal cancer associated with the variant *CYP2E1* genotype (OR: 2.2, 95% CI: 1.3-3.8), this was no longer evident after adjustment for age and gender[35].

The reason for the inconsistent findings for the *CYP2E1* polymorphism is unknown but clearly variation with ethnicity and gender could contribute to differences in influence on neoplasia. The rare *Rsa* I allele is considered to result in increased transcriptional activation of the *CYP2E1* gene[2,3], with elevated expression levels of *CYP2E1* mRNA and protein[3,37]. However, several studies demonstrated common genotype carriers to have the higher *CYP2E1* enzyme activity[4,5]. Differences in *CYP2E1* activity by ethnicity and gender have also been reported, females showing 25% lower activity than males[7,38]. Japanese appear to demonstrate 30%-40% lower activity of *CYP2E1* than Caucasians, even after taking account differences in body size[39].

In the present study, we found a gene-environmental interaction between the *CYP2E1* polymorphism and smoking. Thus, increased risk of colon or rectal cancer was associated with the *CYP2E1 Rsa* I c2/c2 genotype among smokers, but not non-smokers. A similar phenomenon was also found in another study[40]. It has been shown that among non-smokers, urinary styrene metabolites are significantly decreased in subjects with c1/c1 alleles of *CYP2E1* as compared with those with the c1/c2 genotype, whereas no significant differences in urinary metabolites were noted among smokers[41].

We found alcohol drinking to significantly increase risk of cancer development, especially in the rectum, and there was a significant interaction with the *CYP2E1 Rsa* I c2/c2 genotype in both the colon and rectum. Our results are consistent with previous investigations indicating that alcohol consumption is associated with an increased risk for cancers of many organs, such as oral cavity, pharynx, larynx, esophagus, breast, liver, ovary; colon, rectum, stomach and pancreas[42]. Chronic ethanol consumption may promote carcinogenesis by (1) production of acetaldehyde, which is a weak mutagen and carcinogen; (2) induction of *CYP2E1* and associated oxidative stress and conversion of pro-carcinogens to carcinogens; (3) depletion of S-adenosylmethionine and, consequently, induction of global DNA hypomethylation; (4) induction of increased production of inhibitory guanine nucleotide regulatory proteins and components of extracellular signal-regulated kinase-mitogen-activated protein kinase signaling; (5) accumulation of iron and associated oxidative stress; (6) inactivation of the tumor suppressor gene BRCA1 and increased estrogen responsiveness (primarily in breast); and (7) impairment of retinoic acid metabolism[43]. Alcohol also can affect the pharmacokinetics of drugs by altering gastric emptying

or liver metabolism by inducing *CYP2E1*[43]. *CYP2E1* is the key microsomal enzyme that metabolizes alcohol in the non-alcohol dehydrogenase pathway. Choi *et al*[44] also discovered that "ever"-drinking women with the *CYP2E1* c2 allele containing genotypes had an increased risk of developing breast cancer compared to non-drinkers with the *CYP2E1* c1/c1 genotype in the Korean population.

Finally, some limitations require discussion. Because the frequency of the *CYP2E1 Rsa* I c2/c2 genotype is lower in subjects, only relatively small numbers were available for subgroup analyses, with consequent reduction in the magnitude of statistical power and increase in the potential for random error. Another possible problem is selection bias for controls, these being recruited by local health staff, albeit from the general population with a high response rate. The proportional distribution of female in controls was higher than that in colorectal cases, which may have caused a lower prevalence of smokers and alcohol drinkers in the present controls, though we adjusted for sex and age in all statistical analyses.

In summary, the present study revealed a link between the *CYP2E1 Rsa* I polymorphism and increased risk of rectal cancer, with a significant interaction between the *Rsa* I polymorphism and smoking and alcohol drinking habits regarding development of both colon and rectal cancers. The data provide support for our hypothesis that cancer susceptibility with the *CYP2E1* polymorphisms may be altered by background environmental factors.

ACKNOWLEDGMENTS

The authors would like to thank the medical staff of the Huaian City Municipal Hospital, and the staff of the Public Health Center of Huaian City and Jintan City for their assistance in data collection.

COMMENTS

Background

Colorectal cancer is the fifth most commonly occurring cancer in China. Cytochrome P450 (CYP) enzymes in epithelial cells lining the alimentary tract play an important role in both the elimination and activation of (pro-) carcinogens. To estimate the role of *CYP2E1* in colorectal cancer development, we conducted a population based case-control study of colorectal cancer in Jiangsu Province of China.

Research frontiers

A lot of carcinogens from environment must be metabolized for their elimination and activation. Genetic polymorphisms of metabolizing enzymes may affect the metabolism of carcinogens and the risk of cancer formation in humans. Susceptibility to cancer is generally thought to be the sum of complex interactions between environmental and genetic factors. Thereby, how interaction between environmental and genetic factors is a hotspot of cancer epidemiological study. We Regarding to the hotspot, we studied interactions between *CYP2E1* and habits of smoking and alcohol drinking in colorectal cancer development.

Innovations and breakthroughs

In present study, we demonstrate a correlation between *CYP2E1 Rsa* I polymorphism in c2/c2 genotype is associated with rectal and not colon cancer. This increased risk associated with this polymorphism was negated in smokers. Furthermore, a significant cooperative action was seen between the c2/c2 genotype and alcohol consumption in both colon and rectal cancers.

Applications

This research exposes a screenable genetic risk factor and the effects of gene-environment interactions in identifying individuals at risk for colon or rectal cancer. These results have some theoretical and application values in the etiology and prevention of colorectal cancer.

Terminology

CYP2E1: cytochrome P450 2E1. *CYP2E1 Rsa* I polymorphism: *Rsa* I enzyme recognized polymorphism in *CYP2E1* gene.

Peer review

Gao *et al* demonstrate a correlation between *CYP2E1 Rsa* I polymorphisms in c2/c2 genotypes are associated with rectal and not colon cancer. This increased risk associated with this polymorphism was negated in smokers. Furthermore, a significant cooperative action was seen between the c2/c2 genotype and alcohol consumption in both colon and rectal cancers. The experiments contain appropriate controls and weightings of the data taking into consideration age, sex, smoking status and alcohol consumption. This research exposes a screenable genetic risk factor and the effects of gene-environment interactions in identifying patients at risk for colon or rectal cancer.

REFERENCES

1 **Guengerich FP**, Kim DH, Iwasaki M. Role of human cytochrome P-450 IIE1 in the oxidation of many low molecular weight cancer suspects. *Chem Res Toxicol* 1991; **4**: 168-179
2 **Hayashi S**, Watanabe J, Kawajiri K. Genetic polymorphisms in the 5'-flanking region change transcriptional regulation of the human cytochrome P450IIE1 gene. *J Biochem* 1991; **110**: 559-565
3 **Watanabe J**, Hayashi S, Kawajiri K. Different regulation and expression of the human CYP2E1 gene due to the RsaI polymorphism in the 5'-flanking region. *J Biochem* 1994; **116**: 321-326
4 **Marchand LL**, Wilkinson GR, Wilkens LR. Genetic and dietary predictors of CYP2E1 activity: a phenotyping study in Hawaii Japanese using chlorzoxazone. *Cancer Epidemiol Biomarkers Prev* 1999; **8**: 495-500
5 **Lucas D**, Ménez C, Girre C, Berthou F, Bodénez P, Joannet I, Hispard E, Bardou LG, Ménez JF. Cytochrome P450 2E1 genotype and chlorzoxazone metabolism in healthy and alcoholic Caucasian subjects. *Pharmacogenetics* 1995; **5**: 298-304
6 **Uematsu F**, Kikuchi H, Motomiya M, Abe T, Sagami I, Ohmachi T, Wakui A, Kanamaru R, Watanabe M. Association between restriction fragment length polymorphism of the human cytochrome P450IIE1 gene and susceptibility to lung cancer. *Jpn J Cancer Res* 1991; **82**: 254-256
7 **O'Shea D**, Davis SN, Kim RB, Wilkinson GR. Effect of fasting and obesity in humans on the 6-hydroxylation of chlorzoxazone: a putative probe of CYP2E1 activity. *Clin Pharmacol Ther* 1994; **56**: 359-367
8 **Dilger K**, Metzler J, Bode JC, Klotz U. CYP2E1 activity in patients with alcoholic liver disease. *J Hepatol* 1997; **27**: 1009-1014
9 **Girre C**, Lucas D, Hispard E, Menez C, Dally S, Menez JF. Assessment of cytochrome P4502E1 induction in alcoholic patients by chlorzoxazone pharmacokinetics. *Biochem Pharmacol* 1994; **47**: 1503-1508
10 **Leclercq I**, Desager JP, Horsmans Y. Inhibition of chlorzoxazone metabolism, a clinical probe for CYP2E1, by a single ingestion of watercress. *Clin Pharmacol* Ther 1998; **64**: 144-149
11 **Yang CS**, Smith TJ, Hong JY. Cytochrome P-450 enzymes as targets for chemoprevention against chemical carcinogenesis and toxicity: opportunities and limitations. *Cancer Res* 1994; **54**: 1982s-1986s
12 **Reicks MM**, Crankshaw DL. Modulation of rat hepatic cytochrome P-450 activity by garlic organosulfur compounds. *Nutr Cancer* 1996; **25**: 241-248
13 **Kharasch ED**, Thummel KE, Mhyre J, Lillibridge JH. Single-dose disulfiram inhibition of chlorzoxazone metabolism: a clinical probe for P450 2E1. *Clin Pharmacol Ther* 1993; **53**: 643-650
14 **Gebhardt AC**, Lucas D, Ménez JF, Seitz HK. Chlormethiazole inhibition of cytochrome P450 2E1 as assessed by chlorzoxazone hydroxylation in humans. *Hepatology* 1997; **26**: 957-961

15 **Bouchardy C**, Hirvonen A, Coutelle C, Ward PJ, Dayer P, Benhamou S. Role of alcohol dehydrogenase 3 and cytochrome P-4502E1 genotypes in susceptibility to cancers of the upper aerodigestive tract. *Int J Cancer* 2000; **87**: 734-740

16 **Lin DX**, Tang YM, Peng Q, Lu SX, Ambrosone CB, Kadlubar FF. Susceptibility to esophageal cancer and genetic polymorphisms in glutathione S-transferases T1, P1, and M1 and cytochrome P450 2E1. *Cancer Epidemiol Biomarkers Prev* 1998; **7**: 1013-1018

17 **Tan W**, Song N, Wang GQ, Liu Q, Tang HJ, Kadlubar FF, Lin DX. Impact of genetic polymorphisms in cytochrome P450 2E1 and glutathione S-transferases M1, T1, and P1 on susceptibility to esophageal cancer among high-risk individuals in China. *Cancer Epidemiol Biomarkers Prev* 2000; **9**: 551-556

18 **Yu MW**, Gladek-Yarborough A, Chiamprasert S, Santella RM, Liaw YF, Chen CJ. Cytochrome P450 2E1 and glutathione S-transferase M1 polymorphisms and susceptibility to hepatocellular carcinoma. *Gastroenterology* 1995; **109**: 1266-1273

19 **Wu X**, Shi H, Jiang H, Kemp B, Hong WK, Delclos GL, Spitz MR. Associations between cytochrome P4502E1 genotype, mutagen sensitivity, cigarette smoking and susceptibility to lung cancer. *Carcinogenesis* 1997; **18**: 967-973

20 **Le Marchand L**, Sivaraman L, Pierce L, Seifried A, Lum A, Wilkens LR, Lau AF. Associations of CYP1A1, GSTM1, and CYP2E1 polymorphisms with lung cancer suggest cell type specificities to tobacco carcinogens. *Cancer Res* 1998; **58**: 4858-4863

21 **Hung HC**, Chuang J, Chien YC, Chern HD, Chiang CP, Kuo YS, Hildesheim A, Chen CJ. Genetic polymorphisms of CYP2E1, GSTM1, and GSTT1; environmental factors and risk of oral cancer. *Cancer Epidemiol Biomarkers Prev* 1997; **6**: 901-905

22 **Hildesheim A**, Anderson LM, Chen CJ, Cheng YJ, Brinton LA, Daly AK, Reed CD, Chen IH, Caporaso NE, Hsu MM, Chen JY, Idle JR, Hoover RN, Yang CS, Chhabra SK. CYP2E1 genetic polymorphisms and risk of nasopharyngeal carcinoma in Taiwan. *J Natl Cancer Inst* 1997; **89**: 1207-1212

23 **Ladero JM**, Agúndez JA, Rodríguez-Lescure A, Diaz-Rubio M, Benítez J. RsaI polymorphism at the cytochrome P4502E1 locus and risk of hepatocellular carcinoma. *Gut* 1996; **39**: 330-333

24 **Kiss I**, Sándor J, Pajkos G, Bogner B, Hegedüs G, Ember I. Colorectal cancer risk in relation to genetic polymorphism of cytochrome P450 1A1, 2E1, and glutathione-S-transferase M1 enzymes. *Anticancer Res* 2000; **20**: 519-522

25 **Yu WP**, Chen K, Ma XY, Yao KY, Jiang QT, Zou Y, Zhou HG. Genetic polymorphism in cytochrome P450 2E1, salted food and colorectal cancer susceptibility: a case-control study. *Zhonghua Yufang Yixue Zazhi* 2004; **38**: 162-166

26 **Matthias C**, Bockmühl U, Jahnke V, Jones PW, Hayes JD, Alldersea J, Gilford J, Bailey L, Bath J, Worrall SF, Hand P, Fryer AA, Strange RC. Polymorphism in cytochrome P450 CYP2D6, CYP1A1, CYP2E1 and glutathione S-transferase, GSTM1, GSTM3, GSTT1 and susceptibility to tobacco-related cancers: studies in upper aerodigestive tract cancers. *Pharmacogenetics* 1998; **8**: 91-100

27 **Morita S**, Yano M, Shiozaki H, Tsujinaka T, Ebisui C, Morimoto T, Kishibuti M, Fujita J, Ogawa A, Taniguchi M, Inoue M, Tamura S, Yamazaki K, Kikkawa N, Mizunoya S, Monden M. CYP1A1, CYP2E1 and GSTM1 polymorphisms are not associated with susceptibility to squamous-cell carcinoma of the esophagus. *Int J Cancer* 1997; **71**: 192-195

28 **Kato S**, Onda M, Matsukura N, Tokunaga A, Tajiri T, Kim DY, Tsuruta H, Matsuda N, Yamashita K, Shields PG. Cytochrome P4502E1 (CYP2E1) genetic polymorphism in a case-control study of gastric cancer and liver disease. *Pharmacogenetics* 1995; **5** Spec No: S141-S144

29 **Nishimoto IN**, Hanaoka T, Sugimura H, Nagura K, Ihara M, Li XJ, Arai T, Hamada GS, Kowalski LP, Tsugane S. Cytochrome P450 2E1 polymorphism in gastric cancer in Brazil: case-control studies of Japanese Brazilians and non-Japanese Brazilians. *Cancer Epidemiol Biomarkers Prev* 2000; **9**: 675-680

30 **Kato S**, Shields PG, Caporaso NE, Hoover RN, Trump BF, Sugimura H, Weston A, Harris CC. Cytochrome P450IIE1 genetic polymorphisms, racial variation, and lung cancer risk. *Cancer Res* 1992; **52**: 6712-6715

31 **Persson I**, Johansson I, Bergling H, Dahl ML, Seidegård J, Rylander R, Rannug A, Högberg J, Sundberg MI. Genetic polymorphism of cytochrome P4502E1 in a Swedish population. Relationship to incidence of lung cancer. *FEBS Lett* 1993; **319**: 207-211

32 **Hirvonen A**, Husgafvel-Pursiainen K, Anttila S, Karjalainen A, Vainio H. The human CYP2E1 gene and lung cancer: DraI and RsaI restriction fragment length polymorphisms in a Finnish study population. *Carcinogenesis* 1993; **14**: 85-88

33 **London SJ**, Daly AK, Cooper J, Carpenter CL, Navidi WC, Ding L, Idle JR. Lung cancer risk in relation to the CYP2E1 Rsa I genetic polymorphism among African-Americans and Caucasians in Los Angeles County. *Pharmacogenetics* 1996; **6**: 151-158

34 **Anwar WA**, Abdel-Rahman SZ, El-Zein RA, Mostafa HM, Au WW. Genetic polymorphism of GSTM1, CYP2E1 and CYP2D6 in Egyptian bladder cancer patients. *Carcinogenesis* 1996; **17**: 1923-1929

35 **van der Logt EM**, Bergevoet SM, Roelofs HM, Te Morsche RH, Dijk Yv, Wobbes T, Nagengast FM, Peters WH. Role of epoxide hydrolase, NAD(P)H:quinone oxidoreductase, cytochrome P450 2E1 or alcohol dehydrogenase genotypes in susceptibility to colorectal cancer. *Mutat Res* 2006; **593**: 39-49

36 **Gao C**, Takezaki T, Wu J, Li Z, Wang J, Ding J, Liu Y, Hu X, Xu T, Tajima K, Sugimura H. Interaction between cytochrome P-450 2E1 polymorphisms and environmental factors with risk of esophageal and stomach cancers in Chinese. *Cancer Epidemiol Biomarkers Prev* 2002; **11**: 29-34

37 **Carrière V**, Berthou F, Baird S, Belloc C, Beaune P, de Waziers I. Human cytochrome P450 2E1 (CYP2E1): from genotype to phenotype. *Pharmacogenetics* 1996; **6**: 203-211

38 **Kim RB**, O'Shea D. Interindividual variability of chlorzoxazone 6-hydroxylation in men and women and its relationship to CYP2E1 genetic polymorphisms. *Clin Pharmacol Ther* 1995; **57**: 645-655

39 **Kim RB**, Yamazaki H, Chiba K, O'Shea D, Mimura M, Guengerich FP, Ishizaki T, Shimada T, Wilkinson GR. In vivo and in vitro characterization of CYP2E1 activity in Japanese and Caucasians. *J Pharmacol Exp Ther* 1996; **279**: 4-11

40 **Huang WY**, Olshan AF, Schwartz SM, Berndt SI, Chen C, Llaca V, Chanock SJ, Fraumeni JF, Hayes RB. Selected genetic polymorphisms in MGMT, XRCC1, XPD, and XRCC3 and risk of head and neck cancer: a pooled analysis. *Cancer Epidemiol Biomarkers Prev* 2005; **14**: 1747-1753

41 **Ma M**, Umemura T, Mori Y, Gong Y, Saijo Y, Sata F, Kawai T, Kishi R. Influence of genetic polymorphisms of styrene-metabolizing enzymes and smoking habits on levels of urinary metabolites after occupational exposure to styrene. *Toxicol Lett* 2005; **160**: 84-91

42 **Purohit V**, Khalsa J, Serrano J. Mechanisms of alcohol-associated cancers: introduction and summary of the symposium. *Alcohol* 2005; **35**: 155-160

43 **Fraser AG**. Pharmacokinetic interactions between alcohol and other drugs. *Clin Pharmacokinet* 1997; **33**: 79-90

44 **Choi JY**, Abel J, Neuhaus T, Ko Y, Harth V, Hamajima N, Tajima K, Yoo KY, Park SK, Noh DY, Han W, Choe KJ, Ahn SH, Kim SU, Hirvonen A, Kang D. Role of alcohol and genetic polymorphisms of CYP2E1 and ALDH2 in breast cancer development. *Pharmacogenetics* 2003; **13**: 67-72

S- Editor Zhu LH **L- Editor** Negro F **E- Editor** Yin DH

Online Submissions: wjg.wjgnet.com
www.wjgnet.com
wjg@wjgnet.com

World J Gastroenterol 2007 November 21; 13(43): 5731-5735
World Journal of Gastroenterology ISSN 1007-9327

RAPID COMMUNICATION

Mycobacterium avium subspecies *paratuberculosis* infects and multiplies in enteric glial cells

Leonardo A Sechi, Anne Ruehl, Niyaz Ahmed, Donatella Usai, Daniela Paccagnini, Giovanna E Felis, Stefania Zanetti

Leonardo A Sechi, Donatella Usai, Daniela Paccagnini, Giovanna E Felis, Stefania Zanetti, Department of Biomedical Sciences, Microbiology Section, University of Sassari, Viale S Pietro 43/B, Sassari 07100, Italy
Anne Ruehl, Department of Human Biology, Technical University of Munich, Hochfeldweg 2, D-85350 Freising-Weihenstephan, Germany
Leonardo A Sechi, Niyaz Ahmed, Stefania Zanetti, International Society of Genetic and Evolutionary Microbiology, Working Group on Mycobacterial Disease, Sassari, Italy
Niyaz Ahmed, Pathogen Evolution Group, Centre for DNA Fingerprinting and Diagnostics, Hyderabad, India
Correspondence to: Leonardo A Sechi, Dipartimento di Scienze Biomediche, Sezione di Microbiologia Sperimentale e Clinica, Università degli studi di Sassari, Viale S. Pietro 43/B, Sassari 07100, Italy. sechila@uniss.it
Telephone: +39-79-228303 Fax: +39-79-212345
Received: April 17, 2007 Revised: August 23, 2007

Abstract

AIM: To establish the role of enteric glial cells during infection with *Mycobacterium avium* subspecies paratuberculosis (MAP) in Crohn's disease.

METHODS: In order to establish the role of enteric glial cells during infection with *M. avium* subspecies *paratuberculosis* (MAP) in Crohn's disease, Map adhesion experiments on enteric glial cells were performed as well as expression analysis of Map sigma factors during infection.

RESULTS: In this study, for the first time, we found a high affinity of MAP to enteric glial cells and we analyzed the expression of MAP sigma factors under different conditions of growth.

CONCLUSION: The fact that Map showed a high affinity to the glial cells raises concerns about the complicated etiology of the Crohn's disease. Elucidation of the mechanisms whereby inflammation alters enteric neural control of gut functions may lead to novel treatments for Crohn's disease.

Key words: *Mycobacterium avium* subspecies *Paratuberculosis*; Enteric glial cells; Inflammatory bowel diseases; Crohn's disease; Sigma factors expression

Sechi LA, Ruehl A, Ahmed N, Usai D, Paccagnini D, Felis GE, Zanetti S. *Mycobacterium avium* subspecies *paratuberculosis* infects and multiplies in enteric glial cells. *World J Gastroenterol* 2007; 13(43): 5731-5735

http://www.wjgnet.com/1007-9327/13/5731.asp

INTRODUCTION

Several cell lines of the gut have been extensively studied such as intestinal epithelial cells, immune cells, smooth muscle cells and enteric neurons[1-4]. However, very little is known about enteric glial cells which belong to the enteric nervous system (ENS) along with the neurons[5]. The ENS, comprised of several plexuses, is located alongside the intestinal wall. The enteric glia are localised within the mucosal plexuses and the glial processes make close contact with the epithelial cell layers. The epithelial crypt bases, in particular, are surrounded by a dense network of glial cells[6]. These glial cells are small, star shaped with different processes of various length and shape[6]; they are morphologically and immunohistochemically different from microglia of the central nervous system and from all other peripheral glia and appear more closely related to astrocytes although functionally different[6]. Evidence for functional heterogeneicity of enteric glia has recently been described[7]. The enteric glial cells (EGC) could participate in neurotransmitter synthesis/inactivaction or in synaptic transmission. Moreover, they may also interact with intestinal capillaries to modulate endothelial permeability[8].

It has been shown that the enteric nervous system regulates intestinal barrier functions by regulating the zonula occludens-tight junctions[9]. Regarding EGC, it has been shown in a mouse model that EGC ablation results in fulminant intestinal inflammation due to disregulation and rupture of the epithelial intestinal barrier[8,10]. It has been suggested that there is a direct interaction between EGC (releasing soluble factors) and epithelial cells to enhance the intestinal epithelial cells[5]. Moreover they could have a role in the prevention of epithelial barrier disorganization and hyperproliferation during bacterial infection, inflammatory processes and neoplasia[11-13]. All these findings indicate that glial cells may be an important component of the intestinal mucosal defense system.

On the other hand, *Mycobacterium avium* subspecies *paratuberculosis* is the causative agent of Johne's disease, a chronic and incurable disease affecting ruminants and other animals[14]. Moreover, there is increasing evidence of its involvement in the enteric granulomatous syndrome of

Table 1 PCR primers, targets, position on the sequences

Target	Primer name	5'-3' sequence	Position[1]
16S	MAP16Sfor	ATCATGCCCCTTATGTCCAG	1179-1198
	MAP16Srev	TGAGACCGGCTTTAAAAGGA	1259-1278
sigA	sigAfor	GTACGCCACCCAGCTGATGTCG	714-735
	sigArev	CGTCGCGGCAGATCCACAT	787-805
sigB	sigBfor	GACCTGCTCGAGCACAGC	646-663
	sigBrev	CAGCACGCTGCGGATGTCGGTG	783-804
sigC	sigCfor	ACATCCGTCACCTGCAGTC	1088-1106
	sigCrev	GTCACCTCGACCAGATCCTC	1177-1195
sigD	sigDfor	CTTCCTGGCTTTCCTGTACG	249-268
	sigDrev	GATGGACTCGGTCGGGTAG	324-242
sigE	sigEfor	CACCCAGGAGACCTTCATCC	327-346
	sigErev	GACCATGTCCAGGAACAG	418-435
sigF	sigFfor	GGCAGCTCCTACAACACCTT	493-512
	sigFrev	ACTCCTGGTCCTCGATCCGG	597-616
sigF-like	sigF-likefor	ATGACCAACGCAATCGCTCC	1-20
	sigF-likerev	GGCATCCGGCGCAGTTCCA	88-107
sigG	sigGfor	GCGTTCGAAAGCTACGACAT	622-641
	sigGrev	CTGATACCACCCGGTGTACG	692-711
sigH	sigHfor	AATCTCAAGGCGTGGCTCTA	385-404
	sigHrev	TGATTTCCTCGGTCGGATAC	465-484
sigI	sigIfor	GGGCGACATCGACGACGTGC	150-169
	sigIrev	GACATCGCCCGGACGTTCGTG	235-255
sigJ	sigJfor	GCATCTACACGGCGGGCCTG	740-759
	sigJrev	GGCGAACCGGTGAACTTGT	857-875
sigL	sigLfor	CGTGATCGAACGGTCCTACT	399-418
	sigLrev	CCGCACCGCATAGTGTAGT	491-504
sigM	sigMfor	TGGCTGCACCGCATCGTG	238-255
	sigMrev	TCGGCGACCGGATAGTAGTCT	315-335
Other ECF-1	sigECF1for	GTTCTCCGCCGAGTCGATTT	310-328
	sigECF1rev	GTCGAATCCGAACACCTCAC	492-411
Other ECF-2	sigECF2for	GCATCCACACGATCGACAT	839-857
	sigECF2rev	GGTTGTGATGTTCCTGAACC	914-933
Other ECF-3	sigECF3for	GTCGGTCATGGGTTTCGT	780-797
	sigECF3rev	GCACCCAGCTCCAGTTTC	855-873
Other ECF-4	sigECF4for	GATCTCGTCGGCATCTCG	502-519
	sigECF4rev	TCCAATTCGTTTCGGAGATT	592-611
Other ECF-5	sigECF5for	GCAATTGACCCGTTCACC	945-962
	sigECF5rev	CTCCTCCAAAGCGGCTAAG	1020-1038
Other ECF-6	sigECF6for	TGCAAGGTAATTCGATCAAGG	419-439
	sigECF6rev	TCCCTCGTTGACCTGTGC	511-528

[1]longest sequence available (primary and TIGR annotation). ECF: Extracitoplasmatic function; TIGR: The Institute for Genomic Research.

humans called Crohn's disease[15-17]. For all these reasons we analyzed the interactions between EGC and M. paratuberculosis *in vitro*.

Sigma factors are part of the transcriptional regulators family and are responsible for binding to the RNA polymerase complex (composed of four distinct subunits); to recognize promoters and separate DNA strands[18]. In fact, every sigma factor has its own specificity, allowing the initiation of transcription of different subset of genes[18,19]. Some sigma factors (sigD, sigE, sigC, sigH and sigL) play a role in the virulence of *M. tuberculosis*[20,21]. The number and abundance of sigma factors reflect the ability of the bacterium to cope with various environmental conditions, stresses and insults[18,22].

In this study the expression of all 19 sigma factors of M. paratuberculosis were also tested during EGC infection.

MATERIALS AND METHODS

Bacterial strains and culture conditions

M. paratuberculosis ATCC 43015, of human source was obtained from The RIVM, Bilthoven, The Netherlands. *M. paratuberculosis* for DNA extraction was grown in Mycobacteria Growth Indicator Tube (MGITl) medium supplemented with Mycobactin J and egg yolk. Murine enteric glial cells were previously isolated and characterized by Dr. Anne Ruhel[23].

Identification of M. avium subsp. paratuberculosis putative sigma factors

Identification of individual sigma factors in *M. avium* subspecies. paratuberculosis was obtained by text annotation searches and by BlastP similarity searches using *M. smegmatis* and *M. tuberculosis* H37Rv Sigma ORF as queries. Primers used in real time PCR are described in Table 1.

DNA extraction

DNA extraction was performed using the Ribolyser system (HYBAID, USA) and purified as previously described[17].

PCR conditions

Oligonucleotide sequences and position are reported in

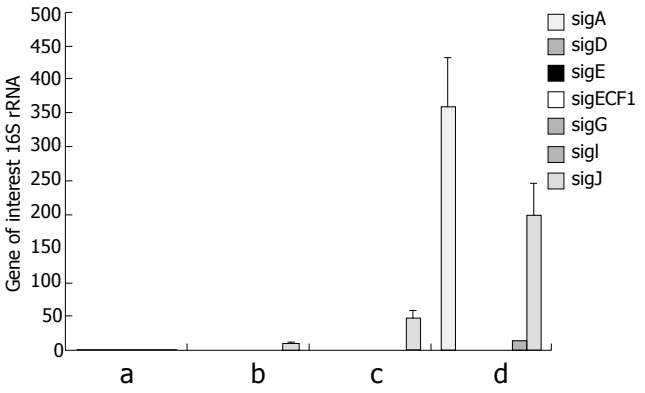

Figure 1 Relative quantification of expression of MAP sigma factors relative to the expression of the 16S rRNA MAP gene (calculated by the Biorad software) by Real Time PCR after different conditions of growth. a: After growth in 7H9 medium plus mycobactin J; b: Infection of EGC after 6 h of incubation; c: Infection of EGC after 48 h of incubation; d: Infection of EGC cells after 7 d of incubation.

Table 1. Specificity of primer pairs was ascertained with PCR with the following conditions: $MgCl_2$ 1.5 mmol/L, deossi Nucleotide Triphosphate (dNTPS) 150 μmol/L, primers 0.2 μmol/L each, Taq 0.025 U/μL reaction volume. After an initial denaturation of 3 min at 94℃, 30 cycles of 1 min at 94℃, 1 min at 58℃, 1 min at 72℃ and a final extension at 72℃ for 5 min were performed. Only the amplification products of the expected length were obtained.

RNA extraction

RNA was extracted using the Ribolyser instrument[17]. RNA was extracted from MAP cells after different conditions: (1) growth in 7H9 medium plus Mycobactin J, (2) after addition of lysozyme at 24 h and 7 d; (3) after infection of EGC line, after 6 h, 24 h, 48 h and 7 d. RNA was quantified for further experiments and samples were stored at -80℃ until further use. cDNA was prepared by an initial incubation at 65℃ for 10 min of the reaction mixture containing 100 μmol/L oligo-dT and 10 μL of extracted RNA; this first step was followed by a second incubation of 1 h at 42℃ of the mixture containing 50 U/reaction of reverse transcriptase (Mooloney-Murine Leukemia Virus M-MLV 200 U/μL), 0.1 mol/L buffer 5 × Tris HCl pH 8.3 (Life Technologies) with 150 mmol/L KCl, 7 mmol/L $MgCl_2$ and 20 mmol/L dithiothreitol (DTT); 0.1 mol/L DTT, 10 mmol/L dNTPs, 40 U/μL RNase inhibitor.

Real time PCR analyses

Real Time PCR was performed using the iCycler Detection System (Biorad) with the SyberGreen assay (Applied Biosystems). Gene expression of all the Sigma factors (except Extracytoplasmic function 3 ECF3) was determined using quantitative Real-Time PCR by comparing the fluorescence produced by test samples to that of the 16S rRNA gene expression (house-keeping gene). Five micro liters of cDNA was subjected to PCR (1 cycle at 94℃ for 1 min; 50 cycles at 94℃ for 30 s and at 60℃ for 40 s) with primers that amplified 16S rRNA, all 19 sigma factor genes. PCR was carried out with the following reaction-mixture in a total volume of 30 μL: 1 × of 10 × buffer, $MgCl_2$ 1.5 mmol/L, dNTPs 0.2 mmol/L, primers 0.5 μmol/L each, DNA polymerase 0.5 U/sample. PCR was performed in a 96 well plate, for each sample 2 wells were utilized to guarantee uniformity in results. The quantitative analysis of the data obtained was performed by Biorad's method of relative quantitation of gene expression (Bio-Rad Laboratories, USA).

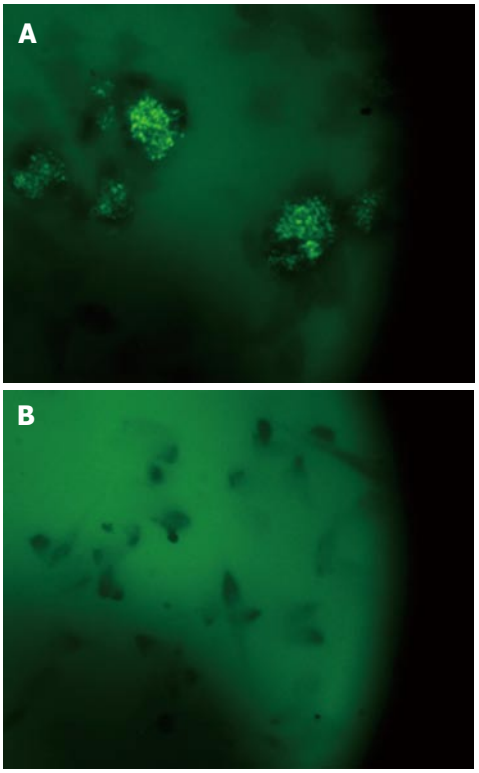

Figure 2 MAP cells stained with auramine rodhamine at 6 h after infection of EGC (**A**) and without infection (**B**) and visualized under a fluorescence microscope (× 100).

Infection experiments

Glial Enteric cell lines were cultivated in 24 well plastic dishes. The EGCs were cultivated in Dulbecco's modified Eagle medium supplemented with 15% fetal bovine serum and 4 mmol of L-glutamine per liter. All tissue culture reagents were obtained from Sigma (Sigma Chemical Co.). Cells were seeded at 2×10^4 cells per well and incubated at 37℃ in 5% CO_2. EGC cells were used when they were semiconfluent. MAP grown over night in 7H9 broth (with mycobactin J) was diluted in cell medium. One milliliter containing 10^6 bacteria was added to each well containing EGCs (cells were infected at a ratio of bacteria/cells of 10:1). After two hours infected EGCs were washed with cell medium containing Kanamycin 100 μg/mL and incubated with the same medium. Cells were stained with auramine rodhamine at the different incubation times (6 h, 48 h and 7 d at 37℃) to visualize MAP, and counted as previously described[17].

RESULTS

Expression of sigma factors in different conditions of Growth

7H9 broth plus mycobactin J: MAP during growth in

broth 7H9 supplemented with Mycobactine J, expressed several sigma factors as expected (Figure 1A). SigA, Sig D, SigE, Sig G and Sig I were among the most expressed ones as compared to the 16S rRNA expression taken as house keeping gene whereas ECF1 and sig J were expressed in lower quantity (Figure 1A).

Infection of EGC: The expression of the 19 sigma factors of MAP was observed and quantified after growth infection of EGC at 6 h, 48 h and 7 d (Figure 1 B-D). Soon after infection, expression of all sigma factors shut down, except for sig J which was expressed in high quantity (Figure 1B). The expression of sig J increased after 48 h (Figure 1C) and 7 d. SigA was overexpressed after seven days (Figure 1D), at the same time an expression of sig I was also detected. Figure 2 reveals an example of EGC infection by MAP where bacteria were visualized within the intestinal glial cells after staining with auramine rodamine as compared to control cells not infected.

DISCUSSION

Enteric glias are distinct from all other glial cell types[5,7]. No gastrointestinal disorder has been reported linked to glial defect yet, most probably because subtle changes in glial function might be involved in the etiopathogenesis of enteric disorders. Crohn's disease with neuroinflammation and neurodegeneration components may be associated with EGC alteration[23-25]. Indeed EGC interact with enteric neurons, endothelial cells, immune cells and the intestinal epithelium; all these factors can contribute to the pathogenesis of Crohn's disease. In our experiments, we found that MAP has a high affinity to EGCs. Experiments "*in vitro*" show a high adhesion and intracellular multiplication as confirmed by the active expression of sigA (the housekeeping sigma factor) after seven days of infection along with the expression of sigJ and sigI (expressed in different conditions of cellular stress).

The fact that this dangerous intestinal pathogen has a demonstrated affinity to the glial cells and that MAP has recently been reported in substantial percentages of Crohn's patients[15-17] raises concerns about the complicated etiology of the Crohn's disease.

MAP expression of sigma factors in EGC is very similar to sigma factor expression after infection of the Caco2 intestinal epithelial cell line (manuscript in preparation) and shows how there is a rapid change in gene expression after cell infection.

EGCs are an active part of an intestinal network system essential for a healthy and functional gut[23,26,27]. The role of EGC in Crohn's and other enteric diseases is not well studied and this is the first report that attempts to unravel interaction between an intestinal pathogen and EGC. Future work is certainly needed to elucidate this complex interaction.

COMMENTS

Background

Enteric glia might play a role in regulating barrier functions in mucosal epithelia. *Mycobacterium avium subspecies paratuberculosis* (MAP) is the causative agent of Johne's disease, a chronic and incurable disease affecting ruminants and other animals. Moreover, evidence of its involvement in Crohn's disease is accumulating. MAP enter the host through Peyer's patches and intestinal epithelium and are sampled by intestinal dendritic cells; they survives inside macrophages. Nothing is known about the role of enteric glial cells during MAP infection thus we performed this study to establish the role of enteric glial cells during infection with *Mycobacterium avium subspecies paratuberculosis* (MAP) in Crohn's disease.

Research frontiers

It is firmly established that intestinal inflammation is accompanied by functional and structural alterations of the Enteric Nervous System to which belong Enteric Glial Cells. In Crohn's disease patients, a compromised glial network that responds poorly to inflammatory stimuli has been suggested. Our report will open a new frontier on the interaction of MAP and enteric glia cells supporting the idea that Crohn's disease is associated with the invasion and persistence of a multi host pathogen as it is MAP.

Innovations and breakthroughs

This is the first research that highlights the interaction of a true enteric pathogen such as Map with Enteric glial cells. This study will open the research field in this matter.

Applications

Enteric glial cells may be the target of a series of cytokine modulators or drugs. Map will be recognized as a pathogen associated with intestinal disorders.

Terminology

EGCs: enteric glial cells; Map: Mycobacterium avium subs. Paratuberculosis; ENS: Enteric nervous system; Johne's disease: Enteric granulomatous infection of ruminants caused by Map; Crohn's disease: Enteric granulomatous chronic inflammation in humans with ulcerative colitis (UC) forms inflammatory bowel disease (IBD).

Peer review

The manuscript by Sechi *et al* describes the expression of MAP sigma factors during infection of enteric glial cells. The first findings that sigma factors are differentially expressed during infection are very promising.

REFERENCES

1 **Liévin-Le Moal V**, Servin AL. The front line of enteric host defense against unwelcome intrusion of harmful microorganisms: mucins, antimicrobial peptides, and microbiota. *Clin Microbiol Rev* 2006; **19**: 315-337
2 **Niess JH**, Reinecker HC. Dendritic cells in the recognition of intestinal microbiota. *Cell Microbiol* 2006; **8**: 558-564
3 **Ozaki H**, Hori M, Kinoshita K, Ohama T. Intestinal dysmotility in inflammatory bowel disease: mechanisms of the reduced activity of smooth muscle contraction. *Inflammopharmacology* 2005; **13**: 103-111
4 **Grundy D**, Schemann M. Enteric nervous system. *Curr Opin Gastroenterol* 2005; **21**: 176-182
5 **Rühl A**. Glial cells in the gut. *Neurogastroenterol Motil* 2005; **17**: 777-790
6 **Rühl A**, Nasser Y, Sharkey KA. Enteric glia. *Neurogastroenterol Motil* 2004; **16** Suppl **1**: 44-49
7 **Rühl A**. Glial regulation of neuronal plasticity in the gut: implications for clinicians. *Gut* 2006; **55**: 600-602
8 **Neunlist M**, Aubert P, Bonnaud S, Van Landeghem L, Coron E, Wedel T, Naveilhan P, Rühl A, Lardeux B, Savidge T, Paris F, Galmiche JP. Enteric glia inhibit intestinal epithelial cell proliferation partly through a TGF-beta1-dependent pathway. *Am J Physiol Gastrointest Liver Physiol* 2007; **292**: G231-G241
9 **Aubé AC**, Cabarrocas J, Bauer J, Philippe D, Aubert P, Doulay F, Liblau R, Galmiche JP, Neunlist M. Changes in enteric neurone phenotype and intestinal functions in a transgenic mouse model of enteric glia disruption. *Gut* 2006; **55**: 630-637
10 **Cabarrocas J**, Savidge TC, Liblau RS. Role of enteric glial cells in inflammatory bowel disease. *Glia* 2003; **41**: 81-93
11 **Bassotti G**, Villanacci V, Maurer CA, Fisogni S, Di Fabio F, Cadei M, Morelli A, Panagiotis T, Cathomas G, Salerni B.

The role of glial cells and apoptosis of enteric neurones in the neuropathology of intractable slow transit constipation. *Gut* 2006; **55**: 41-46

12 **Lomax AE**, Fernández E, Sharkey KA. Plasticity of the enteric nervous system during intestinal inflammation. *Neurogastroenterol Motil* 2005; **17**: 4-15

13 **Tjwa ET**, Bradley JM, Keenan CM, Kroese AB, Sharkey KA. Interleukin-1beta activates specific populations of enteric neurons and enteric glia in the guinea pig ileum and colon. *Am J Physiol Gastrointest Liver Physiol* 2003; **285**: G1268-G1276

14 **Chacon O**, Bermudez LE, Barletta RG. Johne's disease, inflammatory bowel disease, and Mycobacterium paratuberculosis. *Annu Rev Microbiol* 2004; **58**: 329-363

15 **Bull TJ**, McMinn EJ, Sidi-Boumedine K, Skull A, Durkin D, Neild P, Rhodes G, Pickup R, Hermon-Taylor J. Detection and verification of Mycobacterium avium subsp. paratuberculosis in fresh ileocolonic mucosal biopsy specimens from individuals with and without Crohn's disease. *J Clin Microbiol* 2003; **41**: 2915-2923

16 **Naser SA**, Ghobrial G, Romero C, Valentine JF. Culture of Mycobacterium avium subspecies paratuberculosis from the blood of patients with Crohn's disease. *Lancet* 2004; **364**: 1039-1044

17 **Sechi LA**, Scanu AM, Molicotti P, Cannas S, Mura M, Dettori G, Fadda G, Zanetti S. Detection and Isolation of Mycobacterium avium subspecies paratuberculosis from intestinal mucosal biopsies of patients with and without Crohn's disease in Sardinia. *Am J Gastroenterol* 2005; **100**: 1529-1536

18 **Wösten MM**. Eubacterial sigma-factors. *FEMS Microbiol Rev* 1998; **22**: 127-150

19 **Dove SL**, Darst SA, Hochschild A. Region 4 of sigma as a target for transcription regulation. *Mol Microbiol* 2003; **48**: 863-874

20 **Manganelli R**, Voskuil MI, Schoolnik GK, Smith I. The Mycobacterium tuberculosis ECF sigma factor sigmaE: role in global gene expression and survival in macrophages. *Mol Microbiol* 2001; **41**: 423-437

21 **Manganelli R**, Provvedi R, Rodrigue S, Beaucher J, Gaudreau L, Smith I. Sigma factors and global gene regulation in Mycobacterium tuberculosis. *J Bacteriol* 2004; **186**: 895-902

22 **Li L**, Bannantine JP, Zhang Q, Amonsin A, May BJ, Alt D, Banerji N, Kanjilal S, Kapur V. The complete genome sequence of Mycobacterium avium subspecies paratuberculosis. *Proc Natl Acad Sci USA* 2005; **102**: 12344-12349

23 **Rühl A**, Franzke S, Collins SM, Stremmel W. Interleukin-6 expression and regulation in rat enteric glial cells. *Am J Physiol Gastrointest Liver Physiol* 2001; **280**: G1163-G1171

24 **Bush TG**. Enteric glial cells. An upstream target for induction of necrotizing enterocolitis and Crohn's disease? *Bioessays* 2002; **24**: 130-140

25 **Cornet A**, Savidge TC, Cabarrocas J, Deng WL, Colombel JF, Lassmann H, Desreumaux P, Liblau RS. Enterocolitis induced by autoimmune targeting of enteric glial cells: a possible mechanism in Crohn's disease? *Proc Natl Acad Sci USA* 2001; **98**: 13306-13311

26 **Nasser Y**, Ho W, Sharkey KA. Distribution of adrenergic receptors in the enteric nervous system of the guinea pig, mouse, and rat. *J Comp Neurol* 2006; **495**: 529-553

27 **von Boyen GB**, Steinkamp M, Reinshagen M, Schäfer KH, Adler G, Kirsch J. Proinflammatory cytokines increase glial fibrillary acidic protein expression in enteric glia. *Gut* 2004; **53**: 222-228

S- Editor Zhu LH **L- Editor** Alpini GD **E- Editor** Yin DH

Online Submissions: wjg.wjgnet.com
www.wjgnet.com
wjg@wjgnet.com

World J Gastroenterol 2007 November 21; 13(43): 5736-5740
World Journal of Gastroenterology ISSN 1007-9327

RAPID COMMUNICATION

Early prediction of major depression in chronic hepatitis C patients during peg-interferon α-2b treatment by assessment of vegetative-depressive symptoms after four weeks

Geert Robaeys, Jozef De Bie, Marieke C Wichers, Liesbeth Bruckers, Frederik Nevens, Peter Michielsen, Marc Van Ranst, Frank Buntinx

Geert Robaeys, Department of Gastroenterology and Hepatology, Ziekenhuis Oost Limburg, Genk, Belgium
Jozef De Bie, Department of Psychiatry, Ziekenhuis Oost Limburg, Genk, Belgium
Marieke C Wichers, Department of Psychiatry and Neuropsychiatry, South Limburg Mental Health Research and Teaching Network, EURON, Maastricht University, Maastricht, The Netherlands
Liesbeth Bruckers, Center for Statistics, Limburgs Universitair Centrum, Diepenbeek, Belgium
Frederik Nevens, Department of Hepatology, Katholieke Universiteit Leuven, Leuven, Belgium
Peter Michielsen, Division of Gastroenterology and Hepatology, University Hospital, Antwerp, Belgium
Marc Van Ranst, Laboratory of Clinical and Epidemiological Virology, Department of Microbiology and Immunology, Rega Institute and University Hospitals, Katholieke Universiteit Leuven, Leuven, Belgium
Frank Buntinx, Department of General Practice, Katholieke Universiteit Leuven, Leuven, Belgium and Department of General Practice, Maastricht University, The Netherlands
Supported by a received logistic support by Schering Plough
Correspondence to: Dr. Geert Robaeys, Ziekenhuis Oost Limburg, Department of Gastroenterology and Hepatology, Schiepse Bos 6, B 3600 Genk, Belgium. geert.robaeys@zol.be
Telephone: +32-89-326505 Fax: +32-89-327916
Received: March 19, 2007 Revised: August 25, 2007

Abstract

AIM: To study the predictive value of the vegetative-depressive symptoms of the Zung Depression Rating Scale for the occurrence of depression during treatment with peg-interferon α-2b of chronic hepatitis C (CHC) patients.

METHODS: The predictive value of vegetative-depressive symptoms at 4 wk of treatment for the occurrence of a subsequent diagnosis of major depressive disorder (MDD) was studied in CHC patients infected after substance use in a prospective, multicenter treatment trial in Belgium. The presence of vegetative-depressive symptoms was assessed using the Zung Scale before and 4 wk after the start of antiviral treatment.

RESULTS: Out of 49 eligible patients, 19 (39%) developed MDD. The area under the ROC curve of the vegetative Zung subscale was 0.73, $P = 0.004$. The sensitivity at a cut-point of > 15/35 was 95% (95% CI: 74-100). The positive predictive value equalled 44% (95% CI: 29-60).

CONCLUSION: In this group of Belgian CHC patients infected after substance use, antiviral treatment caused a considerable risk of depression. Seven vegetative-depressive symptoms of the Zung scale at wk 4 of treatment predicted 95% of all emerging depressions, at a price of 56% false positive test results.

Key words: Interferons; Hepatitis C; Chronic; Substance-related disorders; Depression; Zung self rating scale; Prognosis

Robaeys G, De Bie J, Wichers MC, Bruckers L, Nevens F, Michielsen P, Van Ranst M, Buntinx F. Early prediction of major depression in chronic hepatitis C patients during peg-interferon α-2b treatment by assessment of vegetative-depressive symptoms after four weeks. *World J Gastroenterol* 2007; 13(43): 5736-5740

http://www.wjgnet.com/1007-9327/13/5736.asp

INTRODUCTION

Following the recent expert consensus, patients with chronic hepatitis C (CHC) should now receive interferon (IFN) and ribavirin regardless of psychiatric status, except in uncontrolled psychiatric disease[1-3]. As 23%-44% of patients treated with IFN develop depressive symptoms during treatment[4,5] and since, more patients are treated, interferon-induced psychiatric illness is likely to become an increasingly important clinical problem[4,6-14].

IFN-induced depression appears to be a depressive disorder that is unusually responsive to antidepressant treatment. Approximately 80% of patients are responsive within 4 wk[15]. This high response rate may be related to the usually short duration of this illness when treatment is initiated, to the mild to moderate severity of illness in most cases[1], but also to the mainly interferon-induced influences on the central nervous system[16].

Based on the results of a small scale study ($n = 16$), it has been hypothesised that vegetative symptoms are

early predictors for the emergence of full depression[9]. We wanted to confirm or refute this finding in a larger patient group of CHC positive substance users, classically considered as predisposed for depression[17].

Therefore, the predictive value of an increase in the score of the seven vegetative-depressive symptoms from the 20-item Zung Depression Rating Scale[18] was studied in a new study in substance users, using the emergence of a DSM-IV based major depression during treatment as the outcome measure.

MATERIALS AND METHODS

Subjects

Previously untreated patients, 18 years or older, with compensated chronic HCV infection acquired after substance use, with a serum alanine aminotransferase level above the upper limit of normal, and positive serum HCV RNA were eligible for the study.

HCV patients infected after substance use were defined as patients who were HCV-positive and who had used cocaine, heroin or LSD at least once. All of them were currently or previously cared for in multidisciplinary and specialised programs, according to criteria defined in the Belgian guidelines for the treatment of CHC patients infected after substance use (Table 1)[1]. Patients, who had co-infections such as hepatitis B virus or human immunodeficiency virus, or patients with a diagnosis of uncontrolled neurological, cardiovascular, endocrine, haematological, hepatic or renal disease or patients with insufficient knowledge of the Dutch or French language were excluded.

The study was approved by the ethical review board of the Catholic University of Leuven Medical School and by the Medical Ethical Committees of each of the different centres, and carried out in accordance with the Declaration of Helsinki. Written informed consent was obtained from each subject prior to participation.

Methods

Patients were treated in a prospective, randomised, multi-center study in Belgium between November 2001 and February 2004 with pegylated interferon α-2b, 1.5 μg/kg weekly by subcutaneous injection in combination with ribavirin (administered orally, 1000-1200 mg/d, depending on body weight) or interferon α-2b PEN 3 MIU subcutaneously 3 times/wk in combination with ribavirin (administered orally, 1000-1200 mg/d, depending on body weight). The total duration of therapy for the two study medication arms was 48 wk if the patient was infected with genotype non-2-3 and 24 wk if the patient was infected with genotype 2-3. The patients were required to use effective birth control. A subgroup out of the study centers that collaborated to the study, also recorded the emergence of depression. In this group we systematically investigated the occurrence of depression during therapy in patients who were not already depressed at baseline.

A complete medical history, physical examination, laboratory blood test and liver biopsy were performed before study entry. A liver biopsy was performed before randomisation.

Table 1 Characteristics at baseline of chronic hepatitis C patients infected by substance use in a Belgian population eligible for treatment in a randomised trial

Characteristics at baseline	*n*	Thrice in wk 3 MIU interferon	Weekly pegylated interferon	Total	Wilcoxon rank sum test or fishers exact test
Age at baseline (yr)	49	37	37	37	0.99
at exposure (yr)	49	27	28	27	0.55
at infection (yr)	49	33	36	35	0.58
Body mass index	33	25	25	25	0.93
Genotype (%)					
-non 2-3	25	73	36	53	0.02[a]
-5	22	27	64	47	
Gender (%)					
F	11	26	19	22	0.73
M	38	74	81	78	
Methadone user (%)	49	39	35	37	0.77
Drug user active (%)	48	59	54	56	0.77
IVDU (%)	49	91	92	92	1.00
Activity[1]					
A0 + 1	40	81	96	89	0.17
A2 + 3	5	19	4	11	
Fibrosis[1]					
F0 + 1	20	38	50	44	0.19
F2 + 3	22	48	50	49	
-F4	3	14	0	7	
Steatosis[1]					
S0	20	40	52	47	0.73
S1	12	30	26	28	
S2 + 3	11	30	22	26	
ASAT at baseline (IU/L)	49	59	77	68	0.2098
ALAT at baseline (IU/L)	49	87	127	108	0.0635

IVDU: Intravenous drug users; ASAT: Aspartate aminotransferase; ALAT: Alanine aminotransferase. [1]According to metavir score for liver biopsy. [a]$P < 0.05$ between genotype-2-3 and non 2-3.

Risk determination

In total, 12 hepatologists in collaborating treatment centres (in whom 49 patients were treated) agreed to apply a 20-item Zung self-rating depression scale (SDS) at wk 0, 4 wk after start of treatment and after the treatment regimen was completed. Zung scale results could score between 25 (normal) and 100 points. A high score indicates a depressive attitude. A cut-off of equal to and higher than 60/100 was considered as indicative for diagnosable depression[18].

Cognitive-depressive and vegetative-depressive symptom dimensions were constructed as described earlier[19]. The vegetative-depressive symptoms (Diurnal variation, lack of sleep, loss of appetite, loss of sex drive, weight loss, constipation, fatigue) were scored from 1 to 4 (in the analysis multiplied with 5/4).

Outcome measures

Clinical diagnosis of depression was confirmed by a qualified psychiatrist on the basis of DSM-IV criteria for major depression[20].

Statistical analysis

Quantitative measures are expressed as mean or as median. Qualitative variables are presented as counts and percentages.

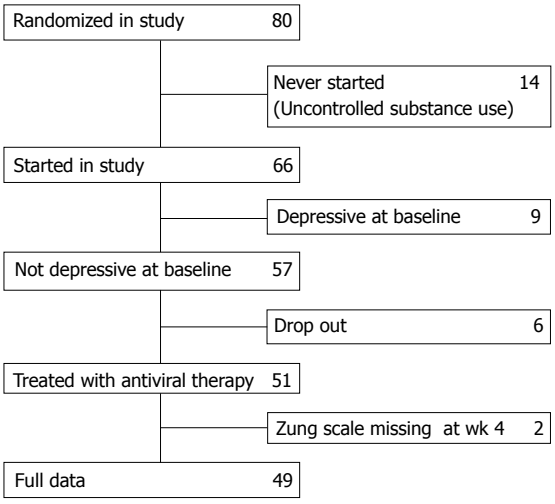

Figure 1 Flow chart of the patients included in the study.

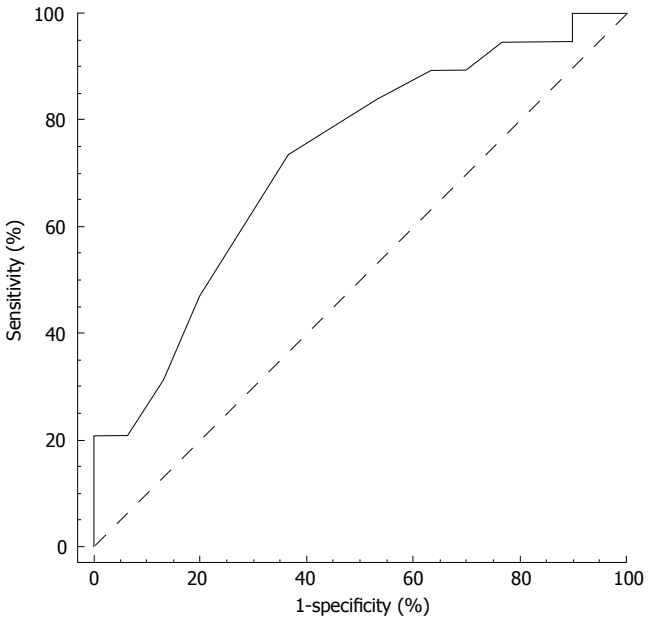

Figure 2 ROC prediction of depression based on vegetative Zung scale at wk 4.

The χ^2 test statistic and logistic regression methodology were used to compare two patient subgroups with respect to categorical outcome measures. *T*-tests for independent samples and linear regression methodology were applied to compare subgroups for differences in means of continuous variables. Non-parametric test statistics such as the Wilcoxon Rank Sum test were used if normality was absent.

In identifying an optimal cut-point for the Zung-vegetative symptoms score, we searched for a maximal sensitivity with a positive predictive value of at least around 50%. We report the full ROC curve, the AUC and its confidence interval for the four-week vegetative subscale of the Zung and the AUC and the *P*-values for possible alternative measures.

RESULTS

Participants

Eighty patients in whom chronic hepatitis C was diagnosed as acquired after substance use were randomised to treatment with either interferon α-2b or pegylated interferon α-2b combined with ribavirin and were followed by a hepatologist who accepted to apply the Zung rating scales. Fourteen patients never started the study because they were still consuming substances in an uncontrolled way. Nine had major depressive disorder (MDD) at baseline and were therefore excluded. For 8 patients data collection was incomplete. In total 49 eligible patients were included in this analysis (Figure 1).

Baseline characteristics

Demographic characteristics and clinical data for all eligible patients not having depression at baseline (n = 49) are summarized in Table 1. There were no baseline differences between the two treatment groups, with the exception of HCV genotype distribution (P = 0.02) and alanine aminotransaminase (ALT) level (P = 0.06).

Depression (DSM *IV*)

Nineteen patients became depressed during antiviral treatment. Median time to depression ranged from 4 to 26 wk and was distributed over this whole period with a mean of 10 wk.

Zung scale

At baseline there was no difference in total, vegetative or cognitive Zung score between patients who subsequently became depressed or not.

At wk 4 after treatment start the mean vegetative Zung scale was higher among the patients developing depression later on compared to other patients (P = 0.008). It decreased slightly from baseline to wk 4 (difference: -0.72; P = 0.49) for patients not getting depressed. Patients getting depressed increased on average 4.13 points on the vegetative Zung scale during the first four weeks of therapy (P = 0.03).

Diagnostic accuracy characteristics

The ROC curve for the prediction of depression emerging during treatment by the vegetative subscale at wk 4 is reported in Figure 2. The area under the curve (AUC) was 0.73 (95% CI 0.58-0.84; P = 0.004). At a cut-off point of > 17/35, the sensitivity and specificity of the vegetative subscale at wk 4 were 90% and 30%, respectively. The positive and negative predictive value equalled 45% and 82%. For a sensitivity of 95% (95% CI 74-100) the vegetative subscale criterion was > 15 and the corresponding specificity 23% (95% CI 10-42), the positive predictive value 44% (95% CI 39-60) and negative predictive value 88% (95% CI 47-100).

The increased vegetative Zung scale was not merely a measure of depression at that moment, but predicted the occurrence of depression scattered over the weeks and months afterwards. Results were not different according to gender, age and genotype.

The change in vegetative symptoms between wk 0 and 4 was marginally predictive (AUC = 0.68; P = 0.06).

The cognitive subscale at wk 4 was not able to predict a clinical diagnosis of depression (AUC = 0.62; $P = 0.15$). The total Zung at wk 4 did only have marginal predictive power (AUC = 0.67; $P = 0.05$).

DISCUSSION

The early presence of vegetative symptoms seems to be predictive for the occurrence of depression later on. In a small scale prospective study ($n = 16$)[9] it was found that the increase in the vegetative subscale score of the Montgomery Asberg Depression Rating Scale (MADRS) or the Hamilton Depression Rating Scale scales after one week of antiviral treatment following the start of antiviral treatment in CHC patients was predictive for MDD. We could confirm these findings in this prospective study during treatment with regular interferon or pegylated interferon in combination with ribavirin. Our study was larger and we had a more vulnerable population resulting in a higher number of patients becoming depressed during treatment. In this study, we found that a cut-off point of > 15/35 at the vegetative subscales at wk 4 resulted in a sensitivity of 95% at an acceptable positive predictive value of 44%.

This high sensitivity was found using a questionnaire of 7 items, part of the 20-item Zung scale. A similar sensitivity was found using the Minnesota Multiphasic Personality Inventory[21]. However, this rating scale includes 566 items and is more elaborate to perform in a routine outpatient clinic.

There was no relation between a higher score or a significant increase in the cognitive subscale at wk 4 and a higher risk of subsequent clinical depression. This is in agreement with the hypothesis formulated in reference[9].

Also, the Zung depression rating scale as a whole was not predictive for the development of depression in substance use patients, at least after exclusion of the patients that were already depressed at baseline. In other studies the baseline value was found to be predictive for patients with the Minnesota Multiphasic Personality Inventory[22], the Hamilton Depression Rating Scale score (HDRSS)[23] and the Centre for Epidemiological Studies-Depression Scale, CES-D[24] higher than a certain cut-off level[21,25,26]. However, in these studies people that were depressed at baseline were not always excluded[25,26].

In our study, an increased vegetative subscale score at 4 wk of treatment predicted diagnosis of major depression scattered over the weeks and months afterwards. This scatter is comparable to results found in other recent studies[4,7-10,25].

Although depressive symptomatology occurring in patients treated with interferon has usually been called 'depression' or 'major depressive episode', the more appropriate term according to new DSM-Ⅳ -TR should be 'substance induced mood disorder'. There are psychopathological (e.g., more irritability)[27], epidemiological (the gender difference in major depressive episode is different from the gender difference in interferon induced mood disorder)[28], genetic[29] and treatment (more patients than in major depressive episode respond well to SSRIs)[30] arguments to support this really to be a different disorder.

This study has some limitations. It was restricted to substance users with CHC infection and antiviral treatment. Therefore, it is not possible to extrapolate to other patient groups. However, from small studies there seems no difference in the development or the mechanism of depression in other patient groups[9,30]. Secondly, although larger than previous studies[9] our sample size is still relatively low resulting in large confidence intervals.

In conclusion, the development of depression can reliably be predicted at wk 4 after start of interferon treatment by an increase in vegetative symptoms of depression (subscale score) to at least 15/35. This results in a prediction with a sensitivity of 95%, at the price of 56% false-positive test results, which for a screening test is considered to be acceptable. Treatment with antidepressants may cure or prevent depression and so increase the treatment adherence. This may improve the SVR in patients evolving to depression and make the SVR comparable to SVR in non-depressed patients. To formally prove this, however, it should be the subject of another study.

COMMENTS

Background

Interferon derived treatment will remain the cornerstone for antiviral therapy in chronic hepatitis C patients in the near future. Interferon induced depression is a frequent side effect that may influence the outcome of the treatment. Since interferon-induced depression is unusually responsive to antidepressant treatment, it is important to detect the patients who are at risk for depression and who can benefit from antidepressive treatment.

Research frontiers

At this moment very few tools have been extensively studied to detect the patients at risk of depression during treatment with interferon. The Minnesota Multiphasic Personality Inventory is thoroughly studied but questioning 566 items makes it very elaborate to perform in a routine outpatient clinic.

Innovations and breakthroughs

Using only seven questions at week four of treatment from the vegetative-depressive symptoms of the Zung scale, it is possible to predict 95% of all emerging depressions, at a price of 56% false positive test results.

Applications

Treatment with antidepressants may cure or prevent depression and so increase the treatment adherence. This may improve the SVR in patients evolving to depression and make the SVR comparable to SVR in non-depressed patients. To formally prove the hypothesis that antidepressants may improve SVR in patients at risk for depression, should be the subject of further studies.

Peer review

Dr. Robaeys and co-workers-including the BASL Steering Committee and the Belgian Study Group: M Adler in Erasme University Hospital, Brussels; B Bastens in St Joseph Hospital, Liège; N Bourgeois, S Bourgeois in Ziekenhuis Netwerk Antwerpen (Stuivenberg), Antwerpen; R Brenard in St Joseph Hospital, Gilly; C Brixko in Hôpital de la Citadelle, Liège; Ph Caenepeel in Ziekenhuis Oost-Limburg, Genk; B Caucheteur in University Hospital St Pierre, Brussels; I Colle in University Hospital, Gent; C de Galocsy in Bracops Hospital, Brussels; J Delwaide in CHU Univertity of Liege, Liege; S Francque University Hospital Antwerpen, Antwerpen; J Henrion in Hôpital de Jolimont, Haine-Saint-Paul; J Holvoet in Ziekenhuis Netwerk Antwerpen (Middelheim), Antwerpen; Y Horsmans in Cliniques universitaires St-Luc UCL, Brussels; Ph Langlet in Clinique Edith Cavell, Brussels; P Laukens in St Jansziekenhuis, Brugge; V Lefebvre in CHR de Namur, Namur; H Louis1, P Michielsen10, JP Mulkay7, F Nevens in UZ Gasthuisberg KUL, Leuven; C Preux in Centre Hospitalier de Tivoli, La Louvière; G Robaeys6, H Van Vlierberghe8,

Ph Warzée in Reine Fabiola Hospital, Montignies sur Sambre - have presented a clinical study in which they aimed to show the predictive value of vegetative-depressive symptoms according to the Zung depression rating for subsequent clinical depression of HCV infected patients during antiviral treatment with interferon and Ribavirin after 4 wk of treatment. The manuscript is well written and presents a very interesting clinical study showing convincing data.

REFERENCES

1 **Robaeys G**, Buntinx F, Bottieau E, Bourgeois S, Brenard R, Colle I, De Bie J, Matheï C, Mulkay JP, Van Damme P, Van Ranst M, Verrando R, Michielsen P, Bourgeois N, Brenard R, de Galocsy Ch, Delwaide J, Henrion J, Horsmans Y, Michielsen P, Reynaert H, Robaeys G, Sprengers D. Guidelines for the management of chronic hepatitis C in patients infected after substance use. *Acta Gastroenterol Belg* 2005; **68**: 38-45

2 **Sylvestre D**. Hepatitis C treatment in drug users: perception versus evidence. *Eur J Gastroenterol Hepatol* 2006; **18**: 129-130

3 **Robaeys G**, Van Vlierberghe H, Matheï C, Van Ranst M, Bruckers L, Buntinx F. Similar compliance and effect of treatment in chronic hepatitis C resulting from intravenous drug use in comparison with other infection causes. *Eur J Gastroenterol Hepatol* 2006; **18**: 159-166

4 **Horikawa N**, Yamazaki T, Izumi N, Uchihara M. Incidence and clinical course of major depression in patients with chronic hepatitis type C undergoing interferon-alpha therapy: a prospective study. *Gen Hosp Psychiatry* 2003; **25**: 34-38

5 **Miyaoka H**, Otsubo T, Kamijima K, Ishii M, Onuki M, Mitamura K. Depression from interferon therapy in patients with hepatitis C. *Am J Psychiatry* 1999; **156**: 1120

6 **Edlin BR**, Seal KH, Lorvick J, Kral AH, Ciccarone DH, Moore LD, Lo B. Is it justifiable to withhold treatment for hepatitis C from illicit-drug users? *N Engl J Med* 2001; **345**: 211-215

7 **Dieperink E**, Ho SB, Thuras P, Willenbring ML. A prospective study of neuropsychiatric symptoms associated with interferon-alpha-2b and ribavirin therapy for patients with chronic hepatitis C. *Psychosomatics* 2003; **44**: 104-112

8 **Hauser P**, Khosla J, Aurora H, Laurin J, Kling MA, Hill J, Gulati M, Thornton AJ, Schultz RL, Valentine AD, Meyers CA, Howell CD. A prospective study of the incidence and open-label treatment of interferon-induced major depressive disorder in patients with hepatitis C. *Mol Psychiatry* 2002; **7**: 942-947

9 **Wichers MC**, Koek GH, Robaeys G, Praamstra AJ, Maes M. Early increase in vegetative symptoms predicts IFN-alpha-induced cognitive-depressive changes. *Psychol Med* 2005; **35**: 433-441

10 **Capuron L**, Gumnick JF, Musselman DL, Lawson DH, Reemsnyder A, Nemeroff CB, Miller AH. Neurobehavioral effects of interferon-alpha in cancer patients: phenomenology and paroxetine responsiveness of symptom dimensions. *Neuropsychopharmacology* 2002; **26**: 643-652

11 **Dalakas MC**, Mock V, Hawkins MJ. Fatigue: definitions, mechanisms, and paradigms for study. *Semin Oncol* 1998; **25**: 48-53

12 **Dusheiko G**. Side effects of alpha interferon in chronic hepatitis C. *Hepatology* 1997; **26**: 112S-121S

13 **Licinio J**, Kling MA, Hauser P. Cytokines and brain function: relevance to interferon-alpha-induced mood and cognitive changes. *Semin Oncol* 1998; **25**: 30-38

14 **Schaefer M**, Schmidt F, Folwaczny C, Lorenz R, Martin G, Schindlbeck N, Heldwein W, Soyka M, Grunze H, Koenig A, Loeschke K. Adherence and mental side effects during hepatitis C treatment with interferon alfa and ribavirin in psychiatric risk groups. *Hepatology* 2003; **37**: 443-451

15 **Kraus MR**, Schäfer A, Faller H, Csef H, Scheurlen M. Paroxetine for the treatment of interferon-alpha-induced depression in chronic hepatitis C. *Aliment Pharmacol Ther* 2002; **16**: 1091-1099

16 **Asnis GM**, De La Garza R. Interferon-induced depression in chronic hepatitis C: a review of its prevalence, risk factors, biology, and treatment approaches. *J Clin Gastroenterol* 2006; **40**: 322-335

17 **De Bie J**, Robaeys G, Buntinx F. Hepatitis C, interferon alpha and psychiatric co-morbidity in intravenous drug users (IVDU): guidelines for clinical practice. *Acta Gastroenterol Belg* 2005; **68**: 68-80

18 **Zung WW**. A self-rating depression scale. *Arch Gen Psychiatry* 1965; **12**: 63-70

19 **Miura H**, Kitagami T, Ohta T. Application of the Zung self-rating depression scale to patients before and after introduction to haemodialysis. *Psychiatry Clin Neurosci* 1999; **53**: 381-385

20 **American Psychiatric Association**. Diagnostic and statistical manual of mental disorders. 4th ed. Washington DC, USA: Swets & Zeitlinger BV, 1994: 210-216

21 **Scalori A**, Pozzi M, Bellia V, Apale P, Santamaria G, Bordoni T, Redaelli A, Avolio A, Parravicini P, Pioltelli P, Roffi L. Interferon-induced depression: prevalence and management. *Dig Liver Dis* 2005; **37**: 102-107

22 **Mosticoni R**, Chiari G. Una descrizione obiettiva della personalit`a. Il Minnesota Multphasic Personality Inventory (MMPI). Firenze, Italy: Organizzazioni Speciali. Rot Off Set, 1993: 15–28

23 **Hamilton M**. Development of a rating scale for primary depressive illness. *Br J Soc Clin Psychol* 1967; **6**: 278-296

24 **Bono C**, Ried LD, Kimberlin C, Vogel B. Missing data on the Center for Epidemiologic Studies Depression Scale: a comparison of 4 imputation techniques. *Res Social Adm Pharm* 2007; **3**: 1-27

25 **Beratis S**, Katrivanou A, Georgiou S, Monastirli A, Pasmatzi E, Gourzis P, Tsambaos D. Major depression and risk of depressive symptomatology associated with short-term and low-dose interferon-alpha treatment. *J Psychosom Res* 2005; **58**: 15-18

26 **Guadagnino V**, Trotta MP, Carioti J, Caroleo B, Antinori A. Does depression symptomatology affect medication compliance during the first weeks of anti-HCV therapy in intravenous drug users? *Dig Liver Dis* 2006; **38**: 119-124

27 **Constant A**, Castera L, Dantzer R, Couzigou P, de Ledinghen V, Demotes-Mainard J, Henry C. Mood alterations during interferon-alfa therapy in patients with chronic hepatitis C: evidence for an overlap between manic/hypomanic and depressive symptoms. *J Clin Psychiatry* 2005; **66**: 1050-1057

28 **Kessler RC**, McGonagle KA, Swartz M, Blazer DG, Nelson CB. Sex and depression in the National Comorbidity Survey. I: Lifetime prevalence, chronicity and recurrence. *J Affect Disord* 1993; **29**: 85-96

29 **Rifai MA**. Implementing genomic research in Psychosomatic Medicine, studying vulnerability to depression in patients with hepatitis C receiving interferon-alpha and ribavirin. *Psychosomatics* 2007; **48**: 107-110

30 **Kraus MR**, Schäfer A, Csef H, Scheurlen M. Psychiatric side effects of pegylated interferon alfa-2b as compared to conventional interferon alfa-2b in patients with chronic hepatitis C. *World J Gastroenterol* 2005; **11**: 1769-1774

S- Editor Zhu LH **L- Editor** Rippe RA **E- Editor** Lu W

Online Submissions: wjg.wjgnet.com
www.wjgnet.com
wjg@wjgnet.com

World J Gastroenterol 2007 November 21; 13(43): 5741-5744
World Journal of Gastroenterology ISSN 1007-9327

RAPID COMMUNICATION

Acute pancreatitis in acute viral hepatitis

Pankaj Jain, Sandeep Nijhawan, Ramesh Roop Rai, Subhash Nepalia, Amit Mathur

Pankaj Jain, Sandeep Nijhawan, Ramesh Roop Rai, Subhash Nepalia, Amit Mathur, Department of Gastroenterology, SMS Medical College, Jaipur, Rajasthan, India
Correspondence to: Sandeep Nijhawan, Professor, Department of Gastroenterology, SMS Medical College, Jaipur, Rajasthan, India. dr_nijhawan@yahoo.com
Telephone: +91-141-2722335 Fax: +91-141-2560994
Received: May 10, 2007 Revised: September 6, 2007

Abstract

AIM: To elucidate the frequency and characteristics of pancreatic involvement in the course of acute (nonfulminant) viral hepatitis.

METHODS: We prospectively assessed the pancreatic involvement in patients with acute viral hepatitis who presented with severe abdominal pain.

RESULTS: We studied 124 patients with acute viral hepatitis, of whom 24 presented with severe abdominal pain. Seven patients (5.65%) were diagnosed to have acute pancreatitis. All were young males. Five patients had pancreatitis in the first week and two in the fourth week after the onset of jaundice. The pancreatitis was mild and all had uneventful recovery from both pancreatitis and hepatitis on conservative treatment. The etiology of pancreatitis was hepatitis E virus in 4, hepatitis A virus in 2, and hepatitis B virus in 1 patient. One patient had biliary sludge along with HEV infection. The abdominal pain of remaining seventeen patients was attributed to stretching of Glisson's capsule.

CONCLUSION: Acute pancreatitis occurs in 5.65% of patients with acute viral hepatitis, it is mild and recovers with conservative management.

Key words: Acute hepatitis; Pancreatitis; Viruses; Pain; Abdomen

Jain P, Nijhawan S, Rai RR, Nepalia S, Mathur A. Acute pancreatitis in acute viral hepatitis. *World J Gastroenterol* 2007; 13(43): 5741-5744

http://www.wjgnet.com/1007-9327/13/5741.asp

INTRODUCTION

Although hepatitis viruses have a strong tropism for hepatocytes, viral antigens have also been detected in other tissues such as the pancreas and gallbladder[1,2]. Several viral infections have been implicated as an aetiological factor of acute pancreatitis. The viruses most frequently responsible are mumps virus, Coxsackie B virus, Epstein-Barr virus and measles virus[3-6].

Acute pancreatitis is not uncommon in fulminant hepatic failure (FHF) and has been confirmed based on histology or serology[7-9]. Acute pancreatitis has been reported very rarely in acute (nonfulminant) viral hepatitis. It has been reported with hepatitis A (HAV), hepatitis B (HBV) and non-A-non-B (blood-borne) and hepatitis E virus (HEV) infection[10-20].

The aim of this study was to determine the frequency and characteristics of pancreatic involvement in the course of acute viral hepatitis.

MATERIALS AND METHODS

Materials

Patients seen at the gastroenterology clinic and ward of SMS hospital, Jaipur between January 2004 and December 2006 were included in this prospective study. Acute viral hepatitis was defined as patients with prodromal symptoms, deep jaundice, markedly raised transaminases, presence of markers of hepatitis B (positive for HBsAg, IgM anti-HBc, HBeAg, but negative for anti-HBe), hepatitis A (IgM anti-HAV), hepatitis C (anti-HCV), hepatitis E (IgM-anti-HEV) viruses in serum and ultrasound abdomen showing thick walled gallbladder and hypoechoic liver. Patients with other causes of acute hepatitis, chronic liver disease, history of alcohol intake and fulminant hepatic failure were excluded from the study.

The diagnosis of acute pancreatitis was based on pancreatic type abdominal pain, raised amylase and lipase levels to three times the upper limit of normal and ultrasound (US) or contrast enhanced computed tomography (CECT) of abdomen suggestive of acute pancreatitis.

Methods

The acute viral hepatitis group underwent hemogram, serum bilirubin, serum aspartate aminotransferase (AST), serum alanine aminotransferase (ALT), serum alkaline phosphatase, prothrombin time, HBsAg, IgM anti-HBc, HBe Ag, anti-HBe, IgM anti-HAV, anti-HCV, IgM anti-HEV and ultrasound abdomen. Serum amylase and lipase, US of the abdomen and/or CECT were done in patients who had severe abdominal pain. Informed consent was obtained from each patient.

Table 1 Clinical and laboratory characteristics of 124 patients of acute viral hepatitis

	Acute viral hepatitis A (n = 16)	Acute viral hepatitis B (n = 54)	Acute viral hepatitis E (n = 54)
Male: Female	13:3	42:12	39:15
Age (yr)[1]	18.3 (8-35)	36 (20-74)	33.6 (17-62)
Clinical features			
Jaundice	15 (93.8)	54 (100)	54 (100)
Prodromal symptoms	16 (100)	54 (100)	54 (100)
Pain abdomen	4 (25)	8 (14.8)	12 (22.2)
Pruritis	4 (25)	9 (16.6)	19 (35.2)
Hepatomegaly (%)	6 (37.5)	16 (29.6)	21 (38.9)
Splenomegaly (%)	2 (12.5)	6 (11.1)	5 (9.2)
Hemoglobin (gm/dL)[1]	12.3 (9.6-14.5)	12.4 (9-15.1)	12.6 (9-14.7)
Platelets ($\times 10^5/mm^3$)[1]	2.5 (1.8-3.2)	1.8 (1.2-2.5)	1.6 (1-3.4)
Total leucocyte count ($\times 1000/mm^3$)[1]	7.9 (6.4-10.5)	8.4 (5-10.1)	7.2 (6-10.6)
Bilirubin (mg/dL)[1]	9.4 (0.67-35.8)	12.4 (3-36.5)	10.7 (3.3-26.3)
AST (IU/L)[1]	1969 (60-7715)	824 (223-3600)	1621.1 (240-3684)
ALT (IU/L)[1]	2134.3 (56-5165)	1024 (489-4900)	1830.6 (240-5549)
Serum alkaline phosphatase (IU/L)[1]	521.9 (196-1426)	424.5 (110-860)	324 (114-647)
Protein/Albumin (gm/dL)[1]	7.2 (6.5-7.8)/4.0 (3.5-4.6)	7 (6-8)/3.9 (3.4-4.8)	6.5 (5.5-8)/3.8 (3.4-4.6)
Prothrombin time prolongation[1]	4 (2-14)	5.5 (1-11)	6 (3-18)
Ultrasonography of the abdomen			
Thickened gallbladder	14 (87.5)	38 (70.4)	44 (81.5)
Hypoechoic liver	8 (50)	24 (44.6)	26 (48.1)
Gallbladder sludge	2 (12.5)	2 (3.7)	3 (5.5)
Ascites	1 (6.25)	3 (5.5)	26 (48.1)
Bulky pancreas	2 (12.5)	1 (1.8)	4 (7.4)

[1]Mean (range).

RESULTS

We had 124 patients with acute viral hepatitis over the three-year period, consisting of 94 males and 30 females, with a mean age of 32.7 years (range 8-65). The viral serology assays showed HBsAg and IgM-anti-HBc in 54 patients, IgM anti-HEV in 54 and IgM anti-HAV in 16 (Table 1). Twenty-four patients (19.4%) presented with history of severe abdominal pain, and 7 of these (29.2%) had evidence of acute pancreatitis. So, 5.65% of patients with acute viral hepatitis presented with acute pancreatitis. In the remaining 17 patients, the amylase and lipase were less than three times the upper limit of the normal. They did not have evidence of acute (calculous or acalculous) cholecystitis. We attributed the abdominal pain to stretching of the Glisson's capsule.

The clinical, laboratory and radiological profile of the patients with acute pancreatitis is given in Tables 2 and 3. The mean age was 23.9 (range 11-32) years, all were males. Abdominal pain occurred 2-30 (mean 12) days after the onset of jaundice. The duration of abdominal pain ranged from 24 to 120 h. None of the patients had a past history of jaundice, abdominal pain, alcoholism, trauma, hyperparathyroidism or drug intake. All patients had jaundice at presentation, mild hepatomegaly and epigastric tenderness. Three patients also had features of ileus.

On investigation, mean bilirubin was 16.4 mg/dL (range 5.8-32.4 mg/dL), mean AST 519 (range 182-1313) U/L and mean ALT 1371.1 (range 702-2438) U/L. Amylase and lipase ranged from 275-596 (mean 364.6) U/L and 520-7258 (mean 2495.4) U/L respectively. Serum lipid profile and calcium levels were normal in all patients. IgM anti-HEV, IgM anti-HAV, IgM anti-HBc were positive in 4, 2 and 1 patient respectively. US could detect pancreatitis in three patients, minimal ascites and biliary sludge in one patient. An abdominal CECT showed edematous and enlarged pancreas in all patients. There was no evidence of necrosis. The patient with sludge showed complete resolution in 2 wk. None of the other patients had evidence of biliary sludge during follow-up. The pancreatitis and hepatitis responded to conservative treatment in all patients. All patients are asymptomatic after a mean follow-up of 12 (range 8-24) mo.

DISCUSSION

Most cases of acute pancreatitis due to hepatitis viruses had been reported in association with acute liver failure (ALF). In the autopsy series of Ham and Fitzpatrick, 14 of the 42 (33%) patients with ALF had acute pancreatitis[8], the majority being of viral etiology. Similar findings had been reported by Parbhoo *et al*[9] in 21 out of 59 patients (36%) with ALF who had acute pancreatitis. Autopsy findings of pancreatitis in seven of 16 (44%) patients with fulminant viral hepatitis, versus two of 33 (6%) patients with fulminant hepatic failure secondary to halothane, support the role of viral infection rather than liver failure per se in causing pancreatitis[21].

There are only a few case reports of symptomatic pancreatitis occurring in the setting of acute viral hepatitis[10]. Most of the patients reported had presented with symptomatic pancreatitis in the early phase of the hepatitic illness[11-20] whereas Mishra *et al*[10] reported 6 patients at wk 2 or 3 after the onset of jaundice. Our series had five patients presenting in the first week and two in the fourth week after the onset of jaundice. One patient had biliary sludge and presented in the first week of jaundice. Ultrasound was done weekly in all the patients until clinical and biochemical resolution. Gallbladder wall thickness

Table 2 Clinical Profile of viral hepatitis patients with acute pancreatitis

	Case 1	Case 2	Case 3	Case 4	Case 5	Case 6	Case 7
Age (yr)	11	30	32	21	30	20	23
Gender	M	M	M	M	M	M	M
Pain interval after onset of jaundice (d)	30	28	3	2	5	6	5
Pain duration (h)	96	72	120	96	24	48	72
Hepatomegaly (cm; subcostal)	5	2	2	3	3	2	3
Etiology	Hepatitis A	Hepatitis B	Hepatitis E	Hepatitis E	Hepatitis E	Hepatitis A	Hepatitis E
Recovery from pancreatitis (d)	8	6	12	6	3	6	4
Recovery from hepatitis (wk)	8	6	12	8	8	12	10

Table 3 Laboratory profile of viral hepatitis patients with acute pancreatitis

Parameter	Case 1	Case 2	Case 3	Case 4	Case 5	Case 6	Case 7
Bilirubin (mg/dL)	32.4	21.3	14.6	11.8	5.8	13.1	15.8
AST (IU /L)	682	1210	1313	182	388	1223	765
ALT (IU/L)	895	702	2238	702	412	2438	814
Alkaline phosphates (IU/L)	560	300	607	420	531	503	231
Albumin (mg/dL)	3.8	4	3.5	3.8	3.5	3.9	3.5
Prothrombin time prolongation (s)	14	11	12	9	11	10	18
Amylase (IU/L)	475	460	275	278	462	319	596
Lipase (IU/L)	7258	520	3297	990	760	2926	2060
Corrected Serum calcium (mg/dL)	9.2	9.1	9	8.9	9.2	9.3	8.1
Serum triglyceride (mg/dL)	140	168	131	165	141	160	154
Ultrasonography (Gallbladder)	Normal	Normal	Normal	Normal	Normal	Normal	Biliary sludge

(more than 3 mm) was found in 96.8% of patients, which is in agreement with a previous study by Sharma *et al*[22]. None of the two patients who presented later had any evidence of biliary sludge on US.

The etiology of pancreatitis was considered to be due to a hepatitis virus in all patients, as there was no evidence of gallstones, sludge, alcohol, drugs, trauma or metabolic causes. The remaining patient had biliary sludge on US. The disappearance of biliary sludge at 2 wk occurred a week later than previously reported[23]. None of the 7 patients with biliary sludge had an episode of acute pancreatitis and gallbladder contraction was similar in the hepatitis and control group in the Portincasa *et al*[23] group. So, the patient might had HEV-associated pancreatitis and had biliary sludge during the acute phase of the viral illness which resolved on follow-up ultrasound abdomen. Basaranoglu *et al*[24] reported a case of gallbladder sludge and acute pancreatitis induced by acute hepatitis A.

Acute pancreatitis in nonfulminant acute viral hepatitis covers the full range of clinical severity. Subclinical pancreatic involvement in viral hepatitis may occur more commonly than is appreciated[25]. The pancreatitis was mild as reported previously[10,13-20]. One of our patients had minimal ascites which resolved in 2 wk. There were no local or systemic complications and all had uneventful recovery from both pancreatitis and hepatitis. No relation was found between the level of amylase and severity of pancreatitis.

The frequency of acute pancreatitis in acute viral hepatitis in the present series is 5.65%, which is 2% higher than reported by Joshi *et al*[26] in their autopsy series of 108 cases. Joske *et al*[27] noted 8 cases of acute viral hepatitis out of 90 patients of acute pancreatitis.

The mechanism of pancreatitis in patients with acute viral hepatitis (nonfulminant) is unknown, and it may be multifactorial. One proposed pathogenesis of pancreatitis associated with hepatitis is the development of edema of the ampulla of Vater with obstruction to the outflow of pancreatic fluid[28]. There is no direct evidence for the routes by which hepatitis viruses reach the pancreas; however, the proposed routes are most likely blood or bile[14].

A more plausible mechanism for viral associated acute pancreatitis is direct inflammation and destruction of pancreatic acinar cell by the virus. This latter theory is supported by the autopsy finding of hepatitis B virus antigens within the cytoplasm of pancreatic acinar cells of patients with hepatitis B surface antigenemia[1,2]. It is possible that the severity of pancreatitis is related to the magnitude of exposure of pancreatic acinar cells to the hepatitis virus[2].

The hepatitis viruses might injure the pancreatic acinar cell membrane, resulting in the leakage of intracellular enzymes, and/or precipitate a network of intracellular events culminating in cell death by a mechanism analogous to hepatocyte necrosis[29]. Another mechanism can be the release and circulation of lysosomal enzymes from the inflamed liver with the activation of trypsinogen to trypsin.

When acute pancreatitis is associated with fulminant hepatitis, the virus may cause tissue damage directly, but there are several other factors which can play an important role in the development of pancreatitis (clinical or silent) and these include acute liver failure, hypotension, infections and drug induced damage[13]. Intrapancreatic

hemorrhage due to hypoprothrombinemia or disseminated intravascular coagulation may result in pancreatic damage and subsequent pancreatitis[8].

In conclusion, acute pancreatitis is not uncommon. In a patient with acute viral hepatitis and acute or disproportionate abdominal pain, acute pancreatitis should be kept as a possibility. Conservative treatment leads to recovery in all the patients.

COMMENTS

Background

The association of hepatitis viruses with acute pancreatitis in the setting of acute (nonfulminant) viral hepatitis is rare. The frequency and characteristics of pancreatic involvement in the course of acute viral hepatitis needs to be elucidated.

Research frontiers

Studies with larger number of patients of acute viral hepatitis with pain abdomen are necessary to determine the frequency and characteristics of pancreatitis as there are only case reports and one case series of six patients.

Innovations and breakthrough

Recent reports describe acute pancreatitis as a cause of acute or dispropionate abdominal pain complicating acute viral hepatitis.

Applications

Patients of acute viral hepatitis with severe pain abdomen should undergo serum amylase, lipase and ultrasonography or contrast-enhanced computed tomography of the abdomen to prove acute pancreatitis as a cause of abdominal pain. The prognosis of patients with acute pancreatitis in the setting of acute viral hepatitis is good and patients recover on conservative treatment.

Terminology

Acute viral hepatitis is defined as presence of prodromal symptoms, deep jaundice, markedly raised transaminases, presence of markers of hepatitis B (positive for HBsAg, IgM anti-HBc, HBeAg, but negative for anti-HBe), hepatitis A (IgM anti-HAV), hepatitis C (anti-HCV), hepatitis E (IgM-anti-HEV) viruses in serum and ultrasound abdomen showing thick walled gallbladder and hypoechoic liver . Patients with other causes of acute hepatitis, chronic liver disease, history of alcohol intake and fulminant hepatic failure were excluded from the study. The diagnosis of acute pancreatitis was based on pancreatic type abdominal pain, raised amylase and lipase levels to three times upper limit of the normal and ultrasound (US) or contrast enhanced computed tomography (CECT) of the abdomen suggestive of acute pancreatitis.

Peer review

This article describes the clinical findings of acute pancreatitis in acute viral hepatitis. The main content of the manuscript is good.

REFERENCES

1 **Hoefs JC**, Renner IG, Askhcavai M, Redeker AG. Hepatitis B surface antigen in pancreatic and biliary secretions. *Gastroenterology* 1980; **79**: 191-194
2 **Shimoda T**, Shikata T, Karasawa T, Tsukagoshi S, Yoshimura M, Sakurai I. Light microscopic localization of hepatitis B virus antigens in the human pancreas. Possibility of multiplication of hepatitis B virus in the human pancreas. *Gastroenterology* 1981; **81**: 998-1005
3 **Parenti DM**, Steinberg W, Kang P. Infectious causes of acute pancreatitis. *Pancreas* 1996; **13**: 356-371
4 **Wislocki LC**. Acute pancreatitis in infectious mononucleosis. *N Engl J Med* 1966; **275**: 322-323
5 **Ursing B**. Acute pancreatitis in coxsackie B infection. *Br Med J* 1973; **3**: 524-525
6 **Naficy K**, Nategh R, Ghadimi H. Mumps pancreatitis without parotitis. *Br Med J* 1973; **1**: 529
7 **Ede RJ**, Moore KP, Marshall WJ, Williams R. Frequency of pancreatitis in fulminant hepatic failure using isoenzyme markers. *Gut* 1988; **29**: 778-781
8 **Ham JM**, Fitzpatrick P. Acute pancreatitis in patients with acute hepatic failure. *Am J Dig Dis* 1973; **18**: 1079-1083
9 **Parbhoo SP**, Welch J, Sherlock S. Acute pancreatitis in patients with fulminant hepatic failure. *Gut* 1973; **14**: 428
10 **Mishra A**, Saigal S, Gupta R, Sarin SK. Acute pancreatitis associated with viral hepatitis: a report of six cases with review of literature. *Am J Gastroenterol* 1999; **94**: 2292-2295
11 **Maity SG**, Ray G. Severe acute pancreatitis in acute hepatitis E. *Indian J Gastroenterol* 2002; **21**: 37-38
12 **Batra Y**, Chakravarty S, Bhatt G. Severe acute pancreatitis associated with acute hepatitis A: a case report. *Trop Gastroenterol* 2003; **24**: 27-28
13 **Lopez Morante A**, Rodriguez de Lope C, San Miguel G, Pons Romero F. Acute pancreatitis in hepatitis A infection. *Postgrad Med J* 1986; **62**: 407-408
14 **Davis TV**, Keeffe EB. Acute pancreatitis associated with acute hepatitis A. *Am J Gastroenterol* 1992; **87**: 1648-1650
15 **Amarapurkar DN**, Begani MM, Mirchandani K. Acute pancreatitis in hepatitis A infection. *Trop Gastroenterol* 1996; **17**: 30-31
16 **Eugene C**, Cadranel JF, Bergue A, Anciaux ML. Acute pancreatitis associated with non-A-non-B hepatitis. Report of a case. *J Clin Gastroenterol* 1990; **12**: 195-197
17 **de Oliveira LC**, Rezende PB, Ferreira AL, de Freitas AA, de Carvalho AM, Guedes CA, Costa WO. Concurrent acute hepatitis and pancreatitis associated with hepatitis B virus: case report. *Pancreas* 1998; **16**: 559-561
18 **Jaroszewicz J**, Flisiak R, Kalinowska A, Wierzbicka I, Prokopowicz D. Acute hepatitis E complicated by acute pancreatitis: a case report and literature review. *Pancreas* 2005; **30**: 382-384
19 **Makharia GK**, Garg PK, Tandon RK. Acute pancreatitis associated with acute hepatitis E infection. *Trop Gastroenterol* 2003; **24**: 200-201
20 **Khanna S**, Vij JC. Severe acute pancreatitis due to hepatitis A virus infection in a patient of acute viral hepatitis. *Trop Gastroenterol* 2003; **24**: 25-26
21 **Geokas MC**, Olsen H, Swanson V, Rinderknecht H. The association of viral hepatitis and acute pancreatitis. *Calif Med* 1972; **117**: 1-7
22 **Sharma MP**, Dasarathy S. Gallbladder abnormalities in acute viral hepatitis: a prospective ultrasound evaluation. *J Clin Gastroenterol* 1991; **13**: 697-700
23 **Portincasa P**, Moschetta A, Di Ciaula A, Palmieri VO, Milella M, Pastore G, Palasciano G. Changes of gallbladder and gastric dynamics in patients with acute hepatitis A. *Eur J Clin Invest* 2001; **31**: 617-622
24 **Basaranoglu M**, Balci NC, Klör HU. Gallbladder sludge and acute pancreatitis induced by acute hepatitis A. *Pancreatology* 2006; **6**: 141-144
25 **Lechi A**, Montesi G, Solbiati M, Dattoli R, Rizzotti P, Zanchetta M, Perobelli L, Burlina A. Serum pancreatic enzyme alterations in acute viral hepatitis. *Hepatogastroenterology* 1983; **30**: 233-235
26 **Joshi RA**, Probstein JG, Blumenthal HT. A survey of experiences with three hundred clinical and one hundred and eight autopsy cases of acute pancreatitis. *Am Surg* 1957; **23**: 34-42
27 **Joske RA**. Aetiological factors in the pancreatitis syndrome. *Br Med J* 1955; **2**: 1477-1481
28 **Tsui CY**, Burch GE, Harb JM. Pancreatitis in mice infected with coxsackievirus B1. *Arch Pathol* 1972; **93**: 379-389
29 **Lever AM**. Mechanisms of virally induced liver damage. *J Hepatol* 1987; **4**: 399-403
30 **Lopez Morante A**, Rodriguez de Lope C, San Miguel G, Pons Romero F. Acute pancreatitis in hepatitis A infection. *Postgrad Med J* 1986; **62**: 407-408

S- Editor Zhu LH **L- Editor** Negro F **E- Editor** Lu W

Online Submissions: wjg.wjgnet.com
www.wjgnet.com
wjg@wjgnet.com

World J Gastroenterol 2007 November 21; 13(43): 5745-5749
World Journal of Gastroenterology ISSN 1007-9327

RAPID COMMUNICATION

Triple non-invasive diagnostic test for exclusion of common bile ducts stones before laparoscopic cholecystectomy

Bahram Pourseidi, Amir Khorram-Manesh

Bahram Pourseidi, Department of Surgery, Kerman University of Medical Science, Kerman, Iran
Amir Khorram-Manesh, Department of Surgery Kungälv and Sahlgrenska University Hospitals, Göteborg, Sweden
Correspondence to: Amir Khorram-Manesh, MD, PhD, Department of General & Orthopedic Surgery, Kungälv Hospital, S-442 83 KUNGÄLV,
Sweden. amir.khorram-manesh@surgery.gu.se
Telephone: +46-303-98008 Fax: +46-303-98326
Received: July 10, 2007 Revised: August 17, 2007

Abstract

AIM: To evaluate the impact of a preoperative "triple non-invasive diagnostic test" for diagnosis and/or exclusion of common bile duct stones.

METHODS: All patients with symptomatic gallstone disease, operated on by laparoscopic cholecystectomy from March 2004 to March 2006 were studied retrospectively. Two hundred patients were included and reviewed by using a triple diagnostic test including: patient's medical history, routine liver function tests and routine ultrasonography. All patients were followed up 2-24 mo after surgery to evaluate the impact of triple diagnostic test.

RESULTS: Twenty-five patients were identified to have common bile duct stones. Lack of history of stones, negative laboratory tests and normal ultrasonography alone was proven to exclude common bile duct stones in some patients. However, a combination of these three components (triple diagnostic), was proven to be the most statistically significant test to exclude common bile duct stones in patients with gallstone disease.

CONCLUSION: Using a combination of routinely used diagnostic components as triple diagnostic modality would increase the diagnostic accuracy of common bile duct stones preoperatively. This triple non-invasive test is recommended for excluding common bile duct stones and to identify patients in need for other investigations.

Key words: Common bile duct stones; Laparoscopic cholecystectomy; Triple non-invasive diagnostic test

Pourseidi B, Khorram-Manesh A. Triple non-invasive diagnostic test for exclusion of common bile ducts stones before laparoscopic cholecystectomy. *World J Gastroenterol* 2007; 13(43): 5745-5749

http://www.wjgnet.com/1007-9327/13/5745.asp

INTRODUCTION

Surgery is the treatment of choice in symptomatic gallstone disease and is also recommended in asymptomatic patients due to complications followed by stone release in common bile duct[1-5]. Coexisting common bile duct stones (CBDS) occur in 7%-20% of all patients undergoing cholecystectomy[2,3,6]. Although intraoperative cholangiography was routinely performed to diagnose CBDS during pre-laparoscopic era, its use in the laparoscopic era has been debated[7-10]. Consequently, other techniques for diagnosing CBDS have been introduced[6-8].

Preoperative liver function test (LFT) results might be diagnostic for CBDS, if abnormal. However, some patients might have normal LFT despite coexisting CBDS[5,7]. Ultrasonography is the major diagnostic modality to diagnose gallstones, but is less helpful for diagnosing CBDS[1-7]. Computed tomography is rarely useful for diagnosing gallstones[5,8]. Magnetic-resonance-cholangio-pancreatography (MRCP) has high specificity and sensitivity and accuracy similar to that of Endoscopic-Retrograde-Cholangio-Pancreatography (ERCP), but its accuracy decreases if gallstones are small (< 4 mm) or if they are located near Vater's papilla[2,5,8,11]. In addition, MRCP is not widely available and unlike ERCP does not allow endoscopic extraction of stones[5,8,12]. ERCP is the most common technique used for both diagnostic and treatment of CBDS. It is however, expensive, invasive, technically demanding and associated with small but significant morbidity[6,7,13].

Clinical history of jaundice, pancreatitis or cholangitis, abnormal LFT results and or dilated common bile duct have been traditionally used to select possible candidates for ERCP preoperatively[5], but to the best of our knowledge, the accuracy of these parameters together in diagnosing and/or excluding CBDS has never been evaluated[5,6,8]. The aim of this retrospective study was to assess the accuracy of these variables alone and in combination for diagnosing/excluding CBDS in a consecutive group of patients with symptomatic gallstones disease operated on by laparoscopic cholecystectomy.

MATERIALS AND METHODS

From March 2004 to March 2006, all consecutive patients with ultrasound verified gallstones, in whom laparoscopic cholecystectomy was indicated, were studied retrospectively. The study was approved by the Afzali Hospital's ethical committee.

All information was collected based on a questionnaire including three different components. Patient's data and medical history, age at operation, gender, history of jaundice (obstructive *vs* non-obstructive), cholangitis or pancreatitis (acute *vs* non-acute) were recorded. The results of ultrasonography, preoperative liver functions tests (LFT), serum-total bilirubin (S-Bil), alkaline phosphatase (S-ALP) and white blood cells counts (WBC) were obtained. The following cut-off values were considered abnormal: S-Bil $\geqslant$ 1.5 dL/L, S-ALP $\geqslant$ 400 Ul/L and WBC $\geqslant$ 10 000/mm^3. CBDS diagnosis was established by either demonstrating a stone in CBD or a wide CBD (diameter $\geqslant$ 10 mm). All patients were operated laparoscopically. No intraoperative cholangiography was performed. All included patients (n = 200) were followed up 2-24 mo postoperatively, by means of a questionnaire, completed by telephone interviews or clinical visit if needed.

Statistical analysis

The statistical analysis was performed using SPSS (version 11.0). The association between occurrence of CBDS and different variables was analyzed using Chi-square test. Sensitivity, specificity, positive and negative predictive values were calculated for all variables individually and in combination. Student t-test with separate variance estimates was performed to test the demographic differences. Fisher exact test and χ^2-test were performed to compare between patients with a different number of suggested variables. $P < 0.05$ was considered statistically significant. Any patient with incomplete medical file or test results or any unclear information was excluded.

RESULTS

Two hundred patients, 43 men (21.5%) and 157 women (78.5%) were consecutively included in this study. The mean age of patients at the time of operation was 56.6 $\pm$ 18.2 and 51.6 $\pm$ 16.5 years for men and women, respectively. The average length of hospital stay was 30 (range 24-72) h for the whole group of patients, with no statistically significant difference between men and women.

Eighteen patients (9%) were found to have CBDS intraoperatively and additional 7 patients were found to have CBDS during the follow-up. The total number of patients with CBDS in this series was 25 patients (12.5%). The review of patient's clinical history did not reveal any clinical evidence for CBDS (jaundice, cholangitis or pancreatitis) in the majority of patients (89.5%). In the remaining patients (10.5%), besides cholangitis, all other clinical variables were more common in men. In 16 out of 25 patients with CBDS (8 women and 8 men), obstructive jaundice was the most frequent variable in both genders (Table 1). The association between clinical evidence for CBDS and occurrence of CBDS was calculated (Table 2). Thirteen patients had one positive clinical variable and 8 patients had two positive clinical variables. Higher number of positive clinical variables was not statistically significant for diagnosing CBDS. CBDS was more common in men with clinical evidence of the disease. The difference between men and women in this aspect was statistically significant (Chi-square: 6.56, df: 2, $P < 0.05$) (Table 2).

Table 1 Frequency of clinical variables in 200 patients with gallstones n (%)

Variables	Total	Women	Men
Obstructive jaundice			
Yes	16 (8)	8 (5.1)	8 (18.6)
No	183 (92)	148 (94.9)	35 (81.4)
Total	199 (100)	156 (100)	43 (100)
History of jaundice			
Yes	5 (2.5)	3 (1.9)	2 (4.7)
No	192 (97.5)	151 (98.1)	41 (95.3)
Total	197 (100)	154 (100)	43 (100)
Cholangitis			
Yes	5 (2.5)	5 (3.2)	0
No	192 (97.5)	149 (96.8)	43 (100)
Total	197 (100)	154 (100)	43 (100)
Acute Pancreatitis			
Yes	1 (0.5)	0	1 (2.3)
No	196 (99.5)	154 (100)	42 (97.7)
Total	197 (100)	154 (100)	43 (100)
History of Pancreatitis			
Yes	2(1)	1 (0.6)	1 (2.3)
No	195(99)	153 (99.4)	42 (97.7)
Total	197(100)	154 (100)	43 (100)

Table 2 Association between the number of positive clinical variables and CBDS n (%)

Patients	Negative history	1 positive findings	2 positive findings	Total
Men	34 (79.1)	6 (14)	3 (7)	43 (100)
Women	145 (92.4)	7 (4.5)	5 (3.2)	157 (100)
Total	179 (89.5)	13 (6.5)	8 (4)	200 (100)

The majority of patients in this cohort had a normal ultrasonography (n = 175, 87.3%). However, in 25 patients with CBDS (12 women and 13 men), 8 patients had a stone in common bile duct, 12 had obstruction in common bile duct, one had both a stone and obstruction of common bile duct, 3 had a widened common bile duct (> 10 mm), and finally one patient had widening of an intrahepatic bile branch. Positive ultrasonographic findings indicating CBDS were more common in men [13 out of 43 men (30%) and 12 out of 157 women (7%)] (Table 3). The difference in ultrasonographic diagnosis between men and women was statistically significant (Chi-square 20.23, df: 5 and $P < 0.05$).

The abnormal S-Bil and S-ALP results in men and women with CBDS are shown in Table 4. The majority of patients had normal laboratory results (> 85%). In 13 men (30.2%) serum bilirubin concentration was higher than 1.5 dL/L [compared to 11 women (7%)] and in 14 men (32.6%) the concentration of alkaline phosphatase was higher than 400 Ul/L [compared to 16 women (10%)]. All

Table 3 The results of ultrasound investigations in 200 patients with gallstones (per gender) *n* (%)

Patients	Men	Women	Total
CBDS	5 (11.9)	3 (1.9)	8 (4.1)
CBD obstruction	6 (14.3)	6 (3.9)	12 (6.1)
CBDS and obstruction	1 (2.4)	0 (0)	1 (0.5)
CBD diameter > 10 mm	1 (2.4)	2 (1.3)	3 (1.5)
Dilated intrahepatic bile duct branches	0 (0)	1 (0.6)	1 (0.5)
Normal	30 (69)	145 (92.3)	175 (87.3)
Total	43 (100)	157 (100)	200 (100)

CBD: Common bile duct; CBDS: Common bile duct stones.

Table 4 Results of liver tests in patients with gallstones (per gender) *n* (%)

Gender	S-bilirubin ⩾ 1.5 dL/L			Alkaline phosphatase ⩾ 400 UL/L		
	Yes	No	Total	Yes	No	Total
Men	13 (30.2)	30 (69.8)	43 (100)	14 (32.6)	29 (67.4)	43 (100)
Women	11 (7)	146 (93)	157 (100)	16 (10.2)	141 (89.8)	157 (100)
Total	24 (12)	176 (88)	200 (100)	30 (15)	170 (85)	200 (100)

patients with S-Bil ⩾ 1.5 dL/L had CBDS. These changes were more common in men and the difference between men and women was statistically significant (Chi-square 17.24, df: 1 and $P < 0.05$).

The sensitivity, specificity, negative predictive value (NPV) and positive predictive value (PPV) of each variable of medical history, LFT results and ultrasonography alone or in different combination for diagnosis/exclusion of CBDS was evaluated statistically (Table 5). As a single diagnostic test, ultrasonography had higher sensitivity (64%), specificity (97.1%), negative and positive predictive values (95% and 76.2%, respectively) than medical history, S-Bil and S-ALP. As a triple diagnostic modality, a combination of medical history, ultrasonographic findings and LFT results was proven to be the best diagnostic modality to exclude CBDS. White blood cells count had no impact in diagnosis of CBDS.

DISCUSSION

Although the majority of patients with gallstone disease have an uncomplicated surgical course, a few may become complicated due to occurrence of CBDS[1-3]. Due to fewer intraoperative cholangiographies during laparoscopic cholecystectomies[6,7], ERCP has been recommended for pre- or postoperative extraction of CBDS. It is however, an invasive investigation with high risk for complications and should be reserved for selected cases[12,14,15]. MRCP is not available in all institutions and its accuracy depends on the size and position of CBDS[4,11,12]. There is thus a need for easy-performing, non-invasive, and reliable test modalities to diagnose or exclude CBDS, by which selected patients can benefit from ERCP, MRCP or other expensive investigations[13-15]. Earlier studies on some clinical, laboratory or radiological variables have been performed[16,17]. There is however, as far as we know, no study performed evaluating a combination of these investigating modalities. The majority of patients with gallstones are routinely evaluated by their clinical history, ultrasonography and LFT (S-Bil and S-ALP)[3,5]. The main object of this study was to evaluate the efficacy of these non-invasive investigation methods for exclusion of CBDS diagnosis.

Table 5 Diagnostic value of each of the triple tests, alone and in combination *n* (%)

Variables	Sensitivity	Specificity	NPV	PPV
1. Medical history	44	92.5	90.5	38.1
2. Ultrasound	64	97.1	95	76.2
3. Alkaline phosphatase ⩾ 400 Ul/L	32	95	90	26.7
4. Serum bilirubin ⩾ 1.5 dL/L	30.3	76.2	89.2	25
2 + 3 + 4	80	82.9	96.7	40
2 + 3 or 2 + 4	32	97.1	90.9	61.5
2 + 1+ 3 or 4	84	81.7	97.3	39.6

NPV: Negative predictive value; PPV: Positive predictive value.

The importance of careful review of patient's history has been reported in many earlier studies. A focused positive patient's history may be an early indication of CBDS[3,6,16-18]. Hyperbilirubinemia preoperatively, had a high diagnostic significant in our study and is also reported by others[7,19]. Ultrasonographic investigation is a reliable diagnostic modality with high availability and lower cost. However, the result of the investigation depends highly on investigators experience[3,14,20]. In our study, ultrasonography was performed by one radiologist and our results are comparable with earlier reports[3,6]. As also earlier reported by others, our study indicates that in patients who lacked clinical, radiological and laboratory signs of CBDS, there is no need for performing ERCP[6,14,21-25]. It also indicates that by using patient's complete medical history (with special focus on the most common clinical complication of gallstone diseases such as pancreatitis), customary laboratory tests such as S-Bil and S-ALP and ultrasonography one may exclude CBDS diagnosis with high accuracy[26-29].

We used different variables as predictors *i.e.,* these variables were used to predict or explain the value(s) of one or more dependent variables (also referred to as dependent or outcome variables statistically). The positive predictive value (PPV), or precision rate, is defined as the proportion of patients with positive test results who are correctly diagnosed. Hence the PPV is used to indicate the probability that, in case of a positive test, the patient really has the specified disease. However there may be more than one cause for a disease and any single potential cause may not always result in the overt disease seen in a patient. In our study only ultrasonographic investigation has highest PPV followed by a combination of ultrasound investigation and LFT results. Since we were interested in evaluating the impact and usefulness of the negative ultrasonography or LFT results and the lack of clinical evidence (negative history of pancreatitis, cholecystitis and cholangitis) of CBDS, in our study, we used the negative predictive value (NPV), which is the proportion of patients with negative test results who are correctly

diagnosed. Higher NPV means then higher sensitivity for excluding CBDS as shown in our study; combining several tests in our study increased the negative predictive value and sensitivity of CBDS exclusion with almost equal specificity[16-18,30].

We concluded that patients with normal ultrasonography, LFT results and no clinical evidence of CBDS "negative triple test" (NPV of 97.3%) may undergo laparoscopic surgery without any need for preoperative MRCP or ERCP. The availability and non-invasiveness of this triple diagnostic test are additional benefits, which makes it more interesting.

COMMENTS

Background

Coexisting common bile duct stones (CBDS) may complicate the course of gallstone disease. During open surgical removal of gallstones (open cholecystectomy), cholangiography is performed to exclude, or if needed, to remove CBDS. With laparoscopic cholecystectomy becoming the first surgical choice for treatment of gallstones, preoperative cholangiography has not been performed routinely and the procedure itself has been debated. Consequently, other techniques have been used to exclude CBDS. These techniques, however, are either invasive, with consequent risk for complications, or only diagnostic; some of them not available at all hospitals. There is thus a need to establish a simple, non-invasive and cheap diagnostic method, available at all units, to identify patients with CBDS for further evaluation with invasive and more expensive techniques.

Research frontiers

The research front in this area is focused on developing different imaging techniques. The most promising technique is Magnetic-Resonance-Cholangio-Pancreatography (MRCP). It has high specificity and sensitivity and accuracy similar to that of ERCP (Endoscopic-Retrograde-Cholangio-Pancreatography), but its accuracy decreases if gallstones are small (< 4 mm) or if they are located near Vater's papilla. In addition MRCP is not widely available and unlike ERCP does not allow endoscopic extraction of stones. ERCP is the most common technique used for both diagnostic and treatment of CBDS. It is however, expensive, invasive, technically demanding and associated with small but significant morbidity.

Innovations and breakthroughs

By using already existed parameters; liver functions test, ultrasonography together with complete review of patient's medical history (triple diagnostic), we offer a simple, cheap and, for all clinicians, available triple technique, to diagnose or exclude CBDS without any extra cost or diagnostic delay.

Applications

The majority of patients without CBDS will be identified by this triple diagnostic technique, leaving the remaining few, to be investigated by MRCP or ERCP. The availability and non-invasiveness of this test are additional benefits, which makes it more interesting.

Terminology

Cholangiography: X-ray examination of the bile ducts following administration of a radiopaque contrast medium. Magnetic-Resonance-Cholangio-Pancreatography: is a medical imaging technique which uses magnetic resonance imaging to visualise the biliary and pancreatic ducts in a non-invasive manner. Endoscopic-Retrograde-Cholangio-Pancreatography: refers to the use of an endoscope; a thin, flexible tube with a tiny video camera and light on the end to diagnose and treat various problems of the GI tract (stomach, intestine, liver, pancreas, and gallbladder).

Peer review

Through retrospective study, the authors concluded that using a combination of routinely used diagnostic components as triple diagnostic modality would increase the diagnostic accuracy of common bile duct stones. The result is reasonable and persuasive.

REFERENCES

1 **Sakorafas GH**, Milingos D, Peros G. Asymptomatic cholelithiasis: is cholecystectomy really needed? A critical reappraisal 15 years after the introduction of laparoscopic cholecystectomy. *Dig Dis Sci* 2007; **52**: 1313-1325

2 **Freitas ML**, Bell RL, Duffy AJ. Choledocholithiasis: evolving standards for diagnosis and management. *World J Gastroenterol* 2006; **12**: 3162-3167

3 **Martin DJ**, Vernon DR, Toouli J. Surgical versus endoscopic treatment of bile duct stones. Cochrane Database Syst Rev 2006; CD003327

4 **Slanetz PJ**, Boland GW, Mueller PR. Imaging and interventional radiology in laparoscopic injuries to the gallbladder and biliary system. *Radiology* 1996; **201**: 595-603

5 **Portincasa P**, Moschetta A, Petruzzelli M, Palasciano G, Di Ciaula A, Pezzolla A. Gallstone disease: Symptoms and diagnosis of gallbladder stones. *Best Pract Res Clin Gastroenterol* 2006; **20**: 1017-1029

6 **Lakatos L**, Mester G, Reti G, Nagy A, Lakatos PL. Selection criteria for preoperative endoscopic retrograde cholangiopancreatography before laparoscopic cholecystectomy and endoscopic treatment of bile duct stones: results of a retrospective, single center study between 1996-2002. *World J Gastroenterol* 2004; **10**: 3495-3499

7 **Livingston EH**, Miller JA, Coan B, Rege RV. Indications for selective intraoperative cholangiography. *J Gastrointest Surg* 2005; **9**: 1371-1377

8 **Majeed AW**, Ross B, Johnson AG, Reed MW. Common duct diameter as an independent predictor of choledocholithiasis: is it useful? *Clin Radiol* 1999; **54**: 170-172

9 **Machi J**, Oishi AJ, Tajiri T, Murayama KM, Furumoto NL, Oishi RH. Routine laparoscopic ultrasound can significantly reduce the need for selective intraoperative cholangiography during cholecystectomy. *Surg Endosc* 2007; **21**: 270-274

10 **Ledniczky G**, Fiore N, Bognár G, Ondrejka P, Grosfeld JL. Evaluation of perioperative cholangiography in one thousand laparoscopic cholecystectomies. *Chirurgia* (Bucur) 2006; **101**: 267-272

11 **Guarise A**, Baltieri S, Mainardi P, Faccioli N. Diagnostic accuracy of MRCP in choledocholithiasis. *Radiol Med* 2005; **109**: 239-251

12 **Chang L**, Lo S, Stabile BE, Lewis RJ, Toosie K, de Virgilio C. Preoperative versus postoperative endoscopic retrograde cholangiopancreatography in mild to moderate gallstone pancreatitis: a prospective randomized trial. *Ann Surg* 2000; **231**: 82-87

13 **Wai CT**, Seto KY, Sutedja DS. Clinics in diagnostic imaging (115). Extraluminal biliary tree obstruction due to compression by pancreatic head tumour. *Singapore Med J* 2007; **48**: 361-366; quiz 367

14 **Ney MV**, Maluf-Filho F, Sakai P, Zilberstein B, Gama-Rodrigues J, Rosa H. Echo-endoscopy versus endoscopic retrograde cholangiography for the diagnosis of choledocholithiasis: the influence of the size of the stone and diameter of the common bile duct. *Arq Gastroenterol* 2005; **42**: 239-243

15 **Nathanson LK**, O'Rourke NA, Martin IJ, Fielding GA, Cowen AE, Roberts RK, Kendall BJ, Kerlin P, Devereux BM. Postoperative ERCP versus laparoscopic choledochotomy for clearance of selected bile duct calculi: a randomized trial. *Ann Surg* 2005; **242**: 188-192

16 **Koo KP**, Traverso LW. Do preoperative indicators predict the presence of common bile duct stones during laparoscopic cholecystectomy? *Am J Surg* 1996; **171**: 495-499

17 **Alponat A**, Kum CK, Rajnakova A, Koh BC, Goh PM. Predictive factors for synchronous common bile duct stones in patients with cholelithiasis. *Surg Endosc* 1997; **11**: 928-932

18 **Bose SM**, Mazumdar A, Prakash VS, Kocher R, Katariya S, Pathak CM. Evaluation of the predictors of choledocholithiasis: comparative analysis of clinical, biochemical, radiological, radionuclear, and intraoperative parameters. *Surg Today* 2001; **31**: 117-122

19 **Hayat JO**, Loew CJ, Asrress KN, McIntyre AS, Gorard DA. Contrasting liver function test patterns in obstructive jaundice due to biliary strictures [corrected] and stones. *QJM* 2005; **98**: 35-40
20 **Pilleul F**. Asymptomatic or paucisymptomatic CBD dilatation on US after cholecystectomy: management. *J Radiol* 2006; **87**: 494-499
21 **Testoni PA**. Preventing post-ERCP pancreatitis: where are we? *JOP* 2003; **4**: 22-32
22 **Freeman ML**, Nelson DB, Sherman S, Haber GB, Herman ME, Dorsher PJ, Moore JP, Fennerty MB, Ryan ME, Shaw MJ, Lande JD, Pheley AM. Complications of endoscopic biliary sphincterotomy. *N Engl J Med* 1996; **335**: 909-918
23 **Freeman ML**, DiSario JA, Nelson DB, Fennerty MB, Lee JG, Bjorkman DJ, Overby CS, Aas J, Ryan ME, Bochna GS, Shaw MJ, Snady HW, Erickson RV, Moore JP, Roel JP. Risk factors for post-ERCP pancreatitis: a prospective, multicenter study. *Gastrointest Endosc* 2001; **54**: 425-434
24 **Varadarajulu S**, Eloubeidi MA, Wilcox CM, Hawes RH, Cotton PB. Do all patients with abnormal intraoperative cholangiogram merit endoscopic retrograde cholangiopancrea tography? *Surg Endosc* 2006; **20**: 801-805
25 **Katz D**, Nikfarjam M, Sfakiotaki A, Christophi C. Selective endoscopic cholangiography for the detection of common bile duct stones in patients with cholelithiasis. *Endoscopy* 2004; **36**: 1045-1049
26 **Rösch T**, Meining A, Frühmorgen S, Zillinger C, Schusdziarra V, Hellerhoff K, Classen M, Helmberger H. A prospective comparison of the diagnostic accuracy of ERCP, MRCP, CT, and EUS in biliary strictures. *Gastrointest Endosc* 2002; **55**: 870-876
27 **Chang L**, Lo SK, Stabile BE, Lewis RJ, de Virgilio C. Gallstone pancreatitis: a prospective study on the incidence of cholangitis and clinical predictors of retained common bile duct stones. *Am J Gastroenterol* 1998; **93**: 527-531
28 **Neoptolemos JP**, London N, Bailey I, Shaw D, Carr-Locke DL, Fossard DP, Moossa AR. The role of clinical and biochemical criteria and endoscopic retrograde cholangiopancreatography in the urgent diagnosis of common bile duct stones in acute pancreatitis. *Surgery* 1986; **100**: 732-742
29 **Leitman IM**, Fisher ML, McKinley MJ, Rothman R, Ward RJ, Reiner DS, Tortolani AJ. The evaluation and management of known or suspected stones of the common bile duct in the era of minimal access surgery. *Surg Gynecol Obstet* 1993; **176**: 527-533
30 **Hariri J**, Øster A. The negative predictive value of p16INK4a to assess the outcome of cervical intraepithelial neoplasia 1 in the uterine cervix. *Int J Gynecol Pathol* 2007; **26**: 223-228

S- Editor Zhu LH **L- Editor** Negro F **E- Editor** Wang HF

Online Submissions: wjg.wjgnet.com
www.wjgnet.com
wjg@wjgnet.com

World J Gastroenterol 2007 November 21; 13(43): 5750-5753
World Journal of Gastroenterology ISSN 1007-9327

RAPID COMMUNICATION

Plasma and platelet serotonin levels in patients with liver cirrhosis

Đorđe M Ćulafić, Duško S Mirković, Miodrag D Vukčević, Jelena S Rudić

Đorđe M Ćulafić, Duško S Mirković, Miodrag D Vukčević, Jelena S Rudić, Clinic of Gastroenterology and Hepatology, Institute of Digestive Diseases; Institute of Medical Biochemistry; Institute of Pulmonary Diseases; Clinical Center of Serbia, Medical Faculty, Belgrade
Correspondence to: Đorđe M Ćulafić, Assistant Professor, Institute of Digestive Diseases, Clinical Center of Serbia, Koste Todorovica 6 street, Belgrade 11000, Serbia. dculafic@eunet.yu
Telephone: +387-11-2629811 Fax: + 387-11-2629811
Received: June 4, 2007 Revised: July 31, 2007

Abstract

AIM: To analyze the relationship between plasma and platelet serotonin levels and the degree of liver insufficiency.

METHODS: The prospective study included 30 patients with liver cirrhosis and 30 healthy controls. The degree of liver failure was assessed according to the Child-Pugh classification. Platelet and platelet poor plasma serotonin levels were determined.

RESULTS: The mean plasma serotonin level was higher in liver cirrhosis patients than in healthy subjects (215.0 ± 26.1 *vs* 63.1 ± 18.1 nmol/L; $P < 0.0001$). The mean platelet serotonin content was not significantly different in patients with liver cirrhosis compared with healthy individuals (4.8 ± 0.6; 4.2 ± 0.3 nmol/platelet; $P > 0.05$). Plasma serotonin levels were significantly higher in Child-Pugh grade A/B than in grade C patients (246.8 ± 35.0 *vs* 132.3 ± 30.7 nmol/L; $P < 0.05$). However, platelet serotonin content was not significantly different between Child-Pugh grade C and grade A/B (4.6 ± 0.7 *vs* 5.2 ± 0.8 nmol/platelet; $P > 0.05$).

CONCLUSION: Plasma serotonin levels are significantly higher in patients with cirrhosis than in the controls and represent the degree of liver insufficiency. In addition, platelet poor plasma serotonin estimation is a better marker for liver insufficiency than platelet serotonin content.

Key words: Serotonin; Plasma; Platelet; Liver cirrhosis

Ćulafić ĐM, Mirković DS, Vukčević MD, Rudić JS. Plasma and platelet serotonin levels in patients with liver cirrhosis. *World J Gastroenterol* 2007; 13(43): 5750-5753

http://www.wjgnet.com/1007-9327/13/5750.asp

INTRODUCTION

The serotonergic system plays a critical role in a wide variety of physiological and behavioral processes. In the circulation, serotonin synthesized by the intestinal enterochromaffin cells, is actively incorporated into platelets and stored in platelet dense-storage granules. Nearly all of the serotonin in circulating blood is concentrated in the platelets and minimally in plasma (which is the interactive pool). The integral membrane protein of mucosal epithelial cells is the major protagonist in regulating the extracellular serotonin concentration[1]. Serotonin is mostly metabolized into 5-hydroxyindoleacetic acid by monoamine oxidase in hepatic and lung endothelial cells[2]. The effects of serotonin are most prominent in the cardiovascular system, with additional effects in the respiratory system and the intestines. Vasoconstriction is a classic response to administration of serotonin. However, serotonin induces smooth muscle cell contraction and proliferation and stimulates endothelial cells to release vasodilating substances and acts as "helper agonist" of platelet aggregation in humans[3,4]. Altered concentrations of circulating serotonin have been implicated in several pathologic conditions including hypertension, primary pulmonary hypertension, liver cirrhosis, and psychiatric disorders[5-8].

The acute and chronic hepatic insufficiency gives rise to serotonin system changes, contributing to the development of hepatic encephalopathy, portal hypertension, and hyperdynamic circulation[9]. Hepatic encephalopathy is followed by changes of serotonin neurotransmission, including the catabolic enzymes, receptors, and metabolites[10]. After application of serotonin inhibitors (ketanserin and ritanserin), portal pressure is decreased in patients with liver cirrhosis, confirming the importance of serotonin in the pathogenesis of portal hypertension[11]. The aim of this study was to characterize the relationship between plasma and platelet serotonin levels and the degree of liver insufficiency.

MATERIALS AND METHODS

Subjects

In the period January-April, 2007, the prospective study included 30 patients with liver cirrhosis and 30 healthy controls, examined at the Institute of Digestive

Diseases, Clinical Center of Serbia, Belgrade. Hepatologic examinations were based on medical history, physical examination, laboratory tests, and liver biopsy. Laboratory tests included hepatocyte integrity, cholestasis, synthetic liver function, and specific (etiological) tests. Puncture liver biopsy was performed in 16 (53.3%) patients, using Menghini needle of 1.4 mm. The degree of liver failure was assessed according to the Child-Pugh classification.

Biochemistry

Platelet and platelet poor plasma (PPP) venous blood was collected in 3 mL original Vacutainer "BD" tubes with 75 g/L K_3EDTA 0.072 mL. Blood samples were taken between 8 and 9 am. Platelet number was immediately determined on "Coulter A^c T Diff" analyser. Platelet rich plasma (PRP) was obtained by low speed centrifugation (200 g, 10 min) on "Heraeus Digifuga GL". Platelet count was determined again and taken into consideration in final determination of serotonin concentration in platelets. Exactly 1 mL of PRP was centrifuged on 1000 × g for 10 min. The obtained PPP was separated, and together with platelet pellets, stored at -20℃, not longer then 20 d[12]. The whole number of platelet pellets and PPP serotonin samples were estimated in one series.

Platelet pellets were spiked with 10 μL N-methyl serotonin solution (Recipe, Munchen) as an internal standard. All pellets were diluted with 100 μL high performance liquid chromatography (HPLC) ultra pure water (Recipe, Munchen). Platelets were destroyed with 100 μL of 700 g/L perchloric acid (Merck Darmstad) and centrifuged at 10 000 × g for 5 min. 100 μL of PPP samples was deproteinized with 100 μL deproteinating reagent (Recipe, Munchen) and centrifuged in same way, as for platelets[13].

Twenty μL of the supernatants were analyzed by reverse phase HPLC (Recipe, Munchen) with original mobile phase for serotonin (Recipe, Munchen). Original, "Recipe" external standard solution has been used for calibration. The HPLC system consisted of "Bio-Rad AS 100" HRLC automatic sampling system with " Rheodine 7125 valve", "Bio-Rad 1350" HPLC pump, and "Bio-Rad 1640" electrochemical detection. Chromatographic data were calculated using the "Chrome Line V 4.20" HPLC software. Amperometric detection has been done on 0.6 V. Duration of chromatographic separation was 10 min.

Statistical analysis

Statistical analyses were performed using SPSS statistical software (SPSS for windows, release 10.0, SPSS, Chicago, Il). Descriptive statistics are presented as mean ± SE. Differences between groups were compared with parametric *t*-test because data had a Gaussian distribution. Because we performed 6 consecutive statistical analyses, we chose a level of significance 0.05/6 = 0.008 (α-adjustment according to the modified Bonferroni procedure).

RESULTS

The most common cause of liver cirrhosis was alcohol in 12 individuals (40.0%). The incidence of cirrhosis due to viral infection was lower with HCV in 6 (20.0%) and HBV in 5 subjects (16.6%); autoimmune diseases were quite rare with 3 cases (10.0%), while etiology was unknown in 4 (13.3%) cases. The patients were classified according to the Child-Pugh system. Child-Pugh class A included 12 (40%) patients, Child-Pugh class B 8 (26.6%), and Child-Pugh class C 10 (33.3%) patients. All patients had clinically evident portal hypertension, none of them had episodes of bacterial peritonitis, and none of them had a beta blocker medication.

The mean plasma free serotonin levels were much higher in liver cirrhosis patients than in healthy individuals. A statistical significant difference was found between serotonin plasma values in patients with liver cirrhosis and healthy subjects (215.0 ± 26.1 *vs* 63.1 ± 18.1 nmol/L; t = 3.868, $P < 0.0001$).

The mean platelet serotonin content was not significantly different in patients with liver cirrhosis compared to healthy individuals. There was no statistically significant difference between platelet serotonin content in patients with liver cirrhosis and healthy subjects (4.8 ± 0.6 *vs* 4.2 ± 0.3 nmol/platelets; t = 0.881, $P > 0.05$).

Plasma free serotonin levels were significantly higher in Child-Pugh grade A/B than in grade C patients (246.8 ± 35.0 *vs* 132.3 ± 30.7 nmol/L; t = 1.938, $P < 0.05$). However, platelet serotonin content was not significantly different between Child-Pugh grade C and grade A/B (4.6 ± 0.7 *vs* 5.2 ± 0.8 nmol/platelets; t = 0.48, $P > 0.05$).

In addition, plasma free serotonin levels were not significantly different between alcohol liver cirrhosis and cirrhosis of other etiology (143.9 ± 29.3 *vs* 224.84 ± 34.8 nmol/L; t = 1.6, $P > 0.05$). Also, platelet serotonin content was not significantly different between alcohol liver cirrhosis and cirrhosis of other etiology (4.2 ± 0.7 *vs* 5.3 ± 0.9 nmol/10^9 platelets; t = 0.91; $P > 0.05$).

DISCUSSION

Marasini *et al*[7] described a significant reduction of serotonin, determined by high-performance liquid chromatography, in platelets of 14 patients with liver cirrhosis, although levels of free circulating plasma serotonin were within the normal range. In the study of Beaudry *et al*[14], the whole-blood serotonin levels were significantly lower in 30 patients with cirrhosis than in age-matched controls, and no correlation was found between these levels and the severity of cirrhosis. This difference might be the result of low platelet count observed in patients with cirrhosis; however, in this series of patients, the significant difference persisted when the whole-blood serotonin levels were expressed by platelet count, but it was less expressed. Thus, in patients with cirrhosis, low whole-blood serotonin levels probably depend on reduction of both uptake, retention of serotonin by platelets, and low platelet number.

However, in the same study of Beaudry *et al*[14], unconjugated plasma serotonin levels, an indication of the active form of serotonin, were significantly higher in patients with cirrhosis than in the controls, and in patients with cirrhosis these levels were higher in Child-Pugh grade A than in grade C patients. In our study, we investigated levels of free or unconjugated serotonin. However, the levels of free serotonin in patients with liver cirrhosis were

also higher than in healthy subjects. Also, the levels of free serotonin in patients with Child-Pugh grade C is less than in grade A/B patients. In addition, platelet serotonin content was not significantly different when patients with liver cirrhosis were compared to healthy subjects.

The discrepancy of our and Beadry's study may be explained by the fact that whole blood is a similar, but not the same kind of biological material, as the platelet pellet is. In addition, we used HPLC as basic technique in our work, which significantly differs from Beadry's study, who also emphasized this difference in his study. The reasons for high levels of plasma serotonin in the liver cirrhosis could be slow uptake and storage of serotonin by the platelets (as could be the sequelae of the kinetic change of serotonin transport mechanisms) or abnormal serotonin release from dense granules of activated platelets.

Laffi *et al*[15] gave the evidence for significant reduction of substances that are deposited in thick (adenosine triphosphate and serotonin) and in alpha granules (B-thromboglobulin and platelet factor 4) in patients with liver cirrhosis in comparison to controls. It is supposed that platelet disorder in deposition of substances mentioned above, in patients with liver cirrhosis, is in relation to platelet activation, a condition defined as "platelet exhaustion".

The causes of platelet activation in liver cirrhosis are complex and not yet fully understood. Hyperdynamic portal circulation and retention in the spleen microcirculation in liver cirrhosis might stimulate platelets. Immunological and inflammatory phenomena in the liver tissue and its influence are other possible reasons for platelet activation. In addition, endotoxemia is often associated with severe liver cirrhosis and it causes platelet activation[16]. In liver cirrhosis, thrombocytopenia is associated with a shorter life span of platelets and is the result of constant platelet activation by cytokines (IL2, IL6, TNFα), it is mediated by subclinical DIC, and intensified elimination by reticuloendothelial system of the spleen and liver[17]. Platelet activation with the increase of both βTG serum concentration and elevation of platelet population (CD62P and CD63 as well as medial intensity of fluorescence CD62P and CD63) becomes higher as liver cirrhosis develops and thrombocytopenia rises. Concurrently with thrombocytopenia in liver cirrhosis, platelet CD63+ population increases, clearly indicating the platelet activation with elevated medial intensity of fluorescence CD62P and CD63[18].

Concentration of circulating serotonin in liver cirrhosis can be influenced by other factors, such as altered serotonin catabolism due to an elevated activity of monoamino oxidase and impaired metabolism of tryptophan, as serotonin precursor[19]. Impaired metabolic function in liver cirrhosis contributes to elevated plasma serotonin. Moreover, vasoactive substances, produced in the splanchnic circulation, bypass the liver in the presence of porto-systemic collaterals and directly enter the systemic circulation. In conclusion, plasma serotonin levels are significantly higher in patients with cirrhosis than in the controls, and represent the degree of liver insufficiency. In addition, PPP serotonin estimation is a better marker of liver insufficiency than platelet serotonin content.

COMMENTS

Background

The acute and chronic hepatic insufficiency gives rise to serotonin system changes, contributing to the development of hepatic encephalopathy, portal hypertension, and hyperdynamic circulation. In patients with liver cirrhosis, low whole-blood serotonin levels depend probably on reduced uptake, retention of serotonin by platelets, and low platelet number. It is supposed that reduced platelet deposition of substances in thick and alfa granules, is in relation to platelet activation, caused by hyperdynamic circulation and endotoxemia. Also, concentration of circulating serotonin in liver cirrhosis can be influenced by other factors, such as altered serotonin catabolism due to elevated activity of monoamino oxidase and impaired metabolism of tryptophan, as a precursor of serotonin.

Research frontiers

The serotonergic system plays a critical role in a wide variety of physiological and behavioral processes. Altered concentrations of circulating serotonin are implicated in several pathologic conditions including hypertension, primary pulmonary hypertension, liver cirrhosis, and psychiatric disorders. The highlight of our research was to characterize the relationship between plasma and platelet serotonin levels and the degree of liver insufficiency.

Innovations and breakthroughs

In Beadry's study, unconjugated plasma serotonin level, an active form of serotonin, was significantly higher in patients with cirrhosis than in the controls, and in cirrhotics this level was higher in Child A than in Child C patients. In our study, the levels of free serotonin in patients with liver cirrhosis were also higher than in healthy subjects. However, the levels of free serotonin in patients with Child C cirrhosis were less compared to Child A/B patients. Furthermore, platelet serotonin content was not significantly different in cirrhotics compared to healthy controls. The discrepancy of our and previous study could be explained by the fact that we used high performance liquid chromatography as basic technique in our work, which significantly differs from the technique used in the previous study.

Applications

The results in the study suggest that plasma serotonin levels may represent the degree of liver insufficiency. Also, platelet poor plasma serotonin estimation is a better marker for liver insufficiency than platelet serotonin content.

Terminology

Serotonin: Serotonin is a vasoactive substance, synthesized by the intestinal enterochromaffin cells, which is actively incorporated into platelets and stored in platelet dense-storage granules. Integral membrane protein of mucosal epithelial cells is the major protagonist in regulating the extracellular serotonin concentration. Serotonin is mostly metabolized into 5-hydroxyindoleacetic acid by monoamine oxidase in hepatic and lung endothelial cells.

Peer review

This is a case controlled study demonstrating that plasma but not platelet serotonin levels are increased in patients with liver cirrhosis and correlate with liver insufficiency. The subject is novel and interesting.

REFERENCES

1 **Pratuangdejkul J**, Schneider B, Jaudon P, Rosilio V, Baudoin E, Loric S, Conti M, Launay JM, Manivet P. Definition of an uptake pharmacophore of the serotonin transporter through 3D-QSAR analysis. *Curr Med Chem* 2005; **12**: 2393-2410
2 **Deacon AC**. The measurement of 5-hydroxyindoleacetic acid in urine. *Ann Clin Biochem* 1994; **31** (Pt 3): 215-232
3 **Li N**, Wallén NH, Ladjevardi M, Hjemdahl P. Effects of serotonin on platelet activation in whole blood. *Blood Coagul Fibrinolysis* 1997; **8**: 517-523
4 **Fanburg BL**, Lee SL. A new role for an old molecule: serotonin as a mitogen. *Am J Physiol* 1997; **272**: L795-L806
5 **Hervé P**, Launay JM, Scrobohaci ML, Brenot F, Simonneau G, Petitpretz P, Poubeau P, Cerrina J, Duroux P, Drouet L. Increased plasma serotonin in primary pulmonary hypertension. *Am J Med* 1995; **99**: 249-254

6 **Humbert M**, Labrune P, Sitbon O, Le Gall C, Callebert J, Hervé P, Samuel D, Machado R, Trembath R, Drouet L, Launay JM, Simonneau G. Pulmonary arterial hypertension and type-I glycogen-storage disease: the serotonin hypothesis. *Eur Respir J* 2002; **20**: 59-65
7 **Marasini B**, Biondi ML, Agostoni A. Platelet and plasma serotonin in patients with liver cirrhosis. *J Clin Chem Clin Biochem* 1989; **27**: 419-421
8 **Quintana J**. Platelet serotonin and plasma tryptophan decreases in endogenous depression. Clinical, therapeutic, and biological correlations. *J Affect Disord* 1992; **24**: 55-62
9 **Borcsiczky D**, Szalay F, Tekes K, Tarcali J, Magyar K, de Châtel R. Platelet serotonin (5-HT) content is decreased in patients with alcoholic liver cirrhosis, but elevated in Gilbert's syndrome. *J Hepatol* 1996; **25**: 781-782
10 **Rao VL**, Giguère JF, Layrargues GP, Butterworth RF. Increased activities of MAOA and MAOB in autopsied brain tissue from cirrhotic patients with hepatic encephalopathy. *Brain Res* 1993; **621**: 349-352
11 **Vorobioff J**, Garcia-Tsao G, Groszmann R, Aceves G, Picabea E, Villavicencio R, Hernandez-Ortiz J. Long-term hemodynamic effects of ketanserin, a 5-hydroxytryptamine blocker, in portal hypertensive patients. *Hepatology* 1989; **9**: 88-91
12 **Fardaee M**, Panjehshahin M, Owji A, Vassei M. Serotonin levels in plasma and platelets of cyclosporin A treated rats. *Irn J Med Sci* 1998; **23**: 89-93
13 **Jovanovic S**, Mirkovic D, Majkic-Sing N. Reference values of serotonin in urine and plasma determined by high-performance liquid chromatography with electrochemical detection. *Clin Lab* 1998; **44**: 263-268
14 **Beaudry P**, Hadengue A, Callebert J, Gaudin C, Soliman H, Moreau R, Launay JM, Lebrec D. Blood and plasma 5-hydroxytryptamine levels in patients with cirrhosis. *Hepatology* 1994; **20**: 800-803
15 **Laffi G**, Marra F, Gresele P, Romagnoli P, Palermo A, Bartolini O, Simoni A, Orlandi L, Selli ML, Nenci GG. Evidence for a storage pool defect in platelets from cirrhotic patients with defective aggregation. *Gastroenterology* 1992; **103**: 641-646
16 **Itoh H**, Cicala C, Douglas GJ, Page CP. Platelet accumulation induced by bacterial endotoxin in rats. *Thromb Res* 1996; **83**: 405-419
17 **Amitrano L**, Guardascione MA, Brancaccio V, Balzano A. Coagulation disorders in liver disease. *Semin Liver Dis* 2002; **22**: 83-96
18 **Panasiuk A**, Zak J, Kasprzycka E, Janicka K, Prokopowicz D. Blood platelet and monocyte activations and relation to stages of liver cirrhosis. *World J Gastroenterol* 2005; **11**: 2754-2758
19 **De Prada M**, Richards JG, Kettler R. Amine storage organelles in platelets In: Gordon JL, eds. Platelets in biology and pathology. Amsterdam: Elsevier, 1981: 105-145

S- Editor Ma N **L- Editor** Mihm S **E - Editor** Wang HF

Online Submissions: wjg.wjgnet.com
www.wjgnet.com
wjg@wjgnet.com

World J Gastroenterol 2007 November 21; 13(43): 5754-5759
World Journal of Gastroenterology ISSN 1007-9327

RAPID COMMUNICATION

Preoperative evaluation with T-staging system for hilar cholangiocarcinoma

Ru-Fu Chen, Zhi-Hua Li, Jia-Jia Zhou, Jie Wang, Ji-Sheng Chen, Qing Lin, Qi-Bing Tang, Ning-Fu Peng, Zhi-Peng Jiang, Quan-Bo Zhou

Ru-Fu Chen, Jia-Jia Zhou, Jie Wang, Ji-Sheng Chen, Qing Ling, Qi-Bing Tang, Ning-Fu Peng, Department of Hepatobiliary Surgery, the Affiliated Second Hospital, Sun Yat-sen University, 107 Yan-Jiang Xi Road, GuangZhou 510120, Guangdong Province, China
Zhi-Hua Li, Department of Oncology, the Affiliated Second Hospital, Sun Yat-sen University, 107 Yan-Jiang Xi Road, GuangZhou 510120, Guangdong Province, China
Zhi-Peng Jiang, Department of Emergency, the Affiliated Second Hospital, Sun Yat-sen University, 107 Yan-Jiang Xi Road, GuangZhou 510120, Guangdong Province, China
Supported by Department of Radiology, The Second Affiliated Hospital, Sun Yat-sen University, Guangdong Province, China
Correspondence to: Quan-Bo Zhou, Department of Hepatobiliary Surgery, the Affiliated Second Hospital, Sun Yat-sen University, 107Yan-Jiang Xi Road, GuangZhou 510120, Guangdong Province, China. hnhszqb@yahoo.com.cn
Telephone: +86-13710782185 Fax: +86-20-81332430
Received: June 5, 2007 Revised: August 9, 2007

Abstract

AIM: To investigate the clinical value of T-staging system in the preoperative assessment of hilar cholangiocarcinoma.

METHODS: From March 1993 to January 2006, 85 patients who had cholangiocarcinoma diagnosed by operative tissue-biopsy were placed into one of three stages based on the new T-staging system, and it was evaluated the resectability and survival correlated with T-staging.

RESULTS: The likelihood of resection and achieving tumor-free margin decreased progressively with increasing T stage ($P < 0.05$). The cumulative 1-year survival rates of T1, T2 and T3 patients were 71.8%, 50.8% and 12.9% respectively, and the cumulative 3-year survival rate was 34.4%, 18.2% and 0% respectively; the survival of different stage patients differed markedly ($P < 0.001$). Median survival in the hepatic resection group was greater than in the group that did not undergo hepatic resection (28 mo *vs* 18 mo; $P < 0.05$). The overall accuracy for combined MRCP and color Doppler Ultrasonagraphy detecting disease was higher than that of combined using CT and color Doppler Ultrasonagraphy (91.4% *vs* 68%; $P < 0.05$). And it was also higher in detecting port vein involvement (90% *vs* 54.5%; $P < 0.05$).

CONCLUSION: The proposed staging system for hilar cholangiocarcinoma can accurately predict resectability, the likelihood of metastatic disease, and survival. A concomitant partial hepatectomy would help to attain curative resection and the possibility of long-term survival. MRCP/MRA coupled with color Doppler Ultrasonagraphy was necessary for preoperative evaluation of hilar cholangiocarcinoma.

Key words: Hilar cholangiocarcinoma; Preoperative staging; Survival rate; Surgical treatment

Chen RF, Li ZH, Zhou JJ, Wang J, Chen JS, Lin Q, Tang QB, Peng NF, Jiang ZP, Zhou QB. Preoperative evaluation with T-staging system for hilar cholangiocarcinoma. *World J Gastroenterol* 2007; 13(43): 5754-5759

http://www.wjgnet.com/1007-9327/13/5754.asp

INTRODUCTION

Cholangiocarcinoma is an adenocarcinoma that arises from the bile duct epithelium and is the second most common primary hepatobiliary cancer, however, cholangiocarcinoma remains a relatively rare disease, accounting for < 2% of all human malignancies[1-3]. Although the entire biliary tree is potentially at risk, hilar cholangiocarcinoma which involved the biliary confluence or the right or left hepatic ducts are most common and account for 40%-60% of all cases[4]. In most instances, the prognosis of hilar cholangiocarcinoma is very poor, with an overall 5-years survival rate of only 1%[5]. At present, surgical resection of early detected tumors is still the optimal treatment method for hilar cholangiocarcinoma[6,7]. Therefore, precise preoperative imaging evaluation including classification and staging of tumor is crucial for planning treatment and assessing prognosis.

Currently, the modified Bismuth-Corlette system and American Joint Committee on Cancer (AJCC) systems are still commonly used in evaluation of hilar cholangiocarcinoma in China, but both of them are failure to identify patients who are operative candidates or to provide prognostic information[5,8,9]. It is possible that the AJCC or Bismuth-Corlette systems has been misused by a

generation of medical oncologists and surgeons who have used staging systems based on postoperative evaluation of the tumor to guide the preoperative, intraoperative, and even postoperative management[9,10].

In an attempt to improve the preoperative clinical and prognostic usefulness of stag system, the organizational structure of the hepatobiliary program at Memorial Sloan-Kettering Cancer Center (MSKCC) have proposed a new T staging that takes into consideration both vascular involvement by local tumor extension and the presence or absence of liver atrophy (Table 1)[11]. This proposed T staging system is predictive of resectability, of the likelihood of nodal or distant metastases, and of overall survival[11]. In this study, we used the proposed T staging system, based on imaging data, to stratifies 85 patients hilar cholangiocarcinoma into one of three stages and evaluate the resectability or survival correlated with T-staging. We also want to find the correlation between the T staging and nodal or distant metastases. In addition, in our study, biliary resections coupled with in-continuity hepatic resection has been proposed, to attain radical resection.

Table 1 Revised preoperative T staging system for patients with hilar cholangiocarcinoma

T Stage	Description
T1	Tumor involving biliary confluence ± unilateral extension to 2° biliary radicles No liver atrophy or portal vein involvement
T2	Tumor involving biliary confluence ± unilateral extension to 2° biliary radicles with ipsilateral portal vein involvement ± ipsilateral hepatic lobar atrophy No main portal vein involvement
T3	Tumor involving biliary confluence + bilateral extension to 2° biliary radicles; OR unilateral extension to 2° biliary radicles with controlateral portal vein involvement; OR unilateral extension to 2° biliary radicles with controlateral hepatic lobar atrophy; ralateral hepatic lobar atrophy; phy; OR main or bilateral portal venous involvement

MATERIALS AND METHODS

Data selection

Data was collected from a database of Hepatobiliary Surgery of the Second Affiliated Hospital of SUN Yat-sen University From March 1993 through January 2006, 85 patients of hilar cholangiocarcinoma underwent laparotomy and diagnosed by tissue-biopsy were retrospectively analyzed in this study. There were 45 men and 40 women and their mean age was 63.5 (median, 65; range, 42-81) years. Follow-up was defined as the number of months between the operation date and the date of death or, if the patient was alive, the end dates of the study period (December 31, 2006). Preoperative baseline examinations were electrocardiogram (ECG), sternite, prothrombin time (PT), hepatic and renal function test. All of 85 patients presented with hilar cholangiocarcinoma had more than one kind of image examinations. Ultrasound (US) or duplex ultrasonography (DUS) coupled with tomographic (CT) scanning were performed on 25 patients; duplex ultrasonography coupled with magnetic resonance cholangiopancreatography (MRCP) was performed on 35 patients; ultrasound, CT coupled with ERCP was performed on 11 patients; ultrasound, CT coupled with MRCP was performed on 14 patients.

T-staging

Tumors were restaged retrospectively using revised preoperative T staging system based on preoperative imaging examinations (Table 1). This staging system, a modification of a previously reported scheme[12], classifies tumors according to three factors related to local tumor extent: the location and extent of bile duct involvement (according to the Bismuth-Corlette system)[13,14], the presence or absence of portal venous invasion, and the presence or absence of hepatic lobar atrophy. The survival data was then compared among the stages. T staging correlated with respectability, Ro resection (margins negative), and the incidence of metastatic disease were reviewed.

Surgical strategies

All 85 patients in this study were treated with laparotomy, the type of therapeutic procedures depended on tumor expansion and clinical conditions of patients. If the tumor was resectable, surgery was the first choice of treatment for patients in good clinical conditions. The two types of operations were: (1) local resection of the bile duct alone; (2) extrahepatic biliary resection with in-continuity hepatic resection. In patients with non-resectable tumors or bad clinical conditions, palliative procedure using endoscopic transpapillary and/or percutaneous transhepatic biliary drainage was performed. In this study the survival of all patients undergoing resection of hilar cholangiocarcinomas by either extrahepatic biliary resection alone or by extrahepatic biliary resection with in-continuity hepatic resection were reviewed.

Statistical analysis

All data were analyzed with SPSS 11.5 statistical package. Cumulative overall survival was calculated by the Kaplan-Meier method using the log rank test with T staging. The correlation between T staging and respectability, Ro resection or the incidence of metastatic disease were analyzed using the χ^2 test. Significance was accepted with 95% confidence.

RESULTS

Proposed T-staging system

The follow-up time of all patients was more than 3 mo. Eighty five patients were staged according to the proposed preoperative clinical system, as described above Table 1. Thirty nine patients had tumor involvement of the biliary confluence (with or without unilateral extension to second-order biliary radicles), no portal vein involvement, and no lobar atrophy and were therefore classified as having T1 tumors. Fifteen patients had T2 lesions because of ipsilateral portal vein involvement or ipsilateral lobar atrophy; or both findings. Thirty one patients had T3 tumors because of biliary extent alone, or main portal vein involvement, or metastatic disease.

Table 2 Resectability, incidence of margins negative and metastatic disease after staging by T stage

T Stage	Operative modus			Margins		Metastatic disease	
	Resected	Drainage	Biopsy	Negative	Positive	Negative	Positive
T1 (n = 39)	29 (74.4)	8 (20.5)	2 (5.1)	22 (75.9)	7 (24.1)	24 (61.5)	15 (38.5)
T2 (n = 15)	9 (60.0)	4 (26.7)	2 (13.3)	3 (33.3)	6 (66.7)	7 (46.7)	8 (53.3)
T3 (n = 31)	2 (6.5)	15 (48.4)	14 (45.1)	0 (0)	2 (100)	9 (30.0)	22 (70.0)
χ^2 value		35.5		8.8		7.3	
P value		0.000		0.012		0.026	

The percentages indicate the proportion of patients within each stage grouping or of the total number of patients. Metastatic disease refers to metastases to N2-level lymph nodes or to distant sites. Median survival was calculated for all patients, including those who died perioperatively.

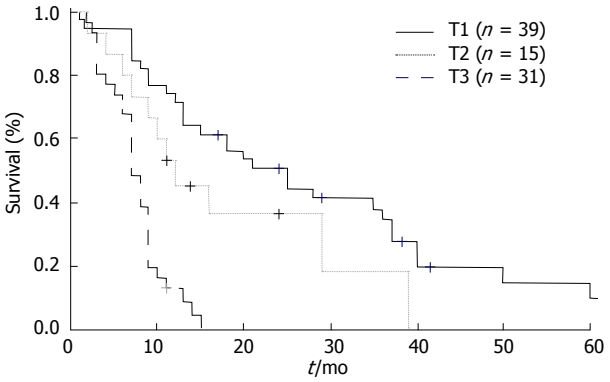

Figure 1 Kaplan-Meier survival analysis stratified by T stage. T stages seemed to be correlated with the survival time (χ^2 = 37.65, P < 0.001), and the survival time decreased progressively with increasing T staging. The cumulative 1-year survival rates of T1, T2 and T3 patients were 71.8%, 50.8% and 12.9%, respectively, and the cumulative 3-year survival rate was 34.4%,18.2% and 0%, respectively, the survival of different stage patients differed markedly (P < 0.001).

The clinical and survival-related factors associated with T stage are detailed in Table 2. Resectability and the likelihood of achieving an R0 resection both decreased progressively with increasing T stage (P < 0.05). A similar proportion of patients with T1 (74.4%) and T2 (60.0%) tumors underwent resection with curative intent. Two patients with T3 tumors (6.5%) were also underwent resection ,but both couldn't achieved R0 resection. In addition, metastatic disease to N2-level lymph nodes or to distant sites (i.e., metastatic disease that contraindicated resection) correlated with increasing T stage (P < 0.05).

Survival analysis

Kaplan-Meier estimate for survival depending on T stages was shown in Figure 1, it showed that T stages seemed to be correlated with the survival time (χ^2 = 37.65, P < 0.001), and the survival time decreased progressively with increasing T staging. The cumulative 1-year survival rates of T1, T2 and T3 patients were 71.8%, 50.8% and 12.9% respectively, and the cumulative 3-years survival rate was 34.4%, 18.2% and 0% respectively; the survival of different stage patients differed markedly (P < 0.001).

In patients with T1 lesions, 12 patients undergoing extrahepatic biliary resections alone and 17 patients underwent in-continuity hepatic resection (Table 3). This is in contrast to patients with T2 lesions, all of patient required a concomitant partial hepatectomy and 3 (33%) of whom required a portal vein resection and reconstruction.

Table 3 Margins negative, complication, operative mortality and survival based on in-continuity hepatic resection

Hepatic resection	n	Margins		Operative mortality, n (%)	Median survival, mo
		Negative, n (%)	Complication, n (%)		
In-continuity Hepatic Resection	28	21 (75)	16 (57)	3 (11)	28
No Hepatic Resection	12	4 (33)	4 (33)	1 (8)	18

Forty of 85 patients underwent resection, 28 (70%) had a concomitant partial hepatectomy, and negative histological margins were attained 75% of the time. The performance of a partial hepatectomy was predictive of a negative histological margin in this series. Median survival in the hepatic resection group was greater than in the group that did not undergo hepatic resection (28 *vs* 18 mo; P < 0.05). And the incident rate of complication and operative mortality in two groups were not different (P > 0.05).

Preoperative imaging evaluation

Most patients were diagnosed after at least a partial radiographic evaluation had been completed, usually consisting in ultrasonography, in a computed tomographic (CT) scan and in some form of direct cholangiography such as ERCP. After referral, further evaluation of tumor extent within the biliary tree and assessment of possible vascular involvement or metastatic disease were performed with MRCP or duplex ultrasonography, which are currently the preferred studies. Some patients who could not be diagnosed preoperatively were considered to have laparotomy for exploration. Altogether, 85 patients had the final diagnosis of hilar cholangiocarcinoma via pathologic diagnosis. The consistent rate with pathological findings of US or duplex ultrasonography coupled with CT, or with MRCP, or with CT and ERCP, or with CT and MRCP was 68% (17/25), 91.4% (32/35), 90.9% (10/11) and 100% (14/14) respectively. And the consistent rate of US combined with CT was significant lower than other combined examinations (P < 0.05). The final diagnosis rate of tumor infiltrated portal vein for duplex ultrasonography combined with MRCP/MRA, duplex ultrasonography combined with CT were 90% (19/21), 54.5% (6/11) respectively. The overall accuracy for combined MRCP and color Doppler Ultrasonagraphy detecting disease and

port vein involvement was higher than that of combined using CT and color Doppler Ultrasonagraphy ($P < 0.05$).

DISCUSSION

Currently, the only curative option for patients with cholangiocarcinoma is aggressive surgical resection. Many authors advocate that patients with suspected cholangiocarcinoma should be considered for operative resection and postoperative adjuvant therapy even if microscopically clear resection margins can not be achieved[15-17]. Therefore, precise preoperative imaging evaluation and staging of tumor are crucial for planning treatment and assessing prognosis.

Great effort has been expended to develop staging systems that are of greater prognostic utility to the surgeon and can be used to guide not only preoperative treatment, but also intra- and postoperative management of patients with cholangiocarcinoma[8,18-20]. There are currently 3 main staging systems utilized for patients with hilar cholangiocarcinomas: AJCC, Bismuth-Corlette, and Blumgart[9]. The AJCC tumor-node-metastasis (TNM) staging system is only applicable to patients who have undergone resection[4]. The Bismuth-Corlette system describes the tumors in terms of their anatomic location. Typically, it has been used to guide treatment (particularly resection), yet it does little to identify patients who are operative candidates or to impart prognostic information[11,12]. The modifications proposed, by Blumgart (Table 1) not only provide anatomic information about the local extent of the tumor but also better stratify patients who are candidates for surgical exploration by taking into account parenchymal characteristics of the liver.

In this study, we retrospectively reviewed 85 patients with cholangiocarcinoma who underwent resection and restaged them into the T-staging system. We have demonstrated the correlation between resectability or R0 resection or survival time and T stage, in 85 patients with hilar cholangiocarcinoma. Resectability and the likelihood of achieving an R0 resection both decreased progressively with increasing T stage. Patients with T1 and T2 have a chance of R0 resection; T3 stage tumors usually have no chance for resection. In our data, a similar proportion of patients with T1 (74.4%) and T2 (60.0%) tumors underwent resection with curative intent. Two patients with T3 tumors (6.5%) also underwent resection, but both couldn't achieve R0 resection. Kaplan-Meier analysis revealed that T-staging seemed to correlate with survival time, and the 1, 3-years accumulative survival time decreased with increasing T stage. The media survival time of patients with T1 stage was significantly higher than that of patients with T2 or T3 stage. In addition, metastatic disease to N2-level lymph nodes or to distant sites (i.e., metastatic disease that contraindicated resection) correlated with increasing T stage. In order to improve operative resectability and curability, hepatic resection has been applied to the treatment for hilar cholangiocar cinoma[21-23]. Whereas, several authors reported that the extent of hepatic resection was closely associated with the occurrence of postoperative complications, such as liver failure, sepsis, and anastomosis leakage[22,24-27]. In this study, we demonstrated a significant survival benefit in those patients who were able to undergo extrahepatic biliary resections coupled with in-continuity hepatic resection as compared with those undergoing to extrahepatic biliary resections alone. Hepatic resection did not increase the incurrence of complication and operative mortality in this series; this results also were supported by Miyazaki *et al*[28]. In our experience, the segments I and Ⅳ resection for hilar cholangiocarcinoma have the benefit of preserving enough hepatic mass for the patient to tolerate surgical stress as compared with major hepatic resection.

Early detection and accurate staging are crucial for planning treatment and improving survival rate of hilar cholangiocarcinomas. Noninvasive methods like magnetic resonance cholangiopancreatography or magnetic resonance angiography (MRCP/MRA) and Doppler ultrasound have been proposed by Jarnagin[29]. In our data analysis, duplex ultrasonography and magnetic resonance cholangiopancreatography have been successful when compared with any other combination of examinations. Ultrasonagraphy detecting disease and port vein involvement was 91.4% and 90%.and was higher than that of combined using CT and color Doppler Ultrasonagraphy. Duplex ultrasonography is noninvasive, and a skilled operator can identify the site of biliary obstruction, as well as the presence or absence of portal venous involvement. The efficacy of MRCP/MRA as a noninvasive means of acquiring reliable and precise information about the anatomy of both the intrahepatic and the extrahepatic biliary tree, as well as the level of tumor involvement, and the presence of nodal or distant metastases, has been well documented and has all but replaced percutaneous and endoscopic cholangiography[30-32].

In conclusion, the T-staging system correlates with respectability, RO resection and overall accumulative survival. Patients with hilar cholangiocarcinoma in T1 and T2 stage have the chance of curative resection, in-continuity hepatic resection, and it is necessary to achieve this with lower complications. Duplex ultrasonography and MRCP/MRA are essential for a preoperative assessment of hilar cholangiocarcinoma.

COMMENTS

Background

Cholangiocarcinoma is a malignancy with poor prognosis, and the best result still comes from surgical resection. However, in many of patients who underwent laparotomy the tumors are found not respectable. Therefore, a precise preoperative evaluation system seems to be particularly important. Whereas, currently the modified Bismuth-Corlette system and American Joint Committee on Cancer (AJCC) systems are still commonly used in evaluation of hilar cholangiocarcinoma in China, but both of them failed to identify patients who are operative candidates or to provide prognostic information.

Research frontiers

This current study retrospectively analyzes 85 patients with cholangiocarcinoma who underwent surgery using the T-staging system, and evaluates whether the resectability or survival correlated with T-staging. We also wanted to find the correlation between the T staging and nodal or distant metastases. Additionally, in our study, biliary resections coupled with in-continuity hepatic resection has been proposed to attain radical resection.

Innovations and breakthroughs

In our data, a similar proportion of patients with T1 (74.4%) and T2 (60.0%) tumors underwent resection with curative intent. Hepatic resection has been applied to the treatment for hilar cholangiocarcinoma, and achieved higher median survival than in the group that did not undergo hepatic resection (28 *vs* 18 mo; $P < 0.05$). In our study, the segments I and IV resection for hilar cholangiocarcinoma have the benefit of preserving enough hepatic mass for the patient to tolerate surgical stress as compared with major hepatic resection. In our data analysis, duplex ultrasonography and magnetic resonance cholangiopancreatography are chosen over any other combination of examinations.

Applications

This study provided important reference as regard to the preoperative assessment for patients with halir cholangiocarcinoma. In conclusion, the T-staging system correlates with resectability, RO resection and overall accumulative survival. Patients with hilar cholangiocarcinoma in T1 and T2 stages have the chance of curative resection, and in-continuity hepatic resection is necessary to achieve this with lower complications. Duplex ultrasonography and MRCP/MRA are necessary for a preoperative assessment of hilar cholangiocarcinoma.

Terminology

In current study, revised preoperative T staging systems were used to preoperatively evaluate the status of patients with hilar cholangiocarcinoma, and it described as follows: T1, Tumor involving biliary confluence ± unilateral extension to 2° biliary radicles, No liver atrophy or portal vein involvement. T2, Tumor involving biliary confluence ± unilateral extension to 2° biliary radicles with ipsilateral portal vein involvement ± ipsilateral hepatic lobar atrophy, No main portal vein involvement T3, Tumor involving biliary confluence + bilateral extension to 2° biliary radicles; OR unilateral extension to 2° biliary radicles with controlateral portal vein involvement; OR unilateral extension to 2° biliary radicles with controlateral hepatic lobar atrophy; OR main or bilateral portal venous involvement.

Peer review

The manuscript retrospectively analyzes 85 patients with cholangiocarcinoma who underwent surgery using the T-staging system. The results show resectability, tumor-free margin resection and cumulative survival of patients decrease with increasing T stage. The study also suggests that MRCP/MRA coupled with Doppler Ultrasonagraphy provides better preoperative evaluation of hilar cholangiocarcinoma. The paper is well written and more importantly it does provide important reference as regard to the preoperative assessment for patient with halir cholangiocarcinoma.

REFERENCES

1 **Carriaga MT**, Henson DE. Liver, gallbladder, extrahepatic bile ducts, and pancreas. *Cancer* 1995; **75**: 171-190
2 **Cormier JN**, Vauthey JN. Biliary tract cancer. *Curr Opin Gastroenterol* 2000; **16**: 437-443
3 **Bathe OF**, Pacheco JT, Ossi PB, Hamilton KL, Franceschi D, Sleeman D, Levi JU, Livingstone AS. Management of hilar bile duct carcinoma. *Hepatogastroenterology* 2001; **48**: 1289-1294
4 **Arai T**, Nagino M, Nimura Y. Surgical treatment for hilar cholangiocarcinoma. *Nihon Rinsho* 2006; **64** Suppl 1: 476-478
5 **Weber A**, Landrock S, Schneider J, Stangl M, Neu B, Born P, Classen M, Rösch T, Schmid RM, Prinz C. Long-term outcome and prognostic factors of patients with hilar cholangiocarcinoma. *World J Gastroenterol* 2007; **13**: 1422-1426
6 **Franco D**, Usatoff V. Surgery for cholangiocarcinoma. *Hepatogastroenterology* 2001; **48**: 53-55
7 **Kawarada Y**, Das BC, Naganuma T, Tabata M, Taoka H. Surgical treatment of hilar bile duct carcinoma: experience with 25 consecutive hepatectomies. *J Gastrointest Surg* 2002; **6**: 617-624
8 **Kim HJ**. TNM staging of hilar cholangiocarcinoma. *Korean J Gastroenterol* 2005; **46**: 20-27
9 **Zervos EE**, Osborne D, Goldin SB, Villadolid DV, Thometz DP, Durkin A, Carey LC, Rosemurgy AS. Stage does not predict survival after resection of hilar cholangiocarcinomas promoting an aggressive operative approach. *Am J Surg* 2005; **190**: 810-815
10 **Chamberlain RS**, Blumgart LH. Hilar cholangiocarcinoma: a review and commentary. *Ann Surg Oncol* 2000; **7**: 55-66
11 **Jarnagin WR**, Fong Y, DeMatteo RP, Gonen M, Burke EC, Bodniewicz BS J, Youssef BA M, Klimstra D, Blumgart LH. Staging, resectability, and outcome in 225 patients with hilar cholangiocarcinoma. *Ann Surg* 2001; **234**: 507-517; discussion 517-519
12 **Burke EC**, Jarnagin WR, Hochwald SN, Pisters PW, Fong Y, Blumgart LH. Hilar Cholangiocarcinoma: patterns of spread, the importance of hepatic resection for curative operation, and a presurgical clinical staging system. *Ann Surg* 1998; **228**: 385-394
13 **Bismuth H**, Corlette MB. Intrahepatic cholangioenteric anastomosis in carcinoma of the hilus of the liver. *Surg Gynecol Obstet* 1975; **140**: 170-178
14 **Bismuth H**, Castaing D, Traynor O. Resection or palliation: priority of surgery in the treatment of hilar cancer. *World J Surg* 1988; **12**: 39-47
15 **Nagorney DM**, Donohue JH, Farnell MB, Schleck CD, Ilstrup DM. Outcomes after curative resections of cholangiocarcinoma. *Arch Surg* 1993; **128**: 871-877; discussion 877-879
16 **Targarona EM**, Zografos G, Habib NA. Liver resection for recurrent hilar cholangiocarcinoma. *Br J Surg* 1993; **80**: 1433
17 **Zervos EE**, Pearson H, Durkin AJ, Thometz D, Rosemurgy P, Kelley S, Rosemurgy AS. In-continuity hepatic resection for advanced hilar cholangiocarcinoma. *Am J Surg* 2004; **188**: 584-588
18 **Lee YJ**. Preoperative diagnosis and management for hilar cholangiocarcinoma. *Korean J Gastroenterol* 2005; **46**: 28-31
19 **Santoro E**, Sacchi M, Carboni F, Santoro R, Scardamaglia F. Diagnostic and surgical features of Klatskin tumors. *Chir Ital* 1999; **51**: 1-7
20 **Otto G**, Romaneehsen B, Bittinger F, Mönch C, Thelen M, Hadian A, Lohse AW. Preoperative imaging of hilar cholangiocarcinoma: surgical evaluation of standard practises. *Z Gastroenterol* 2004; **42**: 9-14
21 **Sugiura Y**, Nakamura S, Iida S, Hosoda Y, Ikeuchi S, Mori S, Sugioka A, Tsuzuki T. Extensive resection of the bile ducts combined with liver resection for cancer of the main hepatic duct junction: a cooperative study of the Keio Bile Duct Cancer Study Group. *Surgery* 1994; **115**: 445-451
22 **Madariaga JR**, Iwatsuki S, Todo S, Lee RG, Irish W, Starzl TE. Liver resection for hilar and peripheral cholangiocarcinomas: a study of 62 cases. *Ann Surg* 1998; **227**: 70-79
23 **Mansfield SD**, Barakat O, Charnley RM, Jaques BC, O'Suilleabhain CB, Atherton PJ, Manas D. Management of hilar cholangiocarcinoma in the North of England: pathology, treatment, and outcome. *World J Gastroenterol* 2005; **11**: 7625-7630
24 **Nakeeb A**, Pitt HA, Sohn TA, Coleman J, Abrams RA, Piantadosi S, Hruban RH, Lillemoe KD, Yeo CJ, Cameron JL. Cholangiocarcinoma. A spectrum of intrahepatic, perihilar, and distal tumors. *Ann Surg* 1996; **224**: 463-473; discussion 473-475
25 **Su CH**, Tsay SH, Wu CC, Shyr YM, King KL, Lee CH, Lui WY, Liu TJ, P'eng FK. Factors influencing postoperative morbidity, mortality, and survival after resection for hilar cholangiocarcinoma. *Ann Surg* 1996; **223**: 384-394
26 **Nagino M**, Nimura Y, Kamiya J, Kanai M, Uesaka K, Hayakawa N, Yamamoto H, Kondo S, Nishio H. Segmental liver resections for hilar cholangiocarcinoma. *Hepatogastroenterology* 1998; **45**: 7-13
27 **Kosuge T**, Yamamoto J, Shimada K, Yamasaki S, Makuuchi M. Improved surgical results for hilar cholangiocarcinoma with procedures including major hepatic resection. *Ann Surg* 1999; **230**: 663-671
28 **Miyazaki M**, Ito H, Nakagawa K, Ambiru S, Shimizu H, Shimizu Y, Okuno A, Nozawa S, Nukui Y, Yoshitomi H, Nakajima N. Segments I and IV resection as a new approach for hepatic hilar cholangiocarcinoma. *Am J Surg* 1998; **175**: 229-231
29 **Georgopoulos SK**, Schwartz LH, Jarnagin WR, Gerdes

H, Breite I, Fong Y, Blumgart LH, Kurtz RC. Comparison of magnetic resonance and endoscopic retrograde cholangiopancreatography in malignant pancreaticobiliary obstruction. *Arch Surg* 1999; **134**: 1002-1007

30 **Fulcher AS**, Turner MA. HASTE MR cholangiography in the evaluation of hilar cholangiocarcinoma. *AJR Am J Roentgenol* 1997; **169**: 1501-1505

31 **Domagk D**, Wessling J, Reimer P, Hertel L, Poremba C, Senninger N, Heinecke A, Domschke W, Menzel J. Endoscopic retrograde cholangiopancreatography, intraductal ultrasonography, and magnetic resonance cholangiopancreatography in bile duct strictures: a prospective comparison of imaging diagnostics with histopathological correlation. *Am J Gastroenterol* 2004; **99**: 1684-1689

32 **Kim HJ**, Lee JM, Kim SH, Han JK, Lee JY, Choi JY, Kim KH, Kim JY, Lee MW, Kim SJ, Choi BI. Evaluation of the longitudinal tumor extent of bile duct cancer: value of adding gadolinium-enhanced dynamic imaging to unenhanced images and magnetic resonance cholangiography. *J Comput Assist Tomogr* 2007; **31**: 469-474

S- Editor Zhu LH **L- Editor** Li M **E- Editor** Yin DH

Online Submissions: wjg.wjgnet.com
www.wjgnet.com
wjg@wjgnet.com

World J Gastroenterol 2007 November 21; 13(43): 5760-5764
World Journal of Gastroenterology ISSN 1007-9327

RAPID COMMUNICATION

Genetic polymorphisms of *ADH2* and *ALDH2* association with esophageal cancer risk in southwest China

Shu-Juan Yang, Hua-Yu Wang, Xiao-Qing Li, Hui-Zhang Du, Can-Jie Zheng, Huai-Gong Chen, Xiao-Yan Mu, Chun-Xia Yang

Shu-Juan Yang, Xiao-Qing Li, Can-Jie Zheng, Huai-Gong Chen, Chun-Xia Yang, Department of Epidemiology, Huaxi Public Health School, Sichuan University, Chengdu 610041, Sichuan Province, China
Hua-Yu Wang, Hui-Zhang Du, Xiao-Yan Mu, Yanting Cancer Prevention and Treatment Institute. Yanting 621600, Sichuan Province, China
Supported partly by Sichuan University Youth Scientific Research Fund (2003) and partly by research fund from Sasakawa Classmate Association (065)
Correspondence to: Dr. Chun-Xia Yang, Department of Epidemiology, Huaxi Public Health School, Sichuan University, Chengdu 610041, Sichuan Province, China. chunxia815@yahoo.com.cn
Telephone: +86-28-85501604 Fax: +86-28-85501295
Received: July 9, 2007 Revised: August 20, 2007

Abstract

AIM: To evaluate the impact of alcohol dehydrogenase *2 (ADH2)* and aldehyde dehydrogenase *2 (ALDH2)* polymorphisms on esophageal cancer risk.

METHODS: One hundred and ninety-one esophageal cancer patients and 198 healthy controls from Yanting County were enrolled in this study. *ADH2* and *ALDH2* genotypes were examined by polymerase-chain-reaction with the confronting-two-pair-primer (PCR-CTPP) method. Unconditional logistic regression was used to calculate the odds ratios (OR) and 95% confidence interval (95% CI).

RESULTS: Both *ADH2*1* allele and *ALDH2*1/*2* allele showed an increased risk of developing esophageal cancer. The adjusted OR (95% CI) for *ADH2*1* allele compared with *ADH2*2/*2* was 1.65 (95% CI = 1.02-2.68) and 1.67 (95% CI = 1.02-2.72) for *ALDH2*1/*2* compared with *ALDH2*1/*1*. A significant interaction between *ALDH2* and drinking was detected regarding esophageal cancer risk, the OR was 1.83 (95% CI = 1.13-2.95). Furthermore, when compared with *ADH2*2/*2* and *ALDH2*1/*1* carriers, *ADH2*1* and *ALDH2*2* carriers showed an elevated risk of developing esophageal cancer among non-alcohol drinkers (OR = 2.46, 95% CI = 0.98-6.14), and a significantly elevated risk of developing esophageal cancer among alcohol drinkers among alcohol drinkers (OR = 9.86, 95% CI = 3.10-31.38).

CONCLUSION: *ADH2* and *ALDH2* genotypes are associated with esophageal cancer risk. *ADH2*1* allele and *ALDH2*2* allele carriers have a much higher risk of developing esophageal cancer, especially among alcohol drinkers.

Key words: Esophageal cancer; Alcohol dehydrogenase 2; Aldehyde dehydrogenase 2; Genetic polymorphisms

Yang SJ, Wang HY, Li XQ, Du HZ, Zheng CJ, Chen HG, Mu XY, Yang CX. Genetic polymorphisms of *ADH2* and *ALDH2* association with esophageal cancer risk in southwest China. *World J Gastroenterol* 2007; 13(43): 5760-5764

http://www.wjgnet.com/1007-9327/13/5760.asp

INTRODUCTION

Epidemiological studies have consistently shown that alcohol drinking is a strong risk factor for esophageal cancer[1-3]. Alcohol is not a carcinogen, but its primary metabolite, acetaldehyde, has been proven carcinogenic in experimental models[4,5]. When consumed through drinking, ethanol is metabolized primarily by class I alcohol dehydrogenase (ADH2) into acetaldehyde, an intermediate metabolite, followed by aldehyde dehydrogenase (ALDH2) into acetic acid in humans[6]. Acetaldehyde, a well-known carcinogen in animals, plays an important role in alcohol toxicity to humans[7]. The encoding genes of the two representative alcohol-metabolizing enzymes display polymorphisms which may modulate individual differences in alcohol-oxidizing capacity and drinking behavior[7,8]. *ADH2*2/*2* has about 40 times higher Vmax than the less-active *ADH2*1/*1*. *ALDH2*2* allele encodes a catalytically inactive subunit for the ALDH2 polymorphism[6,9]. Individuals with the *ALDH2*1/*2* genotype have only 6.25% of normal *ALDH2 *1/*1* activity, indicating a dominant effect of *ALDH2*2*[10]. *ADH2*2* allele and *ALDH2*2* allele, both leading to high acetaldehyde concentrations, are clustered in East Asian populations[6,11,12]. Therefore, polymorphisms of these two genes may exert their effects on esophageal cancer susceptibility. Although several studies on *ADH2* or *ALDH2* polymorphisms and esophageal cancer risk have been conducted to clarify their association[13-15], investigations on non-alcoholic drinkers are limited[16-19].

Yanting, a rural county of Sichuan Province, is one of the areas with the highest esophageal cancer mortality in China[20]. According to the report from Tumor Registry of China, the average incidence rate in this area was $100.5/10^5$ for males and $76.5/10^5$ for females during 1999-2003, which was higher than that in Linxian County and lower than that in Cixian County of Hebei Province, China. Our previous study in Yanting County has shown that alcohol drinking and smoking are common in Yanting County and the main contributors to esophageal cancer[21]. To further study alcohol-related gene polymorphisms and gene-environment interaction on esophageal cancer, a case-control study was conducted in Yanting County.

MATERIALS AND METHODS

Subjects

Esophageal cancer patients were consecutively collected from the Hospital of Yangting Cancer Research Institute (YCRI) from July 2003 to July 2004. All the patients having lived in Yanting County for more than five years were histologically diagnosed as esophageal cancer within 6 mo at the age of 35-85 years. A total of 191 patients (183 with squamous cell carcinoma and 8 with adenocarcinoma) were recruited for the study. One hundred and ninety-one healthy residents from Yanting County served as controls. In total, 191 patients and 198 controls completed a questionnaire and each provided 1 mL blood. The questionnaire included basic demographic data, information on esophageal cancer and habits such as smoking and alcohol drinking, as well as information on food and nutrition.

The ethics committee of each collaborating institution reviewed and approved the study, and informed consent was obtained from all participants.

Genotyping of ALDH2 and ADH2

Genotyping was based upon duplex polymerase-chain-reaction with the confronting-two-pair-primer (PCR-CTPP) method[7]. Briefly, the sequences of four primers used for ADH2 polymorphism are F1 ADH2: 5'-GGG CTTTAGACTGAATAACCTTGG-3'; R1 ADH2: 5'-AAC CACGTGGTCATCTGTGC-3'; F2 ADH2: 5'-GGTGGC TGTAGGAATCTGTCA-5'; R2 ADH2: 5'-AGGGAA AGAGGAAACTCCTGAA-3'. The sequences of primers used for ALDH2 polymorphism are F1 ALDH2: 5'-TGC TATGATGTGTTTGGAGCC-3'; R1 ALDH2: 5'-CCC ACACTCACAGTTTTCACTTC-3'; F2 ALDH2: 5'-GGG CTGCAGGCATACACTA-3'; R2 ALDH2: 5'-GGC TCCGAGCCACCA-3'. Each 25 μL reaction mixture contained 1.3 U Tag biocatalysts, 1.8 mmol/L Mg^{2+}, 0.24 mmol/L dNTPs, 8 primers, 15 pmol of each primer and 5-8 μL template. The PCR conditions were as follows: initial denaturation at 94℃ for 5 min, followed by 35 cycles at 94℃ for 65 s, at 60℃ for 65 s, at 72℃ for 90 s, and a final extension at 72℃ for 5 min. After transient centrifugation, agarose electrophoresis was conducted. The PCR products included 119 bp fragments of *ALDH2*1* allele, 98 bp fragments of *ALDH2*2* allele, 219 bp fragments of *ADH2* and *ADH2*1* allele, 280bp fragments of *ADH2*2* allele. The 176 bp and 219 bp fragments were the common fragments of the two alleles.

Table 1 Characteristics of patients and controls *n* (%)

Characteristic	Patients *n* = 191	Controls *n* = 198	*P*[1]	OR (95% CI)[2]
Age (yr)				
< 50	28 (14.7)	84 (42.9)		
50-64	118 (61.7)	67 (33.4)	*P* < 0.001	-
⩾ 65	45 (23.6)	47 (23.7)		
Mean age (SD)	58.3 (8.3)	52.8 (13.2)	-	-
Sex				
Male	126 (66.0)	122 (61.6)	*P* = 0.372	-
Female	65 (34.0)	76 (38.4)		-
Smoking status				
Non-smokers[3]	75 (39.3)	121 (61.1)	*P* < 0.001	1.00 (References)
Current smokers	116 (60.7)	77 (38.9)		3.76 (2.01-6.73)
Alcohol drinking status				
Non-drinkers[4]	80 (41.9)	128 (64.7)		1.00 (References)
Current alcohol drinkers	111 (58.1)	70 (35.3)	*P* < 0.001	3.16 (1.91-5.24)

[1]*P* value by chi-square test; [2]ORs for smoking and drinking were adjusted for age and sex, rapid food eating, quality of drinking water, consumption of fresh fruits, vegetable and eggs; [3]Non-smokers including ex-smokers; [4]Non-drinkers including ex-drinkers.

Statistical analysis

Statistical analyses were performed using the STATA statistical package (version 8, STATA, College Station, TX). Demographic data, smoking and drinking status were compared between patients and controls by chi-square test. The subjects smoking more than 10 cigarettes per week for at least 6 mo were defined as current smokers. The subjects consuming more than 50 mL of distilled spirits per week for at least 6 mo were defined as current drinkers. The odds ratio (OR) and 95% confidence interval (95% CI) generated in unconditional logistic regression model were used as measures of association for the risk of esophageal cancer. The relationship of ALDH2 and ADH2 polymorphisms with esophageal cancer risk was determined after adjustment for sex, age, smoking, rapid food eating, quality of drinking water, consumption of fresh fruits, vegetables and eggs. The combined effect of alcohol consumption and *ADH2* and *ALDH2* genotypes on esophageal cancer was also examined in this study. Chi-square test was used to check the Hardy-Weinberg equilibrium (HWE) in controls for the assessment of discrepancies between genotype and allele frequencies.

RESULTS

The characteristics of subjects are listed in Table 1. The mean age of 191 patients and 198 controls was 58.3 and 52.8 years, respectively. There was a significant difference in smoking and alcohol drinking status ($P < 0.001$) between patients and controls. When compared with non-smokers, the adjusted OR of current smokers was 3.76 (95% CI = 2.01-6.73). Current alcohol drinkers also showed an increased risk of developing esophageal cancer (OR = 3.16, 95% CI = 1.91-5.24) when compared with non-drinkers. Almost all the alcohol drinkers drank hard

Table 2 *ADH2, ALDH2* **genotype and allele frequencies and ORs for esophageal cancer** *n* **(%)**

ADH2	Cases (*n* = 191)	Controls (*n* = 198)	OR (95% CI)[1]
**2/*2*	78 (40.8)	100 (50.5)	1.00 (Reference)
**1/*2*	80 (41.9)	76 (38.4)	1.89 (1.10-3.22)
**1/*1*	33 (17.3)	22 (11.1)	1.91 (0.92-3.95)
**1/*2 + *1/*1*	113 (59.2)	98 (49.5)	1.65 (1.02-2.68)
ALDH2			
**1/*1*	90 (47.1)	108 (54.5)	1.00 (References)
**1/*2*	98 (51.3)	76 (38.4)	1.67 (1.02-2.72)
**2/*2*	3 (1.6)	14 (7.1)	0.26 (0.06-1.09)
**1/*2 + *2/*2*	101 (52.9)	90 (45.5)	1.43 (0.89-2.30)
Allele frequencies			OR (95% CI)[2]
ADH2			
**2*	236 (61.8)	276 (69.7)	1.00 (References)
**1*	146 (38.2)	120 (30.3)	1.42 (1.06-1.92)
ALDH2			
**1*	278 (72.8)	292 (73.7)	1.00 (References)
**2*	104 (27.2)	104 (26.3)	1.05 (0.76-1.44)

[1]ORs for gene frequencies were adjusted for sex, age, smoking, drinking, rapid food eating, quality of drinking water, consumption of fresh fruits, vegetable and eggs; [2]ORs for allele frequencies were not adjusted.

liquor containing over 48% ethanol in this area and the main tobacco type was cigarette (data not shown).

The genotype and allele distribution of *ADH2* and *ALDH2* and their OR (95% CI) for esophageal cancer risk are listed in Table 2. The ADH2 genotype frequency was 50.5% for *ADH2*2/*2*, 38.4% for *ADH2*1/*2*, and 11.1% for *ADH2*1/*1* in controls, which were in accordance with the HWE (P = 0.20) (data not shown). When compared with the *ADH2*2/*2* genotype, the esophageal cancer risk in subjects harboring *ADH2*1* allele was significantly elevated (OR = 1.65, 95% CI = 1.02-2.68). The OR for *ADH2*1* allele carriers was 1.42 (95% CI = 1.06-1.92) when compared with *ADH2*2* allele carriers. The frequency of *ALDH2*1/*1*, *ALDH2*1/*2* and *ALDH2*2/*2* was 54.6%, 38.4% and 7.1%, respectively, in controls, which were also in accordance with the HWE (P = 0.90) (data not shown). The *ALDH2*1/*2* genotype was associated with an increased risk of developing esophageal cancer (OR = 1.67, 95% CI = 1.02-2.72).

The combined effect of alcohol consumption and *ADH2* and *ALDH2* genotypes on esophageal cancer risk is shown in Table 3. When compared with non-drinkers harboring *ADH2*2/*2* genotype, alcohol drinkers carrying *ADH2*1* showed an increased risk of developing esophageal cancer (OR = 3.94, 95% CI = 1.76-8.81). Similarly, a significantly increased risk of developing esophageal cancer was found in alcohol drinkers harboring *ALDH2*2* genotype (OR = 4.82, 95% CI = 2.06-11.27), compared with non-drinkers harboring *ALDH2*1/*1* genotype. Furthermore, a significant interaction between *ALDH2* and alcohol drinking was detected regarding esophageal cancer risk (adjusted OR = 1.83, 95% CI = 1.13-2.95) (data not shown). When compared with *ADH2*2/*2* and *ALDH2*1/*1* carriers, *ADH2*1* and *ALDH2*2* carriers showed an elevated risk of developing esophageal cancer in non-drinkers (OR = 2.46, 95% CI = 0.98-6.14) and a significantly elevated risk of developing esophageal cancer in alcohol drinkers (OR = 9.86, 95% CI = 3.10-31.38).

DISCUSSION

In the present study, the risk of developing esophageal cancer was significantly increased in *ALDH2*1/*2* gene carriers; subjects with *ADH2*1* allele had a higher risk of developing esophageal cancer than those with *ADH2*2/*2*; carrying both *ALDH2*2* allele and *ADH2*1* allele, suggesting that alcohol drinking greatly increases the susceptibility to esophageal cancer.

*ALDH2*2* allele encoding an inactive subunit of ALDH2 is prevalent in Asian[22]. It was reported that acetaldehyde concentrations after drinking alcohol are mainly dependent on the enzyme activation of *ALDH2*[6,23]. After consumption of alcohol, blood acetaldehyde concentrations in those with *ALDH2*2/*2* and *ALDH2*1/*2* are 19- and 6-fold higher than in those with *ALDH2*1/*1*[24]. Case-control studies of Japanese and Chinese alcohol drinkers[10,15,16,17,19,25,26] consistently demonstrated that inactive *ALDH2*1/*2* is a strong risk factor for esophageal cancer. Our data also show that individuals with *ALDH2*1/*2* (OR = 1.67, 95% CI = 1.02-2.72) had a significantly increased risk of developing esophageal cancer compared to those with *ALDH2*1/*1*. Furthermore, our results reveal that there was a significant interaction between *ALDH2* and alcohol drinking, indicating that esophageal cancer is associated with alcohol drinking, which is influenced by the polymorphism of *ALDH2*.

Previous case-control studies investigating the association between *ADH2* genotype and esophageal cancer demonstrated that *ADH2*1* allele independently enhances esophageal cancer risk[6,10,14,17,19]. In our study, the adjusted OR for subjects carrying *ADH2*1* allele was 1.65 (95% CI = 1.02-2.68), which is in line with former studies[6,10,14,17,19]. There are several reasons which may explain this finding. ADH2 is the predominant enzyme among low-Km class I ADHs expressed in the esophagus[27]. In *ADH2*1/*1* homozygotes, concentrations of ethanol may linger in the esophageal mucosa during the slow oxidation of *ADH2*. Although ethanol is not a cancerogen itself, tobaccos and some other exogenous cancerogens would be assimilated much easier, thus increasing the effect of cancerogen. Besides, ethanol can induce the composition of phase I drug metabolism enzymes such as CYP2E1. Moreover, alcohol drinkers with *ADH2*1* genotype tend to have experienced 'binge-drinking' and withdrawal syndrome earlier in life than those with other genotypes[14,23]. Therefore, *ADH2*1*-mediated alcohol-related events may contribute to the enhancement of esophageal cancer risk in alcohol drinkers.

It was reported that combination of *ADH2*1* allele and *ALDH2*2* allele can greatly enhance cancer risk among alcoholics[10] and general populations[6,19,23]. Carrying these two alleles simultaneously indicates a longer time of exposure to alcohol and highly-concentrated acetaldehyde, thus increasing the individual's susceptibility to esophageal cancer. In the present study, the OR for alcohol drinkers

Table 3 Combined effect of alcohol consumption and *ADH2* and *ALDH2* polymorphisms on esophageal cancer *n* (%)

ADH2		Alcohol drinking status					
		Non-drinkers[2]			Current alcohol drinkers		
		Cases (*n* = 80)	Controls (*n* = 128)	OR (95% CI)[1]	Cases (*n* = 111)	Controls (*n* = 70)	OR (95% CI)[1]
*2/*2		37 (46.3)	65 (50.8)	1.00 (References)	41 (36.9)	35 (50.0)	1.88 (0.86-4.15)
*1/*2 or *1/*1		43 (53.7)	63 (49.2)	1.21 (0.63-2.33)	70 (63.1)	35 (50.0)	3.94 (1.76-8.81)
ALDH2							
*1/*1		33 (41.3)	67 (52.3)	1.00 (References)	57 (51.4)	41 (58.6)	3.15 (1.39-7.13)
*1/*2 or *2/*2		47 (58.7)	61 (47.7)	2.03 (1.03-3.99)	54 (48.6)	29 (41.4)	4.82 (2.06-11.27)
ADH2 and ALDH2							
*2/*2	*1/*1	15 (18.8)	42 (32.8)	1.00 (References)	17 (15.3)	20 (28.6)	2.54 (0.84-7.67)
*1/*2 or *1/*1	*1/*2 or *2/*2	25 (31.3)	38 (29.7)	2.46 (0.98-6.14)	30 (27.0)	14 (20.0)	9.86 (3.10-31.38)

[1]ORs were adjusted for sex, age, smoking, rapid food eating, quality of drinking water, consumption of picked vegetables and fresh fruits, vegetables and eggs; [2]Non-drinkers including ex-drinkers.

with both *ADH2*1* allele and *ALDH2*2* allele was 9.86 (95% CI = 3.10-31.38), which is consistent with former studies[10].

Some limitations of this study should be considered. One is that controls were selected from residents in Yanting County and their basic features are consistent with general people, such as smoking and alcohol drinking. In this study, the genotype distribution among the controls closely conformed to the Hardy-Weinberg equilibrium. So our control group represents the general population of Yanting County. In addition, the present study was not an age matched case control study and age is a risk factor for esophageal cancer. However, our results are age-adjusted and may not be biased by age. The small number of subjects is another limitation, so further studies in a larger scale appear warranted.

In conclusion, *ADH2* and *ALDH2* genotypes are associated with esophageal cancer risk. In addition, the risk of developing esophageal cancer increases in subjects carrying *ADH2*1* allele and *ALDH2*1* allele, especially in alcohol drinkers. Our present findings provide more information on the *ADH2* and *ALDH2* polymorphisms of esophageal cancer in Chinese.

ACKNOWLEDGMENTS

The authors thank the Epidemiology Department of Aichi Cancer Center for providing the primers and Dr. K Matsuo for genotyping technical support.

COMMENTS

Background

Epidemiological studies have consistently shown that alcohol drinking is a strong risk factor for esophageal cancer. When consumed through drinking, ethanol is metabolized primarily by class I alcohol dehydrogenase (ADH2) into acetaldehyde, an intermediate metabolite, followed by aldehyde dehydrogenase (ALDH2) into acetic acid in humans. Acetaldehyde, a well-known carcinogen in animals, plays an important role in alcohol toxicity to humans. *ADH2*2* allele and *ALDH2*2* allele, both leading to high acetaldehyde concentrations, are clustered in East Asian populations. Therefore, the polymorphism of these two genes may exert effect on esophageal cancer susceptibility.

Research frontiers

Esophageal cancer risk is associated with habits and food consumption, such as smoking, alcohol drinking, consumption of fresh fruits and vegetables. However, the effect of gene polymorphisms or gene-environment interaction on esophageal cancer risk has become a hotspot in recent researches. The present study reports the association of ADH2 and ALDH2 gene polymorphisms with esophageal cancer risk. Furthermore, interaction and combination impacts on esophageal cancer risk between gene polymorphisms and alcohol drinking are also analyzed and discussed.

Innovations and breakthroughs

Our study showed that *ADH2* and *ALDH2* polymorphisms were associated with esophageal cancer risk in a high-incidence area of southwest China. Previous studies were mainly conducted in Japanese males or alcoholics. In addition, our controls were collected from the healthy residents and the patients were histologically diagnosed as esophageal cancer within 6 mo, which is superior to hospital-based case-control studies.

Applications

The present study indicates ADH2 and ALDH2 genotypes are associated with esophageal cancer risk, the risk of developing esophageal cancer increases in subjects carrying ADH2*1 allele and ALDH2*2 allele, especially in alcohol drinkers. The present findings can provide more information on the ADH2 and ALDH2 polymorphisms of esophageal cancer in Chinese and help make the prevention strategy against esophageal cancer in China.

Terminology

Alcohol dehydrogenase 2 (*ADH2*): A zinc-containing enzyme which oxidizes primary and secondary alcohols or hemiacetals in the presence of NAD. In alcoholic fermentation, it catalyzes the final step of reducing aldehyde to alcohol in the presence of NADH and hydrogen. Dehydrogenase 2 (*ALDH2*): An enzyme that oxidizes aldehyde in the presence of NAD+ and water to acid and NADH. Genetic polymorphisms: The regular and simultaneous occurrence of two or more discontinuous genotypes in a single interbreeding population. The concept includes differences in genotypes ranging in size from a single nucleotide site to large nucleotide sequences visible at a chromosomal level.

Peer review

This is an interesting paper investigating the association between ADH2 and ALDH2 polymorphisms, environmental factors and esophageal cancer risk in a relatively small cohort of cancer patients. The main conclusion of the manuscript is that ADH2 and ALDH2 genotypes are associated with esophageal cancer risk; the risk of developing esophageal cancer increases greatly in subjects carrying ADH2*1 allele and ALDH2*2 allele, especially in alcohol drinkers.

REFERENCES

1 **Castelletto R**, Castellsague X, Muñoz N, Iscovich J, Chopita N, Jmelnitsky A. Alcohol, tobacco, diet, mate drinking, and esophageal cancer in Argentina. *Cancer Epidemiol Biomarkers Prev* 1994; **3**: 557-564

2 **Brown LM**, Devesa SS. Epidemiologic trends in esophageal and gastric cancer in the United States. *Surg Oncol Clin N Am* 2002; **11**: 235-256

3 **Kinjo Y**, Cui Y, Akiba S, Watanabe S, Yamaguchi N, Sobue

T, Mizuno S, Beral V. Mortality risks of oesophageal cancer associated with hot tea, alcohol, tobacco and diet in Japan. *J Epidemiol* 1998; **8**: 235-243

4 **Woutersen RA**, Appelman LM, Van Garderen-Hoetmer A, Feron VJ. Inhalation toxicity of acetaldehyde in rats. III. Carcinogenicity study. *Toxicology* 1986; **41**: 213-231

5 **Dellarco VL**. A mutagenicity assessment of acetaldehyde. *Mutat Res* 1988; **195**: 1-20

6 **Yokoyama A**, Kato H, Yokoyama T, Tsujinaka T, Muto M, Omori T, Haneda T, Kumagai Y, Igaki H, Yokoyama M, Watanabe H, Fukuda H, Yoshimizu H. Genetic polymorphisms of alcohol and aldehyde dehydrogenases and glutathione S-transferase M1 and drinking, smoking, and diet in Japanese men with esophageal squamous cell carcinoma. *Carcinogenesis* 2002; **23**: 1851-1859

7 **Tamakoshi A**, Hamajima N, Kawase H, Wakai K, Katsuda N, Saito T, Ito H, Hirose K, Takezaki T, Tajima K. Duplex polymerase chain reaction with confronting two-pair primers (PCR-CTPP) for genotyping alcohol dehydrogenase beta subunit (ADH2) and aldehyde dehydrogenase 2 (ALDH2). *Alcohol Alcohol* 2003; **38**: 407-410

8 **Bosron WF**, Li TK. Genetic polymorphism of human liver alcohol and aldehyde dehydrogenases, and their relationship to alcohol metabolism and alcoholism. *Hepatology* 1986; **6**: 502-510

9 **Yoshida A**, Hsu LC, Yasunami M. Genetics of human alcohol-metabolizing enzymes. *Prog Nucleic Acid Res Mol Biol* 1991; **40**: 255-287

10 **Yokoyama A**, Muramatsu T, Omori T, Yokoyama T, Matsushita S, Higuchi S, Maruyama K, Ishii H. Alcohol and aldehyde dehydrogenase gene polymorphisms and oropharyngolaryngeal, esophageal and stomach cancers in Japanese alcoholics. *Carcinogenesis* 2001; **22**: 433-439

11 **Hamajima N**, Takezaki T, Tajima K. Allele Frequencies of 25 Polymorphisms Pertaining to Cancer Risk for Japanese, Koreans and Chinese. *Asian Pac J Cancer Prev* 2002; **3**: 197-206

12 **Oota H**, Pakstis AJ, Bonne-Tamir B, Goldman D, Grigorenko E, Kajuna SL, Karoma NJ, Kungulilo S, Lu RB, Odunsi K, Okonofua F, Zhukova OV, Kidd JR, Kidd KK. The evolution and population genetics of the ALDH2 locus: random genetic drift, selection, and low levels of recombination. *Ann Hum Genet* 2004; **68**: 93-109

13 **Yokoyama A**, Muramatsu T, Ohmori T, Higuchi S, Hayashida M, Ishii H. Esophageal cancer and aldehyde dehydrogenase-2 genotypes in Japanese males. *Cancer Epidemiol Biomarkers Prev* 1996; **5**: 99-102

14 **Yokoyama A**, Muramatsu T, Omori T, Matsushita S, Yoshimizu H, Higuchi S, Yokoyama T, Maruyama K, Ishii H. Alcohol and aldehyde dehydrogenase gene polymorphisms influence susceptibility to esophageal cancer in Japanese alcoholics. *Alcohol Clin Exp Res* 1999; **23**: 1705-1710

15 **Chao YC**, Wang LS, Hsieh TY, Chu CW, Chang FY, Chu HC. Chinese alcoholic patients with esophageal cancer are genetically different from alcoholics with acute pancreatitis and liver cirrhosis. *Am J Gastroenterol* 2000; **95**: 2958-2964

16 **Matsuo K**, Hamajima N, Shinoda M, Hatooka S, Inoue M, Takezaki T, Tajima K. Gene-environment interaction between an aldehyde dehydrogenase-2 (ALDH2) polymorphism and alcohol consumption for the risk of esophageal cancer. *Carcinogenesis* 2001; **22**: 913-916

17 **Hori H**, Kawano T, Endo M, Yuasa Y. Genetic polymorphisms of tobacco- and alcohol-related metabolizing enzymes and human esophageal squamous cell carcinoma susceptibility. *J Clin Gastroenterol* 1997; **25**: 568-575

18 **Boonyaphiphat P**, Thongsuksai P, Sriplung H, Puttawibul P. Lifestyle habits and genetic susceptibility and the risk of esophageal cancer in the Thai population. *Cancer Lett* 2002; **186**: 193-199

19 **Yang CX**, Matsuo K, Ito H, Hirose K, Wakai K, Saito T, Shinoda M, Hatooka S, Mizutani K, Tajima K. Esophageal cancer risk by ALDH2 and ADH2 polymorphisms and alcohol consumption: exploration of gene-environment and gene-gene interactions. *Asian Pac J Cancer Prev* 2005; **6**: 256-262

20 **Kou Y**, Zhang J, Chen G, Wu Z, Yang J, Jiang G, Zhao Y. Mutation of p53 gene in esophageal precancerous cells. *Sichuan Daxue Xuexao Yixueban* 2003; **34**: 306-309

21 **Yang CX**, Wang HY, Wang ZM, Du HZ, Tao DM, Mu XY, Chen HG, Lei Y, Matsuo K, Tajima K. Risk factors for esophageal cancer: a case-control study in South-western China. *Asian Pac J Cancer Prev* 2005; **6**: 48-53

22 **Higuchi S**, Matsushita S, Murayama M, Takagi S, Hayashida M. Alcohol and aldehyde dehydrogenase polymorphisms and the risk for alcoholism. *Am J Psychiatry* 1995; **152**: 1219-1221

23 **Wu CF**, Wu DC, Hsu HK, Kao EL, Lee JM, Lin CC, Wu MT. Relationship between genetic polymorphisms of alcohol and aldehyde dehydrogenases and esophageal squamous cell carcinoma risk in males. *World J Gastroenterol* 2005; **11**: 5103-5108

24 **Mizoi Y**, Yamamoto K, Ueno Y, Fukunaga T, Harada S. Involvement of genetic polymorphism of alcohol and aldehyde dehydrogenases in individual variation of alcohol metabolism. *Alcohol Alcohol* 1994; **29**: 707-710

25 **Yokoyama A**, Muramatsu T, Ohmori T, Yokoyama T, Okuyama K, Takahashi H, Hasegawa Y, Higuchi S, Maruyama K, Shirakura K, Ishii H. Alcohol-related cancers and aldehyde dehydrogenase-2 in Japanese alcoholics. *Carcinogenesis* 1998; **19**: 1383-1387

26 **Tanabe H**, Ohhira M, Ohtsubo T, Watari J, Yokota K, Kohgo Y. Genetic polymorphism of aldehyde dehydrogenase 2 in patients with upper aerodigestive tract cancer. *Alcohol Clin Exp Res* 1999; **23**: 17S-20S

27 **Chao YC**, Wang LS, Hsieh TY, Chu CW, Chang FY, Chu HC. Chinese alcoholic patients with esophageal cancer are genetically different from alcoholics with acute pancreatitis and liver cirrhosis. *Am J Gastroenterol* 2000; **95**: 2958-2964

28 **Yin SJ**, Bosron WF, Magnes LJ, Li TK. Human liver alcohol dehydrogenase: purification and kinetic characterization of the beta 2 beta 2, beta 2 beta 1, alpha beta 2, and beta 2 gamma 1 "Oriental" isoenzymes. *Biochemistry* 1984; **23**: 5847-5853

S- Editor Zhu LH **L- Editor** Wang XL **E- Editor** Liu Y

Online Submissions: wjg.wjgnet.com
www.wjgnet.com
wjg@wjgnet.com

World J Gastroenterol 2007 November 21; 13(43): 5765-5770
World Journal of Gastroenterology ISSN 1007-9327

RAPID COMMUNICATION

Construction of humanized carcinoembryonic antigen specific single chain variable fragment and mitomycin conjugate

De-Jie Chen, Zui Tan, Feng Chen, Tian Du

De-Jie Chen, Zui Tan, Feng Chen, Tian Du, Department of General Surgery, Zhongnan Hospital of Wuhan University, Wuhan 430071, Hubei Province, China
Correspondence to: Professor Zui Tan, Department of General Surgery, Zhongnan Hospital of Wuhan University, 169 Donghu Road, Wuhan 430071, Hubei Province, China. docdj_1130@yahoo.com.cn
Telephone: +86-27-63436739
Received: April 26, 2007 Revised: August 23, 2007

Abstract

AIM: To construct a new target-oriented conjugate of humanized carcinoembryonic antigen (CEA) specific single chain variable fragment (scFv) and mitomycin (MMC) against colorectal cancer, and to investigate its influence on the growth and apoptosis of colorectal cancer cells.

METHODS: The primer was designed according to the gene sequence described in reference 16, which respectively contains restriction enzyme cleavage sites *Bam*H Ⅰ and *Eco*R Ⅰ in its upstream and downstream. PCR was performed with the plasmid as template containing genes of humanized anti-CEA scFv. The product was digested by *Bam*H Ⅰ and *Eco*R Ⅰ, and connected to an expression vector which also has the restriction enzyme cleavage sites *Bam*H Ⅰ and *Eco*R. Expression of the reaction was induced by isopropy-β-D-thiogalactoside (IPTG). Then the expression product was covalently coupled with MMC by dextran T-40. The immunoreactivity of the conjugate against colorectal cancer cells as well as CEA was measured by enzyme linked immunosorbent assay (ELISA). The inhibiting ratio of conjugate on the growth of colorectal cancer cells was also measured by ELISA. The effect of conjugate on the apoptosis of colorectal cancer cells was determined by flow cytometry (FCM).

RESULTS: Restriction endonuclease cleavage and gene sequencing confirmed that the expression vector was successfully constructed. Sodium dodecyl sulfate polyacrylamide gel electropheresis (SDS-PAGE) confirmed that this vector correctly expressed the fusion protein. ELISA confirmed that the conjugate had quite a strong immunoreactivity against colorectal cancer cells and CEA. The conjugate had inhibitory effects on colorectal cancer cells in a concentration-dependent manner and could induce apoptosis of colorectal cancer cells in a concentration-dependent manner.

CONCLUSION: The CEA-scFv-MMC conjugate can be successfully constructed and is able to inhibit the growth and induce apoptosis of colorectal cancer cells.

Key words: Carcinoembryonic antigen; Single chain variable fragment; Mitomycin; Immunoconjugates; Colorectal cancer

Chen DJ, Tan Z, Chen F, Du T. Construction of humanized carcinoembryonic antigen specific single chain variable fragment and mitomycin conjugate. *World J Gastroenterol* 2007; 13(43): 5765-5770

http://www.wjgnet.com/1007-9327/13/5765.asp

INTRODUCTION

Significant improvement has been achieved in the treatment of advanced colorectal cancer in the past decade[1]. New cytotoxic agents and new monoclonal antibodies (mAb) have been shown to substantially improve patient outcomes in randomized trials[2]. Nevertheless, the prognosis of patients with advanced colorectal cancer remains relatively poor with a median survival of approximately 20 mo in optimally treated patients[3]. Therefore, additional treatment strategies are needed in order to further improve the outcomes.

With advances in oncomolecular biology, the mechanism of tumor genesis and development is better understood[4], which provides a new medication pattern against tumors. Since a conception of target-oriented medication against tumors has been recently brought forward[5], we can design and develop medications aiming at target spots of specific molecules and genes to selectively kill tumor cells according to the known abnormal molecules and genes related to the genesis of tumors. Target-oriented medication against tumors provides a new effective way of treating malignant tumors such as mammary cancer, intestinal cancer and lung cancer[6-8], and can directly deliver chemotherapeutics for the tumor and form a high local drug concentration so as to decrease the total dosage and further reduce the toxic and side effects[9].

An ideal target spot of tumor treatment has the following features. (1) It is a kind of macromolecules which are rather critical for malignancy phenotype; (2) It has no obvious expression in important organs and tissues; (3) It has

biological correlativity; (4) It can be repeatedly tested on clinical specimens; (5) It has apparent correlativity with the clinical outcome[10]. Carcinoembryonic antigen (CEA) is a 180 ku cell surface-expressed glycoprotein antigen present in a number of adenocarcinomas, especially in colorectal cancer[11]. The gene sequence and three-dimensional structure of CEA have been reported elsewhere[12]. CEA is a member of the immunoglobulin superfamily and has cell adhesion properties as well as other less clearly defined roles[13]. Since it corresponds to all features of the target spot of tumor treatment, it is the ideal target spot of treating colorectal cancer.

At present, research on target-oriented medication against advanced colorectal cancer involved 3 different target-oriented drugs that have achieved significant curative effect: epidermal growth factor receptor (EGFR) inhibitors, vascular endothelial growth factor receptor (VEGFR) inhibitors, and cyclooxygenase-2 (COX-2) inhibitors[14]. By coupling radio immunity drugs with anti-CEA monoclonal antibody, Vogel[15] has achieved favorable therapeutic effectiveness on nude mice model of liver metastasis of colorectal cancer, thus opening up a new idea for target-oriented medication against advanced colorectal cancer. Based on the above-mentioned theory, we constructed a humanized anti-CEA single-chain antibody (scFv) and coupled it with mitomycin (MMC), a chemotherapeutic agent against colorectal cancer, and investigated the influence of this conjugate on the growth and apoptosis of colorectal cancer cells.

MATERIALS AND METHODS

Materials

Plasmid pUC18 containing humanized anti-CEA-scFv was kindly provided by Professor Mark Sherman (the Berkman Research Institute, USA). *E.coli* DH5α and expression plasmid pGEX-4T-1 were stored in the Virus Research Institute, Medical College of Wuhan University. T4 DNA ligase and restriction endonuclease were purchased from New England Biolabs (USA). High fidelity DNA polymerase and DNA gel extraction kits were purchased from the Promega Company (USA). Plasmid extracting and purifying kits were the products of Vegen Company (Hangzhou, China). Glutathione acyltransferase purification kits were purchased from the Clonetech Company (USA). MMC was purchased from the Roche Company (USA). Bovine serum albumin (BSA), Tween 20, PI dyebath and Hanks solution were bought from Fuzhou Maixin Biology Company (China). Glucosan T-40, cysteine, N-2 N-ethylmaleimide (NEMI), horseradish peroxidase-labeled goat anti-mouse IgG, dimethyl sulphoxide (DMSO) were bought from the Sigma Company (USA). RPMI 1640 culture medium was bought from the Gibico Company (USA). CEA was produced by the Zymed Company (USA). Colorectal cancer cell lines SW480, SW620 and LoVo were provided by China Center for Typical Culture Collection (CCTCC) (Wuhan, China). Primer synthesis and gene sequencing were performed by the Sangon Company (Shanghai, China).

Primers were designed using the program Oligo4.1 and synthesized by Sangon Company (Shanghai, China) as previously described[16], a restriction enzyme cleavage site *Bam*H I was added to the end 5', and a restriction enzyme cleavage site *Eco*R I was added to the end 3'. Upstream primer: 5'CGGGATCCATGGACAGAGTCACA3', downstream primer: 5'CCGAATTCTCCACGTGCACTCGAGACGGTGAC3'. The underlined parts are the restriction enzyme cleavage sites.

Construction of expression vector

Plasmid pUC18 containing humanized anti-CEA scFv T84.66 was taken as the template to perform PCR with its upstream and downstream primers in 50 μL reaction system containing 5 μL template, 5 μL reaction buffer, 2 μL upstream and downstream primers, 0.5 μL high fidelity DNA polymerase, 4 μL dNTP and 33.5 μL deionized water. Samples were heated at 94℃ for 5 min, followed by 35 cycles of heating at 94℃ for 30 s, at 55℃ for 30 s and at 72℃ for 30 s. The temperature was held constant at 72℃ for 7 min to ensure complete extension. The completed PCR reaction mix was electrophoresed on 1% agarose gel and the desired product was extracted from 200 mg gel slice. The purified product was digested with *Bam*H I and *Eco*R. cDNA of anti-CEA scFv T84.66 containing correspondence restriction enzyme sites to pGEX-4T-1 was produced. Prokaryon expression vector pGEX-4T-1 was also digested with *Bam*H I and *Eco*R. After identified by agarose gel electrophoresis, the plasmid with a cohesive end was connected to the cDNA of anti-CEA scFv T84.66 acquired previously. Connection reaction was performed in 10 μL system. The reaction product was transformed into competent cell line DH5α and the positive clone of recombined CEA-scFv-pGEX-4T-1 was acquired. Restriction endonuclease cleavage and gene sequencing confirmed that the scFv fragment was correctly interpolated into pGEX4-T-1. Positive plasmid was extracted and purified with the kits from Vegen Company (Hangzhou, China).

Expression and purification of the fusion protein

Expression of E. coli DH5α containing the positive plasmid was induced by isopropyl-β-D thiogalactoside (IPTG) followed by sodium dodecyl sulfate polyacrylamide gel electropheresis (SDS-PAGE). The level of this protein in total bacterial protein was detected with a thin layer chromatogram (TLC) scanner. The correctly expressed DH5α containing the recombinant plasmid was cultured in 500 mL triangular flask. After IPTG was added to induce expression of the protein, the product was purified with glutathione acyltransferase purification kit according to its manufacturer's instructions. The purified protein was collected with a step-by-step collector containing 500 μL per tube, and the absorbance value was measured at 280 nm to quantify the protein.

Construction of CEA-scFv-MMC conjugate

A pertinent amount of dextran T-40 was admixed with sodium periodate as previously described[17], and the mixture reacted for 3 h at ordinary temperature away from light, then sufficiently dialyzed with deionized water. After cryodesiccation, poly aldehyde dextran (PAD) was produced. Fifty mg of PAD was admixed with 100 mg of MMC, and

the mixture was incubated at 4℃ for 12 h away from light. Then 80 mg of CEA-scFv purified protein was added, stirred reaction was carried out for 12 h and terminated with sodium borohydride. The reaction product was purified with Sephadex G-75 for CEA-scFv-MMC conjugate. The molecular constitution of the conjugate was measured by spectrophotometry. The absorbance value of the conjugate was measured respectively at 280 nm and 488 nm, and at 595 nm after stained with Coomassie brilliant blue. The mole ratio of each composition was recorded.

Detection of immunocompetence of CEA-scFv-MMC conjugate by ELISA

Colorectal tumor cells SW480, SW620 and LoVo were cultured *in vitro* in 96-well culture plates (10^4 cells per well). Twenty-four hours later, 2.5 g/L glutaraldehyde precooled at 4℃ was added (50 μL per well). The cells were fixed at 4℃ for 5min, washed 3 times with PBS and stored at -20℃. When it was used, 10 g/L BSA was added (200 μL per well), sealed overnight at 4℃, then washed with PBS-Tween 20 (PBS-T), and CEA-scFv-MMC diluted with multiple proportion was added (50 μL per well). The mixture was left to react at 37℃ for 1 h, then washed 3 times with PBS-T. Horseradish peroxidase-labeled goat anti-mouse IgG antibody was added (50 μL per well). The mixture was incubated at 37℃ for 1 h, washed 5 times with PBS-T. Enzyme reaction substrate was added (200 μL per well), the mixture was incubated to react for 15 min at room temperature away from light and terminated by adding 2 mol/L sulfuric acid. The absorbance value was measured at 490 nm with enzyme labelling instruments to determine the immunoreactivity of CEA-scFv-MMC against colorectal cancer cells. CEA (pH 7.5) at the concentration of 1.35 g/L was put into culture plates (100 μL per well), the mixture was incubated over night at 4℃. The supernatant was discarded. The mixture was washed 3 times with PBS and stored at -20℃. When it was used, 10 g/L BSA was added (200 μL per well), sealed overnight, and washed with PBS-T buffer solution. Other steps were the same as above, and the immunoreactivity of CEA-scFv-MMC against CEA was detected.

Growth inhibition ratio of conjugate to colorectal cancer cells

The colorectal cancer cells LoVo were cultured in RPMI1640 culture medium, routine serial subculture was carried out in an incubator containing 50 mL/L CO_2 at 37℃. The culture medium was replaced with drug-containing culture medium 24 h after the cells adherently grew to 70%-80% monolayer, then the experiment was carried out. The cells were digested with trypsin and blown to single cell suspension. The cell concentration was counted, adjusted to 1×10^8 cells/L, which were inoculated into 96-well culture plates (0.2 mL per well). The original fluid was discarded after 24 h culture. CEA-scFv-MMC conjugate with different concentrations was added into the wells (0 mg/L in control group; 25 mg/L, 50 mg/L, 100 mg/L, 150 mg/L, 200 mg/L, 300 mg/L and 400 mg/L, respectively, in treatment group) and cultured for 48 h. Twenty μL of MTT solution (2.5 g/L) was added into each well, and cultured for 4 h. After the supernatant was carefully blotted, 150 μL of 100 g/L DMSO was added into each well. The absorbance value (A_{630nm}) of each well was measured by enzyme labelling instruments after gently agitated on the oscillator. The growth inhibition ratio at each concentration in treatment group was calculated according to the following formula: growth inhibition ratio IR (%) = (1-average A_{630nm} of treatment group/A_{630nm} of control group) × 100%.

Influence of conjugate on apoptosis of colorectal cancer cells

Colorectal cancer cells treated with different concentrations of CEA-scFv-MMC conjugate were cultured for 3 d and 10^6 cells were collected, fixed with 700 mL/L ethanol. The dying cell suspension was filtrated through nylon net (400 meshes) and washed 3 times with PBS followed by addition of 10 μL of Annexin V-fluorescein isothiocyanate and PI solution. The mixture was blended in ice bath for 10 min away from light. A flow cytometer (FCM) was used to detect the influence of CEA-scFv-MMC conjugate on the apoptosis of colorectal cancer cells.

Experiments approved by the local ethical committee were performed after the patients gave their informed consent. All the experimental data were expressed as mean ± SD. Comparison between treatment and control groups was made by *t* test and their ratios by χ^2 test. The correlation between the two groups was analyzed with collinearity. $P < 0.05$ was considered statistically significant.

RESULTS

Construction of recombinant plasmid CEA-scFv-pGEX-4T-1

A 810 bp specific band was obtained by PCR amplification with pUC18 as template. cDNA of PCR amplification was completely in accordance with the gene sequence of humanized anti-CEA specific scFv T84.66. The positive clone of recombinant plasmid CEA-scFv-pGEX-4T-1 was identified by double restriction endonuclease cleavage with *Bam*H I and *Eco*R I. Two specific bands were obtained in line 1, one was 4.7 kb and the other was 810 bp, and a 5.5 kb band was obtained in line 2. The 4.7 kb band represented pGEX-4T-1, 810 bp band anti-CEA-scFv, and the 5.5 kb band the recombinant plasmid CEA-scFv-pGEX-4T-1 (Figure 1). The result was completely consistent with our hypothesis. Meanwhile, the scFv gene was correctly inserted to the expression vector.

Expression of scFv gene

After induction of IPTG, expression of the scFv gene inserted to the pGEX-4T-1 was stable. A new protein band was obtained at M_r 49 000 after SDS-PAGE, and its size was in accordance with GST (M_r 26 000) and scFv-CEA (M_r 23 000) fusion protein (Figure 2). This new protein band was preliminarily identified as the expressed CEA-scFv/GST fusion protein. TLC scan showed that the expressed fusion protein amounted to 26% of the total bacterial protein.

Components and immunoreactivity of the conjugate

The components of the conjugate were calculated. The molecule ratio of CEA-scFv: Dextran T-40: MMC in the conjugate was 1:1.2:38. The immunoreactivity of the con-

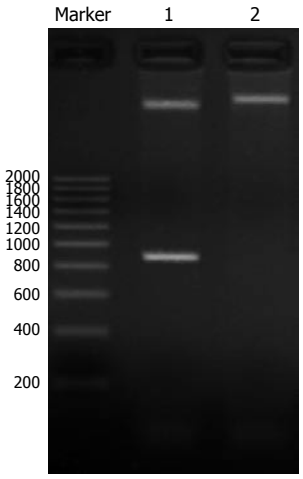

Figure 1 PCR amplification showing 2 specific bands.

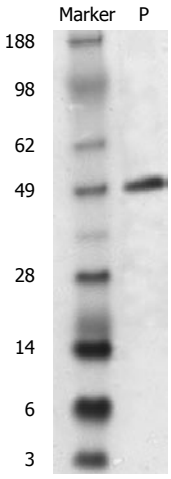

Figure 2 Expression of scFv gene.

jugate against colorectal cancer cells SW480, SW620 and LoVo was strong, and that against LoVo cells was the strongest (Figure 3A). The immunoreactivity of the conjugate against CEA was also strong, especially when the concentration of the conjugate was above 20 mg/L (Figure 3B).

Restraining effect of the conjugate on growth of LoVo cells

After 48 h treatment, LoVo cells were treated with various concentrations of CEA-scFv-MMC, more or less restraining effect of the conjugate on the growth of LoVo cells was shown, significantly depending on the concentration. When the concentration was above 100 mg/L, it had an obvious restraining effect on the growth of the cells ($^aP < 0.05$), and when the concentration was above 200 mg/L, it had a further restraining effect on the cells ($^bP < 0.01$, Table 1).

Effect of conjugate on apoptosis of LoVo cells

Different doses of CEA-scFv-MMC had different effects on apoptosis of LoVo cells. Apoptosis of LoVo cells began at the concentration of 25 mg/L CEA-scFv-MMC. The apoptosis rate increased with the increasing concentration of CEA-scFv-MMC (Figure 4A). Apoptosis of LoVo cells began 12 h after treatment of LoVo cells with CEA-scFv-MMC and the apoptosis rate reached its peak at 72 h (Figure 4B). The results showed that apoptosis of LoVo cells induced by CEA-scFv-MMC was highly dependent on its concentration and its duration of action.

DISCUSSION

Adjuvant chemotherapy has become more and more important in the treatment of colorectal cancer[18]. In recent years, though a variety of anti-cancer drugs are available, most of them could not distinguish cancer cells from normal cells[19]. Therefore, their clinical application is limited due to their toxic and side effects[20]. Target-oriented treatment directly delivers chemotherapeutic drugs to the tumor, resulting in a high drug concentration in the tumor[21]. Through decreasing the total dose, the toxic and side effects of drugs are decreased[22]. Single-chain antibody is an ideal vehicle for delivering chemotherapeutic drugs, because it is easy to reach the tumor due to its small molecular weight and strong penetrating force[23]. The scFv gene applied in this study is derived from monoclonal antibody T84.66, which has been humanized[16] and does not cause (HAMA) reaction in human body[24]. MMC, a broad spectrum anti-tumor drug, is nonspecific for cell cycle. However, it may depolymerize the DNA of cells and inhibit its replication, thus restraining the division of tumor cells[25]. The aim of this study was to construct a drug for target-oriented treatment of colorectal cancer, with MMC as the "warhead" and anti CEA svFv as the vehicle.

Taking plasmid pUC18 as template, we successfully amplified the CEA scFv gene, which is completely consistent with the reported gene sequence[16]. In order to make the fusion gene express effectively and prokaryotic cells express eukaryotic protein, we successfully constructed the GST fusion expressing vector (pGEX-4T-1/CEA-ScFv) and removed the repression effect of lac by IPTG, and made CEA scFv express highly effective in *E.coli* DH5α. The expressed fusion protein amounted to 26% of the total bacterial protein.

In this study, we successfully coupled anti-CEA scFv and MMC with dextran T-40 as a medium. The molecular ratio of scFv: dextran T-40: MMC in the conjugate was 1:1.2:38. Since the molecular weight of the antibody is only 49 ku, the conjugate could meet the requirements of antibody[26]. Measurement of immunoreactivity of the conjugate showed that it had a strong immunological activity against three kinds of colorectal cancer cells, among which immunoreactivity of the conjugate against LoVo cells was the strongest, which may be due to the high CEA expression in LoVo cells[27].

In the study, different concentrations of CEA-scFv-MMC had a different restraining effect on LoVo cells depending on the concentration. When the concentration was above 100 mg/L, it had an obvious restraining effect on the growth of LoVo cells. Apoptosis of LoVo cells began at the concentration of 25 mg/L, the apoptosis ratio increased with the increasing concentration of CEA-scFv-MMC. The optimal dose of CEA-scFv-MMC for inducing apoptosis was 200 mg/L. When time was studied as a variable, the apoptosis began 12 h after treatment of LoVo cells with CEA-scFv-MMC and reached its peak 72 h after CEA-scFv-MMC treatment, suggesting that apoptosis of LoVo cells induced by CEA-scFv-MMC is highly dependent on the concentration of CEA-scFv-MMC and its

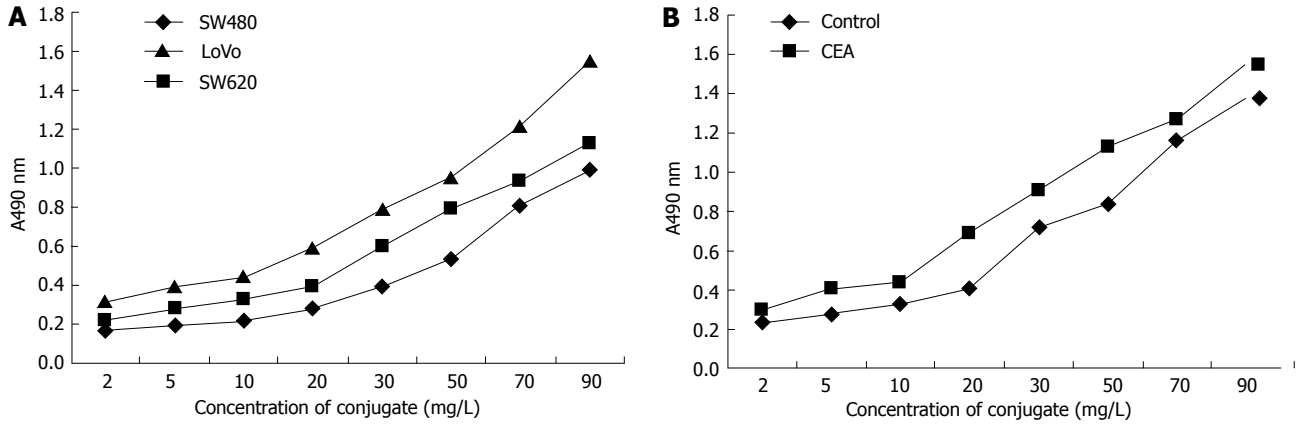

Figure 3 Immunoreactivity of the conjugate against colorectal cancer cells (**A**) and CEA (**B**).

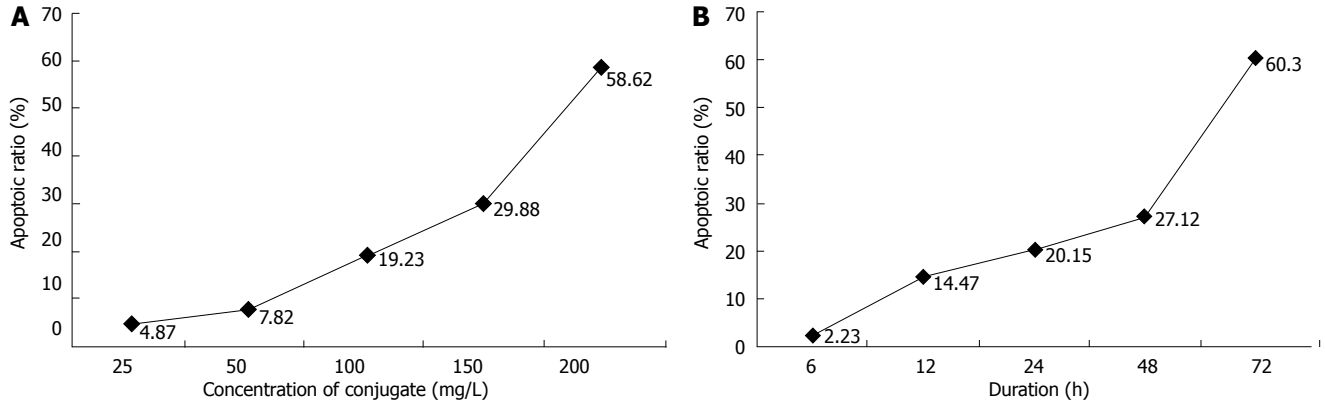

Figure 4 Effect of conjugate on apoptosis of LoVo cells at the concentration of 250 mg/L (**A**) and 200 mg/L (**B**).

duration of action. However, a large dose or a long duration of CEA-scFv-MMC can result in cell necrosis, which may be due to the *in vitro* accumulation of cells undergoing apoptosis without pinocytosis of macrophages[28].

Taking the capacity of the protein yield into consideration, we did not remove GST from the GST/CEA-scFv fusion protein, but directly coupled the fusion protein with MMC. In *in vitro* experiment, GST had no effect on the immune activity of the conjugate and colorectal cancer cells. Further experiments are needed to demonstrate whether the conjugate can be applied *in vivo*. On the other hand, the reaction of the body and immunogenecity do not necessarily parallel the process of humanization[29]. Thus, the in vivo immunogenecity cannot be predicted .The next experiment will focus on more suitable expression vectors to make the expression of CEA-scFv more effectively. Animal experiments will be carried out to explore the target-oriented effect of CEA-scFv-MMC, immunogenecity of the conjugate and its therapeutic effect on colorectal cancer *in vivo*. Since only some kinds of colorectal cancer express CEA[30], this therapy would only be applied to such cancers.

In conclusion, CEA-scFv-MMC conjugate can be successfully constructed and restrains the growth of colorectal cancer cells and induces apoptosis of cancer cells *in vitro*.

Table 1 IR of LoVo cells induced by different concentrations of conjugate

CEA-scFv-MMC (mg/L)	A_{630} (mean ± SD)	Inhibition ratio (%)
Control	0.75 ± 0.10	
25	0.68 ± 0.09	9.3
50	0.62 ± 0.08	17.5
100	0.38 ± 0.06[a]	45.0
150	0.24 ± 0.05[a]	66.9
200	0.11 ± 0.03[b]	84.4
300	0.09 ± 0.02[b]	87.5
400	0.07 ± 0.02[b]	90.0

[a]$P < 0.05$, [b]$P < 0.01$, *vs* control group.

ACKNOWLEDGMENTS

The authors thank the teachers of the Virus Research Institute, Medical College, Wuhan University for their assistance with the experiments and Wuhan University Medical College for offering the scientific research fund.

COMMENTS

Background

Carcinoembryonic antigen (CEA) is present in a number of adenocarcinomas, especially in colorectal cancer. If a humanized anti-CEA single-chain antibody (scFv) can be coupled with a chemotherapeutics, the conjugate would be an ideal target-oriented medication for colorectal cancer.

Research frontiers

An expression vector has been constructed to express the humanized anti-CEA

scFv, with the protein coupled with mitomycin (MMC). The conjugate can restrain the growth of colorectal cancer cells and induce apoptosis of colorectal cancer cells *in vitro*.

Innovations and breakthroughs

Through restriction endonuclease cleavage and gene sequencing, the expression vector was successfully constructed. Applying SDS-PAGE and ELISA, we have confirmed that this vector can correctly express the fusion protein and the conjugate has quite a strong immunoreactivity against colorectal cancer cells and CEA. The conjugate has an inhibitory effect on colorectal cancer cells in a concentration-dependent manner, and induces apoptosis of colorectal cancer cells in a concentration-and time-dependent manner.

Applications

The conjugate may be a potential target-oriented medication for colorectal cancer expressing CEA.

Terminology

CEA is a 180 ku cell-surface expressed glycoprotein antigen present in a number of adenocarcinomas, especially in colorectal cancer. It is a member of the immunoglobulin superfamily and has cell adhesion properties as well as other less clearly defined roles. scFv is an ideal vehicle for delivering chemotherapeutics, as it is easy for single-chain antibody to reach the tumor due to its small molecular weight and strong penetrating force. MMC is a broad spectrum anti-tumor medicine and nonspecific for cell cycle. However, it may depolymerize DNA of cells and inhibit its replication, thus restraining the division of tumor cells.

Peer review

This paper reports the construction and *in vitro* effect of a humanized carcinoembryonic antigen specific single chain fragment mitomycin conjugate. The authors have demonstrated that CEA-scFv-MMC conjugate is able to inhibit the growth and induce the apoptosis of colorectal cancer cells.

REFERENCES

1 **van Laarhoven HW**, Punt CJ. Systemic treatment of advanced colorectal carcinoma. *Eur J Gastroenterol Hepatol* 2004; **16**: 283-289
2 **Krol M**, Koopman M, Uyl-de Groot C, Punt CJ. A systematic review of economic analyses of pharmaceutical therapies for advanced colorectal cancer. *Expert Opin Pharmacother* 2007; **8**: 1313-1328
3 **Punt CJ**. New options and old dilemmas in the treatment of patients with advanced colorectal cancer. *Ann Oncol* 2004; **15**: 1453-1459
4 **Mulders P**, Bleumer I, Oosterwijk E. Tumor antigens and markers in renal cell carcinoma. *Urol Clin North Am* 2003; **30**: 455-465
5 **Elfiky AA**, Saif MW. The developing trend of monoclonal antibodies in the treatment of colorectal cancer. *Expert Opin Biol Ther* 2007; **7**: 871-883
6 **Herbst RS**, Bajorin DF, Bleiberg H, Blum D, Hao D, Johnson BE, Ozols RF, Demetri GD, Ganz PA, Kris MG, Levin B, Markman M, Raghavan D, Reaman GH, Sawaya R, Schuchter LM, Sweetenham JW, Vahdat LT, Vokes EE, Winn RJ, Mayer RJ. Clinical Cancer Advances 2005: major research advances in cancer treatment, prevention, and screening--a report from the American Society of Clinical Oncology. *J Clin Oncol 2006*; **24**: 190-205
7 **Pfeiffer P**, Qvortrup C, Eriksen JG. Current role of antibody therapy in patients with metastatic colorectal cancer. *Oncogene* 2007; **26**: 3661-3678
8 **Takano T**, Ohe Y, Sakamoto H, Tsuta K, Matsuno Y, Tateishi U, Yamamoto S, Nokihara H, Yamamoto N, Sekine I, Kunitoh H, Shibata T, Sakiyama T, Yoshida T, Tamura T. Epidermal growth factor receptor gene mutations and increased copy numbers predict gefitinib sensitivity in patients with recurrent non-small-cell lung cancer. *J Clin Oncol* 2005; **23**: 6829-6837
9 **Guillem EB**, Sampsel JW. Antitumor-associated antigens IgGs: dual positive and negative potential effects for cancer therapy. *Adv Exp Med Biol* 2006; **587**: 341-374
10 **Reichert JM**, Valge-Archer VE. Development trends for monoclonal antibody cancer therapeutics. *Nat Rev Drug Discov* 2007; **6**: 349-356
11 **Gold P**, Freedman SO. Demonstration of tumor-specific antigens in human colonic carcinomata by immunological tolerance and absorption techniques. *J Exp Med* 1965; **121**: 439-462
12 **Zimmermann W**, Ortlieb B, Friedrich R, von Kleist S. Isolation and characterization of cDNA clones encoding the human carcinoembryonic antigen reveal a highly conserved repeating structure. *Proc Natl Acad Sci USA* 1987; **84**: 2960-2964
13 **Shen LZ**, Wu WX, Xu DH, Zheng ZC, Liu XY, Ding Q, Hua YB, Yao K. Specific CEA-producing colorectal carcinoma cell killing with recombinant adenoviral vector containing cytosine deaminase gene. *World J Gastroenterol* 2002; **8**: 270-275
14 **O'Dwyer PJ**. The present and future of angiogenesis-directed treatments of colorectal cancer. *Oncologist* 2006; **11**: 992-998
15 **Vogel CA**, Galmiche MC, Buchegger F. Radioimmunotherapy and fractionated radiotherapy of human colon cancer liver metastases in nude mice. *Cancer Res* 1997; **57**: 447-453
16 **Rodenburg CM**, Mernaugh R, Bilbao G, Khazaeli MB. Production of a single chain anti-CEA antibody from the hybridoma cell line T84.66 using a modified colony-lift selection procedure to detect antigen-positive ScFv bacterial clones. *Hybridoma* 1998; **17**: 1-8
17 **Gladysheva IP**, Polekhina OV, Karmakova TA, Nemtsova ER, Yakubovskaya RI, Shen WC, Kennedy AR, Larionova NI. Potential of block copolymer- and immuno-conjugates for tumor-targeted delivery of Bowman-Birk soybean proteinase inhibitor. *J Control Release* 2001; **74**: 303-308
18 **Balch GC**, De Meo A, Guillem JG. Modern management of rectal cancer: a 2006 update. *World J Gastroenterol* 2006; **12**: 3186-3195
19 **Chung KY**, Saltz LB. Antibody-based therapies for colorectal cancer. *Oncologist* 2005; **10**: 701-709
20 **Puleo S**, Mauro L, Gagliano G, Lombardo R, Li Destri G, Petrillo G, Di Carlo I. Liver damage after transarterial chemoembolization without embolizing agent in unresectable hepatocellular carcinoma. *Tumori* 2003; **89**: 285-287
21 **Sharon J**, Liebman MA, Williams BR. Recombinant polyclonal antibodies for cancer therapy. *J Cell Biochem* 2005; **96**: 305-313
22 **Ng EW**, Adamis AP. Targeting angiogenesis, the underlying disorder in neovascular age-related macular degeneration. *Can J Ophthalmol* 2005; **40**: 352-368
23 **Batra SK**, Jain M, Wittel UA, Chauhan SC, Colcher D. Pharmacokinetics and biodistribution of genetically engineered antibodies. *Curr Opin Biotechnol* 2002; **13**: 603-608
24 **Yazaki PJ**, Sherman MA, Shively JE, Ikle D, Williams LE, Wong JY, Colcher D, Wu AM, Raubitschek AA. Humanization of the anti-CEA T84.66 antibody based on crystal structure data. *Protein Eng Des Sel* 2004; **17**: 481-489
25 **Marinelli A**, Vahrmeijer AL, van de Velde CJ. Phase I/II studies of isolated hepatic perfusion with mitomycin C or melphalan in patients with colorectal cancer hepatic metastases. *Recent Results Cancer Res* 1998; **147**: 83-94
26 **Carter P**. Improving the efficacy of antibody-based cancer therapies. *Nat Rev Cancer* 2001; **1**: 118-129
27 **Li Y**, Chen Y, Dilley J, Arroyo T, Ko D, Working P, Yu DC. Carcinoembryonic antigen-producing cell-specific oncolytic adenovirus, OV798, for colorectal cancer therapy. *Mol Cancer Ther* 2003; **2**: 1003-1009
28 **Morand EF**. New therapeutic target in inflammatory disease: macrophage migration inhibitory factor. *Intern Med J* 2005; **35**: 419-426
29 **Park TG**, Jeong JH, Kim SW. Current status of polymeric gene delivery systems. *Adv Drug Deliv Rev* 2006; **58**: 467-486
30 **Vallejo J**, Torres-Avisbal M, Contreras P, Rodríguez-Liñán M, Rebollo A, González F, Benítez A, Infante J, Mateo A. CEA, CA 19.9 and CA 195 in patients with colorectal carcinoma. ROC analysis. *Rev Esp Med Nucl* 1999; **18**: 281-286

S- Editor Liu Y **L- Editor** Wang XL **E- Editor** Li JL

Online Submissions: wjg.wjgnet.com
www.wjgnet.com
wjg@wjgnet.com

World J Gastroenterol 2007 November 21; 13(43): 5771-5774
World Journal of Gastroenterology ISSN 1007-9327

CASE REPORT

Massive gastrointestinal bleeding: An unusual case of asymptomatic extrarenal, visceral, fibromuscular dysplasia

Paula Andrea Rodriguez Urrego, Mark Flanagan, Wilson S Tsai, Craig Rezac, Nicola Barnard

Paula Andrea Rodriguez Urrego, Nicola Barnard, Department of Pathology, Robert Wood Johnson Medical School-University of Medicine and Dentistry of New Jersey, United States
Mark Flanagan, Craig Rezac, Department of Surgery, RWJMS-UMDNJ, United States
Wilson S Tsai, Department of Heart, Lung and Esophageal Surgery, University of Pittsburgh Medical Center, United States
Supported by Pathology Department RWJMS-UMDNJ, United States
Correspondence to: Paula Andrea Rodriguez Urrego, Pathology Department, New Brunswick NJ 08901, One Robert Wood Johnson PL. MEB 212, United States. rodrigp2@umdnj.edu
Telephone: +1-908-7204531 Fax: +1-732-4188445
Received: June 4, 2007 Revised: August 25, 2007

Abstract

Extrarenal fibromuscular dysplasia causing gastrointestinal bleeding without other manifestations and especially sparing renal vasculature is uncommon. The diagnosis of this entity is usually made by radiographic appearance and the treatment is controversial. To our knowledge only seven cases of visceral fibromuscular dysplasia as a primary manifestation of the disease have been described, symptoms range from abdominal pain to gangrene. This is the first case of visceral fibromuscular dysplasia presenting with otherwise asymptomatic gastrointestinal bleeding, without bowel necrosis or ischemic changes. We provide a review of the literature.

Key words: Fibromuscular dysplasia; Extrarenal; Visceral; Gastrointestinal bleeding; Intimal fibroplasia

Rodriguez Urrego PA, Flanagan M, Tsai WS, Rezac C, Barnard N. Massive gastrointestinal bleeding: An unusual case of asymptomatic extrarenal, visceral, fibromuscular dysplasia. *World J Gastroenterol* 2007; 13(43): 5771-5774

http://www.wjgnet.com/1007-9327/13/5771.asp

INTRODUCTION

Fibromuscular dysplasia (FMD) of extrarenal location, visceral or splanchnic, accounts for a small percentage of cases. Clinical presentation is variable, generally as occlusive or aneurysmal disease, and sometimes associated with a family history of FMD. Treatment is not standardized due to rarity of the entity and includes either segmental resection, with or without angioplasty or medical treatment with anticoagulation and thrombolysis. We present a case report and review of the literature.

CASE REPORT

A 38-year-old man was transferred to our facility with intractable gastrointestinal bleeding. On presentation at the referring institution, he denied shortness of breath, dizziness, lethargy or abdominal pain. Upper esophagogastroduodenosc opy performed at the referring institution, excluded an upper gastrointestinal source of bleeding. An angiogram suggested diffuse severe vasculitis involving celiac trunk, superior mesenteric artery and inferior mesenteric artery.

The patient's medical history was significant for multiple episodes of gastrointestinal bleeding and gastric ulcers. Surgical history was significant for small bowel resection, 6 mo prior to the present admission, where an exposed vessel was identified as the source of bleeding. A pathological diagnosis of angiodysplasia/vasculitis was made. Family history was unremarkable. The patient was a smoker and a social drinker but denied use of illicit drugs.

On admission his physical examination was positive for pallor and compensatory tachycardia with a stable blood pressure. Hemoglobin level was 8.4 g/dL despite multiple transfusions.

The patient was started on steroid therapy due to a history of vasculitis. However, antinuclear antibody titer (ANA) of < 1:16, excluded this possibility. Bleeding scan suggested a bleeding site in the small bowel bleeding most likely in the ileum. On the second day of admission an angiogram was performed with intent of embolization, and showed normal aorta and renal arteries and extensive vascular abnormalities involving all branches of the superior mesenteric artery, which included ectasia, bleading and narrowing; and marked ectasia of the inferior mesenteric artery and areas of hypervascularity. There was no evidence of contrast extravasation. Due to drop of hemoglobin and failure of medical treatment including attempted embolization, the patient was taken to surgery. Intraoperative colonoscopy showed obvious bleeding at the anastomosis site from the previous small bowel resection, in the ileum, with old blood distally. A segment of distal ileum, 6 cm away from the ileocecal valve was resected. No obvious bleeding site was identified.

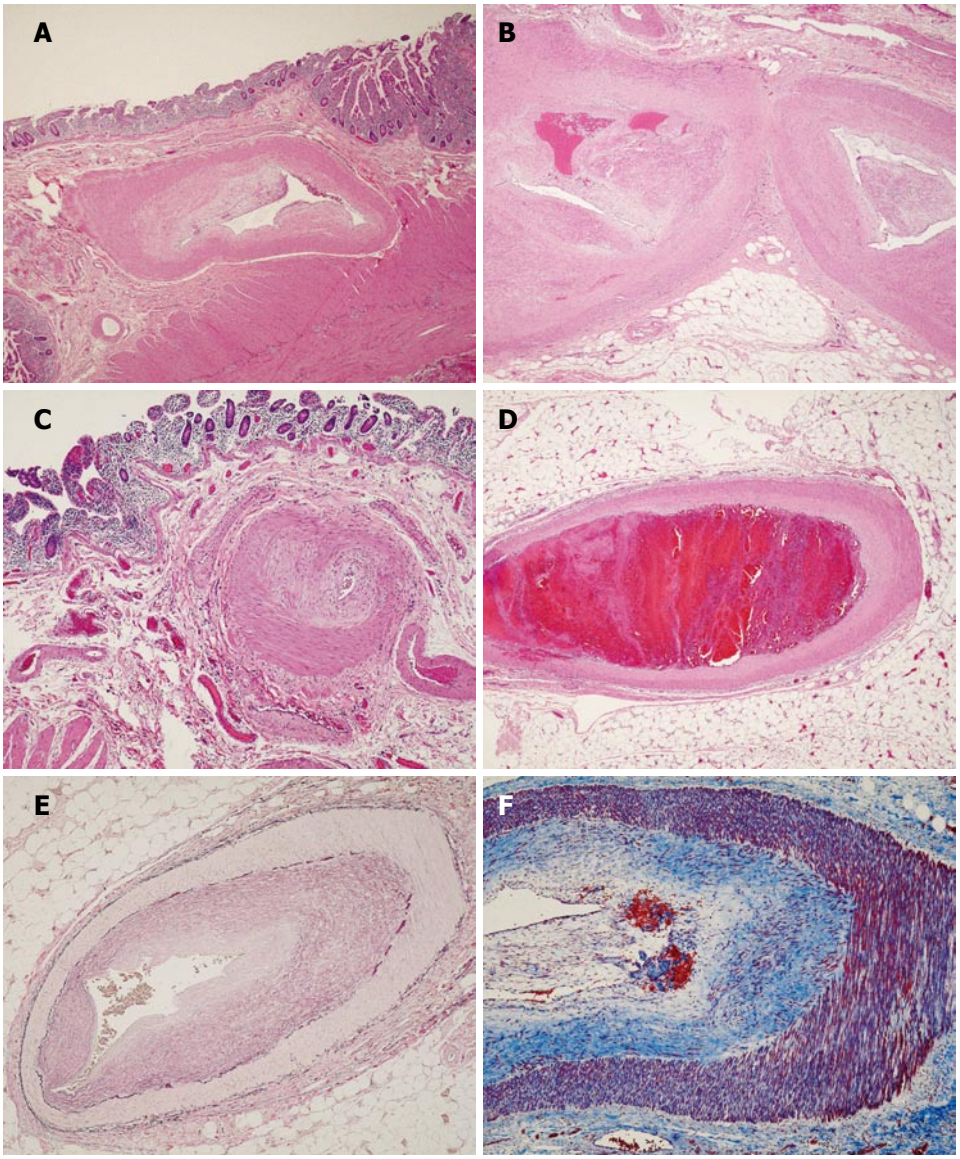

Figure 1 Microscopic sections showing marked thickening (**A**) and hyalinization (**B**) of medium sized vessel walls with prominent eccentric intimal proliferation with no arteritis, necrosis, inflammation and calcification (hematoxylin-eosin, original magnification × 200); sparing of small sized vessels (**C**) (hematoxylin-eosin, original magnification × 200); focal evidence of recent vascular thrombosis with early organization in one vessel (**D**) (hematoxylin-eosin, original magnification × 200); Verhoeff's Van Gieson elastic stain highlighting the prominent intimal hyperplasia (**E**) (original magnification × 200; Masson's trichrome stain highlighting a loose matrix of fibrous tissue replacing and expanding the intima (**F**) (original magnification × 200).

The specimen received consisted of a 37.5 cm segment of small bowel designated as "distal ileum" and a grossly unremarkable vermiform appendix. On opening the small bowel, the mucosal surface was intact without evidence of ulcers or masses. There were multiple yellow, tan slightly elevated areas of the mucosa, giving the appearance of papules, ranging from 0.3 to 0.5 cm. The previous anastomosis site was intact. Sections through the mucosa, perineal fat and mesentery showed thickened and tortuous submucosal, subserosal and mesenteric vessels, some of them contained clotted blood.

Microscopic sections (Figure 1) revealed marked thickening and hyalinization of medium sized vessel walls, with prominent eccentric intimal proliferation (Figure 1A and B) and apparent sparing of small sized vessels (Figure 1C). Focal evidence of recent vascular thrombosis with early organization was noted in one vessel (Figure 1D). Arteritis, necrosis, inflammation and calcification were absent. Verhoeff's Van Gieson elastic stain (Figure 1E) highlighted the prominent intimal hyperplasia. Masson's trichrome stain (Figure 1F) highlighted a loose matrix of fibrous tissue replacing and expanding the intima.

DISCUSSION

FMD was first described more than 68 years ago by Leadbetter, as a cause of hypertension, but was not until 1938 that it received an accurate pathological description by Mc Cormack, who reported four cases as "fibromuscular hyperplasia"[1,3]. Currently, FMD is well recognized as a nonatherosclerotic, noninflammatory vascular disease that most commonly affects young females, involving the renal and internal carotid arteries but has been described in almost all arterial beds in the body[1-9]. This entity accounts for less than 10% of cases of renal-artery stenosis[2]. Among 1200 cases of FMD studied by Meetinger[3], 60% involved renal arteries, 34% extracranial carotid and vertebral arteries, and less than 2.5% involved iliac, celiac and mesenteric arteries.

Two histopathological classifications of renal FMD have been proposed. In 1971, Harrison and McCormack[10] made the first classification, based on the arterial layer in which the lesion predominates: intimal fibroplasias, medial fibroplasias and adventitial fibroplasias. Intimal fibroplasia was found in less than 10% of patients with FMD, and can be confused with arteritis by angiography because it may appear as a focal, concentric stenosis or a long smooth

narrowing. Medial fibroplasia, characterized on imaging studies by a "string of beads appearance", represents the most common dysplastic lesion, with medial compromise and sparing of intimal and adventitial layers. Medial fibroplasias include two uncommon subtypes: perimedial fibroplasia and medial hyperplasia. Perimedial fibroplasia is characterized by a collar of elastic tissue at the junction of the media with the adventitia. Medial hyperplasia, corresponds to less than 1% of causes of renal stenosis, and consists of medial hyperplasia without loose matrix of fibrous tissue formation. The third category, also the rarest type of FMD is adventitial (periarterial) hyperplasia.

In 1975, Stanley[4], subdivided FMD into four categories, instead of three, according to histopathological findings: intimal fibroplasias, medial hyperplasia, medial fibroplasia and perimedial dysplasia. The first category, intimal fibroplasia accounts for 5% of cases of FMD appearing as irregular tubular stenosis in young patients and smooth focal stenosis in older persons, characterized histologically by an accumulation of irregularly arranged subendothelial mesenchymal cells within a loose matrix of fibrous connective tissue, often eccentric, with absence of inflammatory cells or foamy macrophages. The second, medial hyperplasia is characterized by increase in medial muscle, without demonstrable fibrotic changes, and accounts for less than 1% of cases. This category is difficult to differentiate roentographically from intimal fibroplasia. The third and most common category, medial fibroplasia, represents 85% of cases of renal FMD, and is most commonly seen in the pediatric population. It is characterized histologically by compromise of the outer media, or diffuse involvement of the entire media. Involvement of the outer media presents with compact fibrous connective tissue replacing smooth muscle peripherally, and a moderate accumulation of collagen in the inner media, separating disorganized smooth muscle. On the other hand, diffuse medial fibroplasia is characterized by severe disorganization, with disruption and replacement of smooth muscle by haphazard arrangements of fibroblasts and collagen. The last category, perimedial dysplasia, found in 10% of cases of FMD, is characterized by relatively acellular tissue in the region of the external elastic lamina that can be mistaken for dense collagen.

Both authors reported that macroaneurysms and dissections are the common complications of FMD. Aneurysms can present in any subtype, and their presence should not lead to a different diagnosis. To date, classifications are used in the literature, indistinguishably.

The etiology of FMD is unknown, but several factors, genetic, mechanical and hormonal, have been implicated[1-4,7-8]. Hormonal influence is considered due to the prevalence of the disease in hormonally active females. Although no association has been found between FMD and history of use of oral contraceptives or abnormalities of endogenous sex hormones, physiologic preconditioning of cellular elements to fibroblastic activities by estrogen has been shown. Mechanical factors, such as artery traction due to renal ptosis, could explain the increased frequency in the right kidney, compared to the left kidney. The stress involved in the stretch traction may predispose to fibroplasia directly by altering vessel wall tissues or indirectly by disrupting the vasa vasorum. Vasa vasorum of muscular arteries originates from branching of the parent vessel and arteries such as renal, extracranial carotid and external iliac arteries may have a normal paucity of vasa vasorum, making them prone to alteration. Genetic factors may be contributory, since FMD is more common among first degree relatives with renal FMD and among persons with angiotensin-converting-enzyme allele I (ACE-I).

The differential diagnosis is broad, but usually straight forward, once common etiologies are excluded[1,13]. Atherosclerosis typically occurs in older patients with cardiovascular risk factors and usually involves the origin or the proximal portion of the artery. In contrast, renal FMD occurs in younger patients, with few or no cardiovascular risks and frequently involves the middle or distal segments of artery. FMD is distinguished from active vasculitis, based on the absence of inflammation, anemia, thrombocytopenia or acute phase reactants. If histologic diagnosis is unavailable, angiography is unable to differentiate FMD and vasculitis, due to the extreme similarity in radiographic appearance, especially in the case of intimal fibroplasias, where both entities have identical manifestations, as illustrated in this case. Diseases affecting medium size vessels may induce identical histopathological changes in the vessel wall and should be considered in the differential diagnosis, including familial diseases such as neurofibromatosis and Friedreich's ataxia, endocrine diseases such as diabetes and homocystinuria, autoimmune diseases including any type of vasculitis, allograft rejection, infectious vasculitis such as Rickettsia, Rocky Mountain spotted fever, epidemic typhus, scrub typhus, Q-fever, pseudomonas, syphilis, fungi, plague, Whipple's disease, leptospirosis and schistosomiasis, toxic agents such as cocaine, coagulopathies such as thrombotic thrombocytopenic purpura, hemolytic uremic syndrome and disseminated intravascular coagulation, systemic hypertension, neoplastic entities such as intravascular lymphomatosis, endovascular papillary angioendothelioma or intravascular papillary endothelial hyperplasia, amyloidosis or emboli.

Visceral or splanchnic FMD accounts for 2.5% of cases of FMD and its clinical presentation has a wide spectrum[3,5-9,11-13]. When symptomatic, its presentation can be as occlusive disease or as aneurysmal disease. Occlusive disease ranges in spectrum from abdominal angina to intestinal gangrene. Of the seven case reports found in the literature with visceral FMD, two[8,9] had a family history of FMD or associated renal FMD. The other four[5,6,11,13] presented with only visceral involvement. The age ranged from 5 to 78 years. Three cases occurred in women and four in men. The initial presentation was acute abdomen in all the patients, with compromise of superior mesenteric artery in four patients, superior rectal artery in one, jejunal and sigmoid artery and colonic artery in one, and unspecified in the other patient. Two out of the seven patients presented with gastrointestinal bleeding. Histological analysis revealed mucosa with ischemic changes and FMD of different categories, intimal fibroplasia in three patients, medial fibroplasia in two patients, perimedial dysplasia in one patient and adventitial fibroplasia in one patient. Three patients died and four

of the seven survived. Among the successfully treated patients, three had surgery with a segmental resection, one of them combined with angioplasty. One patient was medically treated with anticoagulation and thrombolysis, without requiring any invasive procedure.

Interestingly enough, a study that originated from a case of ischemic proctitis, analyzed 50 rectums and their blood supply in patients with a median age of 61 years[11] showed that adventitial FMD was found in more than 50% of unselected, examined specimens, indicating that a relatively mild, asymptomatic form of adventitial FMD is common in later life.

Treatment for visceral FMD is more anecdotic and based on retrospective case series[1]. Revascularization through angioplasty without stent, segmental resections, anticoagulation and fibrinolysis has been used.

We present a case of extrarenal, visceral FMD, with intimal fibroplasia histopathologic type, causing intractable and recurrent gastrointestinal bleeding, without ischemia or necrosis of the bowel, who was successfully treated surgically with partial jejunectomy. The patient did well, and a year after small bowel resection he developed a ventral hernia, requiring laparoscopic and open repair. The specimen showed a large artery with fibromuscular and intimal hyperplasia. No new episodes of gastrointestinal bleeding or gastrointestinal symptoms have been documented.

REFERENCES

1 **Slovut DP**, Olin JW. Fibromuscular dysplasia. *N Engl J Med* 2004; **350**: 1862-1871

2 **Safian RD**, Textor SC. Renal-artery stenosis. *N Engl J Med* 2001; **344**: 431-442

3 **Mettinger KL**. Fibromuscular dysplasia and the brain. II. Current concept of the disease. *Stroke* 1982; **13**: 53-58

4 **Stanley JC**, Gewertz BL, Bove EL, Sottiurai V, Fry WJ. Arterial fibrodysplasia. Histopathologic character and current etiologic concepts. *Arch Surg* 1975; **110**: 561-566

5 **Mertens J**, Daenens K, Fourneau I, Marakbi A, Nevelsteen A. Fibromuscular dysplasia of the superior mesenteric artery--case report and review of the literature. *Acta Chir Belg* 2005; **105**: 523-527

6 **Yamaguchi R**, Yamaguchi A, Isogai M, Hori A, Kin Y. Fibromuscular dysplasia of the visceral arteries. *Am J Gastroenterol* 1996; **91**: 1635-1638

7 **Pannier-Moreau I**, Grimbert P, Fiquet-Kempf B, Vuagnat A, Jeunemaitre X, Corvol P, Plouin PF. Possible familial origin of multifocal renal artery fibromuscular dysplasia. *J Hypertens* 1997; **15**: 1797-1801

8 **Hamed RM**, Ghandour K. Abdominal angina and intestinal gangrene--a catastrophic presentation of arterial fibromuscular dysplasia: case report and review of the literature. *J Pediatr Surg* 1997**; 32:** 1379-1380

9 **Horie T,** Seino Y, Miyauchi Y, Saitoh T, Takano T, Ohashi A, Yamada N, Tamura K, Yamanaka N. Unusual petal-like fibromuscular dysplasia as a cause of acute abdomen and circulatory shock. *Jpn Heart J* 2002; **43**: 301-305

10 **Harrison EG**, McCormack LJ. Pathologic classification of renal arterial disease in renovascular hypertension. *Mayo Clin Proc* 1971; **46**: 161-167

11 **Quirke P**, Campbell I, Talbot IC. Ischaemic proctitis and adventitial fibromuscular dysplasia of the superior rectal artery. *Br J Surg* 1984; **71**: 33-38

12 **Case records of the Massachusetts General Hospital**. Weekly clinicopathological exercises. Case 9-1995. A 60-year-old man with hypertrophic cardiomyopathy and ischemic colitis. *N Engl J Med* 1995; **332**: 804-810

13 **Safioleas M**, Kakisis J, Manti C. Coexistence of hypertrophic cardiomyopathy and fibromuscular dysplasia of the superior mesenteric artery. *N Engl J Med* 2001; **344**: 1333-1334

S- Editor Zhu LH **L- Editor** Wang XL **E-Editor** Li HY

Online Submissions: wjg.wjgnet.com
www.wjgnet.com
wjg@wjgnet.com

World J Gastroenterol 2007 November 21; 13(43): 5775-5778
World Journal of Gastroenterology ISSN 1007-9327

CASE REPORT

Well to moderately differentiated HCC manifesting hyperattenuation on both CT during arteriography and arterial portography

Soo Ryang Kim, Susumu Imoto, Hirotsugu Ikawa, Kenji Ando, Keiji Mita, Shuichi Fuki, Michiie Sakamoto, Yoshihiro Kanbara, Toshiyuki Matsuoka, Masatoshi Kudo, Yoshitake Hayashi

Soo Ryang Kim, Susumu Imoto, Hirotsugu Ikawa, Kenji Ando, Keiji Mita, Shuichi Fuki, Department of Gastroenterology, Kobe Asahi Hospital, Kobe 653-0801, Japan
Michiie Sakamoto, Department of Pathology, Keio University School of Medicine, Tokyo 160-8582, Japan
Yoshihiro Kanbara, Department of Surgery, Hyogo Cancer Center, Akashi 673-0021, Japan
Toshiyuki Matsuoka, Department of Radiology, Osaka City University Medical School, Osaka 545-8586, Japan
Masatoshi Kudo, Department of Gastroenterology, Kinki University School of Medicine, Osaka-Sayama 589-8511, Japan
Yoshitake Hayashi, Division of Molecular Medicine & Medical Genetics, International Center for Medical Research and Treatment, Kobe University Graduate School of Medicine, Kobe 650-0017, Japan
Correspondence to: Soo Ryang Kim, MD, Department of Gastroenterology, Kobe Asahi Hospital, 3-5-25 Bououji-cho, Nagata-ku, Kobe 653-0801, Japan. info@kobe-asahi-hp.com
Telephone: +81-78-6125151 Fax: +81-78-6125152
Received: July 12, 2007 Revised: August 24, 2007

Abstract

We present a rare case of well- to moderately-differentiated hepatocellular carcinoma (HCC) in a 71-year-old woman with hepatitis C virus-related cirrhosis and unusual radiologic features. A 20-mm hypoechoic nodule disclosed by ultrasound in segment two showed hyperattenuation on both computed tomography hepatic arteriography and computed tomography during arterial portography. Contrast-enhanced ultrasound revealed hypervascularity in the early vascular phase and defect in the post-vascular phase, with the same pattern detected by the two imaging techniques. SPIO-MRI revealed a hyperintense nodule. These findings were compatible with those of moderately-differentiated HCC. An ultrasound-guided biopsy showed histological features of well- to moderately-differentiated HCC characterized by more than two-fold the cellularity of the non-tumorous area, fatty change, clear cell change and mild cell atypia with a thin to mid-trabecular pattern. Further studies may provide insights into the correlation between tumor neovascularity in multistep hepatocarcinogenesis and dual hemodynamics, including the artery and the portal vein.

Key words: Hepatocarcinogenesis; CT hepatic arteriography; CT during arterial portography; Hyperattenuation; Dual hemodynamics; Well- to moderately-differentiated hepatocellular carcinoma

Kim SR, Imoto S, Ikawa H, Ando K, Mita K, Fuki S, Sakamoto M, Kanbara Y, Matsuoka T, Kudo M, Hayashi Y. Well to moderately differentiated HCC manifesting hyperattenuation on both CT during arteriography and arterial portography. *World J Gastroenterol* 2007; 13(43): 5775-5778

http://www.wjgnet.com/1007-9327/13/5775.asp

INTRODUCTION

Recent advances in imaging have enabled clinicians to identify not only advanced HCC but also dysplastic nodules or early hepatocellular carcinoma (HCC). Moreover, clinicians can now obtain images by CT hepatic arteriography (CTA) and CT during arterial portography (CTAP) concurrently, and can evaluate the hemodynamics of lesions preoperatively[1,2].

To determine the treatment of choice for HCC, examinations by both CTA and CTAP are indispensable because of the high sensitivity of CTAP in detecting hepatic lesions and the capability of CTA of characterizing them. Moderately-differentiated HCC is generally demonstrated as a perfusion defect on CTAP and as an enhanced area on CTA, principally because of the reciprocal blood flow of these two features. We investigated a case of well- to moderately-differentiated HCC, manifesting hyperattenuation on both CTA and CTAP.

CASE REPORT

A 71-year-old woman with hepatitis C virus (HCV)-related cirrhosis was admitted to Kobe Asahi Hospital in January 2007 for further examination of a 20-mm hypoechoic nodule in segment two (S2). She had no history of alcohol, blood transfusion, or drug abuse. Six months earlier, the patient had undergone to radiofrequency ablation of a 20-mm totally necrotic HCC in segment 7 (S7).

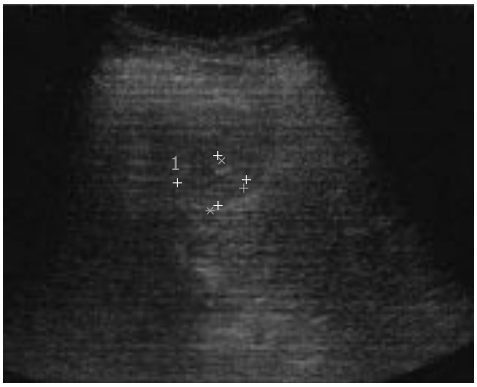

Figure 1 Ultrasound (US) image of a 20-mm hypoechoic nodule in segment 2 (S2).

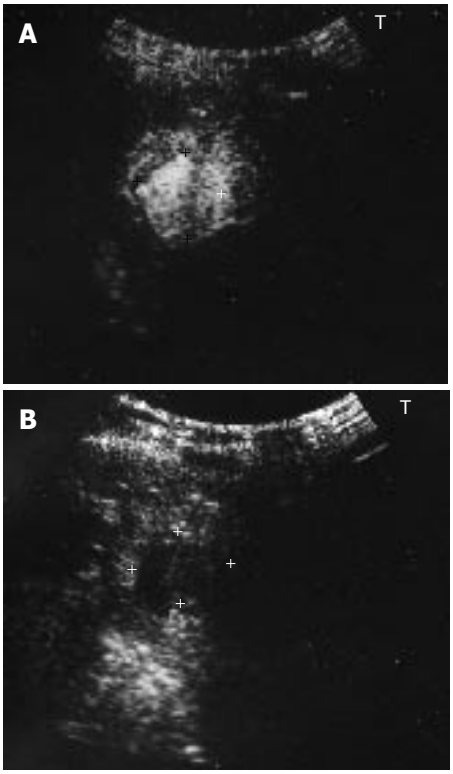

Figure 2 Contrast enhanced US of the nodule in S2. **A**: Hypervascularity in the early vascular phase; **B**: Defect in the post-vascular phase.

On admission, a physical examination showed no remarkable abnormalities. Serum HCV RNA was positive, and the HCV genotype was 1b. Serum hepatitis B virus (HBV) was negative for surface antigen, surface antibody, core antibody, and deoxyribonucleic acid (DNA). Laboratory studies disclosed the following abnormal values: platelets $6.0 \times 10^4/\mu L$ (normal 13.4-34.9), aspartate aminotransferase 50 U/L (10-40), alanine aminotransferase 46 U/L (5-40), alkaline phosphokinase 744 U/L (115-359), thymol turbidity 13.9 U (< 4.0), zinc surface turbidity 25.2 U (2.0-12.0), ICG R15 43% (0-10), γ globulin 52.8% (10.5-20.3). The levels of tumor markers were as follows: alpha-fetoprotein (AFP) 63.8 ng/mL (< 10.0), lens culinaris agglutinin A reactive fraction of alpha fetoprotein (AFP-L3) 4.6% (< 10.0), and protein-induced vitamin K absence (PIVKA II) 91 mAU/mL (<40).

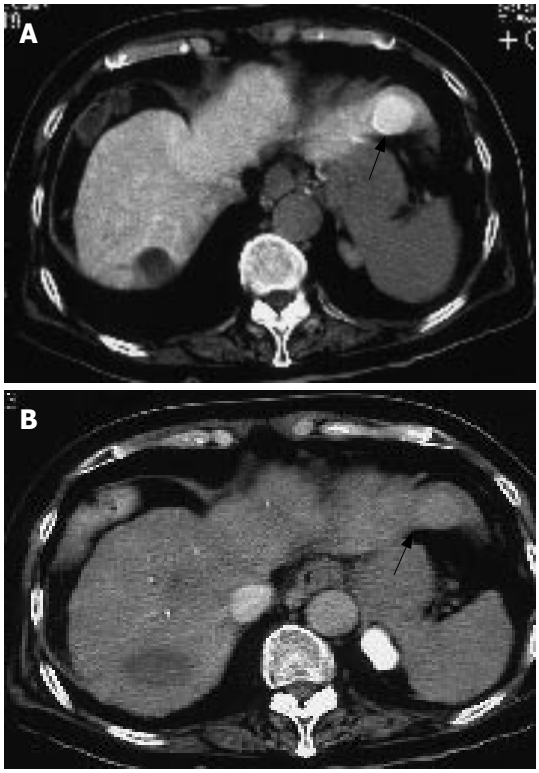

Figure 3 **A**: Hyperattenuation in S2 on computed tomography during arteriography (CTA); **B**: Hyperattenuation in S2 on computed tomography during arterial portography (CTAP).

Ultrasound (US) disclosed a 20-mm hypoechoic nodule in S2 (Figure 1). Contrast-enhanced US revealed hypervascularity in the early vascular phase (Figure 2A), and defect in the post-vascular phase (Figure 2B). Magnetic resonance imaging (MRI) revealed a high intensity nodule at both T1- and T2-weighted sequences. Contrast-enhanced MRI revealed a hypervascular nodule in the early phase and washout in the late phase. SPIO-MRI revealed a hyperintense nodule. Contrast-enhanced CT revealed an enhanced nodule in the early phase and washout in the late phase. Both CTA and CTAP revealed hyperattenuation (Figure 3A and B). Histologically, the nodule was well- to moderately-differentiated HCC characterized by more than two-fold the cellularity of the non-tumorous area, fatty change, clear cell change and mild cell atypia with a thin to mid-trabecular pattern (Figure 4A).

Immunohistochemical staining of heat shock protein (HSP) 70 (Figure 4B) was partly positive, and that of cyclase-associated protein (CAP) 2 was strongly positive (Figure 4C). Immunohistochemical staining of CD34 in HCC was positive in the sinusoidal blood space (Figure 4D). Immunohistochemically, CD68 was significantly underexpressed in the sinusoidal blood space compared with its expression in the non-HCC area (Figure 4E).

DISCUSSION

According to the classification by the International Working Party of the World Congress of Gastroenterology[3], hepatic nodules observed in patients with chronic liver disease can be subdivided into regenerative nodules

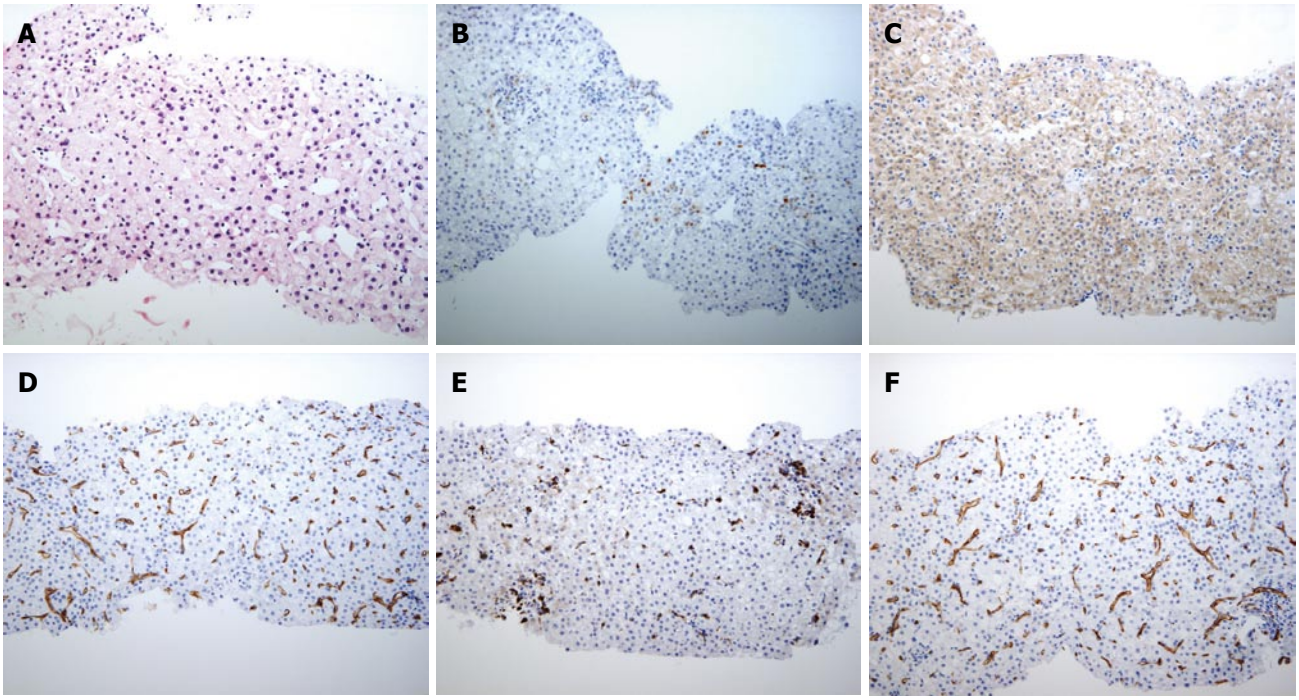

Figure 4 Histological features of a US-guided biopsy of a hyperechoic nodule in S2. **A**: Well- to moderately-differentiated HCC characterized by more than two-fold the cellularity of the non-tumorous area, fatty change, clear cell change and mild cell atypia with a thin to mid-trabecular pattern (HE×100); **B**: Immunohistochemical finding, HSP70 partly positive HCC cells; **C**: Immunohistochemical finding, CAP2 strongly positive HCC cells; **D**: Immunohistochemical staining of CD34 in the sinusoidal blood space is positive, showing capillarization; **E**: Immunohistochemical staining of CD68 Kupffer cells in the sinusoidal blood space is relatively less positive; **F**: Non-HCC area of immunohistochemical staining of CD68 Kupffer cells in the sinusoidal blood space.

(monoacinar and multiacinar), low-grade dysplastic nodules (LGDS), high-grade dysplastic nodules (HGDS), well-differentiated HCC (wHCC), moderately-differentiated HCC (mHCC), and poorly-differentiated HCC (pHCC), in the ascending order of histologic grades, representing a sequence of multistep hepatocarcinogenesis.

Several studies have shown sequential changes of hemodynamics in such hepatocellular neoplastic nodules and have reached similar conclusions: in the multistep developmental process of HCC, first, intratumoral hepatic arterial flow transiently decreases in the early stages of hepatocarcinogenesis and corresponds, histopathologically, to the obliteration of pre-existing hepatic arteries[2]; next intratumoral portal flow decreases gradually with the elevation of the histopathologic grades of hepatocellular nodules; and then hepatic arterial flow shows a gradual increase[4].

As is well documented through imaging techniques, such as CTA and CTAP, and histopathologically, the hepatocarcinogenetic process involves a gradual decrease in portal blood flow within the lesion and a reciprocal increase in hepatic arterial blood.

Although the HCC lesion is usually demonstrated as an iso- or hypoattenuated mass on CTAP, hyperattenuated lesions on CTAP are rare and limited to observations made in Japan[5-7].

Hyperattenuation on CTAP has been postulated as being reciprocal compensation for portal venous flow and hepatic arterial flow[5]; however, it is difficult to explain such hyperattenuation on CTAP by this premise because of the crucial gradual pressure between the hepatic artery and the portal vein. Although this hypothesis has not been pathophysiologically proven yet, one possible explanation[8] could be the following.

Abnormal thick-walled tumor vessels or tumor neovascularity may not necessarily carry arterial blood, considering the unique dual blood supply system of the originating organ, the liver. Tumor vessels may be communicating predominantly with the portal venous system through pre-existing intratumoral portal veins at the early stage of hepatocarcinogenesis (LGDN to wHCC), when both pre-existing arteries and portal veins decrease in number and when tumor angiogenesis may already have begun.

Net portal perfusion seen on CTAP in such tumors may reflect the sum or an additional effect of the reduced preexisting portal vein and the increased tumor vessels. These two factors may thus cancel out each other, resulting in isoperfusion on CTAP. When tumor angiogenesis exceeds the loss of a preexisting portal vein, the lesion may exhibit hyperattenuation on CTAP. Despite the communication between tumor vessels and portal veins, the tumor may become hypoxic because of the paucity of oxygen in portal venous blood compared with arterial blood. The hypoxia may thus induce gradual angiogenesis. As the histologic grades of the liver nodule advance, tumor vessels increase and may start to communicate with the arterial system as well, either through preexisting arteries or directly through outside arteries. Portal communication of the tumor vessels may gradually decrease; instead, arterial communication becomes gradually dominant. In mHCC and pHCC, therefore, the tumor may be fed exclusively by

arterial supply.

We have previously presented a rare case of well-differentiated HCC manifesting hypoattenuation on CTA and hyperattenuation on CTAP[7]. Takayasu et al[6] also have presented three such cases of HCC. These observations give rise to one possible explanation of the present case manifesting hyperattenuation on both CTA and CTAP: in the course of dedifferentiation from well- to moderately-differentiated HCC, there may be an intermediate phase between the manifestation of hypoattenuation on CTA and hyperattenuation on CTAP and the manifestation of hyperattenuation on CTA and hypoattenuation on CTAP. To the best of our knowledge, this is the first case of well- to moderately-differentiated HCC manifesting hyperattenuation on both CTA and CTAP.

Histopathologically, the tumor showed well- to moderately-differentiated HCC characterized by more than two-fold the cellularity of the non-tumorous area, fatty change, clear cell change and mild cell atypia with a thin to mid-trabecular pattern. Varying degrees of fatty changes may be one of the significant morphological markers of malignant transformation in the nodule, as observed in our US guided biopsy specimen.

Immunohistochemically, HSP70 is significantly overexpressed in early HCC, compared with its expression in dysplastic nodules, reaching 80% in most cases of well-differentiated HCC[9].

All cases of dysplastic nodules have been negative or focally positive (5%-10% of the lesions) for CAP2; in contrast, most cases of HCC (27 of 29 cases) have been partly positive for CAP2. Of the lesions, 70%-100% have been positive in the advanced components, and the positivity of well-differentiated HCC has ranged from 10% to 100%[10].

Positive immunohistochemical staining of both HSP70 and CAP2 confirmed the diagnosis of well- to moderately-differentiated HCC in the present case.

Positive immunohistochemical staining of CD34 in endothelial cells in the sinusoidal blood space has shown capillarization[11]. The immunohistochemical staining of CD34 was compatible with the hypervascularity of our tumor, as shown by imaging studies. Relatively less positive staining of CD68 of Kupffer cells in the sinusoidal blood space revealed the dedifferentiation. This finding was compatible with the imaging studies based on SPIO-MRI.

Further studies on sequential homodynamic change in hepatocarcinogenesis are indicated.

REFERENCES

1 **Hayashi M**, Matsui O, Ueda K, Kawamori Y, Gabata T, Kadoya M. Progression to hypervascular hepatocellular carcinoma: correlation with intranodular blood supply evaluated with CT during intraarterial injection of contrast material. *Radiology* 2002; **225**: 143-149

2 **Tajima T**, Honda H, Taguchi K, Asayama Y, Kuroiwa T, Yoshimitsu K, Irie H, Aibe H, Shimada M, Masuda K. Sequential hemodynamic change in hepatocellular carcinoma and dysplastic nodules: CT angiography and pathologic correlation. *AJR Am J Roentgenol* 2002; **178**: 885-897

3 **Terminology of nodular hepatocellular lesions**. *Hepatology* 1995; **22**: 983-993

4 **Kudo M**. Imaging blood flow characteristics of hepatocellular carcinoma. *Oncology* 2002; **62** Suppl 1: 48-56

5 **Hirano K**, Kondo Y, Teratani T, Obi S, Fujishima T, Hoshida Y, Tateishi R, Sato S, Koike Y, Shiina S, Imai Y, Shiratori Y, Omata M. Hepatocellular carcinoma depicted as hypoattenuation on CT hepatic arteriography (CTA) and hyperattenuation on CT during arterial portography (CTAP). *J Gastroenterol* 2001; **36**: 346-349

6 **Takayasu K**, Muramatsu Y, Wakao F, Mizuguchi Y, Iwata R, Maeda T, Moriyama N, Sakamoto M. Hepatic nodules with early enhancement during computed tomography portography: report of six cases. *J Gastroenterol Hepatol* 2002; **17**: 779-784

7 **Kim SR**, Kim KI, Maekawa Y, Imoto S, Ninomiya T, Mita K, Ando K, Fukuda K, Fuki S, Kudo M, Matsuoka T, Sasase N, Taniguchi M, Hayashi Y. Well-differentiated HCC manifesting hyperattenuation on CT during arterial portography. *Hepatogastroenterology* 2005; **52**: 1559-1562

8 **Yoshimitsu K,** Honda H, Tajima T, Irie H, Aibe H, Shinozaki K, Nishie A. Multistep carcinogenesis and development of hepatocellular carcinoma: a new concept based on sequential hemodynamic change as observed on CT angiography. Res Adv Cancer 2002. 01

9 **Chuma M**, Sakamoto M, Yamazaki K, Ohta T, Ohki M, Asaka M, Hirohashi S. Expression profiling in multistage hepatocarcinogenesis: identification of HSP70 as a molecular marker of early hepatocellular carcinoma. *Hepatology* 2003; **37**: 198-207

10 **Shibata R**, Mori T, Du W, Chuma M, Gotoh M, Shimazu M, Ueda M, Hirohashi S, Sakamoto M. Overexpression of cyclase-associated protein 2 in multistage hepatocarcinogenesis. *Clin Cancer Res* 2006; **12**: 5363-5368

11 **Nakashima Y**, Nakashima O, Hsia CC, Kojiro M, Tabor E. Vascularization of small hepatocellular carcinomas: correlation with differentiation. *Liver* 1999; **19**: 12-18

S- Editor Liu Y **L- Editor** Li M **E- Editor** Wang HF

Online Submissions: wjg.wjgnet.com
www.wjgnet.com
wjg@wjgnet.com

World J Gastroenterol 2007 November 21; 13(43): 5779-5780
World Journal of Gastroenterology ISSN 1007-9327

CASE REPORT

Minute signet ring cell carcinoma occurring in gastric hyperplastic polyp

Shoji Hirasaki, Seiyuu Suzuki, Hiromitsu Kanzaki, Kohei Fujita, Shuji Matsumura, Eiji Matsumoto

Shoji Hirasaki, Seiyuu Suzuki, Hiromitsu Kanzaki, Kohei Fujita, Shuji Matsumura, Eiji Matsumoto, Department of Internal Medicine, Sumitomo Besshi Hospital, 3-1 Ohji-cho, Niihama 792-8543, Japan
Correspondence to: Dr. Shoji Hirasaki, Second Department of Internal Medicine, Sumitomo Besshi Hospital, 3-1 Ohji-cho, Niihama 792-8543, Japan. shoji_hirasaki@ni.sbh.gr.jp
Telephone: +81-897-377111 Fax: +81-897-377121
Received: August 24, 2007 Revised: September 10, 2007

Abstract

We describe a 45-year-old woman with minute signet ring cell carcinoma occurring in a gastric hyperplastic polyp. A biopsy specimen obtained from the gastric hyperplastic polyp revealed signet ring cell carcinoma. Endoscopic mucosal resection (EMR) was performed to confirm the diagnosis. Histological examination of the EMR specimen revealed focal signet ring cell carcinoma in the hyperplastic polyp. There are few cases of gastric hyperplastic polyp associated with signet ring cell carcinoma.

Key words: Minute gastric cancer; Signet ring cell; Endoscopic mucosal resection

Hirasaki S, Suzuki S, Kanzaki H, Fujita K, Matsumura S, Matsumoto E. Minute signet ring cell carcinoma occurring in gastric hyperplastic polyp. *World J Gastroenterol* 2007; 13(43): 5779-5780

http://www.wjgnet.com/1007-9327/13/5779.asp

INTRODUCTION

Patients with gastric hyperplastic polyps may present with anemia, abdominal pain or gastric outlet obstruction[1,2]; therefore, most endoscopists agree that large gastric polyps or polyps associated with complications should be removed endoscopically or surgically. On the other hand, signet ring cell carcinoma rarely occurs in gastric hyperplastic polyps; however, no standardized therapy for such cases has been established. Herein, we report a rare case of a Japanese woman diagnosed with minute signet ring cell carcinoma in a gastric hyperplastic polyp and treated with endoscopic mucosal resection (EMR).

CASE REPORT

A 45-year-old woman visited our hospital for a follow-up study of a gastric polyp. She had been diagnosed with gastric hyperplastic polyp on the posterior wall of the middle third area 5 years previously. Her body temperature was 36.4℃, blood pressure was 126/78 mmHg, and radial pulse rate was 66 beats/min and regular. She had neither anemia nor jaundice. A neurological examination revealed no abnormal findings and there was no lymphadenopathy. No specific family history was identified. Routine hematological examination and biochemical tests were within normal limits. Serum anti-*H pylori* immunoglobulin G (IgG) antibody was positive. Endoscopic examination of the upper digestive tract revealed a small gastric hyperplastic polyp in the posterior wall of the gastric body (Fig. 1). The first biopsy specimen obtained from the polyp showed signet ring cell carcinoma. However, the biopsy specimen obtained repeatedly (three times) from the lesion revealed hyperplastic foveolar epithelium. Thus, the definite diagnosis could not be made. The patient underwent an EMR for histological confirmation. The protruding lesion, 6 × 5 mm in size, was resected completely with a safe lateral and vertical margin (Fig. 2). Histological examination showed neoplastic cells with signet ring features surrounded by the tissue of the hyperplastic polyp (Fig. 2). The protruding lesion was diagnosed as minute signet ring cell carcinoma in a hyperplastic polyp with mucosal invasion, ly0, and v0.

DISCUSSION

This case involved the unusual association of a gastric hyperplastic polyp and focal signet ring cell carcinoma. Histological features in this case fulfilled the criteria of Nakamura *et al*[3] for the malignant transformation of hyperplastic polyps: (1) coexistence of benign and malignant parts in the same polyp; (2) existence of sufficient evidence that the benign area had previously been a benign polyp; and existence of sufficient cellular and structural atypia in the malignant area to be diagnosed as cancer.

The relationship between gastric hyperplastic polyp and gastric cancer remains unknown. In a study of gastric polyps[2,4] we found that hyperplastic polyps are the most common; nearly 85%-91% of all polyps were hyperplastic polyps. In another report, the incidence of gastric hyperplastic polyps was reported to be 28.3% in one series of 5515 gastric polyps by Stolte *et al*[5]. As gastric

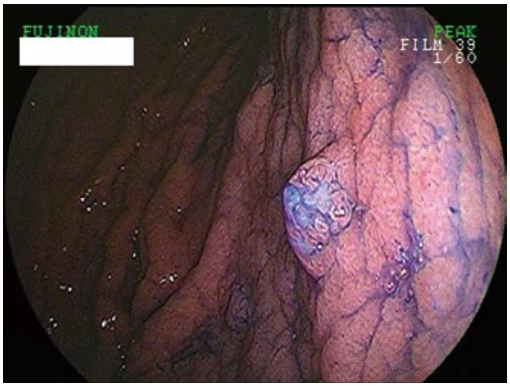

Figure 1 Endoscopic appearance of the gastric hyperplastic polyp in the posterior wall of the gastric body.

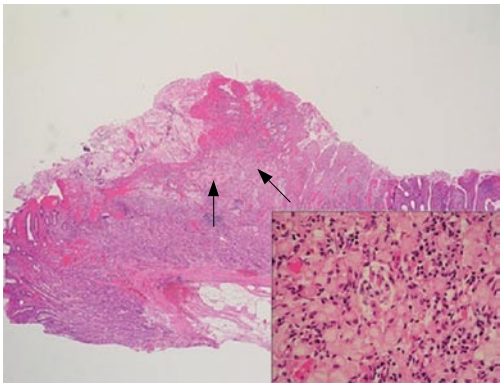

Figure 2 The resected specimen obtained by endoscopic mucosal resection showing localized neoplastic cells with signet ring features limited to the mucosal layer (arrows) (HE, × 10, × 100).

hyperplastic polyps are common, we should identify the relationship between gastric hyperplastic polyps and gastric cancer. It is generally acknowledged that the natural course of hyperplastic polyps does not include transformation to carcinoma, although hyperplastic polyps occasionally associate with gastric cancer[6-8]. In these reports, most hyperplastic polyps harboring cancer were larger than 1 cm in size[6-8]. The malignant transformation of a hyperplastic polyp is considered to relate to the size and macroscopic type; as the polyp grows larger and becomes semipedunculated or pedunculated, adenomatous or dysplastic foci appear first, followed by the cancerous lesion. Most adenocarcinomas found within hyperplastic polyps are the differentiated type. Few cases of signet ring cell carcinoma occurring in gastric hyperplastic polyps have been reported[4,9].

In the present case, the hyperplastic polyp, 6 mm in diameter, was associated with focal signet ring cell carcinoma and was diagnosed by endoscopic biopsy by chance. However, we could not locate the cancer in the polyp by careful observation with endoscopy. Thus, association of hyperplastic polyp and gastric cancer should generally be taken into consideration when endoscopists detect gastric hyperplastic polyps. Endoscopists should aggressively obtain biopsy specimens from hyperplastic polyps even if they are small.

In conclusion, we report the case of a woman diagnosed with minute signet ring cell carcinoma in a hyperplastic gastric polyp. This case emphasizes that small gastric hyperplastic polyp may be associated with gastric cancer, and periodic follow-up endoscopy and careful observation are necessary when treating patients with gastric hyperplastic polyp, even when it is less than 1 cm.

REFERENCES

1 **Alper M**, Akcan Y, Belenli O. Large pedinculated antral hyperplastic gastric polyp traversed the bulbus causing outlet obstruction and iron deficiency anemia: endoscopic removal. *World J Gastroenterol* 2003; **9**: 633-634
2 **Gencosmanoglu R**, Sen-Oran E, Kurtkaya-Yapicier O, Tozun N. Antral hyperplastic polyp causing intermittent gastric outlet obstruction: case report. *BMC Gastroenterol* 2003; **3**: 16
3 **Nakamura T**, Nakano G. Histopathological classification and malignant change in gastric polyps. *J Clin Pathol* 1985; **38**: 754-764
4 **Zea-Iriarte WL**, Itsuno M, Makiyama K, Hara K, Haraguchi M, Ajioka Y. Signet ring cell carcinoma in hyperplastic polyp. *Scand J Gastroenterol* 1995; **30**: 604-608
5 **Stolte M**, Sticht T, Eidt S, Ebert D, Finkenzeller G. Frequency, location, and age and sex distribution of various types of gastric polyp. *Endoscopy* 1994; **26**: 659-665
6 **Daibo M**, Itabashi M, Hirota T. Malignant transformation of gastric hyperplastic polyps. *Am J Gastroenterol* 1987; **82**: 1016-1025
7 **Yamaguchi K**, Shiraishi G, Maeda S, Kitamura K. Adenocarcinoma in hyperplastic polyp of the stomach. *Am J Gastroenterol* 1990; **85**: 327-328
8 **Gotoh Y**, Fujimoto K, Sakata Y, Fujisaki J, Nakano S. Poorly differentiated adenocarcinoma in a gastric hyperplastic polyp. *South Med J* 1996; **89**: 453-454
9 **Fry LC**, Lazenby AJ, Lee DH, Mönkemüller K. Signet-ring-cell adenocarcinoma arising from a hyperplastic polyp in the stomach. *Gastrointest Endosc* 2005; **61**: 493-495

S- Editor Liu Y **L- Editor** Alpini GD **E- Editor** Wang HF

Online Submissions: wjg.wjgnet.com
www.wjgnet.com
wjg@wjgnet.com

World J Gastroenterol 2007 November 21; 13(43): 5781-5782
World Journal of Gastroenterology ISSN 1007-9327

CASE REPORT

Mucinous cyst exhibiting severe dysplasia in gastric heterotopic pancreas associated withe gastrointestinal stromal tumour

Antony Kaufman, David Storey, Cheok Soon Lee, Rajmohan Murali

Antony Kaufman, Cheok Soon Lee, Rajmohan Murali, Department of Anatomical Pathology, Sydney Cancer Centre, Royal Prince Alfred Hospital, Camperdown, New South Wales, Australia
David Storey, Department of Surgery, Royal Prince Alfred Hospital, Camperdown, New South Wales, Australia
Rajmohan Murali, Sydney Melanoma Unit, Sydney Cancer Centre, Royal Prince Alfred Hospital, Camperdown, New South Wales, Australia
Correspondence to: Dr. Rajmohan Murali, Department of Anatomical Pathology, Royal Prince Alfred Hospital, Missenden Road, Camperdown, NSW 2050, Sydney, Australia. rajmohan.murali@email.cs.nsw.gov.au
Telephone: +61-2-95157458 Fax: +61-2-95158405
Received: September 28, 2006 Revised: September 3, 2007

Abstract

Heterotopic pancreatic tissue within the stomach is rare and dysplasia within heterotopic pancreatic tissue is very rare. We present the first report of a patient with concurrent occurrence of heterotopic pancreas in the stomach with a gastrointestinal stromal tumour.

Key words: Dysplasia; Gastrointestinal stromal tumour; Heterotopic pancreas; Mucinous cyst; Stomach

Kaufman A, Storey D, Lee CS, Murali R. Mucinous cyst exhibiting severe dysplasia in gastric heterotopic pancreas associated with gastrointestinal stromal tumour. *World J Gastroenterol* 2007; 13(43): 5781-5782

http://www.wjgnet.com/1007-9327/13/5781.asp

INTRODUCTION

Heterotopic pancreas is a relatively common lesion found in approximately 1 in 500 abdominal laparotomies[1] with approximately 62% found in the stomach[2]. Pancreatic heterotopia is defined as pancreatic tissue lacking vascular or anatomical continuity with the normal pancreas[1]. Symptoms associated with heterotopic pancreas are rare, but when present are usually associated with a gastric site. Symptoms may be due to mass effect such as pyloric obstruction, ulceration or bleeding, or due to pancreatic diseases such as pancreatitis, cyst formation or pancreatic neoplasia. Dysplasia and malignancy within pancreatic heterotopia are rare events[3]. The synchronous occurrence of gastrointestinal stromal tumour (GIST) and heterotopic pancreas has not, to our knowledge, been previously reported.

CASE REPORT

A 71 year-old female was admitted to our hospital for melaena (77 g/L haemoglobin). She underwent endoscopy, and two lesions were visualised in the gastric antrum, one with overlying mucosal ulceration. The lesions were not biopsied as they were scheduled for resection. On the following day, both lesions were resected. Macroscopically the lesions measured 70 mm × 50 mm × 40 mm and 15 mm × 15 mm × 12 mm. The former was a solid tumour with a fleshy tan cut surface, while the latter was a solid and cystic lesion containing a single cyst (10 mm in diameter) filled with mucinous material. The solid lesion with surface ulceration was a gastrointestinal stromal tumour (intermediate risk, uncertain malignant potential)[4] composed of fascicles of spindle cells exhibiting mild nuclear pleomorphism and up to 4 mitotic figures per 50 high power fields (Figure 1). Large areas of tumour necrosis were present. Surface ulceration was present, which was the likely source of melaena.

The smaller lesion was composed of pancreatic ducts and acini within the gastric submucosa and focally extended into the muscularis propria. Within this area was a cyst partly lined by mucinous epithelium while in some areas the lining epithelium was denuded. The mucinous epithelium exhibited moderate to severe dysplastic cytoarchitectural features (tufted and micropapillary architecture, along with nuclear enlargement, stratification, coarsely granular chromatin and nucleolar prominence) (Figure 2). Around the cyst there were small pools of extracellular mucin, associated with a chronic inflammatory response suggestive of partial rupture. Adjacent smaller dilated ducts were lined by non-dysplastic columnar mucinous epithelium. No evidence of stromal invasion was present. The cyst lining cells were positive for CK7 and CK20 (Figure 2), the latter was localized in the dysplastic areas. The intracytoplasmic mucin was positive for alcian blue pH 0.5 and periodic acid Schiff.

The gastric mucosa adjacent to the lesions showed active chronic gastritis, *H pylori* organisms and intestinal metaplasia.

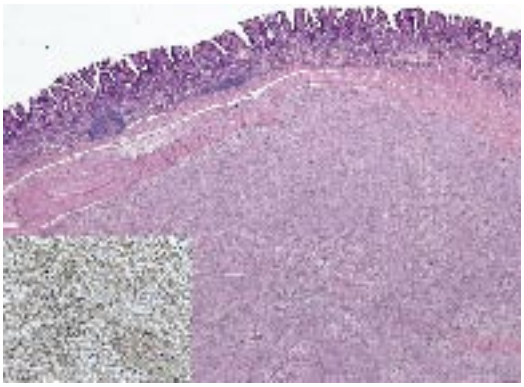

Figure 1 Gastrointestinal stromal tumour composed of fascicles of spindle cells. The tumour cells are positive for CD117 (inset).

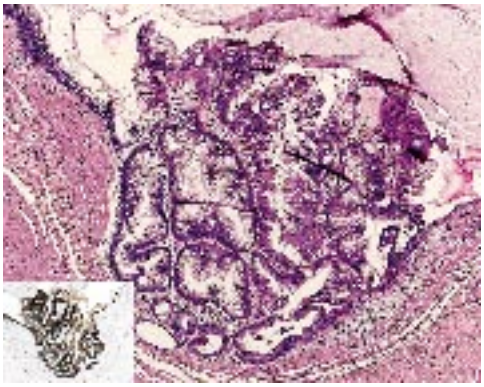

Figure 2 Severely dysplastic mucinous epithelium lining mucin-filled cyst in heterotopic pancreas. The dysplastic epithelium is positive for CK20 (inset).

DISCUSSION

Heterotopic pancreas is a relatively common lesion most often present in the gastric antrum seen macroscopically as a round or lobulated white to yellow which can be up to a few centimetres in dimension[2]. Diagnosis is difficult and often not made until surgical removal of the lesion. Heterotopic pancreas has been classified into three types by Heinrich: class I is typical pancreatic tissue with acini, ducts and islet cells, class Ⅱ shows a large number of acini and few ducts, and class Ⅲ shows numerous ducts with few acini or islet cells[5]. Neoplasms arising in heterotopic pancreatic tissue are rare[6] and include borderline mucinous cystic tumour[7], adenocarcinoma[6], mucinous cystadenocarcinoma[8], acinar cell carcinoma[2], islet cell tumour[9], or solid and papillary neoplasm[10]. Cystic degeneration without malignant change appears to be more common and may mimic mucinous carcinoma from another primary site[11]. The case report by Naqvi *et al*[7] includes a description of jejunal pancreatic heterotopia with cystically dilated ducts lined by mucinous epithelium showing low grade dysplastic cytoarchitectural features. They diagnosed a borderline mucinous cystic tumour without documenting the presence of ovarian type stroma. Of the reported cases of malignancy few have included reference to dysplastic or pre-malignant change[8,12]. These reports note the presence of dysplasia or carcinoma *in-situ* within the heterotopic pancreas adjacent to invasive ductal adenocarcinoma. Given the morphological appearances of the severe dysplasia seen in our patient, it is likely that the changes represent a pre-malignant change akin to that reported in orthotopic pancreas under the rubric "pancreatic intraepithelial neoplasia" (PanIN). Although malignant change within heterotopic pancreas is rare, we recommend that in the presence of dysplastic change within heterotopic pancreas tissue, the entire lesion should be sampled and examined histologically to exclude the presence of invasive malignancy.

REFERENCES

1 **Solcia E**, Capella C, Kloppel G. Tumors of the pancreas. Washington: Armed Forces Institute of Pathology, 1995; 231-232

2 **Makhlouf HR**, Almeida JL, Sobin LH. Carcinoma in jejunal pancreatic heterotopia. *Arch Pathol Lab Med* 1999; **123**: 707-711

3 **Kloppel G**, Hruban RH, Longnecker DS, Adler G, Kern SE, Partanen TJ. Ductal adenocarcinoma of the pancreas. In: World Health Organisation classification of tumours. Pathology and genetics of tumours of the digestive system. Lyon: IARC Press, 2000; 221

4 **Fletcher CD**, Berman JJ, Corless C, Gorstein F, Lasota J, Longley BJ, Miettinen M, O'Leary TJ, Remotti H, Rubin BP, Shmookler B, Sobin LH, Weiss SW. Diagnosis of gastrointestinal stromal tumors: A consensus approach. *Hum Pathol* 2002; **33**: 459-465

5 **Song DE**, Kwon Y, Kim KR, Oh ST, Kim JS. Adenocarcinoma arising in gastric heterotopic pancreas: a case report. *J Korean Med Sci* 2004; **19**: 145-148

6 **Emerson L**, Layfield LJ, Rohr LR, Dayton MT. Adenocarcinoma arising in association with gastric heterotopic pancreas: A case report and review of the literature. *J Surg Oncol* 2004; **87**: 53-57

7 **Naqvi A**, de la Roza G. Borderline mucinous cystic tumor in jejunal pancreatic heterotopia. *Ann Diagn Pathol* 2004; **8**: 151-155

8 **Nisar PJ**, Zaitoun AM, Lobo DN, Rowlands BJ. Heterotopic pancreas in the spleen: malignant degeneration to mucinous cystadenocarcinoma. *Eur J Gastroenterol Hepatol* 2002; **14**: 793-796

9 **Tolentino LF**, Lee H, Maung T, Stabile BE, Li K, French SW. Islet cell tumor arising from a heterotopic pancreas in the duodenal wall with ulceration. *Exp Mol Pathol* 2004; **76**: 51-56

10 **Ishikawa O**, Ishiguro S, Ohhigashi H, Sasaki Y, Yasuda T, Imaoka S, Iwanaga T, Nakaizumi A, Fujita M, Wada A. Solid and papillary neoplasm arising from an ectopic pancreas in the mesocolon. *Am J Gastroenterol* 1990; **85**: 597-601

11 **Nopajaroonsri C**. Mucus retention in heterotopic pancreas of the gastric antrum. A lesion mimicking mucinous carcinoma. *Am J Surg Pathol* 1994; **18**: 953-957

12 **Osanai M**, Miyokawa N, Tamaki T, Yonekawa M, Kawamura A, Sawada N. Adenocarcinoma arising in gastric heterotopic pancreas: clinicopathological and immunohistochemical study with genetic analysis of a case. *Pathol Int* 2001; **51**: 549-554

S- Editor Liu Y **L- Editor** Wang XL **E- Editor** Wang HF

Online Submissions: wjg.wjgnet.com
www.wjgnet.com
wjg@wjgnet.com

World J Gastroenterol 2007 November 21; 13(43): 5783-5786
World Journal of Gastroenterology ISSN 1007-9327

CASE REPORT

Association of liver cirrhosis related IgA nephropathy with portal hypertension

Georgios Kalambokis, Leonidas Christou, Dimitrios Stefanou, Evdokia Arkoumani, Epameinondas V Tsianos

Georgios Kalambokis, Leonidas Christou, Epameinondas V Tsianos, 1st Division of Internal Medicine and Hepato-gastroenterology Unit, University Hospital, Ioannina, Greece
Dimitrios Stefanou, Evdokia Arkoumani, Department of Pathology, University Hospital, Ioannina, Greece
Correspondence to: Dr. Epameinondas V Tsianos, Professor, Medical School of Ioannina, 45110 Ioannina, Greece. geodora@mail.gr
Telephone: +30-26510-97501 Fax: +30-26510-97016
Received: June 7, 2007 Revised: September 6, 2007

Abstract

A high incidence of IgA nephropathy has been reported in patients with liver cirrhosis, though, clinically evident nephrotic syndrome is very uncommon. Impaired hepatic clearance of circulating IgA immune complexes and subsequent deposition in renal glomeruli has been considered principally in the pathogenesis of liver cirrhosis associated IgA nephropathy. Here we report on a patient with cryptogenic liver cirrhosis and splenic vein thrombosis, who presented with nephrotic syndrome. Renal biopsy showed findings consistent with IgA nephropathy. Lower endoscopy showed features of portal hypertensive colopathy. Following initiation of propranolol and anticoagulant treatment to reduce portal pressure, a gradual decrease of proteinuria and hematuria to normal range was noted. The potential pathogenetic role of portal hypertension in the development of IgA nephropathy in cirrhotic patients is discussed.

Key words: IgA nephropathy; Nephrotic syndrome; Portal hypertension; Liver cirrhosis

Kalambokis G, Christou L, Stefanou D, Arkoumani E, Tsianos EV. Association of liver cirrhosis related IgA nephropathy with portal hypertension. *World J Gastroenterol* 2007; 13(43): 5783-5786

http://www.wjgnet.com/1007-9327/13/5783.asp

INTRODUCTION

IgA nephropathy (IgAN) is a well known concomitant of liver cirrhosis (LC) with largely unknown pathogenesis[1,2]. Most of the literature has focused on the causative role of impaired clearance of circulating IgA immune complexes (IgAIC) by the diseased liver with subsequent intraglomerular deposition[1,3-5]. Other reports suggested that some etiological factors of chronic liver disease may be associated per se with development of IgAN[6-11]. We report the case of a patient with portal hypertension (PH) due to cryptogenic LC and splenic vein thrombosis (SVT) presented as nephrotic syndrome (NS), caused by IgAN. Proteinuria resolved after the introduction of propranolol and oral anticoagulation. The association of PH with IgAN is reviewed and potential pathogenetic mechanisms through which PH can cause IgAN in cirrhotic patients are proposed.

CASE REPORT

A 34-year-old man was evaluated for nephrotic range proteinuria and LC. Seven days before, he was admitted to another hospital with a 6-mo history of ankle swelling and periorbital oedema, and a 3-wk history of increased abdominal distention. Abdominal ultrasound showed a nodular liver, moderate ascites, and splenomegaly; the kidneys had normal dimensions and structure. Diagnostic aspiration of peritoneal fluid showed no evidence of infection; the serum ascites albumin gradient was consistent with PH (1.2). A large volume paracentesis was performed and daily treatment with furosemide 40 mg and spironolactone 100 mg was initiated.

On admission, the patient had mild peripheral oedema and ascites. Past history, including blood transfusion and alcohol consumption, was unremarkable, and he denied taking regular medication. There was no history of family renal or liver disease. Abnormal laboratory results were as follows: hemoglobin 114 g/L (normal range, 130-180), platelet count 79 000/mm^3 (130 000-400 000), international normalized ratio 1.2, fibrinogen 3.2 g/L (2-4), plasma D-dimers 1310 mg/L (< 200), serum urea 9.86 mmol/L (1.7-8.3), serum creatinine 88.4 μmol/L (53-106), total bilirubin 20.5 μmol/L (5.1-17), alanine aminotransferase 59 U/L (4-36), serum total protein 56 g/L (60-78), and serum albumin 22 g/L (32-45). Urinary protein was 3.6 g/day (< 0.06), red cell content 80-100 per field, white cell content 0-2 per field. Serum IgA was 7.1 g/L (0.9-3.2), IgG 15.7 g/L (8-15), and IgM 2.3 g/L (0.5-3). Serum C3 and C4 were 0.76 g/L (0.86-1.84) and 0.1 g/L (0.2-0.58), respectively. Chest radiography and echocardiography were normal. Stool examination for occult blood was positive with a ferritin of 5 ng/mL (6-80).

Liver biopsy confirmed LC but failed to disclose the aetiology of liver disease. The results of a thorough diagnostic work-up, including PCR for HBV and HCV, antimitochondrial antibodies, antinuclear antibodies, anti-smooth muscle antibodies, anti-liver-kidney microsomal antibodies, soluble liver antigen, alpha1-antitrypsin, copper and iron studies, and cryoglobulins, were also negative. Upper gastrointestinal endoscopy showed 1st degree esophageal varices and congested gastric mucosae. Colonoscopy revealed hyperemia, mucosal oedema, and friability throughout the entire colon, indicative of PHC. Abdominal computed tomography and venography revealed SVT and extensive venous collateral circulation; there was no evidence of splenorenal shunt, and portal or renal vein thrombosis. Investigation for acquired and inherited thrombophilic factors revealed the G20210A heterozygous mutation of prothombin. Other coagulation defects, including deficiencies of natural inhibitors of coagulation (protein C, protein S, antithrombin), factor V Leiden mutation, TT677 mutation of methylene-tetrahydrofolate reductase, and anticardiolipin antibodies, were not detected.

A renal biopsy demonstrated a diffuse endocapillary glomerulonephritis with a small proportion of crescends. The immunofluorescent study revealed IgA deposits of high intensity, localized within the mesangium of all glomeruli, as well as lesser amounts of IgM and C3. The electron-microscopic study showed electron-dense deposits under the basement membrane of capillaries that extended to the paramesangial region. A few intramembranous deposits were also seen (Figure 1).

Propranolol, increasing to 60 mg daily to achieve a reduction of heart rate by 25%, the vitamin K antagonist acenocoumarol, targeting an INR in the range of 2-3, and iron sulfate were added to diuretic treatment. Renal protein excretion decreased to normal range within 20 d together with a reduction of IgA levels (3.4 g/L) and disappearance of hematuria; ascites and oedema gradually resolved. One month later, repeated tomography showed patent splenic vein and a decrease in collateral circulation and size of spleen.

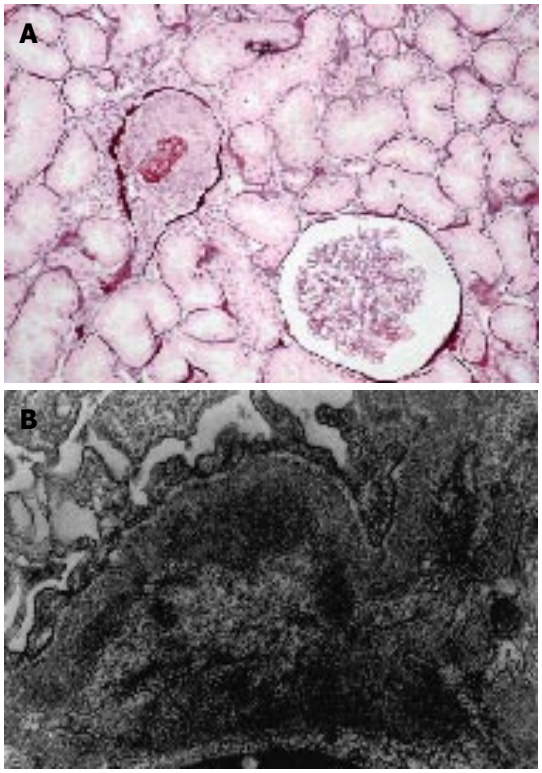

Figure 1 **A**: Light microscopy study showing endocapillary and extracapillary proliferation. A large cellular crescend is observed in the left upper glomerulus (silver methoxamine stain, × 200); **B**: Electron-microscopic study showing intramembranous and paramesangial electron-dense deposits (× 13 000).

DISCUSSION

IgAN associated with liver disease is the commonest form of secondary IgAN[12]. Glomerular deposits of IgA and fewer amounts of other immunoglobulins and C3 have been noted in 35% to 90% of cirrhotic patients[1,2]. The majority of IgA synthesis in human is mucosal, predominantly polymeric (pIgA) with two isotypes, IgA1 and IgA2, in about equal proportions. Normally, little mucosal pIgA reaches the circulation[12]. In patients with chronic liver disease, increased circulating IgA against gut flora and IgAIC have been reported[5,13]. Serum complement factor levels may be low due to activation of complement components by immune complexes, hepatic hyposynthesis, or both[14]. PIgA2 is mainly eliminated through the hepatic asialoglycoprotein receptor (ASGR) whereas only a small percentage of pIgA1 is cleared through this pathway[15], which explains the higher proportion of circulating IgA2 in chronic liver disease[16]. The majority of pIgA is then released back to the circulation in degraded forms[17]. Kupffer cells participate in the removal of IgA expressing specific Fc receptors[18]. PIgA1 is the predominant form in mesangial deposits[19], yet no antigens have been identified within the mesangial deposits.

LC-related IgAN is usually clinically silent[1]. Nakamoto *et al*[20] reported NS in 1.6% of a series of 752 cirrhotic patients. Microscopic but rarely gross hematuria may occur, but it is less common than in patients with primary IgAN[1,20].

The pathogenesis of LC-related IgAN remains uncertain. Impaired hepatic clearance of IgAIC due to reduced phagocytic[1,3-5] or ASGR[6] activity, which subsequently are deposited in the renal glomeruli, have been considered principally in the literature. However, there is no correlation between the degree of liver damage and the IgAIC levels[16]. In addition, a direct association of various causes of chronic liver disease, such as hepatitis viruses B[6] and C[7] infections, heavy alcohol consumption[8], autoimmune hepatitis[9], primary hemochromatosis[10], and alpha1-antitrypsin deficiency[11] with immunological renal injury has been suggested.

In the present case, IgAN was secondary to LC of unknown etiology complicated by PH and portosystemic shunting, as shown by the imaging results, and the presence of PHC[21] and esophageal varices. Proteinuria and hematuria resolved after introduction of propranolol to improve PHC[21] by decreasing portal pressure and tributary flow[22]. No significant renal effects of propranolol have been reported in cirrhotic patients to

justify decrease of proteinuria[23]. SVT has been associated with left-sided PH in non-cirrhotic subjects[24]. Therefore, acenocumarol may have exerted an additive portal hypotensive effect in our patient by restoring SVT, possibly related to PTHR A20210 mutation[25] or NS per se[26]. Renal vein thrombosis[26] or spontaneous splenorenal shunt[27], which might have been involved in the development and progress of IgAN in our patient, were not confirmed by computed tomography and venography.

Consistent with our observations, three previous case reports highlighted the pivotal role of PH in the development of LC-related IgAN[28-30]. Nakamura *et al*[28] reported a progressive fall in proteinuria together with clinical remission of NS after initiation of propranolol in a patient with cryptogenic LC. In another case of non-cirrhotic PH and IgAN induced NS, portacaval anastomosis decreased portal pressure causing proteinuria and hematuria to disappear[29]. Finally, Babbs *et al*[30] described a case of IgAN in a non-cirrhotic patient with a large splenic artery aneurysm causing PH and extensive collateral circulation. Splenectomy and aneurysm resection induced remission of the NS and hematuria.

The portosystemic shunting that results from PH may cause IgA to deviate from hepatic uptake and depolymerization[1]. Therefore, reduction of PH is expected to increase hepatic processing of IgAIC. PH also decreases small intestinal motility promoting bacterial overgrowth[31,32], while in the same time increases intestinal permeability[33]. In this regard, increased circulating IgA and IgAIC may represent an exaggerated response of immune system to excess gut antigen exposure[34,35], resulting from diminished mucosal integrity and spillage of IgA into the circulation. Another mechanism could involve the endotoxemia that frequently accompanies LC with PH[36], suggested to be generated by gut flora through bacterial translocation[37,38] favored by dysfunction of intestinal barrier[33,37]. Previous literature showed that endotoxemia may decrease hepatic ASGR binding[39]. Therefore, portal hypotensive treatment may decrease bacterial translocation and endotoxin levels[40], which could restore ASGR function.

In conclusion, PH seems to play a significant role in the pathogenesis of IgAN associated with LC. In this point of view, a decrease in PH is likely to reduce renal protein excretion in patients with significant proteinuria. Further studies are needed to assess if the severity of PH is related with the magnitude of renal IgA deposition.

REFERENCES

1 **Newell GC**. Cirrhotic glomerulonephritis: incidence, morphology, clinical features, and pathogenesis. *Am J Kidney Dis* 1987; **9**: 183-190
2 **Sinniah R**. Heterogeneous IgA glomerulonephropathy in liver cirrhosis. *Histopathology* 1984; **8**: 947-962
3 **Endo Y**, Matsushita H, Nozawa Y, Nishikage S, Matsuya S, Hara M. Glomerulonephritis associated with liver cirrhosis. *Acta Pathol Jpn* 1983; **33**: 333-346
4 **Iida H**, Izumino K, Matsumoto M, Takata M, Mizumura Y, Sugimoto T. Glomerular deposition of IgA in experimental hepatic cirrhosis. *Acta Pathol Jpn* 1985; **35**: 561-567
5 **Sancho J**, Egido J, Sánchez-Crespo M, Blasco R. Detection of monomeric and polymeric IgA containing immune complexes in serum and kidney from patients with alcoholic liver disease. *Clin Exp Immunol* 1982; **47**: 327-335
6 **Lai KN**, Lai FM, Tam JS, Vallance-Owen J. Strong association between IgA nephropathy and hepatitis B surface antigenemia in endemic areas. *Clin Nephrol* 1988; **29**: 229-234
7 **Couser WG**. Glomerulonephritis. *Lancet* 1999; **353**: 1509-1515
8 **Cecchin E**, De Marchi S. Alcohol misuse and renal damage. *Addict Biol* 1996; **1**: 7-17
9 **Singri N**, Gleason B, Flamm SL, Kanwar YS, Ghossein C. Secondary IgA nephropathy presenting as nephrotic syndrome with glomerular crescentic changes and acute renal failure in a patient with autoimmune hepatitis. *J Nephrol* 2004; **17**: 125-129
10 **Gouet D**, Fort E, Roblot P, Maréchaud R, Sudre Y, Touchard G. Glomerulopathy with mesangial IgA deposits in primary hemochromatosis. *Rev Med Interne* 1987; **8**: 311-312
11 **Szönyi L**, Dobos M, Vásárhelyi B, Héninger E, Vas T, Nagy J, Kovács T. Prevalence of alpha1-antitrypsin phenotypes in patients with IgA nephropathy. *Clin Nephrol* 2004; **62**: 418-422
12 **Pouria S**, Feehally J. Glomerular IgA deposition in liver disease. *Nephrol Dial Transplant* 1999; **14**: 2279-2282
13 **Coppo R**, Aricò S, Piccoli G, Basolo B, Roccatello D, Amore A, Tabone M, De la Pierre M, Sessa A, Delacroix DL. Presence and origin of IgA1- and IgA2-containing circulating immune complexes in chronic alcoholic liver diseases with and without glomerulonephritis. *Clin Immunol Immunopathol* 1985; **35**: 1-8
14 **Nochy D**, Callard P, Bellon B, Bariety J, Druet P. Association of overt glomerulonephritis and liver disease: a study of 34 patients. *Clin Nephrol* 1976; **6**: 422-427
15 **Rifai A**, Fadden K, Morrison SL, Chintalacharuvu KR. The N-glycans determine the differential blood clearance and hepatic uptake of human immunoglobulin (Ig)A1 and IgA2 isotypes. *J Exp Med* 2000; **191**: 2171-2182
16 **Delacroix DL**, Elkom KB, Geubel AP, Hodgson HF, Dive C, Vaerman JP. Changes in size, subclass, and metabolic properties of serum immunoglobulin A in liver diseases and in other diseases with high serum immunoglobulin A. *J Clin Invest* 1983; **71**: 358-367
17 **Finck MH**, Reichen J, Vierling JM, Kloppel TM, Brown WR. Hepatic uptake and disposition of human polymeric IgA1 in perfused rat liver: evidence for incomplete biliary excretion and intrahepatic degradation. *Am J Physiol* 1985; **248**: G450-G455
18 **Rifai A**, Mannik M. Clearance of circulating IgA immune complexes is mediated by a specific receptor on Kupffer cells in mice. *J Exp Med* 1984; **160**: 125-137
19 **Lomax-Smith JD**, Zabrowarny LA, Howarth GS, Seymour AE, Woodroffe AJ. The immunochemical characterization of mesangial IgA deposits. *Am J Pathol* 1983; **113**: 359-364
20 **Nakamoto Y**, Iida H, Kobayashi K, Dohi K, Kida H, Hattori N, Takeuchi J. Hepatic glomerulonephritis. Characteristics of hepatic IgA glomerulonephritis as the major part. *Virchows Arch A Pathol Anat Histol* 1981; **392**: 45-54
21 **Ohashi K**, Orihata G, Ohta S, Takamori S, Kojima K, Fukazawa M, Beppu T, Futagawa S. Portal hypertensive gastropathy and colopathy. *Nihon Rinsho* 1998; **56**: 2369-2375
22 **Lebrec D**, Hillon P, Muńoz C, Goldfarb G, Nouel O, Benhamou JP. The effect of propranolol on portal hypertension in patients with cirrhosis: a hemodynamic study. *Hepatology* 1982; **2**: 523-527
23 **Henriksen JH**, Ring-Larsen H. Renal effects of drugs used in the treatment of portal hypertension. *Hepatology* 1993; **18**: 688-695
24 **Evans GR**, Yellin AE, Weaver FA, Stain SC. Sinistral (left-sided) portal hypertension. *Am Surg* 1990; **56**: 758-763
25 **Rosendaal FR**, Doggen CJ, Zivelin A, Arruda VR, Aiach M, Siscovick DS, Hillarp A, Watzke HH, Bernardi F, Cumming AM, Preston FE, Reitsma PH. Geographic distribution of the 20210 G to A prothrombin variant. *Thromb Haemost* 1998; **79**: 706-708
26 **Sagripanti A**, Barsotti G. Hypercoagulability, intraglomerular coagulation, and thromboembolism in nephrotic syndrome.

Nephron 1995; **70**: 271-281
27 **Carrión JA**, Bellot P, Colmenero J, Garcia Pagan JC. Large spontaneous splenorenal shunt as a cause of chronic hepatic encephalopathy. *J Hepatol* 2004; **40**: 868
28 **Nakamura M**, Ohishi A, Watanabe R, Kaneko K, Aosaki N, Iigaya T, Monma T, Sugiura H, Miyoshi Y, Hamaguchi K. IgA nephropathy associated with portal hypertension in liver cirrhosis due to non-alcoholic and non-A, non-B, non-C hepatitis. *Intern Med* 1994; **33**: 488-491
29 **Laurent J**, Lagrue G, Bruneau C, Kazandjian M. Does portal hypertension play a role in IgA mesangial glomerulonephritis (IgG GN)? *Kidney Int* 1986; **30**: 640 (Abstract)
30 **Babbs C**, Warnes TW, Torrance HB, Ballardie FW. IgA nephropathy in non-cirrhotic portal hypertension. *Gut* 1991; **32**: 225-226
31 **Gunnarsdottir SA**, Sadik R, Shev S, Simrén M, Sjövall H, Stotzer PO, Abrahamsson H, Olsson R, Björnsson ES. Small intestinal motility disturbances and bacterial overgrowth in patients with liver cirrhosis and portal hypertension. *Am J Gastroenterol* 2003; **98**: 1362-1370
32 **Reilly JA**, Quigley EM, Forst CF, Rikkers LF. Small intestinal transit in the portal hypertensive rat. *Gastroenterology* 1991; **100**: 670-674
33 **Yao GX**, Shen ZY, Xue XB, Yang Z. Intestinal permeability in rats with CCl4-induced portal hypertension. *World J Gastroenterol* 2006; **12**: 479-481
34 **Macpherson AJ**. IgA adaptation to the presence of commensal bacteria in the intestine. *Curr Top Microbiol Immunol* 2006; **308**: 117-136
35 **Woodroffe AJ**, Gormly AA, McKenzie PE, Wootton AM, Thompson AJ, Seymour AE, Clarkson AR. Immunologic studies in IgA nephropathy. *Kidney Int* 1980; **18**: 366-374
36 **Lumsden AB**, Henderson JM, Kutner MH. Endotoxin levels measured by a chromogenic assay in portal, hepatic and peripheral venous blood in patients with cirrhosis. *Hepatology* 1988; **8**: 232-236
37 **Chiva M**, Guarner C, Peralta C, Llovet T, Gómez G, Soriano G, Balanzó J. Intestinal mucosal oxidative damage and bacterial translocation in cirrhotic rats. *Eur J Gastroenterol Hepatol* 2003; **15**: 145-150
38 **Albillos A**, de la Hera A, González M, Moya JL, Calleja JL, Monserrat J, Ruiz-del-Arbol L, Alvarez-Mon M. Increased lipopolysaccharide binding protein in cirrhotic patients with marked immune and hemodynamic derangement. *Hepatology* 2003; **37**: 208-217
39 **Leveille-Webster CR**, Rogers J, Arias IM. Use of an asialoglycoprotein receptor-targeted magnetic resonance contrast agent to study changes in receptor biology during liver regeneration and endotoxemia in rats. *Hepatology* 1996; **23**: 1631-1641
40 **Pérez-Paramo M**, Muñoz J, Albillos A, Freile I, Portero F, Santos M, Ortiz-Berrocal J. Effect of propranolol on the factors promoting bacterial translocation in cirrhotic rats with ascites. *Hepatology* 2000; **31**: 43-48

S- Editor Liu Y **L- Editor** Mihm S **E- Editor** Wang HF

Online Submissions: wjg.wjgnet.com
www.wjgnet.com
wjg@wjgnet.com

World J Gastroenterol 2007 November 21; 13(43): 5787-5793
World Journal of Gastroenterology ISSN 1007-9327

CASE REPORT

Cerebral metastasis from hepatoid adenocarcinoma of the stomach

Sheng Zhang, Mi Wang, Yi-Hui Xue, Yu-Peng Chen

Sheng Zhang, Mi Wang, Yi-Hui Xue, Yu-Peng Chen, Department of Pathology, The First Affiliated Hospital of Fujian Medical University, Fuzhou 350005, Fujian Province, China
Correspondence to: Dr. Sheng Zhang, Department of Pathology, The First Affiliated Hospital of Fujian Medical University, Fuzhou 350005, Fujian Province, China. zhgshg@126.com
Telephone: +86-591-87982733 Fax: +86-591-83318716
Received: August 24, 2007 Revised: September 9, 2007

Key words: Cerebral metastasis; Gastric hepatoid adenocarcinoma; Immunohistochemistry

Zhang S, Wang M, Xue YH, Chen YP. Cerebral metastasis from hepatoid adenocarcinoma of the stomach. *World J Gastroenterol* 2007; 13(43): 5787-5793

http://www.wjgnet.com/1007-9327/13/5787.asp

Abstract

We first report a rare case of metastasis from gastric hepatoid adenocarcinoma (HAC) to cerebral parenchyma, in a 50-year-old Chinese patient. He complained of a one-month history of a paroxysm of headache in the left temple and pars parietalis accompanied with binocular caligation caligo, insensible feeling of limbs and transient anepia. Magnetic resonance (MR) imaging revealed a spherical occupying lesion in the left posterior-temple lobe which was clinically diagnosed as a metastatic tumor. Three years ago, the patient accepted total gastrectomy as he was pathologically diagnosed at gastroscopy having an adenocarcinoma. Eight months after gastrectomy, the occupying lesion in liver was detected by ultrasound and CT, and he accepted transcatheter arterial embolization. Before operation of the brain metastasis, no obvious abnormality was found in liver by ultrasound. Histopathological characteristics of the brain tumor were identical to those of stomach tumor. The growth pattern of both tumors showed solid cell nests. The tumor cells were polygonal, and had abundant eosinophilic cytoplasm and round nuclei with obvious nucleoli. Sinusoid-like blood spaces were located between nodular tumor cells. Immunohistochemistry-stained tumor cells were positive for AFP and negative for Hep-Par-1. According to these histopathological findings, both tumors were diagnosed as HAC and metastatic HAC. The patient remained alive 16 mo after tumorectomy of the cerebral metastasis. The differential diagnosis of brain metastasis from metastatic tumors should use a panel of antibodies to avoid confusing with the brain metastasis of hepatocellular carcinoma (HCC). This paper describes this rare case of metastasis from gastric hepatoid adenocarcinoma to cerebral parenchyma, and provides a review of the literature concerning its histopathological and immunohistochemical characteristics.

INTRODUCTION

Gastric carcinoma is one of the most frequent tumors in the world. Its histological types include well- and poorly-differentiated adenocarcinoma, hepatoid adenocarcinoma (HAC), adenosquamous carcinoma, *etc*[1]. Metastasis of gastric carcinoma occurs mainly in organs and lymph nodes in venter imus, rarely in distant sites. Since Bourreille *et al*[2,3] reported the first case of gastric carcinoma with an increased level of serum alpha fetoprotein (AFP) in 1970, other cases have been reported[4,5]. In 1985, the term of hepatoid adenocarcinoma was used as malignant epithelial tumor derived from stomach by Ishikura *et al*[6]. The incidence rate of HAC is about 1.3%-1.5%. HAC produces a large amount of AFP, and is characterized by histopathological features, such as hepatoid differentiation, metastasis and poor prognosis. The number of brain metastases from gastric carcinoma, especially from gastric hepatoid adenocarcinoma is small. Only one case of cerebellar metastasis from gastric cancer with a higher level of AFP has been reported by Goda *et al*[7]. We present the first case of gastric hepatoid adenocarcinoma metastasis to cerebral parenchyma.

CASE REPORT

History and examination

A 50-year-old patient was admitted to our hospital with complaint of a one-month history of a paroxysm of headache in the left temple and pars parietalis accompanied with binocular caligation caligo, insensible feeling of limbs and transient anepia. The patient had no history of nausea and vomiting, spasm, palsy, aconuresis and copracrasia. Physical examination revealed decreased visual acuity and papilledema.

Radiological studies

Magnetic resonance (MR) imaging revealed a spherical occupying lesion of about 6.0 cm × 4.8 cm × 4.0 cm in

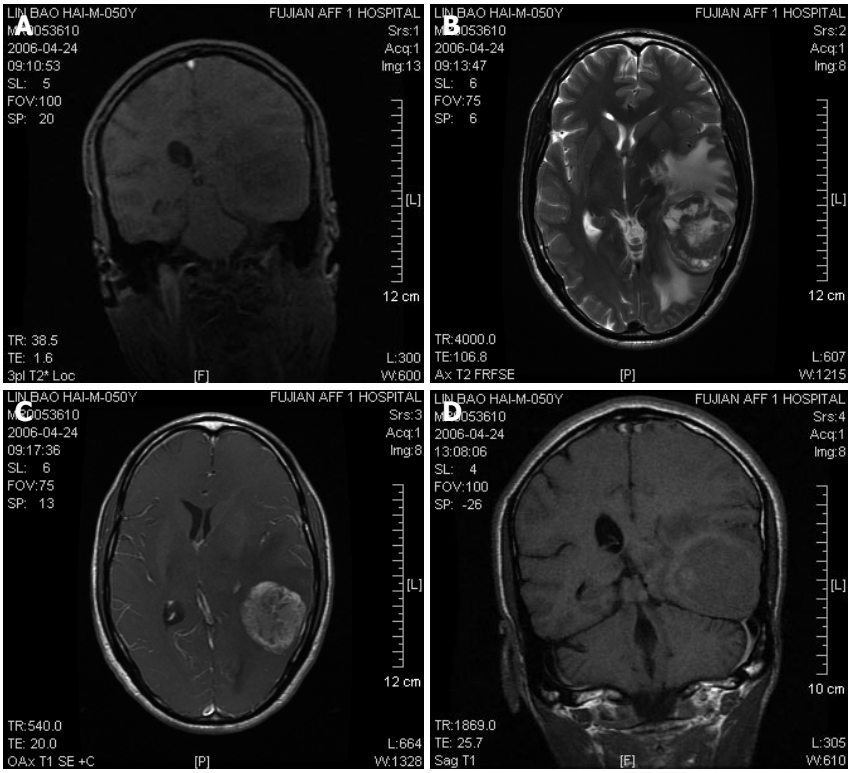

Figure 1 MR imaging revealing a spherical occupying lesion in the left posterior-temple lobe with a high intensity on T_2-weighted images and irregular contrast enhancement with a clear boundary and uneven signal in size of about 6.0 cm × 4.8 cm × 4.0 cm after administration of gadolinium-diethylene triamino pentaacetic acid (Gd-DTPA). **A**: Coronal gradient-recalled echo; **B**: Cross-sectional T2WI; **C**: Cross-sectional contrast enhancement T1WI; **D**: Coronal T1WI-delayed scan 4 h after contrast media injected *via* veins.

the left posterior-temple lobe with a high intensity on T_2-weighted images and irregular contrast enhancement with a clearly boundary and uneven signal after administration of gadolinium-diethylene triamino pentaacetic acid (Gd-DTPA). The lesion displayed an occupying effect, an out-inferior border close to the left transverse sinus, a perilesional irregular edema zone, compressed and deformed left posterior ventricle, and median line turned to dextroposition (Figure 1). The lesion was clinically diagnosed as a metastatic tumor.

Operation

On the 7th d after admission, the patient underwent tumorectomy. A tumor was found in subcortex of the left temporal lobe of about 0.3 cm and resected. A sample of about 4.0 cm × 5.0 cm × 5.0 cm was taken for pathological examination.

Pathological findings

Pathological analysis of the tumor sample revealed the growth pattern of solid cell nests. The polygonal tumor cells had abundant eosinophilic cytoplasm and round nuclei with obvious nucleoli. A pseudoglandular configuration containing proteic fluid was found in some parts of the tumor. Sinusoid-like blood spaces were located between nodular tumor cells (Figure 2). Metastasis of hepatocellular carcinoma was suspected.

Immunohistochemistry

Immunohistochemistry-stained hepatoid cells were positive for alpha-fetoprotein (AFP) and negative for Hep-Par-1 (Table 1, Figure 3), which did not match the immunohistochemical features of hepatocellular carcinoma metastasis.

Clinical history

Three years ago the patient was admitted to hospital due to recurrent pain in the epigastrium and accepted total gastrectomy because he was diagnosed having adenocarcinoma in cardia and corpora of the stomach with lymph node metastasis (Figure 4). No abnormal acoustic image in liver, pancreas, spleen and other organs was found on ultrasonograph. After surgery the patient received 6 mo of chemotherapy [calcium folinate (CF), 5-fluorouracil (5-FU) and cis-diamminedichloroplatinum (DDDP)]. The histopathological characteristics of brain tumor were identical to those of the sample sections. Immunohistochemistry-stained specimen of gastric carcinoma was positive for AFP and negative for Hep-Par-1 (Figure 5). Eight months after gastrectomy, an occupying lesion was detected in liver by ultrasound. CT scan also revealed a nodular or lump-like, high-density contrast mass in liver lobes during arterial phase, but the size of liver did not change, liver boundary was smooth and hepatic lobes were normal. The density of a larger mass of about 6.7 cm × 5.5 cm was uneven and the interior density was low at portal venous phase. The architecture of porta hepatis was clear (Figure 6). The diagnosis was liver metastasis from gastric carcinoma. Transcatheter arterial embolization for hepatic metastatic tumors with CF, 5-FU and DDDP was performed. The liver was rechecked by ultrasound every 6 mo after embolization. Before operation of the brain metastasis, ultrasound displayed no obvious abnormalities in liver and kidney and color Doppler flow imaging revealed no obvious bloodstream signals (Figure 7). Based on the results of histopathology and immunohistochemistry, the lesions were finally diagnosed as hepatoid adenocarcinoma (HAC) of cardia and corpora of the stomach and

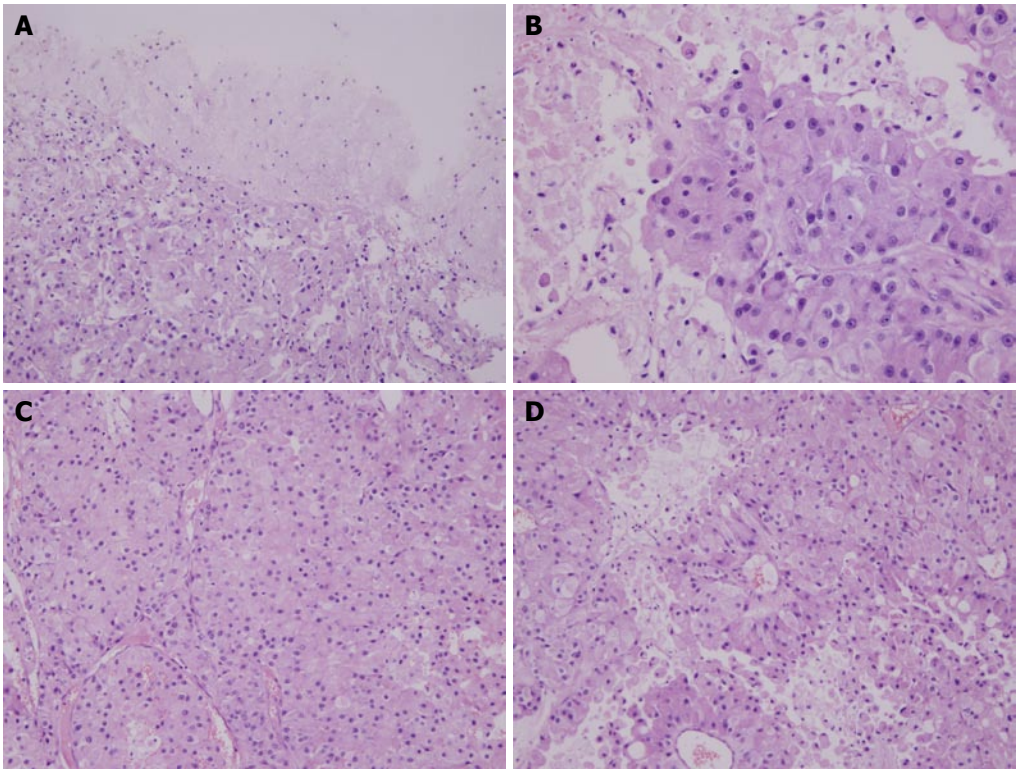

Figure 2 Brain metastatic tumor showing the growth pattern of solid cell nests (HE stain). **A**: Polygonal tumor cells with abundant eosinophilic cytoplasm, rich blood vessels and clear boundary of tumor and brain parenchyma (× 100); **B**: Polygonal tumor cells showing epitheliod and abundant eosinophilic cytoplasm, rich chromatin nuclei with obvious nucleoli (× 200); **C**: Round nuclei with obvious nucleoli, rich blood vessels resembling sinusoid-like blood spaces in hepatocellular carcinoma (× 200); **D**: Tumor cells exhibiting radial pattern surrounding thin- walled vessels (× 200).

metastatic hepatoid adenocarcinoma in the left posterior temple lobe, respectively. The patient was alive in the 16-mo follow-up period after operation of brain tumor.

DISCUSSION

Most patients with advanced gastric carcinoma die of metastasis and progressive cachexia. Metastasis of gastric carcinoma mainly occurs in peritoneal organs such as liver and lymph nodes; distant metastasis is rare. The incidence of intracranial metastasis from gastric carcinoma carcinoma ranges 1.3%-9.8%[8-10]. However, autopsy showed that the incidence of intracranial metastasis from gastric carcinoma is over 10.87%[11].

HAC is a special type of extrahepatic adenocarcinoma and its morphology is strikingly similar to that of hepatocellular carcinoma (HCC). Tumor cells consist of polygonal tumor cells with large central nuclei, prominent nucleoli, and abundant eosinophilic cytoplasm, showing solid growth pattern and less trabecular and glandular as well as frequent lymphatic and vascular invasiveness, regional prominent mitoses, but no bile secretion and periodic acid-Schiff-positive diastase-resistant hyaline globules. HAC has been found in different organs, such as the stomach, lung, pancreas, esophagus, papilla of Vater, colon, bladder, kidney, ovary, uterus, cervix and peritoneal organs[4,5,12-21]. Most patients are males, ranging in age from 40 to 77 years. The antrum and pylorus are the frequent locations of gastric HAC. Most patients with HAC show an elevated AFP serum level. The clinical course of HAC patients is aggressive and poor in survival. The biological behavior of HAC is associated mainly with extensive hematogenous metastasis to the liver and early involvement of lymph nodes. Up to date, only one case of cerebellum metastasis from gastric carcinoma with an elevated AFP level has been reported[7]. However, no report on supratentorial cerebral parenchymal metastasis of gastric HAC is available.

Table 1 Immunohistochemical characteristics of cerebral metastasis and primary gastric carcinoma

	Cerebral metastasis	Primary gastric carcinoma
AE1/AE3	+	+
EMA	+	-
CK7	+	-
CK20	-	-
Villin	-	±
AFP	+	+
E-Cadherin	+	+
Hep-Par-1	-	-
CK8	+	+
CK19	+	+
34βE12	-	-
AACT	+	+
CD10	-	-
CD68	-	-
CK17	-	-
CK5/6	-	-
S-100	-	
GFAP	-	
SYN	-	
NSE	+	

Kodama *et al*[22] have reported two histological types of AFP-producing gastric carcinoma: medullary type and well-differentiated papillary or tubular type[22]. HAC of the medullary type is positive for AFP and well-differentiated adenocarcinomatous type is negative for AFP[6]. HAC of the medullary type has a striking morphologic similarity to HCC, and both of them produce high levels of AFP. Our patient had the morphology of the medullary type and was positive for AFP. Ishikura *et al*[6] suggested that this may be

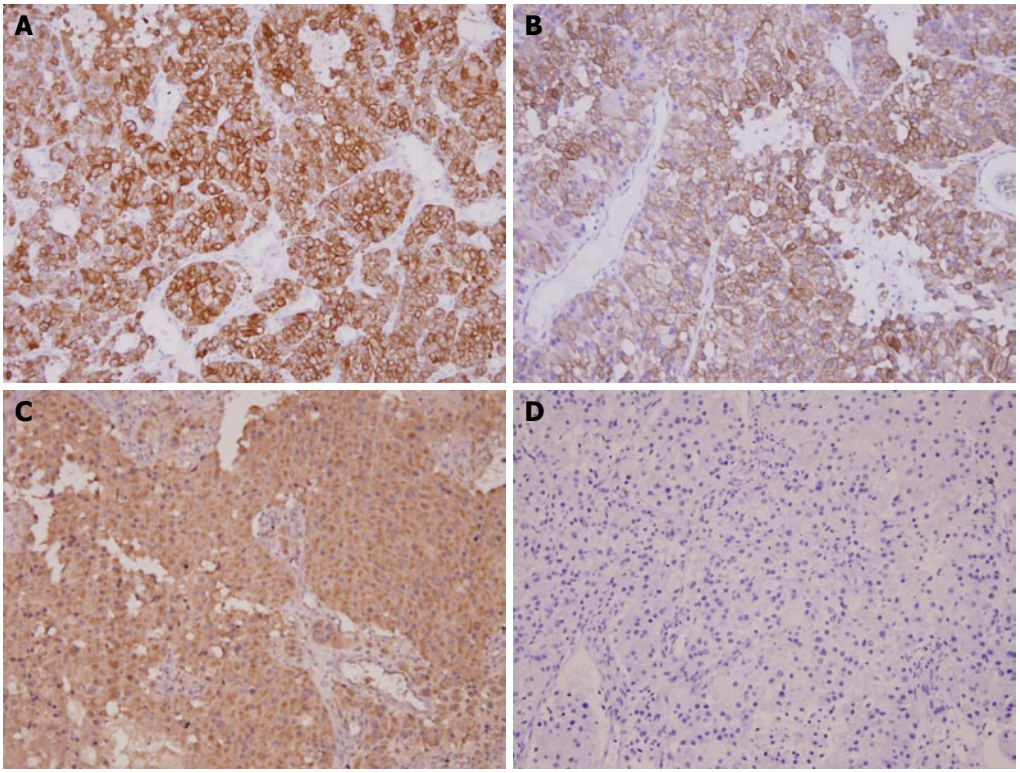

Figure 3 Immunoreactive characteristics of brain metastatic tumor (EnVision). **A**: Positively- stained cytokeratin AE1/AE3 (× 200); **B**: Positively-stained cytokeratin 8 (× 200); **C**: Positively-stained AFP (× 200); **D**: Negatively-stained Hep-Par-1 (× 200).

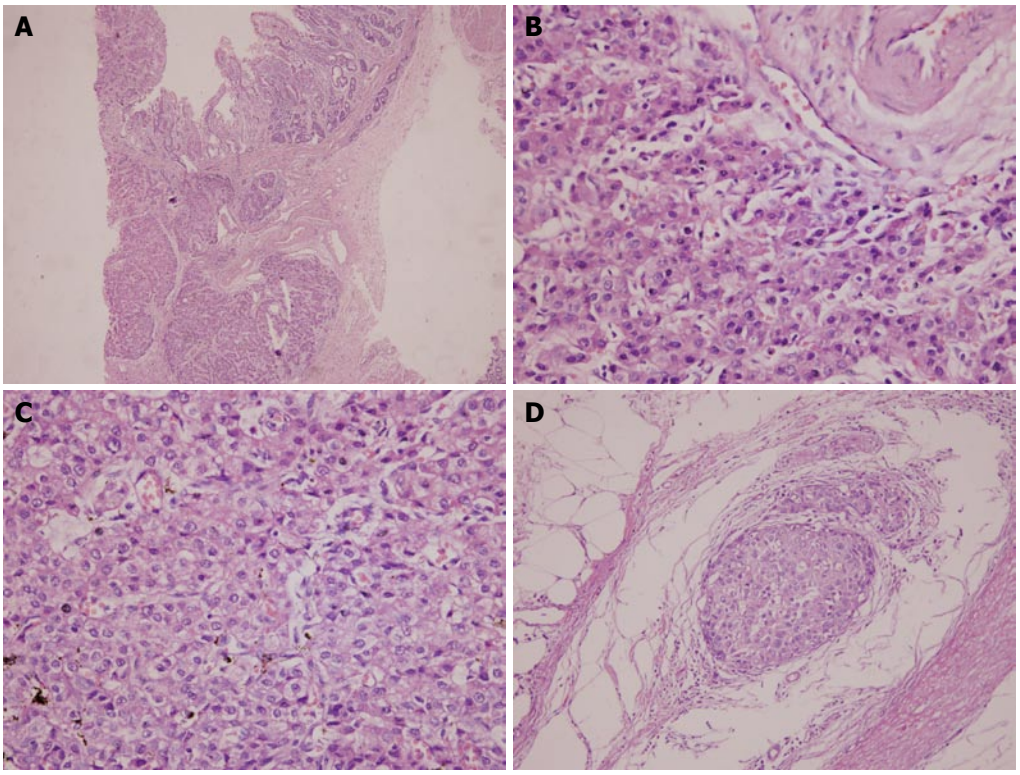

Figure 4 Histopathological features of primary gastric hepatoid adenocarcinoma. **A**: Tumor located at submucosa and intramuscle showing the growth pattern of solid cell nests (× 40); **B**: Part of tumor grown in cords separated by sinusoid-like blood spaces (× 200); **C**: Part of tumor grown in solid appearance showing polygonal epithelioid tumor cells with abundant eosinophilic cytoplasm, round nuclei with obvious nucleoli (× 200); **D**: Intralymph vascular tumor thrombosis in primary carcinoma (× 200).

due to the fact that the stomach and liver are both derived from primitive foregut of the embryo, and disturbances of differentiation may ultimately result in the development of foci of hepatocellular differentiation.

HAC and HCC share numerous clinicopathological features, such as elevated AFP serum level, hepatoid morphology and immunoreactivity with AFP, polyclonal carcinoembryonic antigen (CEA), and alpha-1 antitrypsin[23]. The histopathology of HAC and HCC is extremely similar, thus making the differential diagnosis difficulty, especially when the primary tumor is unknown. Immunohistochemistry of extrahepatic HAC and HCC is positive for AFP, CEA and cytokeratins 8 and 19, but not for cytokeratin 7[23,24]. The immunoreactivity of CK7 was positive in brain metastasis of our patient but negative in primary gastric carcinoma. The inconsistent phenomenon

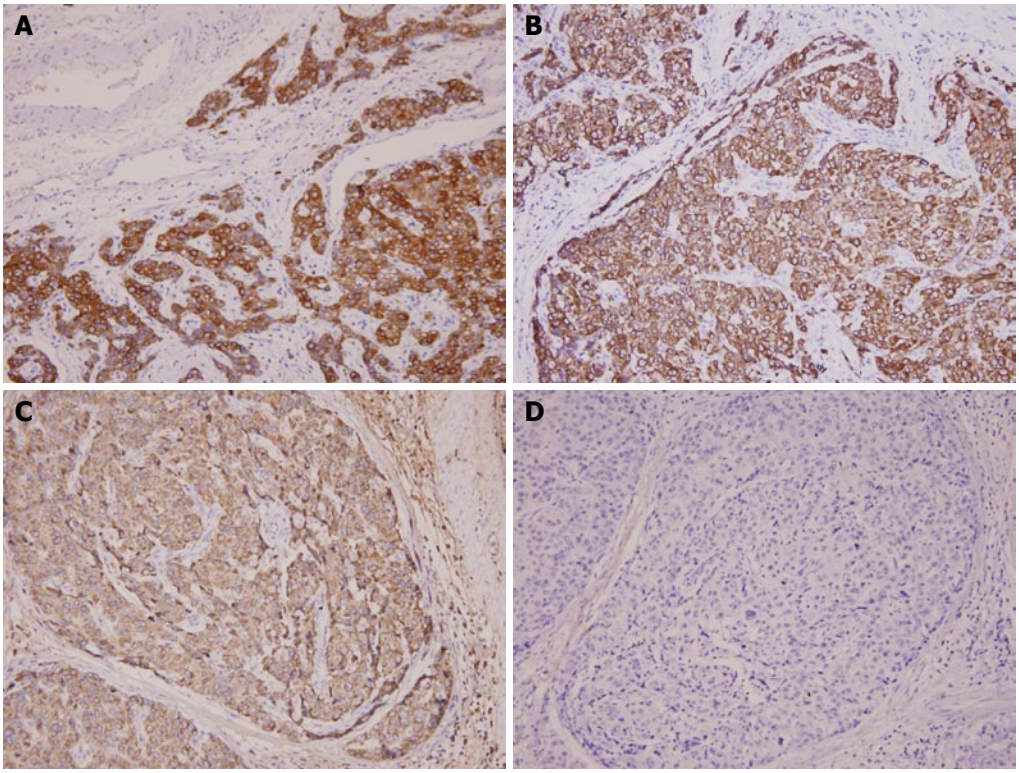

Figure 5 Immunohistochemical characteristics of primary gastric hepatoid adenocarcinoma. **A**: Positively-stained cytokeratin AE1/AE3 (× 200); **B**: Positively-stained cytokeratin 8 (× 200); **C**: Positively-stained AFP (× 200); **D**: Negatively-stained Hep-Par-1 (× 200).

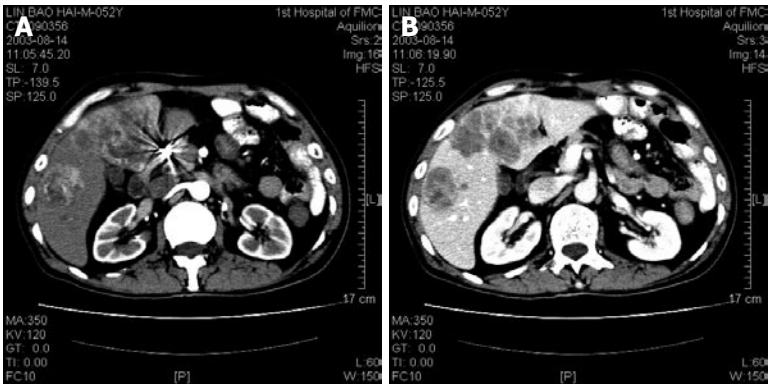

Figure 6 CT imaging features of liver metastatic tumor. **A**: CT scan revealing nodular or lump-like, high-density contrast mass in liver lobes during arterial phase; **B**: Uneven enhancement during portal venous phase.

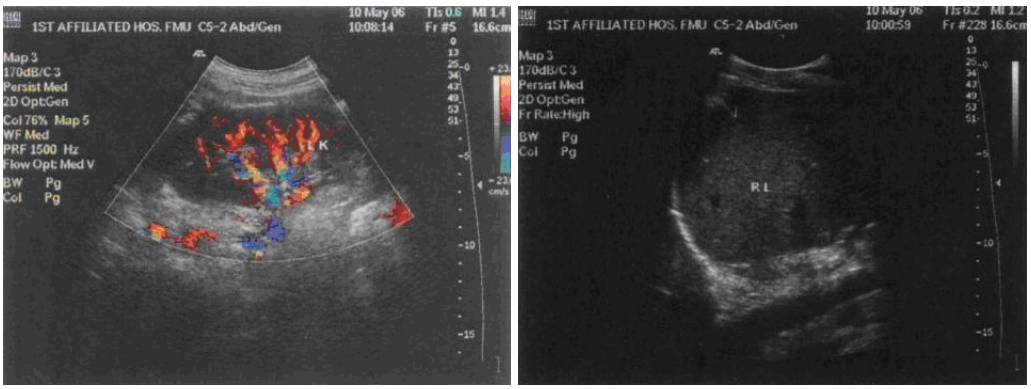

Figure 7 Features of ultrasound examination before operation of the brain metastasis.

of CK7 immunostaining is unable to explain. Therefore, it is uncertain that the brain metastasis is derived from liver metastasis from gastric HAC or from the primary gastric carcinoma.

Hep-Par-1 is a recently developed new monoclonal antibody that reacts with a hepatocyte-specific epitope. It was reported that the sensitivity and specificity of Hep-Par-1 in HCC are 82% and 90%, respectively[25], suggesting that this antibody is the most sensitive and specific immunohistochemical marker for hepatocyte differentiation[26-28]. In our patient, immunostaining showed that HCC was positive for Hep-Par-1 and extrahepatic

HAC was negative for Hep-Par-1.

Brain is one of the frequent hematogenous metastatic sites. It was reported that metastasis accounts for 13% of all brain tumors[9]. Usually, intracranial metastases and primary gliomas can be differentiated based on conventional MRI findings and clinical history. However, in some circumstances, especially when the lesion is solitary and its clinical features are nonspecific, conventional MRI alone is difficult to differentiate them. Although the management of metastases and primary gliomas is different, their morbidity and mortality are similar.

It was reported that the frequent symptoms of brain metastasis in recipients are headache, psychiatric symptom, hemicrania, vision disorder, cortical epilepsy[9]. The present patient had a similar clinical situation and intracranial metastases confirmed by MRI. Of the intracranial metastases, malignant melanomas account for 90%, chorioepithelioma malignum 60%, lung cancers 20%, breast cancers 16%, renal carcinomas 13% and thyroid carcinomas 9%. Brain metastasis of gastric cancer has been found only in about 0.5%-5% of cases reported, in which poorly-differentiated adenocarcinomas account for 27.3%-50%[9,29,30]. Most intracranial metastases from gastric cancer are lymphogenous and occur at meninges. Metastasis to the cerebral parenchyma *via* the arterial blood flow is rare. In general, patients with brain metastasis from gastric carcinoma have a higher stage of cancer and lymphovascular invasion or lymph node metastasis[9]. It is difficult to predict brain metastasis. If the patients have lymph node metastasis, lymphovascular invasion, or metastasis of other organs, they should be monitored carefully in order to detect brain metastases.

Treatment of brain metastasis depends mainly on whether it is solitary or multiple. Solitary metastasis is treated through resection, and multiple metastases are treated mainly with radiotherapy and chemotherapy. It was reported that multiple brain metastases account for 60%-70%, the prognosis of patients with brain metastasis is generally poor, and the mean postoperative survival time is about 6 mo[9]. The present patient remained alive 16 mo after the operation of brain metastasis. A longer survival time may be associated with the complete resection of brain metastasis and sensitivity to chemotherapy and radiotherapy.

In conclusion, metastasis of gastric hepatoid adenocarcinoma to the brain is rare. The differential diagnosis of metastatic tumors needs to use a panel of antibodies to avoid confusing with the brain metastasis of HCC. Long-term follow-up and close observation are required to find the symptoms of nervous system after gastrectomy, and early CT or MRI should be performed for the diagnosis of brain metastases. Solitary brain metastases are usually treated with surgery, radiotherapy and chemotherapy.

REFERENCES

1 **Fenoglio-Preiser C**, Munoz N, Carneiro F, Powell SM, Correa P, Rugge M, Guilford P, Sasako M, Lambert R, Stolte M, Megraud F, Watanabe H. Gastric carcinoma. In: Hamilton SR, Aaltonen LA. WHO classification of tumours, Pathology and genetics of tumours of the digestive system. Lyon: IARC Press, 2000: 37-67

2 **Kataoka H**, Miura Y, Joh T, Seno K, Tada T, Tamaoki T, Nakabayashi H, Kawaguchi M, Asai K, Kato T, Itoh M. Alpha-fetoprotein producing gastric cancer lacks transcription factor ATBF1. *Oncogene* 2001; **20**: 869-873

3 **Nagai E**, Ueyama T, Yao T, Tsuneyoshi M. Hepatoid adenocarcinoma of the stomach. A clinicopathologic and immunohistochemical analysis. *Cancer* 1993; **72**: 1827-1835

4 **Inagawa S**, Shimazaki J, Hori M, Yoshimi F, Adachi S, Kawamoto T, Fukao K, Itabashi M. Hepatoid adenocarcinoma of the stomach. *Gastric Cancer* 2001; **4**: 43-52

5 **Adachi Y**, Tsuchihashi J, Shiraishi N, Yasuda K, Etoh T, Kitano S. AFP-producing gastric carcinoma: multivariate analysis of prognostic factors in 270 patients. *Oncology* 2003; **65**: 95-101

6 **Ishikura H**, Fukasawa Y, Ogasawara K, Natori T, Tsukada Y, Aizawa M. An AFP-producing gastric carcinoma with features of hepatic differentiation. A case report. *Cancer* 1985; **56**: 840-848

7 **Goda K**, Tsunoda S, Sakaki T, Morimoto T, Hashimoto H, Yoshimura Y, Horikawa N, Nakagawa H, Iwasaki S. AFP producing gastric cancer manifested by metastasis to the tentorium cerebelli; case report and review of the literature. *No Shinkei Geka* 1992; **20**: 183-185

8 **Nomura T**, Yoshikawa T, Kato H, Nikkuni K, Sasaki K, Shirai Y, Hatakeyama K. Early gastric cancer manifested as brain metastasis: report of a case. *Surg Today* 1997; **27**: 334-336

9 **Kasakura Y**, Fujii M, Mochizuki F, Suzuki T, Takahashi T. Clinicopathological study of brain metastasis in gastric cancer patients. *Surg Today* 2000; **30**: 485-490

10 **Kim M**. Intracranial involvement by metastatic advanced gastric carcinoma. *J Neurooncol* 1999; **43**: 59-62

11 **Nathoo N**, Chahlavi A, Barnett GH, Toms SA. Pathobiology of brain metastases. *J Clin Pathol* 2005; **58**: 237-242

12 **Hayashi Y**, Takanashi Y, Ohsawa H, Ishii H, Nakatani Y. Hepatoid adenocarcinoma in the lung. *Lung Cancer* 2002; **38**: 211-214

13 **Shih NN**, Tsung JS, Yang AH, Tsou MH, Cheng TY. A unique pancreatic tumor with exclusive hepatocytic differentiation. *Ann Clin Lab Sci* 2006; **36**: 216-221

14 **Tanigawa H**, Kida Y, Kuwao S, Uesugi H, Ojima T, Kobayashi N, Saigenji K, Okayasu I. Hepatoid adenocarcinoma in Barrett's esophagus associated with achalasia: first case report. *Pathol Int* 2002; **52**: 141-146

15 **Gardiner GW**, Lajoie G, Keith R. Hepatoid adenocarcinoma of the papilla of Vater. *Histopathology* 1992; **20**: 541-544

16 **Lopez-Beltran A**, Luque RJ, Quintero A, Requena MJ, Montironi R. Hepatoid adenocarcinoma of the urinary bladder. *Virchows Arch* 2003; **442**: 381-387

17 **Ishikura H**, Ishiguro T, Enatsu C, Fujii H, Kakuta Y, Kanda M, Yoshiki T. Hepatoid adenocarcinoma of the renal pelvis producing alpha-fetoprotein of hepatic type and bile pigment. *Cancer* 1991; **67**: 3051-3056

18 **Kwon JE**, Kim SH, Cho NH. No ancillary finding is valid to distinguish a primary ovarian hepatoid carcinoma from metastatic hepatocellular carcinoma. *Int J Gynecol Cancer* 2006; **16**: 1691-1694

19 **Takeuchi K**, Kitazawa S, Hamanishi S, Inagaki M, Murata K. A case of alpha-fetoprotein-producing adenocarcinoma of the endometrium with a hepatoid component as a potential source for alpha-fetoprotein in a postmenopausal woman. *Int J Gynecol Cancer* 2006; **16**: 1442-1445

20 **Thamboo TP**, Wee A. Hep Par 1 expression in carcinoma of the cervix: implications for diagnosis and prognosis. *J Clin Pathol* 2004; **57**: 48-53

21 **Kitamura H**, Ikeda K, Honda T, Ogino T, Nakase H, Chiba T. Diffuse hepatoid adenocarcinoma in the peritoneal cavity. *Intern Med* 2006; **45**: 1087-1091

22 **Kodama T**, Kameya T, Hirota T, Shimosato Y, Ohkura H, Mukojima T, Kitaoka H. Production of alpha-fetoprotein, normal serum proteins, and human chorionic gonadotropin in stomach cancer: histologic and immunohistochemical analyses of 35 cases. *Cancer* 1981; **48**: 1647-1655

23 **Terracciano LM**, Glatz K, Mhawech P, Vasei M, Lehmann

FS, Vecchione R, Tornillo L. Hepatoid adenocarcinoma with liver metastasis mimicking hepatocellular carcinoma: an immunohistochemical and molecular study of eight cases. *Am J Surg Pathol* 2003; **27**: 1302-1312

24 **Tickoo SK**, Zee SY, Obiekwe S, Xiao H, Koea J, Robiou C, Blumgart LH, Jarnagin W, Ladanyi M, Klimstra DS. Combined hepatocellular-cholangiocarcinoma: a histopathologic, immunohistochemical, and in situ hybridization study. *Am J Surg Pathol* 2002; **26**: 989-997

25 **Maitra A**, Murakata LA, Albores-Saavedra J. Immunoreactivity for hepatocyte paraffin 1 antibody in hepatoid adenocarcinomas of the gastrointestinal tract. *Am J Clin Pathol* 2001; **115**: 689-694

26 **Chu PG**, Ishizawa S, Wu E, Weiss LM. Hepatocyte antigen as a marker of hepatocellular carcinoma: an immunohistochemical comparison to carcinoembryonic antigen, CD10, and alpha-fetoprotein. *Am J Surg Pathol* 2002; **26**: 978-988

27 **Leong AS**, Sormunen RT, Tsui WM, Liew CT. Hep Par 1 and selected antibodies in the immunohistological distinction of hepatocellular carcinoma from cholangiocarcinoma, combined tumours and metastatic carcinoma. *Histopathology* 1998; **33**: 318-324

28 **Minervini MI**, Demetris AJ, Lee RG, Carr BI, Madariaga J, Nalesnik MA. Utilization of hepatocyte-specific antibody in the immunocytochemical evaluation of liver tumors. *Mod Pathol* 1997; **10**: 686-692

29 **Adachi Y**, Mori M, Maehara Y, Sugimachi K. Poorly differentiated medullary carcinoma of the stomach. *Cancer* 1992; **70**: 1462-1466

30 **York JE**, Stringer J, Ajani JA, Wildrick DM, Gokaslan ZL. Gastric cancer and metastasis to the brain. *Ann Surg Oncol* 1999; **6**: 771-776

S- Editor Liu Y **L- Editor** Wang XL **E- Editor** Lu W

Online Submissions: wjg.wjgnet.com
www.wjgnet.com
wjg@wjgnet.com

World J Gastroenterol 2007 November 21; 13(43): 5794
World Journal of Gastroenterology ISSN 1007-9327

ACKNOWLEDGMENTS

Acknowledgments to Reviewers of *World Journal of Gastroenterology*

Many reviewers have contributed their expertise and time to the peer review, a critical process to ensure the quality of *World Journal of Gastroenterology*. The editors and authors of the articles submitted to the journal are grateful to the following reviewers for evaluating the articles (including those published in this issue and those rejected for this issue) during the last editing time period.

Francesco Negro, MD
Divisions of Gastroenterology and Hepatology and of Clinical Pathology, Hôpital Cantonal Universitaire, 24 rue Micheli-du-Crest, CH-1211 Genève 14, Switzerland

Seyed-Moayed Alavian, Professor
P.O.Box: 14155-3651, Tehran, Iran

Hitoshi Asakura, Director, Professor
International Medical Information Center, Shinanomachi Renga Bldg.35, Shinanomachi, Shinjukuku, Tokyo 160-0016, Japan

Yvan Vandenplas, Professor
Department of Pediatrics, AZ-VUB, Laarbeeklaan 101, Brussels 1090, Belgium

Phillip S Oates, PhD
Department of Physiology, School of Biomedical and Chemical Sciences, The University of Western Australia, Perth, WA, Australia

Yaron Niv, Professor
Department of Gastroenterology, Rabin Medical Center, Beilinson Campus, Tel Aviv University, 2 Hadekel St., Pardesia 42815, Israel

Josep M Bordas, MD
Department of Gastroenterology IMD, Hospital Clinic", Llusanes 11-13 at, Barcelona 08022, Spain

James Michael Millis, Professor
University of Chicago, Section of Transplantation, MC 5027, 5841 S. Maryland Avenue, Chicago, IL 60637, United States

Lucia Malaguarnera, Associate Professor, MD, PhD
Dept of Biomedical Sciences, University, Via E. De Amicis, 24 Trecastagni Catania, 95039, Italy

Shu Zheng, Professor
Scientific Director of Cancer Institute, Zhejiang University, Secondary Affiliated Hospital, Zhejiang University, 88# Jiefang Road, Hangzhou 310009, Zhejiang Province, China

Richard A Rippe, PhD
Department of Medicine, The University of North Carolina at Chapel Hill, Chapel Hill, NC 27599-7038, United States

Sharon DeMorrow, PhD
Division of Research and Education, Scott and White Hospital and The Texas A&M University System, Health Science Center College of Medicine, Temple, Texas 76504, United States

John Frank Di Mari, PhD
Internal Medicine, Gastroenterology, 9.138 MRB 301 University Blvd. Galveston, Texas 77555-1064, United States

Thomas Langmann, Associate Professor
University of Regensburg, Institute of Human Genetics, Franz-Josef-Strauss-Allee 11, Regensburg 93053, Germany

Markus Reiser, Professor, PhD
Gastroenterology-Hepatology, Ruhr-Universit?t Bochum, Bürkle-de-la-Camp-Platz 1, Bochum 44789, Germany

James F Trotter, MD, Associate Professor
University of Colorado, Division of Gastroenterology, 4200 E. 9th Avenue, b-154, Denver, CO 80262, United Stetes

Thomas Bock, PhD, Professor
Department of Molecular Pathology, Institute of Pathology, University Hospital of Tuebingen, D-72076 Tuebingen, Germany

Chang Hong Lee, MD
Department of Internal Medicine, Konkuk University Hospital, Konkuk University School of Medicine, 4-12 Hwayang-dong, Gwangjin-gu, Seoul, 143-729, Korea

Masayoshi Ito, MD
Department of Endoscopy, Yotsuya Medical Cube, 5-5-27-701 Kitashinagawa, Shinagawa-ku, Tokyo 1410001, Japan

Paolo Del Poggio, PhD
Hepatology Unit, Department of Internal Medicine, Treviglio Hospital, Piazza Ospedale 1, Treviglio Bg 24047, Italy

Kurt Lenz, Professor
Department of Internal Medicine, Konventhospital Barmherzige Brueder, A-4020 Linz, Austria

Xupeng Ge, MD, PhD
Transplant Biology Research Center, Massachusetts General Hospital, Harvard Medical School, MGH East, Building 149-5102, 13th street, Boston MA 02129, United States

Peter Laszlo Lakatos, MD, PhD
1st Department of Medicine, Semmelweis University, Koranyi S 2A, Budapest H1083, Hungary

Shingo Tsuji, Professor
Department of Internal Medicine and Therapeutics, Osaka University Graduate School of Medicine(A8), 2-2 Yamadaoka, Suita, Osaka 565-0871, Japan

Manuel Romero-Gómez, MD, Professor
Hepatology Unit, Hospital Universitario de Valme, Ctra de Cádiz s/n, Sevilla 41014, Spain

Wei Tang, MD, Assistant Professor
H-B-P Surgery Division, Artificial Organ and Transplantation Division, Department of surgery, Graduate School of Medicine, The University of Tokyo, Tokyo 113-8655, Japan

Massimo Raimondo
Division of Gastroenterology and Hepatology, Mayo Clinic, 4500 San Pablo Road, Jacksonville, FL 32224, United States

Jia-Yu Xu, Professor
Shanghai Second Medical University, Rui Jin Hospital, 197 Rui Jin Er Road, Shanghai 200025, China

Reza Malekzadeh, Professor
Digestive Disease Research Center, Tehran University of Medical Sciences, Shariati Hospital, Kargar Shomali Avenue, 19119 Tehran, Iran

Dusan M Jovanovic, Professor
Institute of Oncology, Institutski Put 4, Sremska Kamenica 21204, Serbia

Steven David Wexner, MD, Professor of Surgery
The Cleveland Clinic Foundation Health Sciences Center of the Ohio State University, and Clinical Professor, Department of Surgery, Division of General Surgery, University of South Florida College of Medicine, 21st Century Oncology Chair in Colorectal Surgery, Chairman Department of Colorectal Surgery, Chief of Staff, Cleveland Clinic Florida, 2950 Cleveland Clinic Boulevard, Weston, Florida 33331, United States

Rene Lambert, Professor
International Agency for Research on Cancer, 150 Cours Albert Thomas, Lyon 69372 cedex 8, France

Online Submissions: wjg.wjgnet.com
www.wjgnet.com
wjg@wjgnet.com

World J Gastroenterol 2007 November 21; 13(43): 5795
World Journal of Gastroenterology ISSN 1007-9327

Meetings

MAJOR MEETINGS COMING UP

Meeting Falk Research Workshop: Morphogenesis and Cancerogenesis of the Liver
25-26 January 2007
Goettingen
symposia@falkfoundation.de

Meeting Canadian Digestive Diseases Week (CDDW)
16-20 February 2007
Banff-AB
cagoffice@cag-acg.org
www.cag-acg.org/cddw/cddw2007.htm

Meeting Falk Symposium 158: Intestinal Inflammation and Colorectal Cancer
23-24 March 2007
Sevilla
symposia@falkfoundation.de

Meeting BSG Annual Meeting
26-29 March 2007
Glasgow
www.bsg.org.uk/

NEXT 6 MONTHS

Meeting 42nd Annual Meeting of the European Association for the Study of the Liver
11-15 April 2007
Barcelona
easl2007@easl.ch
www.easl.ch/liver-meeting/

Meeting Falk Symposium 159: IBD 2007 - Achievements in Research and Clinical Practice
4-5 May 2007
Istanbul
symposia@falkfoundation.de

Meeting European Society for Paediatric Gastroenterology, Hepatology and Nutrition Congress 2007
9-12 May 2007
Barcelona
espghan2007@colloquium.fr

Digestive Disease Week
19-24 May 2007
Washington Convention Center, Washington DC

Meeting Gastrointestinal Endoscopy Best Practices: Today and Tomorrow, ASGE Annual Postgraduate Course at DDW
23-24 May 2007
Washington-DC
tkoral@asge.org

Meeting ESGAR 2007 18th Annual Meeting and Postgraduate Course
12-15 June 2007
Lisbon
fca@netvisao.pt

Meeting Falk Symposium 160: Pathogenesis and Clinical Practice in Gastroenterology
15-16 June 2007
Portoroz
symposia@falkfoundation.de

Meeting ILTS 13th Annual International Congress
20-23 June 2007
Rio De Janeiro
www.ilts.org

Meeting 9th World Congress on Gastrointestinal Cancer
27-30 June 2007
Barcelona
meetings@imedex.com

EVENTS AND MEETINGS IN 2007

Meeting Falk Research Workshop: Morphogenesis and Cancerogenesis of the Liver
25-26 January 2007
Goettingen
symposia@falkfoundation.de

Meeting Canadian Digestive Diseases Week (CDDW)
16-20 February 2007
Banff-AB
cagoffice@cag-acg.org
www.cag-acg.org/cddw/cddw2007.htm

Meeting Falk Symposium 158: Intestinal Inflammation and Colorectal Cancer
23-24 March 2007
Sevilla
symposia@falkfoundation.de

Meeting BSG Annual Meeting
26-29 March 2007
Glasgow
www.bsg.org.uk/

Meeting 42nd Annual Meeting of the European Association for the Study of the Liver
11-15 April 2007
Barcelona
easl2007@easl.ch
www.easl.ch/liver-meeting/

Meeting Falk Symposium 159: IBD 2007 - Achievements in Research and Clinical Practice
4-5 May 2007
Istanbul
symposia@falkfoundation.de

Meeting European Society for Paediatric Gastroenterology, Hepatology and Nutrition Congress 2007
9-12 May 2007
Barcelona
espghan2007@colloquium.fr

Meeting Gastrointestinal Endoscopy Best Practices: Today and Tomorrow, ASGE Annual Postgraduate Course at DDW
23-24 May 2007
Washington-DC
tkoral@asge.org

Meeting ESGAR 2007 18th Annual Meeting and Postgraduate Course
12-15 June 2007
Lisbon
fca@netvisao.pt

Meeting Falk Symposium 160: Pathogenesis and Clinical Practice in Gastroenterology
15-16 June 2007
Portoroz
symposia@falkfoundation.de

Meeting ILTS 13th Annual International Congress
20-23 June 2007
Rio De Janeiro
www.ilts.org

Meeting 9th World Congress on Gastrointestinal Cancer
27-30 June 2007
Barcelona
meetings@imedex.com

Meeting 15th International Congress of the European Association for Endoscopic Surgery
4-7 July 2007
Athens
info@eaes-eur.org
congresses.eaes-eur.org/

Meeting 39th Meeting of the European Pancreatic Club
4-7 July 2007
Newcastle
www.e-p-c2007.com

Meeting XXth International Workshop on Heliobacter and related bacteria in cronic degistive inflammation
20-22 September 2007
Istanbul
www.heliobacter.org

Meeting Falk Workshop: Mechanisms of Intestinal Inflammation
10 October 2007
Dresden
symposia@falkfoundation.de

Meeting Falk Symposium 161: Future Perspectives in Gastroenterology
11-12 October 2007
Dresden
symposia@falkfoundation.de

Meeting Falk Symposium 162: Liver Cirrhosis - From Pathophysiology to Disease Management
13-14 October 2007
Dresden
symposia@falkfoundation.de

American College of Gastroenterology Annual Scientific Meeting
12-17 October 2007
Pennsylvania Convention Center
Philadelphia, PA

Meeting APDW 2007 - Asian Pacific Digestive Disease Week 2007
15-18 October 2007
Kobe
apdw@convention.co.jp
www.apdw2007.org

15th United European Gastroenterology Week, UEGW
27-31 October 2007
Le Palais des Congrès de Paris, Paris, France

Meeting The Liver Meeting® 2007 - 57th Annual Meeting of the American Association for the Study of Liver Diseases
2-6 November 2007
Boston-MA
www.aasld.org

Gastro 2009, World Congress of Gastroenterology and Endoscopy London, United Kingdom 2009

Online Submissions: wjg.wjgnet.com
www.wjgnet.com
wjg@wjgnet.com

World J Gastroenterol 2007 November 21; 13(43): 5796-5798
World Journal of Gastroenterology ISSN 1007-9327

Instructions to authors

GENERAL INFORMATION

World Journal of Gastroenterology (*WJG, World J Gastroenterol* ISSN 1007-9327 CN 14-1219/R) is a weekly journal of more than 48 000 circulation, published on the 7th, 14th, 21st and 28th of every month.

Original Research, Clinical Trials, Reviews, Comments, and Case Reports in esophageal cancer, gastric cancer, colon cancer, liver cancer, viral liver diseases, *etc*., from all over the world are welcome on the condition that they have not been published previously and have not been submitted simultaneously elsewhere.

Indexed and abstracted in

Current Contents®/Clinical Medicine, Science Citation Index Expanded (also known as SciSearch®) and Journal Citation Reports/Science Edition, *Index Medicus*, MEDLINE and PubMed, Chemical Abstracts, EMBASE/Excerpta Medica, Abstracts Journals, *Nature Clinical Practice Gastroenterology and Hepatology*, CAB Abstracts and Global Health. ISI JCR 2003-2000 IF: 3.318, 2.532, 1.445 and 0.993.

Published by

The WJG Press

SUBMISSION OF MANUSCRIPTS

Manuscripts should be typed double-spaced on A4 (297 mm × 210 mm) white paper with outer margins of 2.5 cm. Number all pages consecutively, and start each of the following sections on a new page: Title Page , Abstract, Introduction, Materials and Methods, Results, Discussion, acknowledgements, References, Tables, Figures and Figure Legends. Neither the editors nor the Publisher is responsible for the opinions expressed by contributors. Manuscripts formally accepted for publication become the permanent property of The WJG Press, and may not be reproduced by any means, in whole or in part without the written permission of both the authors and the Publisher. We reserve the right to put onto our website and copy-edit accepted manuscripts. Authors should also follow the guidelines for the care and use of laboratory animals of their institution or national animal welfare committee.

Authors should retain one copy of the text, tables, photographs and illustrations, as rejected manuscripts will not be returned to the author(s) and the editors will not be responsible for the loss or damage to photographs and illustrations in mailing process.

Online submissions

Online submissions are strongly advised. Manuscripts should be submitted through the Online Submission System at: http://www.wjgnet.com/index.jsp. Authors are highly recommended to consult the ONLINE INSTRUCTIONS TO AUTHORS (http://www.wjgnet.com/wjg/help/instructions.jsp) before attempting to submit online. Authors encountering problems with the Online Submission System may send an email you describing the problem to wjg@wjgnet.com for assistance. If you submit your manuscript online, do not make a postal contribution. A repeated online submission for the same manuscript is strictly prohibited.

Postal submission

Send 3 duplicate hard copies of the full-text manuscript typed double-spaced on A4 (297 mm × 210 mm) white paper together with any original photographs or illustrations and a 3.5 inch computer diskette or CD-ROM containing an electronic copy of the manuscript including all the figures, graphs and tables in native Microsoft Word format or *.rtf format to:

Editorial Office

World Journal of Gastroenterology
Editorial Department: Apartment 1066, Yishou Garden,
58 North Langxinzhuang Road,
PO Box 2345, Beijing 100023, China
E-mail: wjg@wjgnet.com
http: //www.wjgnet.com
Telephone: +86-10-85381892
Fax: +86-10-85381893

MANUSCRIPT PREPARATION

All contributions should be written in English. All articles must be submitted using a word-processing software. All submissions must be typed in 1.5 line spacing and in word size 12 with ample margins. The letter font is Tahoma. For authors from China, one copy of the Chinese translation of the manuscript is also required (excluding references). Style should conform to our house format. Required information for each of the manuscript sections is as follows:

Title page

Full manuscript title, running title, all author(s) name(s), affiliations, institution(s) and/or department(s) where the work was accomplished, disclosure of any financial support for the research, and the name, full address, telephone and fax numbers and email address of the corresponding author should be included. Titles should be concise and informative (removing all unnecessary words), emphasize what is new, and avoid abbreviations. A short running title of less than 40 letters should be provided. List the author(s)' name(s) as follows: initial and/or first name, middle name or initial(s) and full family name.

Abstract

An informative, structured abstract of no more than 350 words should accompany each manuscript. Abstracts for original contributions should be structured into the following sections: AIM: Only the purpose should be included. METHODS: The materials, techniques, instruments and equipments, and the experimental procedures should be included. RESULTS: The observatory and experimental results, including data, effects, outcome, *etc*. should be included. Authors should present *P* value where necessary, and the significant data should accompany. CONCLUSION: Accurate view and the value of the results should be included.

The format of structured abstracts is at: http://www.wjgnet.com/wjg/help/11.doc

Key words

Please list 5-10 key words that could reflect content of the study mainly from *Index Medicus*.

Text

For most article types, the main text should be structured into the following sections: INTRODUCTION, MATERIALS AND METHODS, RESULTS and DISCUSSION, and should include in appropriate Figures and Tables. Data should be presented in the body text or in Figures and Tables, but not in both.

Illustrations

Figures should be numbered as 1, 2, 3 and so on, and mentioned clearly in the main text. Provide a brief title for each figure on a separate page. No detailed legend should be involved under the figures. This part should be added into the text where the figures are applicable. Digital images: black and white photographs should be scanned and saved in TIFF format at a resolution of 300 dpi; color images should be saved as CMYK (print files) but not as RGB (screen-viewing files). Place each photograph in a separate file. Print images: supply images of size no smaller than 126 mm × 85 mm printed on smooth surface paper; label the image by writing the Figure number and orientation using an arrow. Photomicrographs: indicate the original magnification and stain in the legend. Digital Drawings: supply files in EPS if created by freehand and illustrator, or TIFF from photoshops. EPS files must be accompanied by a version in native file format for editing purposes. Existing line drawings should be scanned at a resolution of 1200 dpi and as close as possible to the size where they will appear when printed. Please use uniform legends for the same subjects. For example: Figure 1 Pathological changes of atrophic gastritis after treatment. A: ...; B: ...; C: ...; D: ...; E: ...; F: ...; G: ...

Tables

Three-line tables should be numbered as 1, 2, 3 and so on, and mentioned clearly in the main text. Provide a brief title for each table. No detailed legend should be included under the tables. This part should be added into the text where the tables are applicable. The information should complement but not duplicate that contained in the text. Use one horizontal line under the title, a second under the column heads, and a third below the Table, above any footnotes. Vertical and italic lines should be omitted.

Notes in tables and illustrations

Data that are not statistically significant should not be noted. $^{a}P<0.05$, $^{b}P<0.01$ should be noted ($P>0.05$ should not be noted). If there are other series of *P* values, $^{c}P<0.05$ and $^{d}P<0.01$ are used. Third series of *P* values can be expressed as $^{e}P<0.05$ and $^{f}P<0.01$. Other notes in tables or under

illustrations should be expressed as ^1F, ^2F, ^3F; or some other symbols with a superscript (Arabic numerals) in the upper left corner. In a multi-curve illustration, each curve should be labeled with ●, ○, ■, □, ▲, △, *etc.* in a certain sequence.

Acknowledgments

Brief acknowledgments of persons who have made genuine contributions to the manuscripts and who endorse the data and conclusions are included. Authors are responsible for obtaining written permission to use any copyrighted text and/or illustrations.

REFERENCES

Coding system

The author should code the references according the citation order in text in Arabic numerals, put references codes in square brackets, superscript it at the end of citation content or the author name of the citation. For those citation content as the narrate part, the coding number and square brackets should be typeset normally. For example, Crohn's disease (CD) is associated with increased intestinal permeability[1,2]. If references are directly cited in the text, they would be put together with the text, for example, from references [19,22-24], we know that...

When the authors code the references, please ensure that the order in text is the same as in reference part and also insure the spelling accuracy of the first author's name. Do not code the same citation twice.

PMID requirement

PMID roots in the abstract serial number indexed by PubMed (http://www.ncbi.nlm.nih.gov/entrez/query.fcgi?db=PubMed). The author should supply the PMID for journal citation. For those references that have not been indexed by PubMed, a printed copy of the first page of the full reference should be submitted.

The accuracy of the information of the journal citations is very important. Through reference testing system, the authors and editor could check the authors name, title, journal title, publication date, volume number, start page, and end page. We will interlink all references with PubMed in ASP file so that the readers can read the abstract of the citations online immediately.

Style for journal references

Authors: the first author should be typed in bold-faced letter. The surname of all authors should be typed with the initial letter capitalized and followed by their name in abbreviation (For example, Lian-Sheng Ma is abbreviated as Ma LS, Bo-Rong Pan as Pan BR). Title of the cited article and italicized journal title (Journal title should be in its abbreviation form as shown in PubMed), publication date, volume number (in black), start page, and end page [PMID: 11819634]

Note: The author should test the references through reference testing system (http://www.wjgnet.com/cgi-bin/index.pl)

Style for book references

Authors: the first author should be typed in bold-faced letter. The surname of all authors should be typed with the initial letter capitalized and followed by their name in abbreviation (For example, Lian-Sheng Ma is abbreviated as Ma LS, Bo-Rong Pan as Pan BR) Book title. Publication number. Publication place: Publication press, Year: start page and end page.

Format

Journals

English journal article (list all authors and include the PMID where applicable)

1 **Grover VP**, Dresner MA, Forton DM, Counsell S, Larkman DJ, Patel N, Thomas HC, Taylor-Robinson SD. Current and future applications of magnetic resonance imaging and spectroscopy of the brain in hepatic encephalopathy. *World J Gastroenterol* 2006; **12**: 2969-2978 [PMID: 16718775]

Chinese journal article (list all authors and include the PMID where applicable)

2 **Lin GZ**, Wang XZ, Wang P, Lin J, Yang FD. Immunologic effect of Jianpi Yishen decoction in treatment of Pixu-diarrhoea. *Shijie Huaren Xiaohua Zazhi* 1999; **7**: 285-287

In press

3 **Tian D**, Araki H, Stahl E, Bergelson J, Kreitman M. Signature of balancing selection in Arabidopsis. *Proc Natl Acad Sci U S A* 2006; In press

Organization as author

4 **Diabetes Prevention Program Research Group**. Hypertension, insulin, and proinsulin in participants with impaired glucose tolerance. *Hypertension* 2002; **40**: 679-686 [PMID: 12411462]

Both personal authors and an organization as author

5 **Vallancien G**, Emberton M, Harving N, van Moorselaar RJ; Alf-One Study Group. Sexual dysfunction in 1, 274 European men suffering from lower urinary tract symptoms. *J Urol* 2003; **169**: 2257-2261 [PMID: 12771764]

No author given

6 21st century heart solution may have a sting in the tail. *BMJ* 2002; **325**: 184 [PMID: 12142303]

Volume with supplement

7 **Geraud G**, Spierings EL, Keywood C. Tolerability and safety of frovatriptan with short- and long-term use for treatment of migraine and in comparison with sumatriptan. *Headache* 2002; **42** Suppl 2: S93-99 [PMID: 12028325]

Issue with no volume

8 **Banit DM**, Kaufer H, Hartford JM. Intraoperative frozen section analysis in revision total joint arthroplasty. *Clin Orthop Relat Res* 2002; (**401**): 230-238 [PMID: 12151900]

No volume or issue

9 Outreach: bringing HIV-positive individuals into care. *HRSA Careaction* 2002; 1-6 [PMID: 12154804]

Books

Personal author(s)

10 **Sherlock S**, Dooley J. Diseases of the liver and billiary system. 9th ed. Oxford: Blackwell Sci Pub, 1993: 258-296

Chapter in a book (list all authors)

11 **Lam SK**. Academic investigator's perspectives of medical treatment for peptic ulcer. In: Swabb EA, Azabo S. Ulcer disease: investigation and basis for therapy. New York: Marcel Dekker, 1991: 431-450

Author(s) and editor(s)

12 **Breedlove GK**, Schorfheide AM. Adolescent pregnancy. 2nd ed. Wieczorek RR, editor. White Plains (NY): March of Dimes Education Services, 2001: 20-34

Conference proceedings

13 **Harnden P**, Joffe JK, Jones WG, editors. Germ cell tumours V. Proceedings of the 5th Germ Cell Tumour Conference; 2001 Sep 13-15; Leeds, UK. New York: Springer, 2002: 30-56

Conference paper

14 **Christensen S**, Oppacher F. An analysis of Koza's computational effort statistic for genetic programming. In: Foster JA, Lutton E, Miller J, Ryan C, Tettamanzi AG, editors. Genetic programming. EuroGP 2002: Proceedings of the 5th European Conference on Genetic Programming; 2002 Apr 3-5; Kinsdale, Ireland. Berlin: Springer, 2002: 182-191

Electronic journal (list all authors)

Morse SS. Factors in the emergence of infectious diseases. Emerg Infect Dis serial online, 1995-01-03, cited 1996-06-05; 1(1): 24 screens. Available from: URL: http//www.cdc.gov/ncidod/EID/eid.htm

Patent (list all authors)

16 **Pagedas AC**, inventor; Ancel Surgical R&D Inc., assignee. Flexible endoscopic grasping and cutting device and positioning tool assembly. United States patent US 20020103498. 2002 Aug 1

Inappropriate references

Authors should always cite references that are relevant to their article, and avoid any inappropriate references. Inappropriate references include those that are linked with a hyphen and the difference between the two numbers at two sides of the hyphen is more than 5. For example, [1-6], [2-14] and [1, 3, 4-10, 22] are all considered as inappropriate references. Authors should not cite their own unrelated published articles.

Statistical data

Present as mean ± SD or mean ± SE.

Statistical expression

Express t test as t (in italics), F test as F (in italics), chi square test as χ^2 (in Greek), related coefficient as r (in italics), degree of freedom as γ (in Greek), sample number as n (in italics), and probability as P (in italics).

Units

Use SI units. For example: body mass, m (B) = 78 kg; blood pressure, p(B) = 16.2/12.3 kPa; incubation time, t (incubation) = 96 h, blood glucose concentration, c (glucose) 6.4 ± 2.1 mmol/L; blood CEA mass concentration, p (CEA) = 8.6 24.5 μg/L; CO_2 volume fraction, 50 mL/L CO_2 not 5% CO_2; likewise for 40 g/L formaldehyde, not 10% formalin; and mass fraction, 8 ng/g, *etc.* Arabic numerals such as 23, 243, 641 should be read 23 243 641.

The format about how to accurately write common units and quantum is at: http://www.wjgnet.com/wjg/help/15.doc

Abbreviations

Standard abbreviations should be defined in the abstract and on first mention in the text. In general, terms should not be abbreviated unless they are used repeatedly and the abbreviation is helpful to the reader. Permissible abbreviations are listed in Units, Symbols and Abbreviations: A Guide for Biological and Medical Editors and Authors (Ed. Baron DN, 1988) published by The Royal Society of Medicine, London. Certain commonly used abbreviations, such as DNA, RNA, HIV, LD50, PCR, HBV, ECG, WBC, RBC, CT, ESR, CSF, IgG, ELISA, PBS, ATP, EDTA, mAb, can be used directly without further mention.

Italics

Quantities: *t* time or temperature, *c* concentration, *A* area, *l* length, *m* mass, *V* volume.
Genotypes: *gyr*A, *arg* 1, *c myc*, *c fos*, *etc.*
Restriction enzymes: *Eco*RI, *Hin*dI, *Bam*HI, *Kbo* I, *Kpn* I, *etc.*
Biology: *H pylori, E coli, etc.*

SUBMISSION OF THE REVISED MANUSCRIPTS AFTER ACCEPTED

Please revise your article according to the revision policies of *WJG*. The revised version including manuscript and high-resolution image figures (if any) should be copied on a floppy or compact disk. Author should send the revised manuscript, along with printed high-resolution color or black and white photos, copyright transfer letter, the final check list for authors, and responses to reviewers by a courier (such as EMS) (submission of revised manuscript by e-mail or on the *WJG* Editorial Office Online System is NOT available at present).

Language evaluation

The language of a manuscript will be graded before sending for revision. (1) Grade A: priority publishing; (2) Grade B: minor language polishing; (3) Grade C: a great deal of language polishing; (4) Grade D: rejected. The revised articles should be in grade B or grade A.

Copyright assignment form

Please downloaded CAF from http://www.wjgnet.com/wjg/help/9.doc.

We certify that the material contained in this manuscript:

Ms:

Title:

is original, except when appropriately referenced to other sources, and that written permission has been granted by any existing copyright holders. We agree to transfer to WJG all rights of our manuscript, including: (1) all copyright ownership in all print and electronic formats; (2) the right to grant permission to republish or reprint the stated material in whole or in part, with or without a fee; (3) the right to print copies for free distribution or sale; (4) the right to republish the stated material in a collection of articles or in any other format. We also agree that our article be put on the Internet.

Criteria for authorship: The WJG requests and publishes information about contributions of each author named to the submitted study. Authorship credit should be based on (1)direct participation in the study, including substantial contributions to conception and design of study, or acquisition of data, or analysis and interpretation of data; (2) manuscript writing, including drafting the article, or revising it critically for important intellectual content; (3)supportive work, including statistical analysis of data, or acquisition of funding, or administration, technology and materials support, or supervision, or supportive contributions. Authors should meet at least one of the three conditions. The WJG does not publish co-first authors and co-corresponding authors.

We hereby assign copyright transfer to WJG if this paper is accepted.

Author Name in full (Full names should be provided, with first name first, followed by middle names and family name at the last, eg, Eamonn MM Quigley). Handwritten names are not accepted.

Author Name in abbreviation (Family name is put first in full, followed by middle names and first name in abbreviation with first letter in capital, eg, Quigley EMM). Handwritten names are not accepted.

1 Full Name: _____
Abbreviation Name: _____
Signed: _____
Date: _____

2 Full Name: _____
Abbreviation Name: _____
Signed: _____
Date: _____

3 Full Name: _____
Abbreviation Name: _____
Signed: _____
Date: _____

4 Full Name: _____
Abbreviation Name: _____
Signed: _____
Date: _____

5 Full Name: _____
Abbreviation Name: _____
Signed: _____
Date: _____

6 Full Name: _____
Abbreviation Name: _____
Signed: _____
Date: _____

7 Full Name: _____
Abbreviation Name: _____
Signed: _____
Date: _____

8 Full Name: _____
Abbreviation Name: _____
Signed: _____
Date: _____

9 Full Name: _____
Abbreviation Name: _____
Signed: _____
Date: _____

10 Full Name: _____
Abbreviation Name: _____
Signed: _____
Date: _____

Final check list for authors

The format is at: http://www.wjgnet.com/wjg/help/13.doc

Responses to reviewers

Please revise your article according to the comments/suggestions of reviewers. The format for responses to the reviewers' comments is at: http://www.wjgnet.com/wjg/help/10.doc

Proof of financial support

For paper supported by a foundation, authors should provide a copy of the document and serial number of the foundation.

Publication fee

Authors of accepted articles must pay publication fee.
EDITORIAL and LETTERS TO THE EDITOR are free of charge.